PROTON AND CARBON-13 NMR STUDIES ON THE STEREOCHEMISTRY AND KINETICS OF HINDERED INTERNAL ROTATIONAL PROCESSES IN 1-ARYL HYDANTOINS

SIDDIK ICLI

A THESIS

in

THE DEPARTMENT

of

CHEMISTRY

Presented in Partial Fulfillment of the Requirements for the Degree of DOCTOR OF PHILOSOPHY

Sir George Williams University

Montreal, Canada

April 1974

VITAE

The author was born in Sivas, Turkey on June 2, 1947. He graduated from Kurtulus High School, Ankara, Turkey in June 1964. The same year he entered the University of Ankara where he held a NATO scholarship from the Scientific and Technical Research Council of Turkey. He graduated from the University of Ankara in June 1968, receiving a diploma in Chemistry.

In September 1968 the author began graduate study at the University of Rochester, Rochester, New York, under the direction of Dr. R. W. Kreilick in Chemistry and received the degree of M.Sc. in June 1971. He held the scholarship from the Research Council of Turkey during his graduate studies.

Beginning in January 1971, the author continued graduate study leading to the degree of Doctor of Philosophy at Sir George Williams University under the direction of Dr. L. D. Colebrook. The scholarship from the Research Council of Turkey supported him until January 1972. During the academic years of 1971-72 and 1972-73 he held full-time demonstratorships from Sir George Williams University.

ACKNOWLEDGEMENTS

The author appreciates and gratefully acknowledges the aid and advice of the following, who helped in the preparation of this thesis.

Dr. L. D. Colebrook, for his patient direction and support of these research projects.

The aid and helpful discussions of Dr. N. Gurudata on carbon-13 nmr studies, of Professor J. Lenoir and Dr. O. S. Tee on organic synthesis, of Dr. P. H. Bird and Mr. J. H. Lawson on computer programs.

Dr. R. T. B. Rye, for obtaining the elemental analysis of some hydantoins.

Mr. D. F. Williams, for providing the information in use of the C. W. carbon-13 nmr instrument.

Sir George Williams University, and the Department of Chemistry for the use of their facilities and CDC 3300 and CYBER 70-72 computers.

Ms. K. Bennett, for correcting the English in the thesis.

Research Council of Turkey, Sir George Williams University, for their financial support.

ABSTRACT

Part I

The stereochemistry and the kinetics of conformational change of a series of 1-aryl substituted hydantoins subject to restricted internal rotation about the aryl C-N bond have been investigated by proton magnetic resonance line shape analysis. The barriers to internal rotation caused by polar or non-polar ortho substituents on the aryl group are consistent with the expected relative sizes of these groups, in contrast to the previously studied 3-aryl hydantoins. Rotational barriers are strongly influenced by the bulk effect of the C-5 substituents on the hydantoin ring.

Solvent effects on the thermodynamic parameters for restricted rotation have been examined. Studies in different solvents have revealed that polar and anisotropic interactions between solute and solvent molecules have pronounced effects on the enthalpies and entropies of activation for restricted rotation.

High resolution nuclear magnetic resonance data indicate that the trans isomers of diastereomeric 1-aryl hydantoins mono-substituted in the 5-position have the higher stability in the rotational ground states.

Part II

In a carbon-13 nuclear magnetic resonance study of the 1-aryl hydantoins, the carbon-13 shieldings have been examined with reference to the stereochemistry of these compounds. The relative influences of steric, inductive, and conjugation effects due to aryl and C-5 methyl substituents on the chemical shifts of the various carbon atoms in these compounds were considered. Additive shift parameters found for the 1-aryl hydantoins agree with those found for the previously studied 3-aryl hydantoins.

Carbon shielding values in aryl substituted hydantoins are sensitive to solvent polarity. Carbonyl carbon chemical shifts of the hydantoins are more strongly influenced than other carbon chemical shifts when hydrogen bonding between solute and solvent molecules is present.

The non-equivalence of the enantiotopic, C-5 methyl carbon atoms in the C-13 magnetic resonance spectra of aryl hydantoins with high barriers to internal rotation has indicated the feasibility of using the carbon resonance to study the kinetics of conformational change. The higher chemical shift differences for the carbon relative to the proton spectra result in higher coalescence temperatures, as has been demonstrated for one of the hydantoins with a coalescence temperature near the probe temperature.

Part III

A proton magnetic resonance study of some 1-aryl hydantoins in a chiral solvent environment has resulted in the observation of the non-equivalence of isomeric protons. Splitting of the signals of aromatic methyl protons of aryl substituted hydantoins in optically active carbinol solutions is attributed to specific solute-solvent interactions. The solvent-induced chemical shift differences are attributed to the anisotropic interactions of solute and solvent molecules in hydrogen bonded diastereomeric solvates. The carbon-13 and the proton shielding data and the rotational thermodynamic parameters have enabled a configuration for the hydantoin-carbinol complex to be proposed. The absence of similar non-equivalencies in the C-13 spectra is believed to result from the relatively lower sensitivity of carbon resonances to small chemical shift differences.

TABLE OF CONTENTS

LIST OF FIGURES

LIST OF TABLES

PART I

THE KINETICS OF CONFORMATIONAL CHANGE IN 1-ARYL HYDANTOINS THROUGH PMR LINE SHAPE ANALYSIS

INTRODUCTION

The application of nuclear magnetic resonance (nmr) spectroscopy to the investigation of restricted internal rotational processes has proven to be of immense value relative to other spectroscopic methods (infrared, Raman, microwave, polarimetric).[1,2] It offers the possibility of examining organic compounds with minimal restriction imposed by their molecular sizes or shapes and of determining the kinetic and thermodynamic parameters of conformational changes most efficiently, providing that the barriers hindering internal rotation are sufficiently high. In many cases the rate of rotation may be lowered by either lowering the temperature range of the nmr study or by introducing bulky substituents into the parent molecule to slow the rate of rotation. Since the late 1950's, the nmr technique has permitted the study of many rate processes with rotational free energies of activation ranging from the upper borderline of 20-25 kcal/mol, down to about 5-6 kcal/mol. Over much of this range the conformers are unstable with respect to chemical isolation[2,3]

In basic theory, an nmr study includes a line shape analysis of the distinguishable peaks due to the non-equivalent nuclei of rotational isomers. Line shape analysis is applicable when the average lifetimes of the exchanging species exceed an upper limit on the nmr time scale, so that

the spectrum is observed as the sum of individual entities. In contrast, if the lifetimes fall below the lower limit, a time averaged spectrum of the two species is observed. At intermediate lifetimes, coalescence from the individual spectra to the time averaged spectrum is observed. The analysis of these processes to obtain useful kinetic and thermodynamic data is termed "dynamic nuclear magnetic resonance" (DNMR)[2]. The rate of exchange between diastereomeric rotamers may be obtained through the use of an equilibration method for highly hindered systems. The chemically isolated diastereomer is allowed to reach equilibrium at constant temperature and the changes in peak areas of the diastereotopic nuclei are measured.

The earliest reports of DNMR studies were concerned with the double-bond character of amides and related compounds.[4,5] Later studies were extended to ring inversions[2,6] and some organometallic complexes[7]. Consequently, the hindered rotation process in heterocyclic systems attracted attention. Mislow et al[8] reported kinetic data on hindered rotation about the aryl C-N bond in N-aryl cyclic amides. Subsequently, workers in Colebrook's laboratories have studied the stereochemistry and kinetics of conformational change in some biphenyls[9], amide derivatives, and some new heterocyclic systems. Bentz[10] determined the barriers to hindered rotation in biphenyls and triazines of type I and II respectively, through the use of complete line shape

analysis.

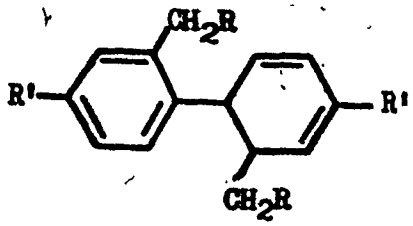

(I)

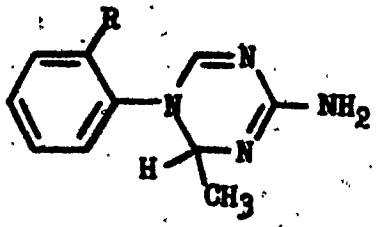

(II)

Hund[11] has studied the influence of structural changes on the rotational kinetic parameters in N-benzyl-N-aryl amides of type III.

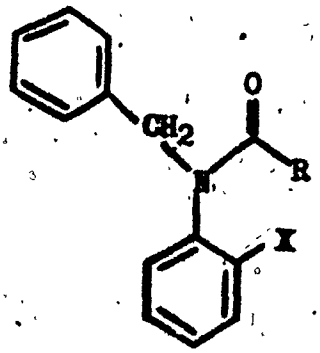

(III)

Fehlner,[12,13] Giles,[14] and Granata[15] have observed high rotational stabilities in quinazolinones,[IV], 3-aryl hydantoins,[V], and 3-aryl-2-thio hydantoins,[V]. These authors have examined the kinetic and thermodynamic parameters calculated from the complete line shape analysis and equilibration methods. Williams[16] made a preliminary investigation of the 3-aryl hydantoins using the carbon-13 nmr technique. His results are discussed in Part II of the thesis.

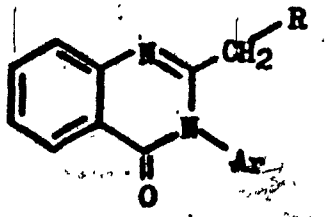

(IV)

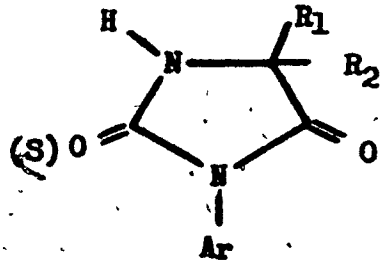

(V)

The use of hydantoins permits the examination of restricted internal rotation processes about aryl C-N bonds involving a hetero ring substituted in two different positions. The investigation of rotational kinetic and thermodynamic parameters in 1-aryl hydantoins, in relation to the stereochemistry of conformational change, the substituent and the solvent effects, is the subject of this study.

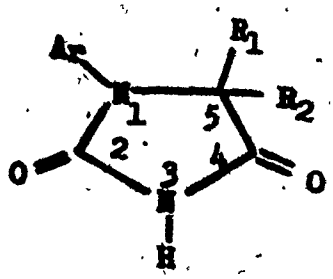

The 1-aryl hydantoins which were synthesized for the purpose of this DNMR study are listed in Table I-1. The comparison of the present results with those obtained for 3-aryl hydantoins has indicated some interesting dissimilarities, both expected and unexpected. Thus, an understanding of the nature of the influences of through-

Table I-1: 1-Aryl Hydantoins Prepared for the Study of C-N Bond Hindered Rotation.

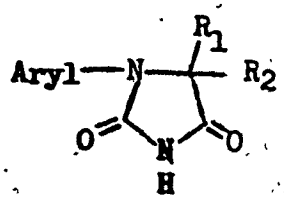

Hydantoin	Aryl	R_1	R_2
I	o-Chlorophenyl	H	H
II	o-Tolyl	H	H
III	o-Trifluoromethylphenyl	H	H
IV	α-Naphthyl	H	H
V	o-Chlorophenyl	CH_3	H
VI	o-Tolyl	CH_3	H
VII	α-Naphthyl	CH_3	H
VIII	2,3-Dimethylphenyl	CH_3	H
IX	o-Chlorophenyl	C_6H_5	H
X	o-Tolyl	C_6H_5	H
XI	α-Naphthyl	C_6H_5	H
XII	o-Chlorophenyl	CH_3	CH_3
XIII	o-Tolyl	CH_3	CH_3
XIV	α-Naphthyl	CH_3	CH_3
XV	β-Naphthyl	CH_3	CH_3
XVI	o-Fluorophenyl	CH_3	CH_3
XVII	o-Methoxyphenyl	CH_3	CH_3
XVIII	2,3-Dimethylphenyl	CH_3	CH_3

bond or through-space steric or electronic effects and of the solvent molecular environment on hindered rotation about the aryl C-N bond in hydantoin derivatives has been achieved.

Causes of Non-equivalence in the NMR Spectra:

The internal bond rotation about the C-N bond joining the aryl and hetero rings results in formation of diastereomeric and enantiomeric rotational isomers in 1-aryl hydantoins.

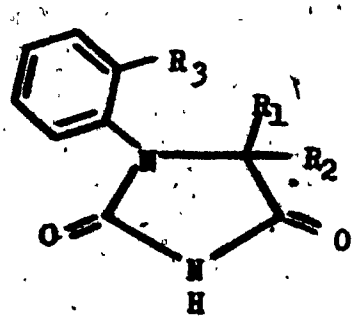

Asymmetry is introduced by the ortho substituted aryl and the C-5 substituents. The aryl and the hetero rings of the rotamers are shown at right angles to each other in the figures below, the molecule being viewed along the C-N bond rotational axis. Due to steric and electronic effects the planes are expected to deviate from 90° angles. In order to simplify the schematic drawings these effects are not considered here, but they are discussed later in the thesis.

A 180° rotation of the ortho substituted aryl ring around the C-N rotational axis forms isomer II from I, and isomer IV from III. When the R_1 and R_2 groups are identical, I and IV, and II and III will be identical. I will be enantiomeric to II. Enantiomers have similar physical properties, so one may expect indistinguishable spectra for the I and II enantiomers. However, R_1 and R_2 are non-equivalent (diastereotopic) due to the presence of asymmetry caused by the ortho aryl substituent R_3. Hence they reside in different magnetic environments and they are expected to show chemical shift differences in the nmr spectra. If R_1 and R_2 are protons, an AB spin system will be present. The protons will couple to each other so that an AB quartet is expected to be observed at slow rates of rotation. In this investigation an AB quartet was not exhibited by the hydantoins studied even at the lowest possible temperatures (~-75° C), presumably because of low barriers to hindered rotation. When the C-5 substituents (R_1 and R_2) are methyl groups a doublet with members of equal intensity was recorded in the pmr spectra at normal probe temperatures. The coupling between the protons of two methyl groups was too small to be observed.

Diastereomeric species may be present only when R_1 and R_2 are not identical. Under these circumstances, I will be diastereomeric to II, and III will be diastereomeric to IV. I and III, and II and IV, will be enantiomeric, with

indistinguishable spectra. R_1 and R_2 were chosen to be a proton and a methyl group, respectively, in the 1-aryl hydantoin diastereomeric series. The lifetimes of the diastereomers were found to be unequal, due to certain steric interactions in the hydantoin molecules, resulting in unequal intensities of the signals arising from corresponding protons on the diastereomeric rotamers. The spectrum is complicated further by coupling of the methine proton to the methyl protons. The methine proton shows a pair of quartets, while the methyl protons show a pair of doublets under conditions of slow rotation. In another case, involving diastereomeric rotamers, in which the C-5 position of the hydantoin is substituted with a proton and a phenyl group, the methine proton signal was recorded as a single peak at the lowest possible temperatures (~-75° C), probably due to lack of sufficiently high barriers to rotation.

THEORY OF LINE-SHAPE ANALYSIS

Quantum Mechanical Line-Shape Theory:

The line shape analysis for an AB set of protons exchanging with each other is given as a sample application. The theoretical line shapes for the case of two interacting nuclei of spin I = 1/2 which undergo an exchange process have been calculated by Alexander[17] and by Kaplan[18], by deriving the Boltzman equation for the average density matrix. The total spin Hamiltonian is given below for a correlated intramolecular exchange process in which the environments of the two interacting nuclei are interchanged in a time interval short compared to the lifetimes of the nuclei in the two different environments.

$$\vec{H} = \vec{W}_o(\vec{I}_z^A + \vec{I}_z^B) + \delta(\vec{I}_z^A + \vec{I}_z^B) + J(\vec{I}^A \cdot \vec{I}^B) + W_1[(I_x^A + I_x^B)\cos Wt + (I_y^A + I_y^B)\sin Wt] \quad (1)$$

where $\vec{W}_o = \gamma\vec{H}_o$ with the Zeeman field $\vec{H}_o$ defining the direction z, and $W_1 = \gamma H_1$. H_1 is the amplitude of the radio-frequency field rotating at frequency W, and γ is the gyromagnetic ratio of the proton; $\vec{I}^A$ and $\vec{I}^B$ are the nuclear spin operators of the protons A and B. J is the scalar coupling constant and $\pm\delta$ are the chemical shift parameters (in frequency units) of the protons A and B respectively,

in the Zeeman field H_o, as observed in the absence of exchange.

In order to simplify the derivation of a set of line shape equations Alexander made the assumption that the natural line width makes little contribution to the line width of the observed lines, so that $1/T_2$ (where T_2 is the transverse relaxation time) was set equal to zero.

If this assumption is made, considerable errors can be introduced to the calculations of the lifetimes of the nuclei on the exchanging sites, when factors which increase the natural line width such as viscosity broadening and long range coupling are present at slow exchange rates. For this reason it is desirable to include the linewidth parameter in the calculations. Line shape equations for an exchanging AB set of protons in which $1/T_2$ was not assumed to be zero have been rederived by Colebrook and Turner[19]. These equations are also given in the Ph. D. thesis of Bentz.[10]

However, quantum mechanical line shape equations of this type are applicable to line shape analysis only when the Boltzman populations of the two exchanging sites are equal. In addition, the equations contain the coupling constant parameters, which would require the inclusion of J values in the calculations. Due to these restrictions, the classical line shape equations of Gutowsky and Holm[3] were preferred for use in the line shape analyses required in

this study, since they could be applied to all the line shapes encountered.

Classical Line Shape Theory:

a) Line Shape of a Pair of Singlets Collapsing to a Single Peak: Classical line shape theory based on the Bloch equations[20] has been employed by Gutowsky and Holm[5] to derive the line shape equations for an exchange process between two sites. If one considers that the rotamers of a molecule which is undergoing internal rotation reside in two different environments, A and B, with chemical shifts $\nu_A = W_A/2\pi$ and $\nu_B = W_B/2\pi$, a first order rate reaction can be assumed to be in progress, due to change in magnetization of both sites. The rate constants for the forward and the reverse reactions are given as $k_A = 1/\tau_A$ and $k_B = 1/\tau_B$, where τ_A and τ_B are the lifetimes of the two rotamers.

The equation for the intensity, I, at any point, W, which has been calculated by the use of Bloch equations modified to include the rate process, is given by;

$$I = K\left\{ \frac{1 + \tau/T_2)P + Q.R}{P^2 + R^2} \right\}$$

where

$$\tau = \frac{\tau_A \cdot \tau_B}{\tau_A + \tau_B}$$

and

$$P = \tau\left\{(1/T_2)^2 - [1/2(W_A + W_B) - W]^2 + 1/4(W_A - W_B)^2\right\} + 1/T_2$$

$$Q = \tau[(\tfrac{1}{2}(W_A + W_B) - W - \tfrac{1}{2}(P_A - P_B)\ (W_A - W_B)]$$

$$R = [\tfrac{1}{2}(W_A + W_B) - W](1 + 2\tau/T_2) + \tfrac{1}{2}(P_A - P_B)\ (W_A - W_B)$$

K is a scaling factor and T_2 is the transverse relaxation time assumed to be the same in both sites. P_A and P_B are the populations of the two rotamers, and are defined as:

$$P_A = \frac{\tau_A}{\tau_A + \tau_B} \quad ; \qquad P_B = \frac{\tau_B}{\tau_A + \tau_B}$$

The simulated spectra in Figure I-1 illustrate the temperature dependence of a system of this type.

b) <u>Line Shape of a pair of Doublets Collapsing to a single Doublet:</u>

The system considered here can be thought of as two superimposed systems of the Gutowsky-Holm type, as in the previous case. Bentz[10] and Fehlner[12] have derived the equations for this system based upon the Gutowsky-Holm formulations.

The intensities of the M and N lines, and the coupling constants J_A and J_B, have been taken into account in this system. These components are shown in the figure below.

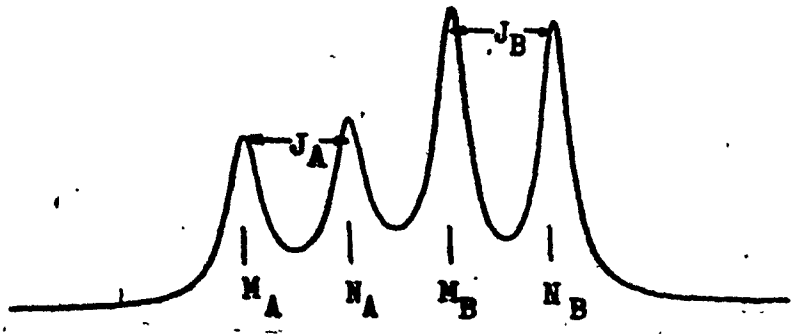

The expression for the intensity, I_T, at any frequency W, is given in the following equation:

$$I_T = K\ [I_M + L(I_N)]$$

where,

$$I_M = \frac{(1 + \tau/T2)P_M + Q_M \cdot R_M}{P_M^2 + R_M^2}$$

$$I_N = \frac{(1 + \tau/T2)P_N + Q_N \cdot R_N}{P_N^2 + R_N^2}$$

$$\tau = \frac{\tau_A \cdot \tau_B}{\tau_A + \tau_B}$$

and

$$P_M = \tau[(1/T_2)^2 - (\tfrac{1}{2}S-W)^2 + (1/4)D^2] + 1/T_2$$

$$P_N = \tau[(1/T_2)^2 - (\tfrac{1}{2}U-W)^2 + (1/4)V^2] + 1/T_2$$

$$Q_M = \tau[\tfrac{1}{2}S-W-\tfrac{1}{2}(P_A-P_B)D]$$

$$Q_N = \tau[\tfrac{1}{2}U-W-\tfrac{1}{2}(P_A-P_B)V]$$

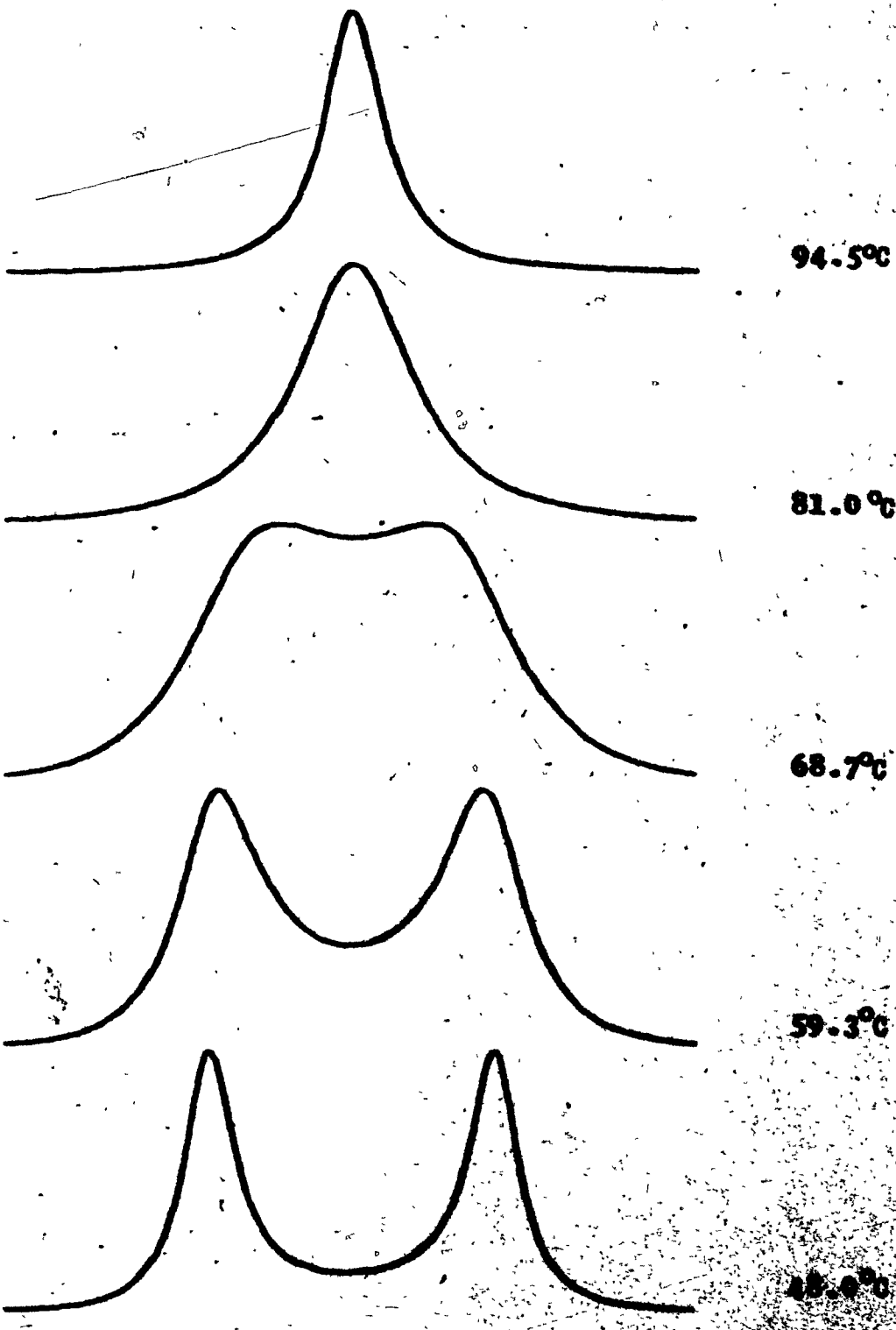

Figure I-1: Computer Simulated Spectra of Coalescence of C-5 Methyl Protons in 1-(p-Chlorophenyl) - 5,5-dimethyl hydantoin, XII, in DMSO-d_6 Solution.

$$R_M = [\tfrac{1}{2}S - W](1+2\tau/T_2) + \tfrac{1}{2}(P_A - P_B)D$$

$$R_N = [\tfrac{1}{2}U - W](1+2\tau/T_2) + \tfrac{1}{2}(P_A - P_B)V$$

$$S = W_A + W_B$$

$$D = W_A - W_B$$

$$U = (W_A + J_A) + (W_B + J_B)$$

$$V = (W_A + J_A) - (W_B + J_B)$$

$$P_A = \tau_A / (\tau_A + \tau_B)$$

$$P_B = \tau_B / (\tau_A + \tau_B)$$

τ_A and τ_B are the mean lifetimes of the two rotamers, while W_A and W_B are the frequencies of the M_A and M_B lines, respectively. J_A and J_B are measured as the shift (in Hz) between the M_A and N_A lines and between the M_B and N_B lines, respectively. W, W_A, W_B, J_A and J_B are all converted to radians/sec. for use in this calculation. L is a factor which allows the intensity of the N lines to be related to that of the M lines. K, the scaling factor, and T_2, the transverse relaxation time, are the same as defined for the AB system. The simulated spectra in Figure I-2 show temperature dependence for a system of this type, where the chemical shift difference is sufficiently large that the doublets are separated. The simulated spectra of 1-(α-naphthyl)-5-methyl hydantoin in Figure I-3 show a triplet at low temperatures

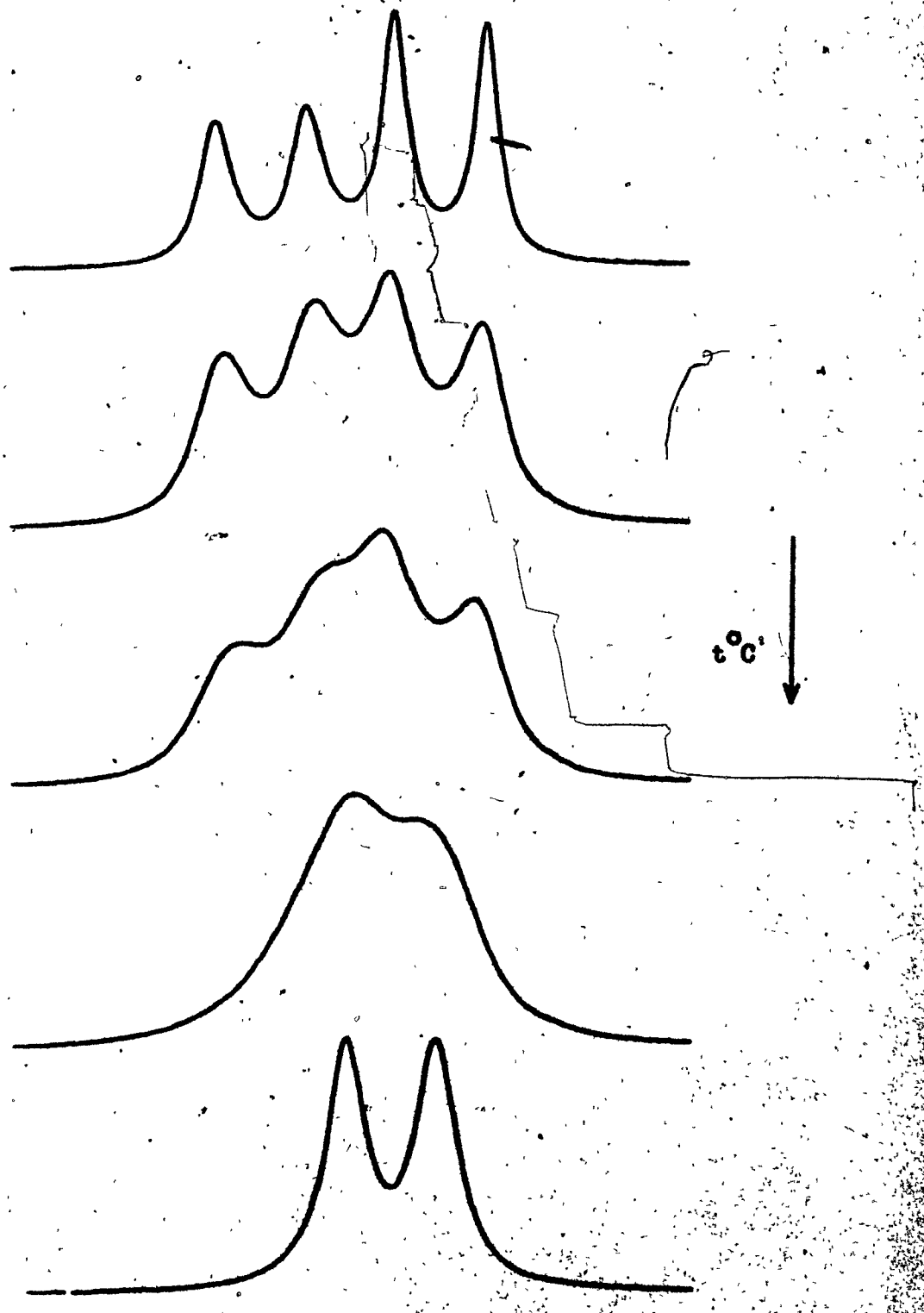

Figure I-2 : Computer Simulated Spectra of Coalescence of Two Doublets with Large Chemical Shift Difference.

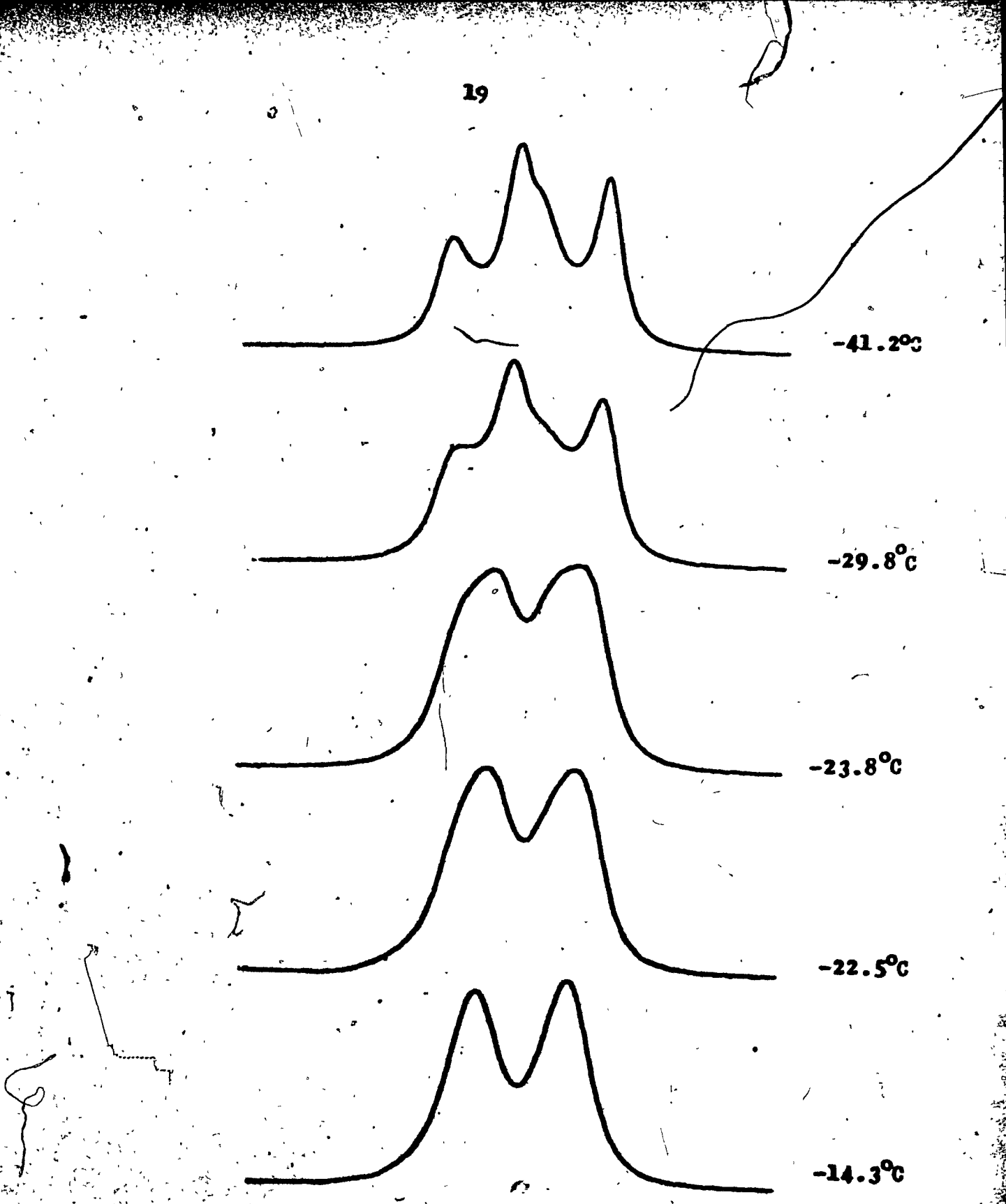

Figure I-3 : Computer Simulated Spectra of Coalescence of C-5 Methyl Protons in 1-(α-Naphthyl)-5-methyl hydantoin, VII, in Acetone-d_6/DMSO-d_6 Solution.

due to coincidence of coupling constants with chemical shift differences.

Use of these equations is valid only in systems which are close to first order.

Comparison of Spectra:

Theoretical spectra can be calculated for any given set of lifetime, chemical shift, and coupling constant parameters for the exchanging sites, using the equations based on the Gutowsky-Holm formulation. In order to obtain the most accurate lifetime values or rate constants for rotamers, at given temperatures, one has to achieve a good fit between the experimental and theoretical spectra. This may be done point by point by computer. A spectrum calculated from initial estimates of the parameters can be compared with the observed spectrum by a least squares method. New parameters are then calculated based upon the differences between observed and calculated intensities, and a resulting new theoretical spectrum is compared with the experimental spectrum. The non-linear regression procedure continues to calculate new parameters and make comparisons until the best fit is found. The programs NLINGH and NLINDD2, which are suitable for this non-linear least squares regression analysis, were developed by Colebrook from the program NLIN2 which was originally obtained from the SHARE library.[21] The basic non-linear regression program is used

in combination with subroutines containing the line-shape equations for the system being considered. The operational procedure for these programs is explained in detail in experimental part. Examples of spectra fitted using these programs are given in Figures I-4 to I-9.

Calculation of Activation Parameters:

The Arrhenius and Eyring activation parameters for the rotational process are calculated through the use of mean lifetimes or rate constants which are obtained from line shape analysis. A computer program, ACTPAR,[22] has been written to calculate all the activation parameters and 90% confidence limits from given lifetimes and temperatures.

The Arrhenius Activation energy, E_a, is defined in the Arrhenius equation;

$$k = A \exp(-E_a/RT)$$

where k is the rate constant for the rotation process, A is the frequency factor, R is the gas constant and T is the temperature in degrees Kelvin. The slope of the plot of lnk versus 1/T ($^{\circ}$K), gives the energy of activation.

The temperature dependent activation parameters: enthalpy of activation, $\Delta H^{\neq}$, free energy of activation, $\Delta G^{\neq}$ and entropy of activation, $\Delta S^{\neq}$, are calculated by the use of the Eyring equations by ACTPAR. These equations are expressed below:

$$\Delta H^{\neq} = E_a - RT$$

$$\Delta G^{\neq} = 2.303RT(10.319 + \log T + \log(T)$$

$$\Delta S^{\neq} = (\Delta H^{\neq} - \Delta G^{\neq})/T$$

ACTPAR finds the best straight line for the plot of lnk versus 1/T through the use of a linear regression method, and also calculates the Eyring parameters for a specified temperature.

EXPERIMENTAL

Preparation of NMR Samples:

The choice of NMR solvents for the aryl substituted hydantoins is somewhat limited because of the poor solubility of these compounds in most solvents. The nmr samples for the hydantoins with high coalescence points (room temperature or above) were prepared in hexadeuterodimethylsulfoxide (DMSO-d_6), or pyridine, obtained from Merck Sharp & Dohme Isotope Chemicals and Fisher Chemicals, respectively. 2-Chloropyridine was used instead of pyridine when the coalescence temperatures of the hydantoins exceeded the boiling point of pyridine. The samples were prepared as concentrated as possible. Concentrations in both types of solvents were approximately two molar.

Hydantoins with spectra that coalesced below room temperature were dissolved in hexadeuteroacetone and hexadeuterodimethylsulfoxide mixtures. DMSO-d_6 solvent was added in 15-20% proportions to increase the solubility of the hydantoins in deuterated acetone. These solutions did not freeze at temperatures as low as -70 and -75°C degrees. Acetone-d_6 was obtained from Merck Sharp & Dohme Isotope Chemicals.

Tetramethylsilane (TMS) and hexamethyldisilane (HMDS, from [illegible] Specialties) were added in small portions as internal standards to the low and high temperature nmr samples, respectively.

Measurement of Spectra:

The nmr spectra of the 1-aryl hydantoins were taken on a Varian HA-100 spectrometer operating at 100 MHz in the field sweep mode. The sweep widths of the spectra were either 50 or 100 Hz, depending on the chemical shift differences of the methyl protons. Standard Varian ethylene glycol and methanol reference samples were used for high and low temperature measurements, respectively. Temperature measurements were carried out by measuring the peak separation from the methylene or methyl peak employed as the lock signal to the hydroxyl peak. The temperatures for each run were calculated from Varian calibration charts, where chemical shift differences are plotted versus temperature.

The temperatures or chemical shift differences were measured before or after each run. Care was taken to make sure that the temperature had come to equilibrium before it was measured. This was done by checking the current stability on the variable temperature controller and finding a reproducible hydroxyl proton signal at a constant chemical shift value. This method is estimated to be good to an accuracy of $\pm 1^{\circ}C$.

Another factor that was also carefully considered during variable temperature studies was homogeneity adjustments. These adjustments had a critical effect on the natural line width measurements. The homogeneity controls were optimized

on the internal reference signal at room temperature, and the natural line width was measured for each series of runs. It was found that a probe temperature change seriously unbalanced the homogeneity adjustments. Before any high or low temperature run the internal reference signal was re-optimized to a level comparable to that obtained on the room temperature run. The best results were obtained when the concentration of the internal reference was chosen to produce a signal similar in intensity to the methyl signals. The power level and other settings were maintained with minimal change for each series of runs in order to obtain the most accurately comparable spectra. Spectra of the nuclei of interest were taken at 2 to 4 °C intervals around the coalescence point. These intervals were increased near the fast and slow exchange limits.

Fitting of the Spectra:

Fitting of theoretical spectra to the experimental spectra was carried out through the use of a non-linear least squares regression program.[22] A series of programs, prepared by Colebrook for the particular line shapes involved in this study, were used for the various steps in the data acquisition, transfer, and processing procedures. The whole process was carried out in three stages; line follower digitization of the spectra, transfer of data from paper tape to magnetic tape and fitting by the non-linear least squares regression

program. A Hewlett-Packard F-3B Line Follower, H-P 7001 AM X-Y Recorder and H-P 2114B computer were used for the first two operations, and fitting was performed on a CDC 6400 computer.

A - Line Follower Digitization of NMR Spectra:

The program LINDI was used in conjunction with the Hewlett-Packard Line Follower, Recorder and 2114B computer to digitize the recorded spectra.[22] Digitized experimental spectra were punched onto paper tape as intensity-frequency data pairs. The main program is written in Fortran and the subroutines which drive the recorder, effect digitization and provide a variable delay to control scanning rate, are written in Assembler. LINDI allows the computer to drive the X-axis sweep of the recorder through an 8 bit digital to analogue converter while the line follower head follows the spectral trace (only in black colour) and a voltage proportional to the spectral intensity is supplied to the analogue to digital converter from the Y-axis slide wire. The computer moves the recorder arm across the spectrum in 250 increments, storing a digitized intensity for each step. Before the run is started the line follower head is adjusted successively to the left and right limits of the portion of the spectrum to be scanned, using the recorder zero and gain controls, the two frequency limits are entered into the computer and the sensor is set on the base line as zero intensity. In order

the computer calculates the frequency corresponding to each intensity. The computer was allowed to output up to 251 baseline corrected intensity-frequency data pairs, which were simultaneously typed and punched on paper tape.

The line follower cannot cope with steep curves, even at the slowest scanning rate. In this case, the line follower head was moved by hand on the curve, point by point, by using the computer switch register to control acquisition of each point. The computer switch register was also used to abort the scan when the line follower head lost the curve and a repeat scan was needed. The frequency interval per intensity measurement was usually selected to be 0.25 or 0.50 Hz, depending upon whether the spectrum contained narrow or broad peaks, respectively.

Digitization of noisy spectra was carried out on a superimposed trace. The spectra were recorded in coloured ink, rather than black, and a best curve estimated by eye and drawn in pencil through the centre of the noise.

B - Transfer of Data:

The programs written for this procedure were used to transfer the digital information from paper tape to magnetic tape together with estimated parameters for the fitting process. In addition to the data pairs from paper tape, original estimates of all the parameters and identification of the parameters which are to be held constant must be

recorded on the magnetic tape. The data on magnetic tape were then transferred to the CDC 6400 computer. The following programs were processed by the H-P 2114B computer for data transfer.

TAPGH

This program was employed for the case of a pair of singlets collapsing to a single peak. Six parameters are needed to describe the line shape and intensity of this system. They are the chemical shifts in Hz, ν_A and ν_B; the lifetimes of the two species in seconds, τ_A and τ_B; a scaling factor, k; and the line width in Hz, W. Any or all of the six parameters can be allowed to vary in the fitting process. It is frequently advisable initially to keep constant the linewidth and chemical shift parameters in order to obtain close estimates to the lifetimes from the non-linear least squares regression programs. Then the chemical shift parameters can be permitted to vary for the best fit. If this procedure is not followed satisfactory convergence may not be obtained.

TPDDJ

This program was used for the use of a pair of doublets collapsing to a single doublet when the coupling constants were unequal. Nine parameters are needed to describe the line shape and intensity of this system. They are the chemical shifts in

Hz, ν_A and ν_B; the lifetimes of the two species in seconds, τ_A and τ_B; the linewidth in Hz, W; the coupling constants in Hz, J_A and J_B; a scaling factor, k; and the relationship factor, R. The relationship factor, R, permits a correction to be made for a small amount of second order character in the spectrum. The linewidth and coupling constant parameters were kept constant in all the cases studied. Chemical shift parameters were not permitted to vary unless reasonable lifetime values were found.

CHKTP

This program was employed to read and type the contents of the magnetic tape. It was useful for a check-up before submitting the run on the CDC 6400 computer. It saved CDC computer and operator time when the digital information was not properly written on to the magnetic tape by the H-P 2114B computer. Unnoticed hardware or software problems affecting the H-P 2114B were also easily identified in some cases by this process.

C - Fitting by Non-Linear Least Squares Regression Program:

The non-linear least squares regression programs NLINDD2 and NLINCH fitted the digitized spectra stored on magnetic tapes by theoretical spectra, using the CDC 6400 computer for two different kinds of systems. The fitting process followed an iterative sequence, varying the line shape and intensity

parameters until a best fit was obtained. The natural line width, and in some cases the chemical shift parameters were held constant during the fitting process at values determined from spectra recorded under conditions of slow exchange. These restrictions were necessary because the fitting procedure cannot make an adequate distinction between the effects of varying the line width parameters and the true lifetimes on exchanging sites. The procedures followed for each type of system are given below.

NLINDD2

This program was employed to fit a pair of doublets collapsing to a doublet system. The fitting process was tedious and difficult. It required care in use due to the large number of parameters and the overlapping of doublets (Figures I-2 and I-3). In order to find accurate values for the chemical shifts the following procedures were followed. The accuracy of the measurement of one of the chemical shift parameters was poor due to the overlapping of doublets. The computer was allowed to find the most accurate chemical shift value from the best fit. The chemical shift, ν_B, for an overlapped peak was allowed to vary while the other chemical shift, ν_A, was kept constant, together with the natural line width and the coupling constant parameters. This procedure was successfully applied to the lowest temperature spectra. The chemical shift parameters for the spectra recorded at

higher temperatures were estimated with the use of the chemical shift difference obtained from fitted lowest temperature spectra. The chemical shift, natural line width, and the coupling constant parameters were held constant in most of the cases, otherwise, the computer fitted the digitized spectrum by a calculated spectrum with unacceptable lifetime and chemical shift parameters.

Experimental and theoretical spectra of some of the 5-monomethyl substituted hydantoins, fitted by NLINDD2, are shown in Figures I-4, I-5 and I-6.

DD

Program DD was employed to calculate and plot a theoretical spectrum for a pair of doublets collapsing to a doublet system, using the H-P 2114B computer. Chemical shift, coupling constant, lifetime, linewidth, relationship factor, and frequency range parameters were entered into the computer. A calculated spectrum was plotted and visually compared with the recorded spectrum.

This program was used when difficulty was found with the fitting procedure for NLINDD2. NLINDD2 failed to give a good fit when the initial estimates of the lifetime parameters were too far away from the optimum values. A calculated spectrum was plotted on the H-P recorder by the use of the DD program and compared to the experimental spectrum by eye. The lifetime parameters were varied until the best similarity

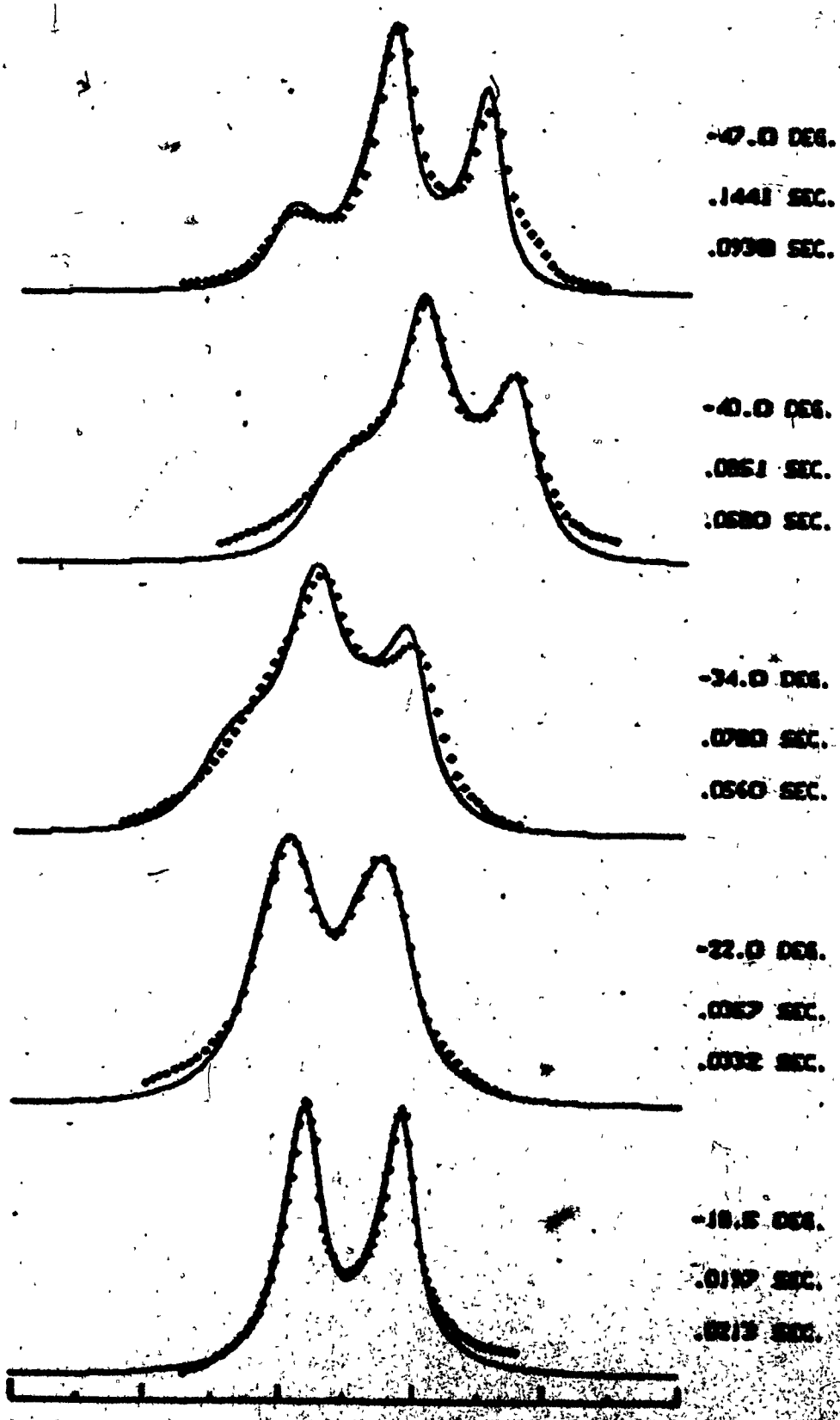

Figure I-4 : Fitted Experimental (·····) and Theoretical (——) Spectra for 1-(α-Furyl)-2-methyl-2-propyl Acetate (5a) in Acetone-d6/DMSO-d6 at Various Temperatures. Exchange Lifetimes are shown.

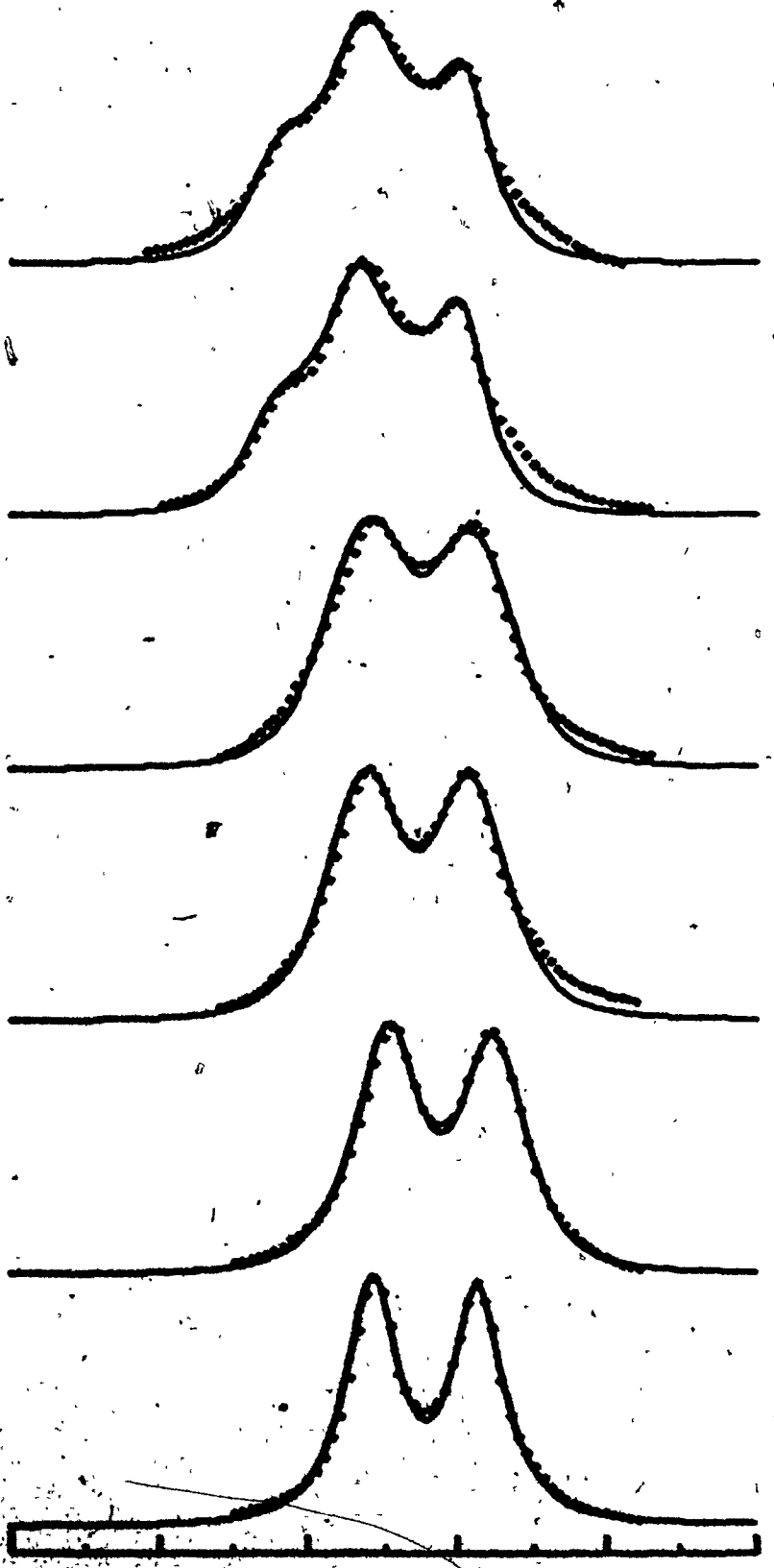

Figure I-5 : Fitted Experimental (•••••) and Theoretical (——) Spectra for 1-(2,3-Dimethylphenyl)-5-methyl hydantoin (VIII) in Pyridine at Various Temperatures. Mean Lifetimes are shown.

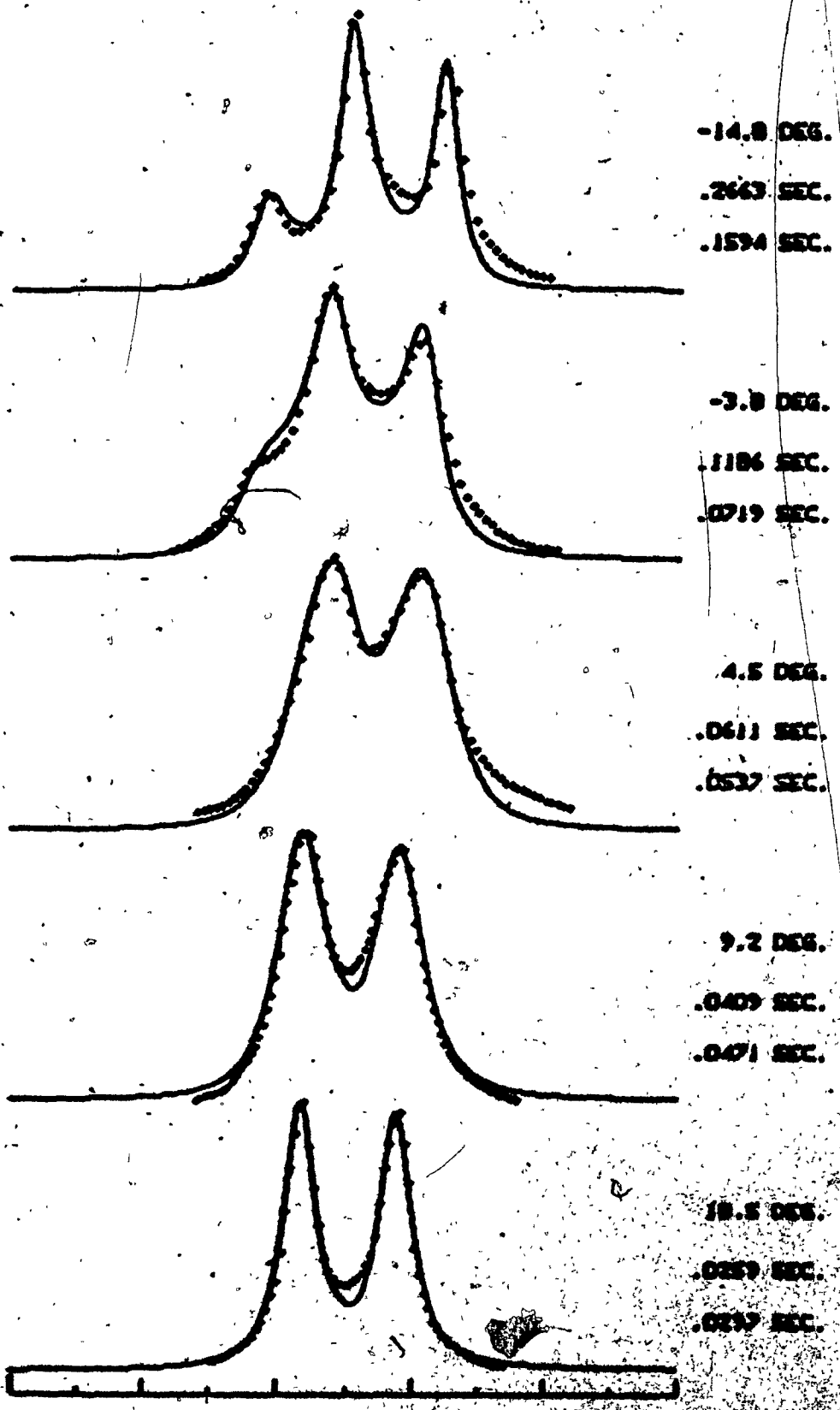

Figure I-6 : Fitted Experimental (•••••) and Theoretical (——) Spectra for 1-(2,3-Dimethyl phenyl)-5-methyl tetrazole (VII) in Acetone-d_6/DMSO-d_6 at Various Temperatures. Rate Information

between the calculated spectrum and the recorded spectrum was obtained. These lifetime values were then used in conjunction with NLINDD2 for line shape analysis.

NLINGH

This program was employed to fit a pair of singlets collapsing to a singlet system. The linewidth and chemical shift parameters were held constant for the spectra near the coalescence temperatures, the remaining three parameters being allowed to vary. If this procedure were not followed large errors in the lifetimes were introduced because of uncertainty in the chemical shift parameters. Although one would expect to find the lifetimes of exchanging sites equal to each other, slightly unequal values were obtained. This inaccuracy was probably caused by experimental errors on recorded spectra and from inaccuracies in linewidth measurements.

Experimental and theoretical spectra of some of the 5,5-dimethyl substituted hydantoins, fitted by NLINGH, are shown in Figures I-7, I-8 and I-9.

Temperature Dependence of Chemical Shift Differences:

The temperature dependence of the chemical shift differences between non-equivalent diastereomeric and enantiomeric protons of 3-aryl hydantoins was found to be relatively small in the line shape analysis studies by

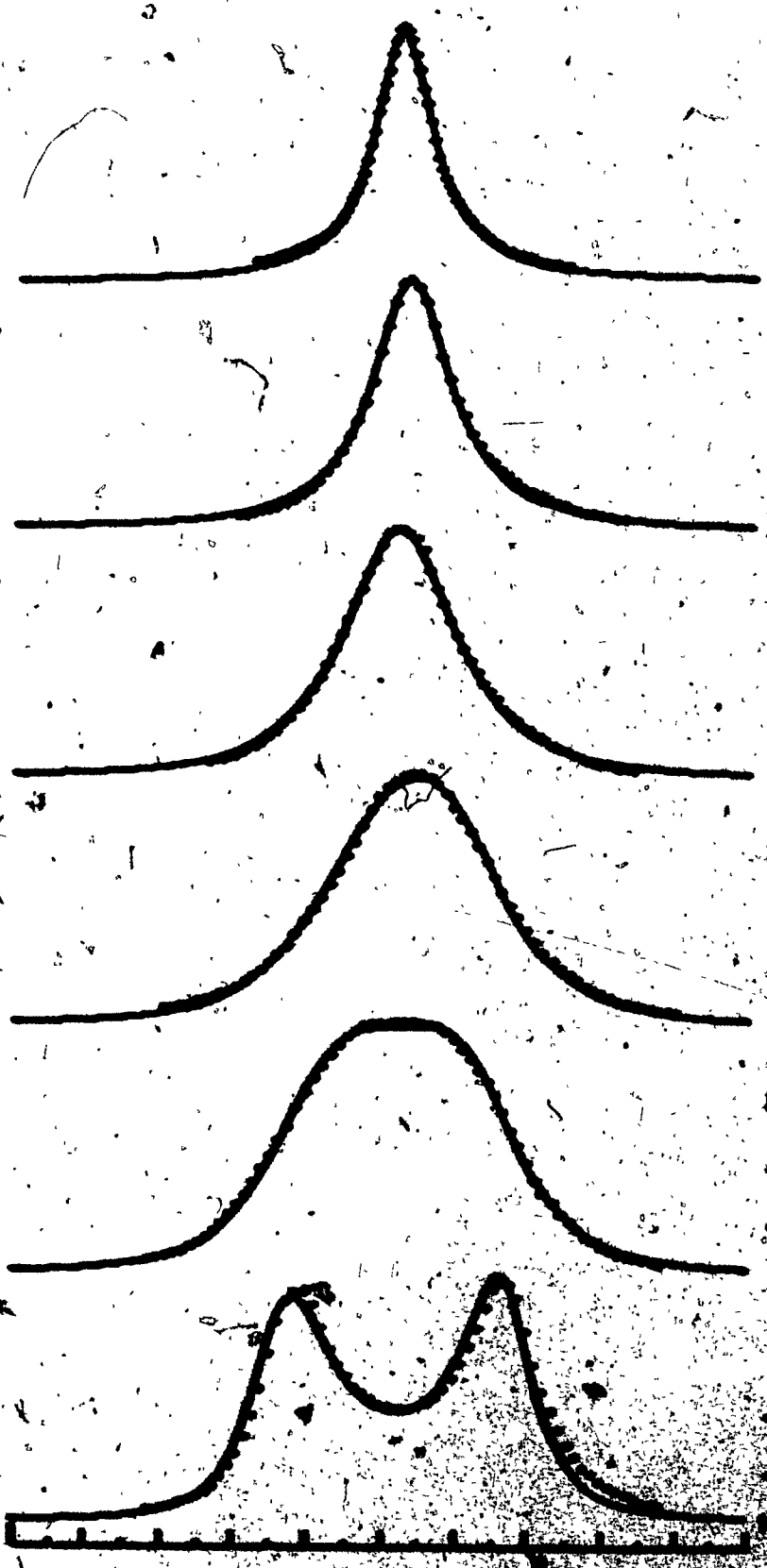

Figure I-7 : Fitted Experimental (·····) and Theoretical (——) Spectra for 1-(α-Naphthyl)-5-Substituted Tetrazoles in 2-Chloropyridine at Various Temperatures. Values of Rotation Time shown.

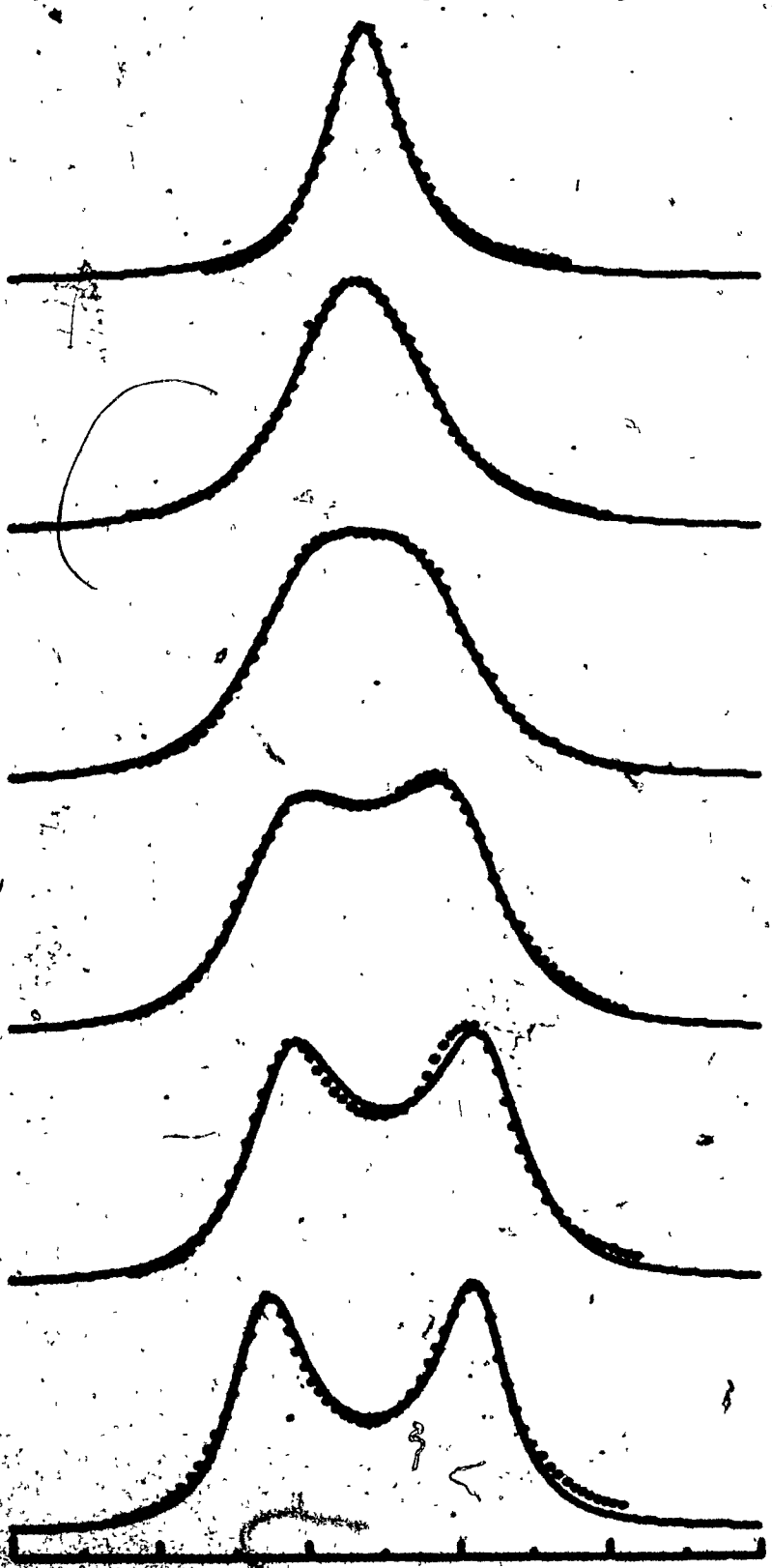

Figure I-5: Fitted Experimental (•••••) and Theoretical (——) Spectra for 1-(p-Chlorophenyl)-5,5-dimethyl hydantoin in Pyridine at Various Temperatures. Mean Lifetimes are shown.

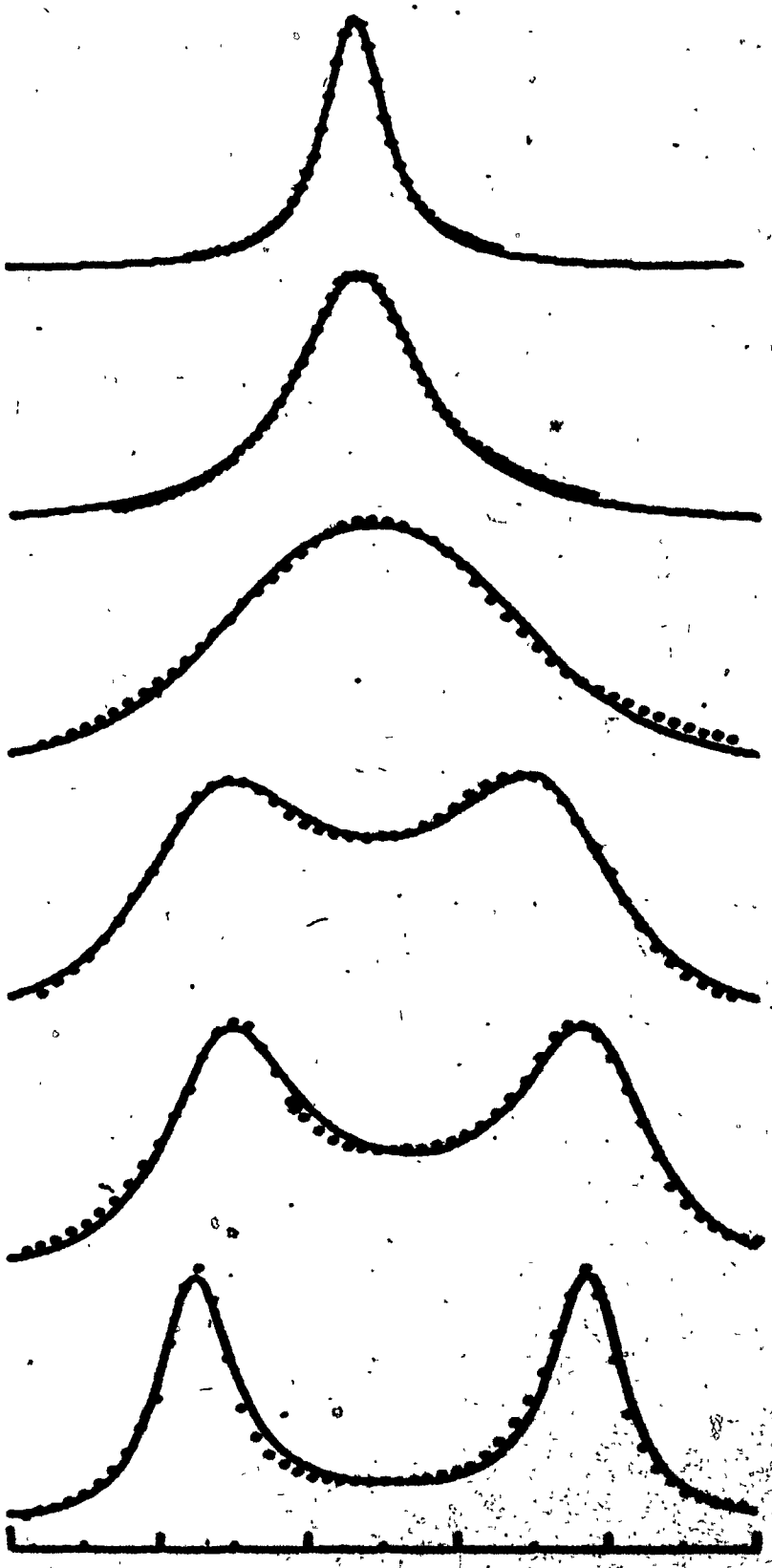

Figure I-9 : Fitted Experimental (••••) and Theoretical (——) Spectra for 1-(p-Tolyl)-5,5-dimethyl hydantoin in Pyridine at various temperatures. Mean lifetimes are shown.

Fehlner[12] and Gramata [15]. For all the cases studied there was not sufficient evidence because of limitations in the precision of the experiments to show whether $\Delta\nu$ had increased or decreased with increasing temperatures. A similar result was obtained for the 1-aryl hydantoins. Figure I-10 shows the chemical shift differences returned by the computer for the C-5 methyl protons of 1-(o-tolyl)-5-methyl hydantoin, VI, at temperatures above and below coalescence temperature. It can be seen that chemical shift differences are scattered about an average of 8.5 Hertz and any temperature dependence is not evident.

These scatterings are expected to be caused by uncertainty in the line shape analysis and by experimental errors on the recorded spectra. It seems that the deviation on $\Delta\nu$ values are relatively small for the hydantoin VI at various temperatures. However, in the cases where the chemical shift difference had to be kept constant, the scattering in the values of $\Delta\nu$ obtained by line shape analysis were appreciably large and brought serious errors to the calculation of lifetimes (Figure I-11). Thus it is assumed that chemical shift differences in the temperature ranges of line shape analysis are independent of temperature. A constant chemical shift difference was chosen for the majority of 1-aryl hydantoins in order to avoid the errors caused by such scattering of chemical shift difference values.

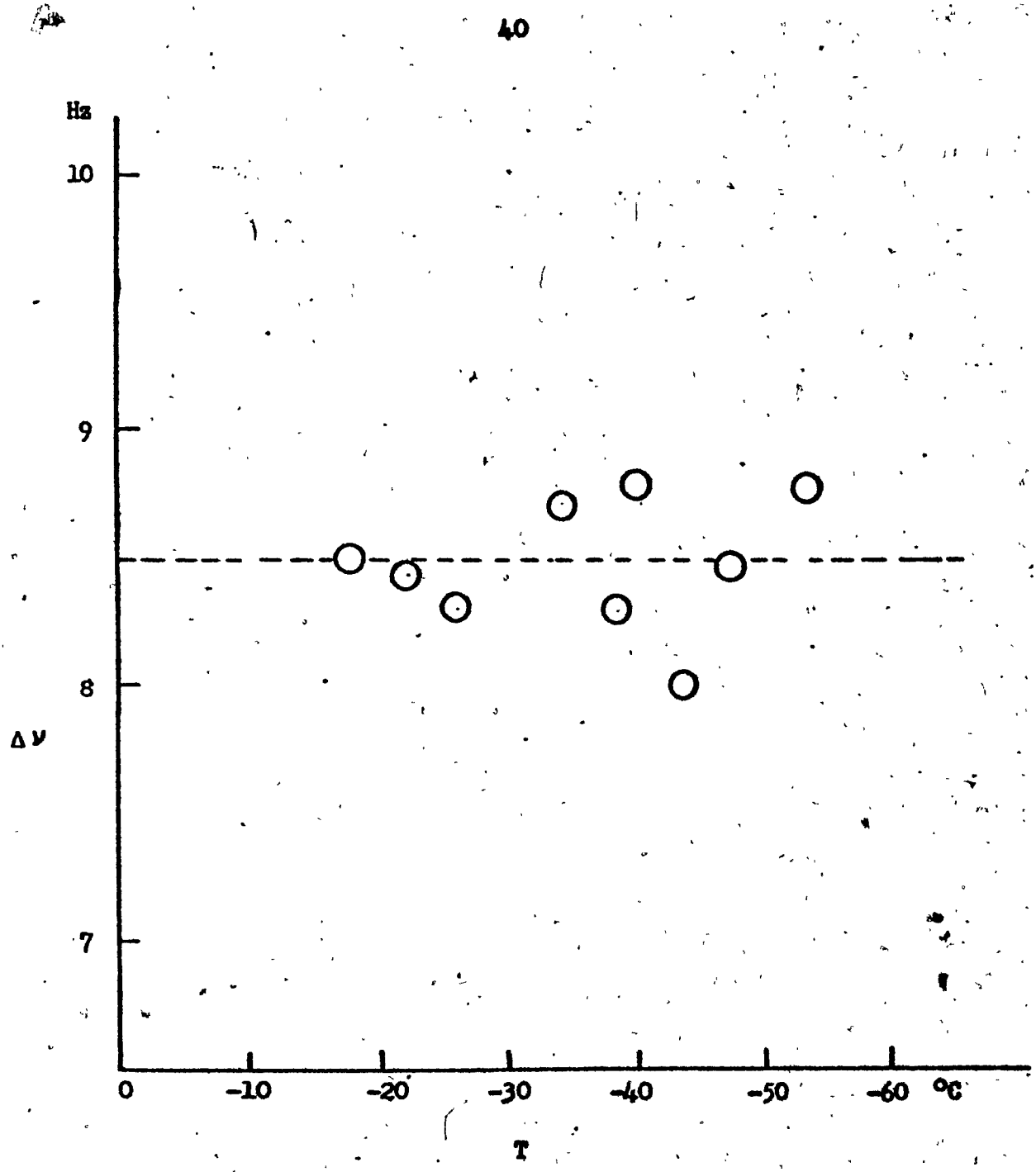

Figure I-10 : Temperature Dependence of the Chemical Shift Difference of the C-5 Methyl Protons in 1-(o-Tolyl)-5-methyl hydantoin, VI.

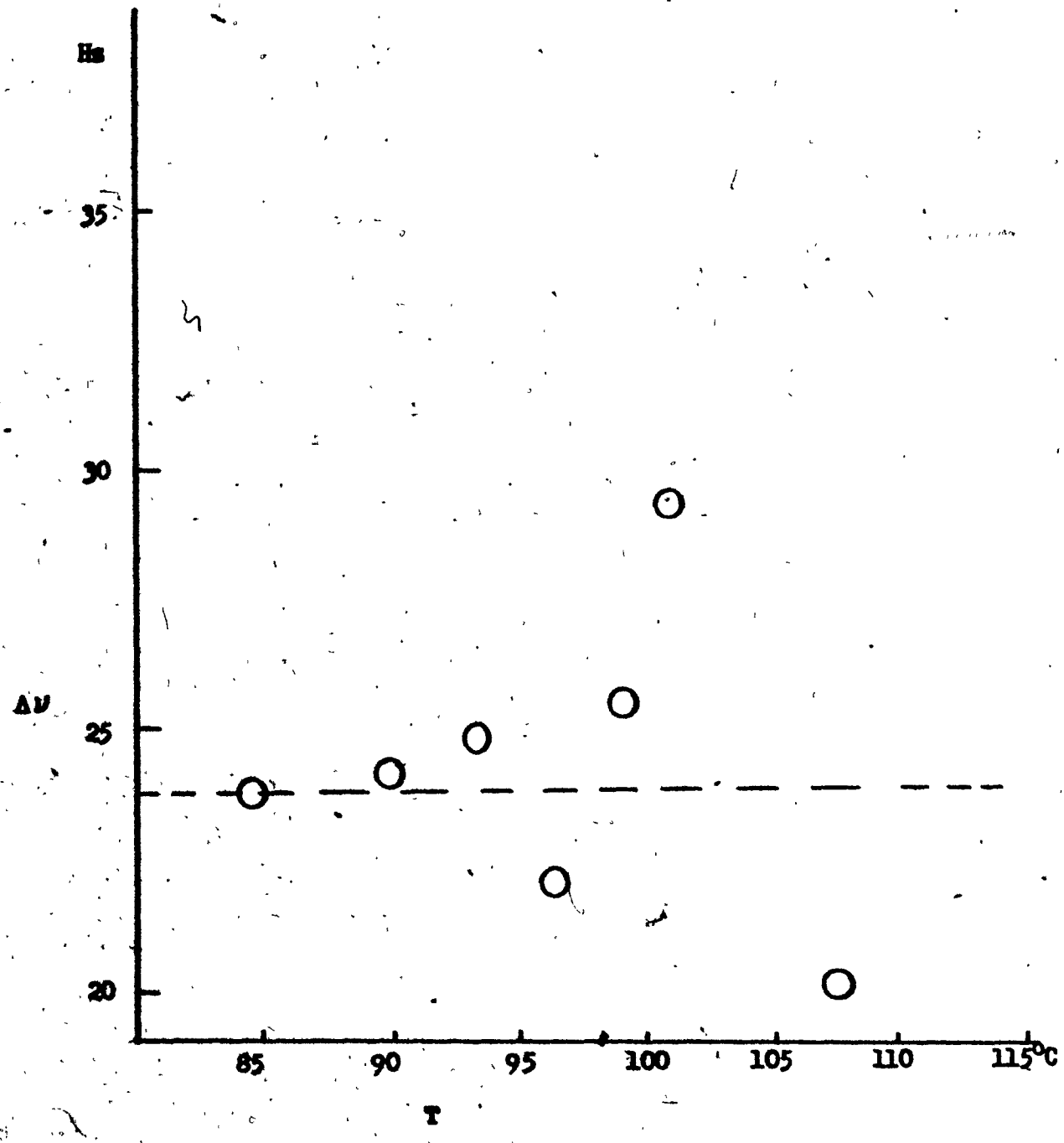

Figure I-11: Temperature Dependence of the Chemical Shift Difference of the C-5 Methyl Protons in 1-(o-Tolyl)-5,5-dimethyl hydantoin, XIII.

DATA AND RESULTS

C-5 Monomethyl Hydantoins :

Line shape analysis data and results for the C-5 monomethyl substituted hydantoins are presented in the following tables and figures. The lifetimes, together with their associated standard errors, were calculated from the best fits of calculated and digitized experimental spectra using the NLINDD2 program. Rate constants are given as reciprocals of lifetime values. For all the hydantoins studied, a triplet for the C-5 methyl protons was observed at low temperatures, instead of the predicted two doublets. Approximate chemical shift differences were estimated from the lowest temperature spectra and the best fit values were obtained by computer simulation, using the regression method. Linewidth parameter values became larger with decreasing temperature, particularly for the compounds with low coalescence temperatures. This affect is attributed to viscosity broadening of the nmr signals at these temperatures.

The ranges of the Arrhenius plots are chosen to present a convenient display, rather than for purposes of comparison. All the Arrhenius plots of C-5 monomethyl hydantoins are drawn on the same scale.

Tables of kinetic data are shown following the experimental data. Arrhenius and Eyring parameters and 90%

confidence limits were calculated by the program ACTPAR. Equilibrium constants were obtained from the ratio of rate constant values for diastereomeric equilibrium.

The appreciable deviation of many points from the regression lines reflects the experimental difficulty in obtaining satisfactory low temperature spectra of the C-5 monomethyl compounds, largely due to overlapping of methyl doublets.

The lifetimes Tau A and Tau B, for the collapse of C-5 methyl signals, are chosen to be the upfield and lowfield peaks in the pmr spectra, respectively.

Table I-2 : Lifetimes and Rotational Rates for 1-(o-Chlorophenyl)-5-methyl hydantoin (V) in Acetone-d_6/DMSO-d_6 Solution at Various Temperatures, Calculated at Constant Chemical Shift Differences

Temperature (oc)	Lifetime (Sec)	Standard Error	Rate Constant (Sec-1)	Line Width (Hz)	Chemical Shift Diff. (Hz)
Tau A, Collapse of C-5 Methyl Signals					
-47.0	0.0386	0.0006	25.9	1.0	6.4
-52.5	0.0471	0.0019	21.2	1.0	6.4
-60.0	0.0777	0.0041	12.9	1.5	6.4
-63.0	0.0939	0.0052	10.6	2.0	6.4
-67.0	0.1135	0.0094	8.8	4.0	6.4
-71.0	0.1500	0.0079	6.7	5.7	6.4
Tau B, Collapse of C-5 Methyl Signals					
-47.0	0.0374	0.0005	26.7	1.0	6.4
-52.5	0.0487	0.0019	20.5	1.0	6.4
-60.0	0.0688	0.0038	14.5	1.5	6.4
-63.0	0.0746	0.0046	13.4	2.0	6.4
-67.0	0.1276	0.0095	7.8	4.0	6.4
-71.0	0.2062	0.0092	4.8	5.7	6.4

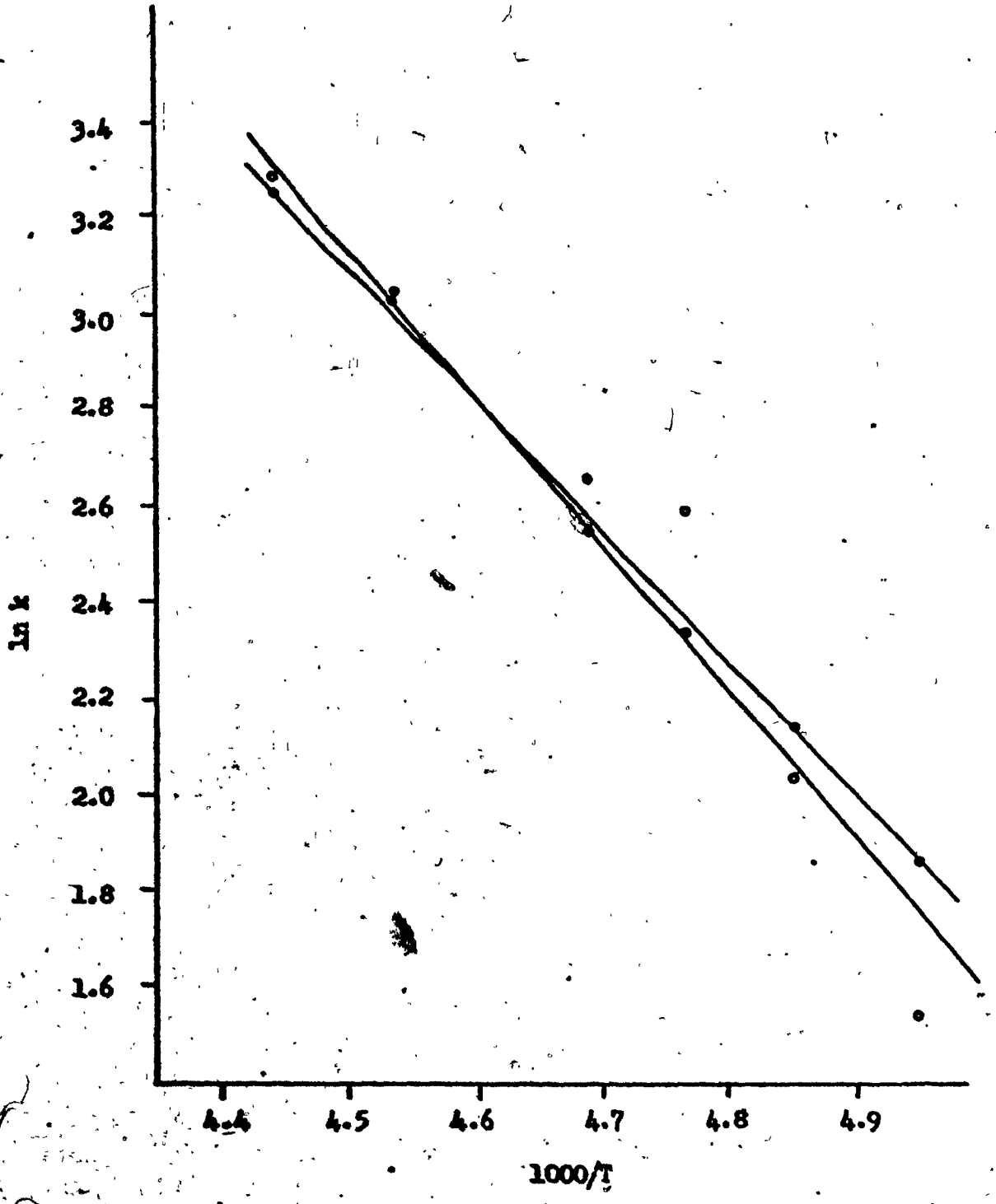

Figure I-12 : Arrhenius Plot for 1-(o-Chlorophenyl)-5-methyl hydantoin (V) in Acetone-d_6/DMSO-d_6 Solution Tau A (•) , Tau B (o).

Table I-3 : Lifetimes, Rotational Rates, and Chemical Shift Differences for 1-(o-Tolyl)-5-methyl hydantoin (VI) in Acetone-d_6/DMSO-d_6 Solution at Various Temperatures.

Temperature (°C)	Lifetime (Sec)	Standard Error	Rate Constant (Sec^{-1})	Line Width (Hz)	Chemical Shift Diff. (Hz)
		Tau A, Collapse of C-5 Methyl Signals			
-18.5	0.0197	0.0004	50.8	1.0	8.5
-22.0	0.0357	0.0006	28.0	1.0	8.4
-25.5	0.0888	0.0036	11.3	1.0	8.3
-34.0	0.0780	0.0025	12.8	1.0	8.7
-37.5	0.0920	0.0051	10.9	1.0	8.3
-40.0	0.0851	0.0026	11.7	1.0	8.8
-43.5	0.1058	0.0056	9.4	1.0	8.0
-47.0	0.1441	0.0070	6.9	1.0	8.5
-52.5	0.1243	0.0055	8.1	1.0	8.8
		Tau B, Collapse of C-5 Methyl Signals			
-18.5	0.0213	0.0005	46.9	1.0	8.5
-22.0	0.0332	0.0006	30.1	1.0	8.4
-25.5	0.0514	0.0035	19.5	1.0	8.3
-34.0	0.0560	0.0028	17.9	1.0	8.7
-37.5	0.0760	0.0062	13.2	1.0	8.3
-40.0	0.0580	0.0030	17.2	1.0	8.8
-43.5	0.0849	0.0051	11.8	1.0	8.0
-47.0	0.0938	0.0098	10.7	1.0	8.5
-52.5	0.0971	0.0068	10.3	1.0	8.8

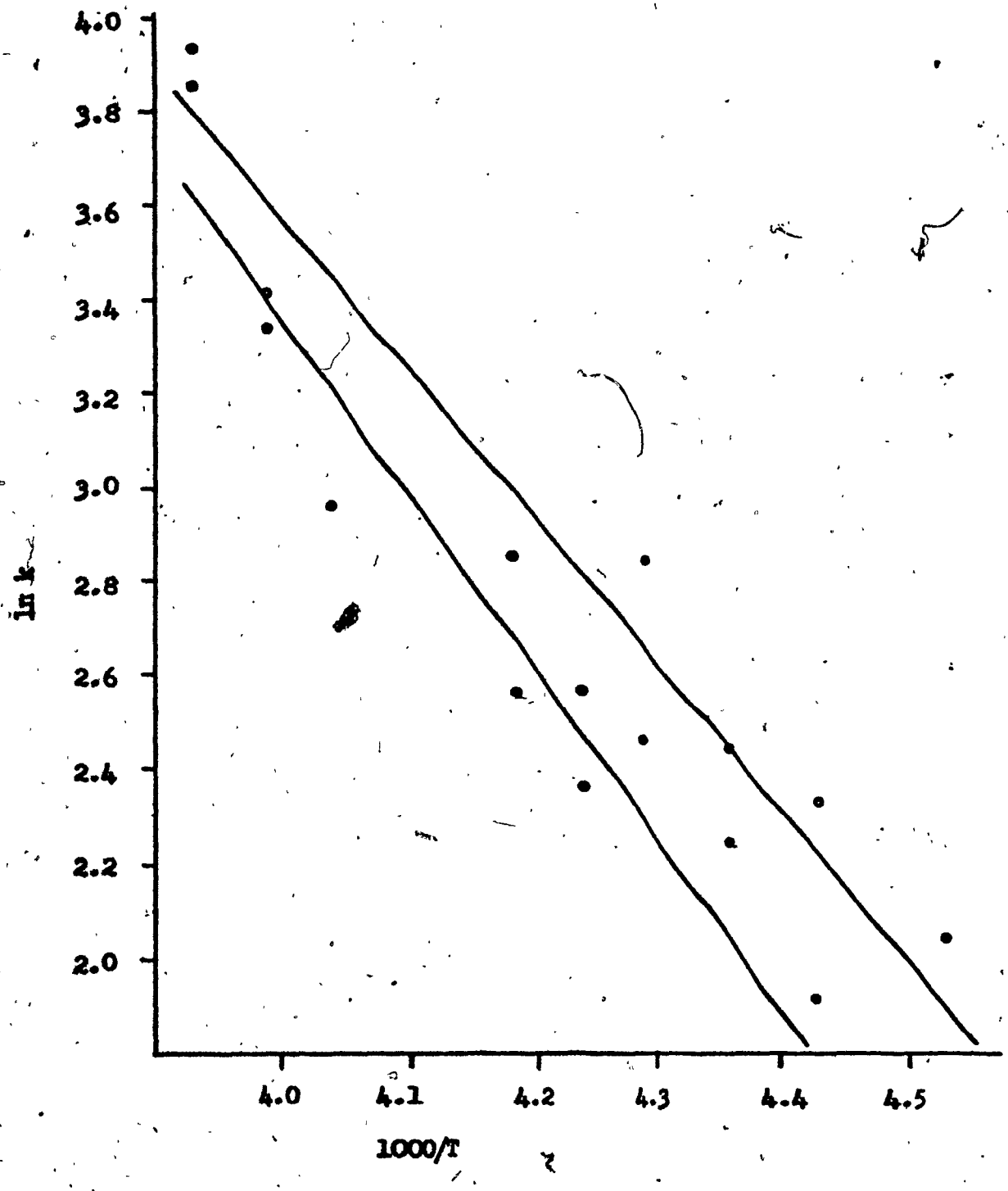

Figure I-13 : Arrhenius Plot for 1-(o-Tolyl)-5-methyl hydantoin (VI) in Acetone-d_6/DMSO-d_6 Solution. Tau A (●), Tau B (○)

Table I-4 = Lifetimes and Rotational Rates for 1-(α-Naphthyl)-5-methyl hydantoin (VII) in Acetone-d_6/DMSO-d_6 Solution at Various Temperatures, Calculated at Constant Chemical Shift Difference.

Temperature (°C)	Lifetime (Sec)	Standard Error	Rate Constant (Sec-1)	Line Width (Hz)	Chemical Shift Diff. (Hz)
Term A, Collapse of C-5 Methyl Signals					
-14.0	0.0651	0.0017	15.4	1.2	5.4
-15.5	0.0705	0.0017	14.2	1.2	5.4
-22.5	0.0830	0.0032	12.0	1.2	5.4
-23.8	0.0893	0.0040	11.2	1.2	5.4
-26.0	0.1103	0.0068	8.9	1.2	5.4
-29.8	0.1620	0.0094	6.2	1.2	5.4
-37.5	0.1958	0.0120	5.1	1.2	5.4
-41.2	0.2518	0.0141	3.9	1.2	5.4
Term B, Collapse of C-5 Methyl Signals					
-14.0	0.0554	0.0015	18.0	1.2	5.4
-15.5	0.0529	0.0014	18.9	1.2	5.4
-22.5	0.0701	0.0029	14.3	1.2	5.4
-23.8	0.0805	0.0037	12.4	1.2	5.4
-26.0	0.0902	0.0060	10.9	1.2	5.4
-29.8	0.1165	0.0074	8.6	1.2	5.4
-37.5	0.1510	0.0109	6.6	1.2	5.4
-41.2	0.1821	0.0110	5.5	1.2	5.4

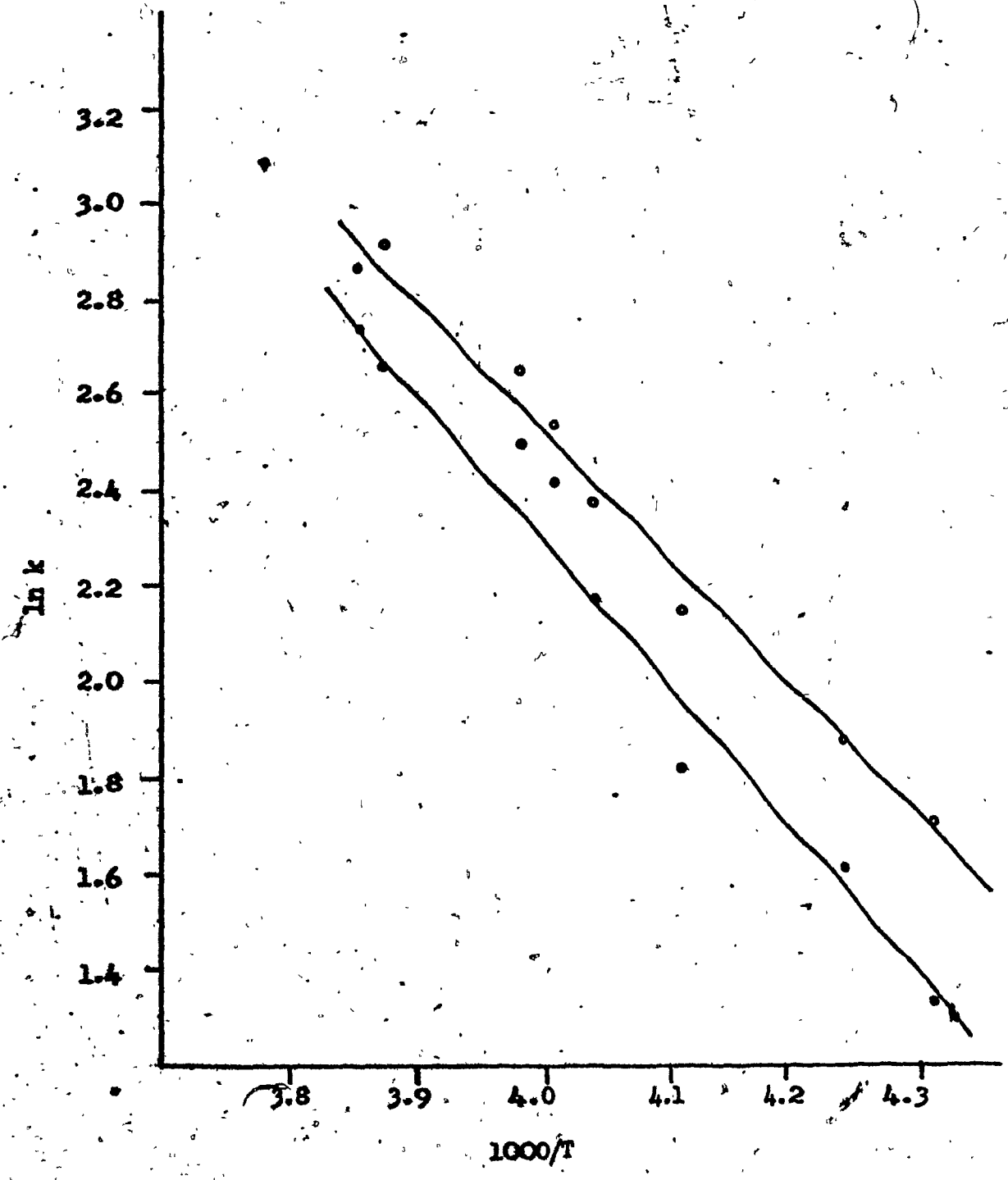

Figure I-14: Arrhenius Plot for 1-(α-Naphthyl)-5-methyl hydantoin (VII) in Acetone-d_6/DMSO-d_6 Solution Tau A (o), Tau B (o).

Table I-5 : Lifetimes, Rotational Rates, and Chemical Shift Difference for 1-(2,3-Dimethylphenyl)-5-methyl hydantoin (VIII) in Acetone-d_6/DMSO-d_6 Solution at Various Temperatures.

Temperature (°C)	Lifetime (Sec)	Standard Error	Rate Constant (Sec^{-1})	Line Width (Hz)	Chemical Shift Diff. (Hz)
Tau A, Collapse of C-5 Methyl Signals					
18.5	0.0259	0.0007	38.6	1.0	6.3
12.0	0.0370	0.0008	27.0	1.0	6.3
9.2	0.0409	0.0009	24.4	1.0	6.3
4.5	0.0611	0.0018	16.4	1.1	6.3
-0.2	0.0957	0.0020	10.5	1.1	6.3
-3.8	0.1186	0.0033	8.4	1.1	6.6
-8.9	0.1757	0.0083	5.7	1.1	6.5
-13.3	0.2218	0.0069	4.5	1.1	6.5
-14.8	0.2663	0.0154	3.8	1.1	6.5
Tau B, Collapse of C-5 Methyl Signals					
18.5	0.0297	0.0008	33.7	1.0	6.3
12.0	0.0413	0.0009	24.2	1.0	6.3
9.2	0.0471	0.0010	21.3	1.0	6.3
4.5	0.0537	0.0016	18.6	1.1	6.3
-0.2	0.0642	0.0019	15.6	1.1	6.3
-3.8	0.0719	0.0025	13.9	1.1	6.6
-8.9	0.1223	0.0070	8.2	1.1	6.5
-13.3	0.1232	0.0050	8.1	1.1	6.5
-14.8	0.1594	0.0118	6.3	1.1	6.5

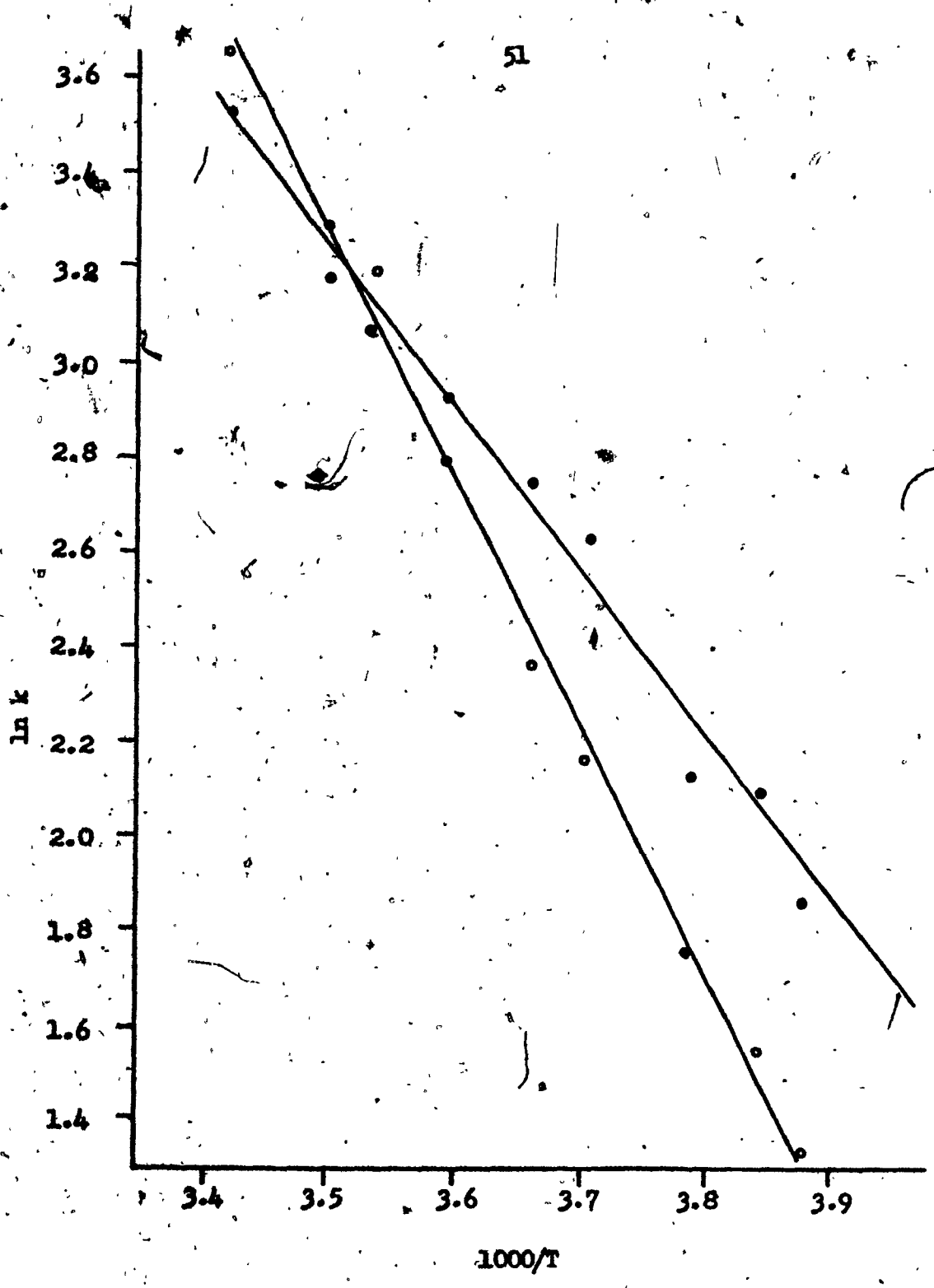

Figure I-15 : Arrhenius Plot for 1-(2,3-Dimethylphenyl)-5-methyl hydantoin (VIII) in Acetone-d_6/DMSO-d_6 Solution. Tau A (o), Tau B (•).

Table I-6 : Lifetimes and Rotational Rates for 1-(2,3-Dimethylphenyl)-5-methyl hydantoin (VIII) in Pyridine Solution at Various Temperatures, Calculated at Constant Chemical Shift Difference.

Temperature (°C)	Lifetime (Sec)	Standard Error	Rate Constant (Sec-1)	Line Width (Hz)	Chemical Shift Diff. (Hz)
Tau A, Collapse of C-5 Methyl Signals					
17.2	0.0280	0.0008	35.7	0.9	7.6
12.2	0.0310	0.0005	32.3	0.9	7.6
8.5	0.0327	0.0007	30.6	0.9	7.6
5.0	0.0394	0.0004	25.4	0.9	7.6
0.6	0.0442	0.0009	22.6	0.9	7.6
-2.5	0.0488	0.0009	20.5	1.0	7.6
-8.8	0.0830	0.0017	12.0	1.0	7.6
-13.9	0.0833	0.0021	12.0	1.0	7.6
-15.7	0.0824	0.0018	12.1	1.1	7.6
-18.5	0.0874	0.0041	11.4	1.1	7.6
Tau B, Collapse of C-5 Methyl Signals					
17.2	0.0283	0.0008	35.3	0.9	7.6
12.2	0.0297	0.0005	33.7	0.9	7.6
8.5	0.0329	0.0007	30.4	0.9	7.6
5.0	0.0370	0.0004	27.0	0.9	7.6
0.6	0.0424	0.0009	23.6	0.9	7.6
-2.5	0.0473	0.0009	21.1	1.0	7.6
-8.8	0.0585	0.0016	17.1	1.0	7.6
-13.9	0.0623	0.0019	16.0	1.0	7.6
-15.7	0.0653	0.0017	15.3	1.1	7.6
-18.5	0.0703	0.0041	14.2	1.1	7.6

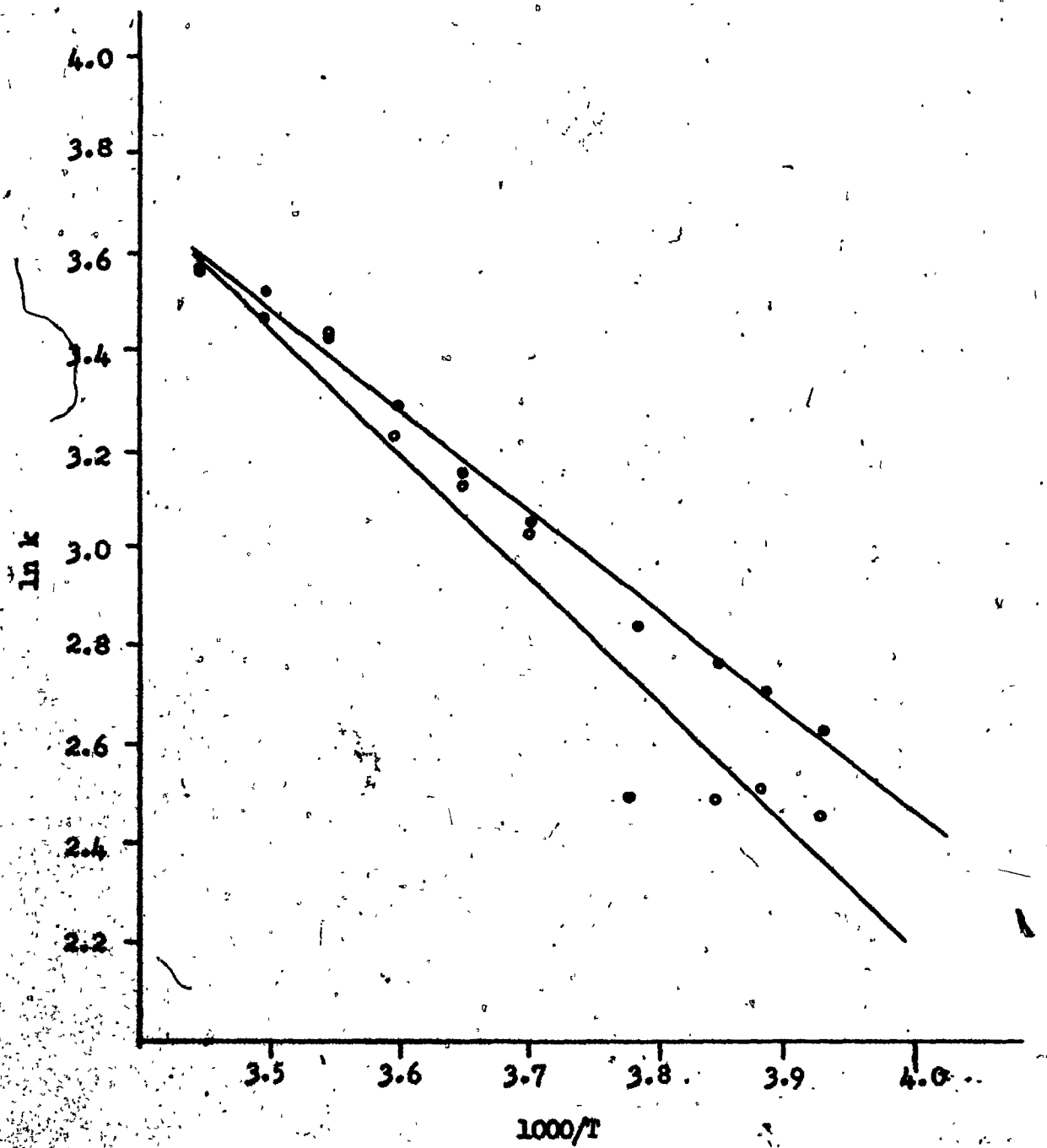

Figure I-16 : Arrhenius Plot for 1-(2,3-Dimethylphenyl)-3-methyl hydantoin (VIII) in Pyridine Solution.

Tau A (o), Tau B (●).

Table I-7 : Kinetic Parameters and Equilibrium Constants for Rotation in Some 1-Aryl-5-methyl Hydantoins, Calculated at Coalescence Temperatures[a]

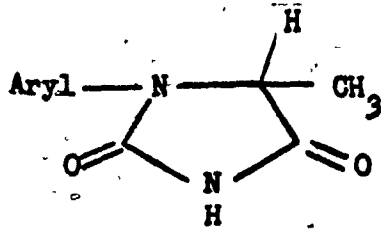

VII Aryl = α-Naphthyl

VIII Aryl = 2,3-Dimethylphenyl

Compound	Solvent	Coales. Temp. (°C)		Ea (kcal/mol)	$\Delta H^{\neq}$ (kcal/mol)	$\Delta S^{\neq}$ (e.u.)	$\Delta G^{\neq}$ (kcal/mol)	τ (sec)	Keq
VII	Acetone-d_6/ DMSO-d_6	-24.0	τ_a	6.1±1.0	5.6±1.0	-31±4	13.6±0.1	0.102	1.25±0.20
			τ_b	5.6±0.6	5.1±0.6	-33±2	13.2±0.1	0.082	
VIII	Acetone-d_6/ DMSO-d_6	-0.2	τ_a	10.7±0.6	10.2±0.6	-16±2	14.6±0.1	0.087	1.26±0.20
			τ_b	7.1±0.8	6.6±0.8	-29±3	14.5±0.1	0.069	
VIII	Pyridine	-4.0	τ_a	5.3±0.7	4.8±0.7	-35±3	14.1±0.1	0.055	1.15±0.20
			τ_b	4.0±0.3	3.5±0.3	-39±1	14.1±0.1	0.048	

[a] Errors are 90% confidence limits

Table I-7 : (Cont.)

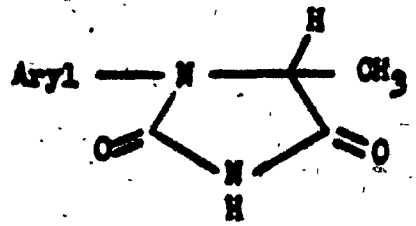

V Aryl = o-Chlorophenyl

VI Aryl = o-Tolyl

Compound	Solvent	Coales. Temp. (°C)		Ea (kcal/mol)	$\Delta H^{\ddagger}$ (kcal/mol)	$\Delta S^{\ddagger}$ (e.u.)	$\Delta G^{\ddagger}$ (kcal/mol)	τ (sec)	Keq
VI	Acetone-d_6/ DMSO-d_6	-32.0	τ_a	5.2±2.3	4.7±2.3	-33±6	12.7±0.1	0.062	1.26±0.20
			τ_b	4.5±1.4	4.0±1.4	-36±10	12.6±0.1	0.049	
V	Acetone-d_6/ DMSO-d_6	-63.0	τ_a	5.2±0.4	4.4±0.4	-30±2	11.1±0.1	0.092	0.96±0.20
			τ_b	6.1±1.7	5.7±1.7	-26±8	11.2±0.1	0.096	

C-5 Dimethyl Hydantoins :

The following tables and figures give the line shape analysis data and results for the C-5 dimethyl substituted hydantoins. The NLINGH program was used to obtain the lifetimes and the standard errors from the best fit spectra. Chemical shift differences were measured at room temperature, where sufficiently minimum enantiomeric exchange process was in progress. The quality of the fitting is better than in the case of the C-5 monomethyl hydantoins. Since all the C-5 dimethyl hydantoins coalesced at high temperatures, more accurate line width and chemical shift parameters were obtained.

The Arrhenius plots, Arrhenius and Eyring parameters and 90% confidence limits were calculated by the program ACTPAR. All the Arrhenius plots for the C-5 dimethyl hydantoins are drawn on the same scale.

Table I-8 : Lifetimes and Rotational Rates for 1-(o-Chlorophenyl)-5,5-dimethyl hydantoin (XII) in DMSO-d_6 Solution at Various Temperatures, Calculated at a Line Width of 1.0 Hz and Constant Chemical Shift Difference

Temperature (°C)	Lifetime (Sec)	Standard Error	Rate Constant (Sec-1)	Chemical Shift Diff. (Hz)
	Average of Tau A and Tau B for the Collapse of the C-5 Methyl Signals			
48.0	0.0845	0.0024	11.8	22.5
53.8	0.0645	0.0020	15.5	22.5
59.3	0.0460	0.0010	21.7	22.5
61.0	0.0391	0.0005	25.6	22.5
63.0	0.0324	0.0005	30.9	22.5
68.7	0.0236	0.0004	42.4	22.5
74.5	0.0159	0.0002	62.9	22.5
81.0	0.0103	0.0002	97.1	22.5
85.5	0.0084	0.0002	119.1	22.5
94.5	0.0055	0.0001	181.8	22.5

Table I-9 : Lifetimes and Rotational Rates for 1-(o-Chlorophenyl)-5,5-dimethyl hydantoin (XII) in pyridine Solution at Various Temperatures, Calculated at a Line Width of 1.0 Hz and Constant Chemical Shift Difference.

	Average of Tau A and Tau B for the Collapse of the C-5 Methyl Signals			
35.3	0.1008	0.0043	9.9	25.6
41.0	0.0738	0.0034	13.5	25.6
44.5	0.0626	0.0010	15.9	25.6
49.9	0.0465	0.0007	21.5	25.6
53.2	0.0356	0.0003	28.1	25.6
56.0	0.0307	0.0004	32.6	25.6
58.0	0.0272	0.0001	36.8	25.6
61.5	0.0200	0.0001	50.0	25.6
66.0	0.0150	0.0002	66.7	25.6
71.5	0.0120	0.0002	83.3	25.6

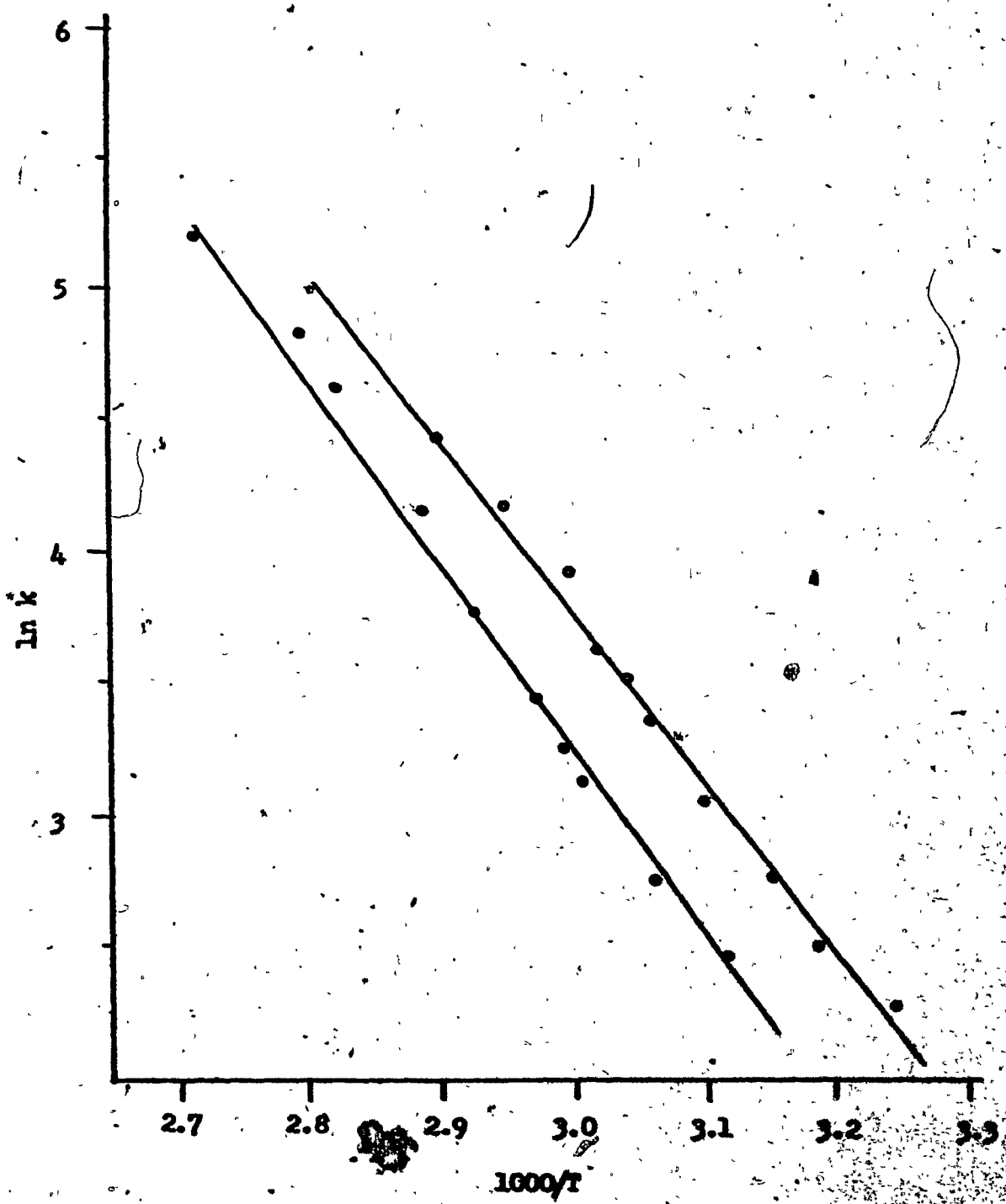

Figure I-17 : Arrhenius Plot for 1-(p-Chlorophenyl)-5,5-dimethyl hydantoin (XII) in DMSO-d_6 (●) and Pyridine (○) Solutions.

Table I-10: Lifetimes and Rotational Rates for 1-(o-Tolyl)-5,5-dimethyl hydantoin (XIII) in DMSO-d_6 Solution at Various Temperatures, Calculated at a Line Width of 1.1 Hz and Constant Chemical Shift Difference.

Temperature (°C)	Lifetime (Sec)	Standard Error	Rate Constant (Sec-1)	Chemical Shift Diff. (Hz)
Average of Tau A and Tau B for the Collapse of the C-5 methyl Signals				
67.5	0.0638	0.0022	15.7	27.6
72.0	0.0452	0.0011	22.1	27.6
77.5	0.0334	0.0010	29.9	27.6
81.5	0.0271	0.0004	36.9	27.6
85.0	0.0215	0.0004	46.5	27.6
88.5	0.0174	0.0002	57.8	27.6
91.5	0.0134	0.0002	74.6	27.6
97.2	0.0094	0.0001	106.4	27.6
103.2	0.0068	0.0001	147.1	27.6
110.5	0.0046	0.0001	217.4	27.6

Table I-11: Lifetimes and Rotational Rates for 1-(o-Tolyl)-5,5-dimethyl hydantoin (XIII) in Pyridine Solution at Various Temperatures, Calculated at a Line Width of 1.4 Hz and Constant Chemical Shift Difference

Temperature (°C)	Lifetime (Sec)	Standard Error	Rate Constant (Sec-1)	Chemical Shift Diff. (Hz)
Average of Tau A and Tau B for the Collapse of the C-5 Methyl Signals				
53.0	0.0698	0.0018	14.3	27.2
59.0	0.0552	0.0011	18.1	27.2
64.5	0.0456	0.0007	21.9	27.2
69.2	0.0341	0.0004	29.3	27.2
75.0	0.0247	0.0002	40.5	27.2
79.5	0.0190	0.0002	52.6	27.2
84.0	0.0140	0.0002	71.4	27.2
90.3	0.0100	0.0002	100.0	27.2
96.0	0.0070	0.0001	142.9	27.2
102.0	0.0051	0.0001	196.1	27.2
107.0	0.0037	0.0001	270.3	27.2
112.8	0.0031	0.0001	322.6	27.2

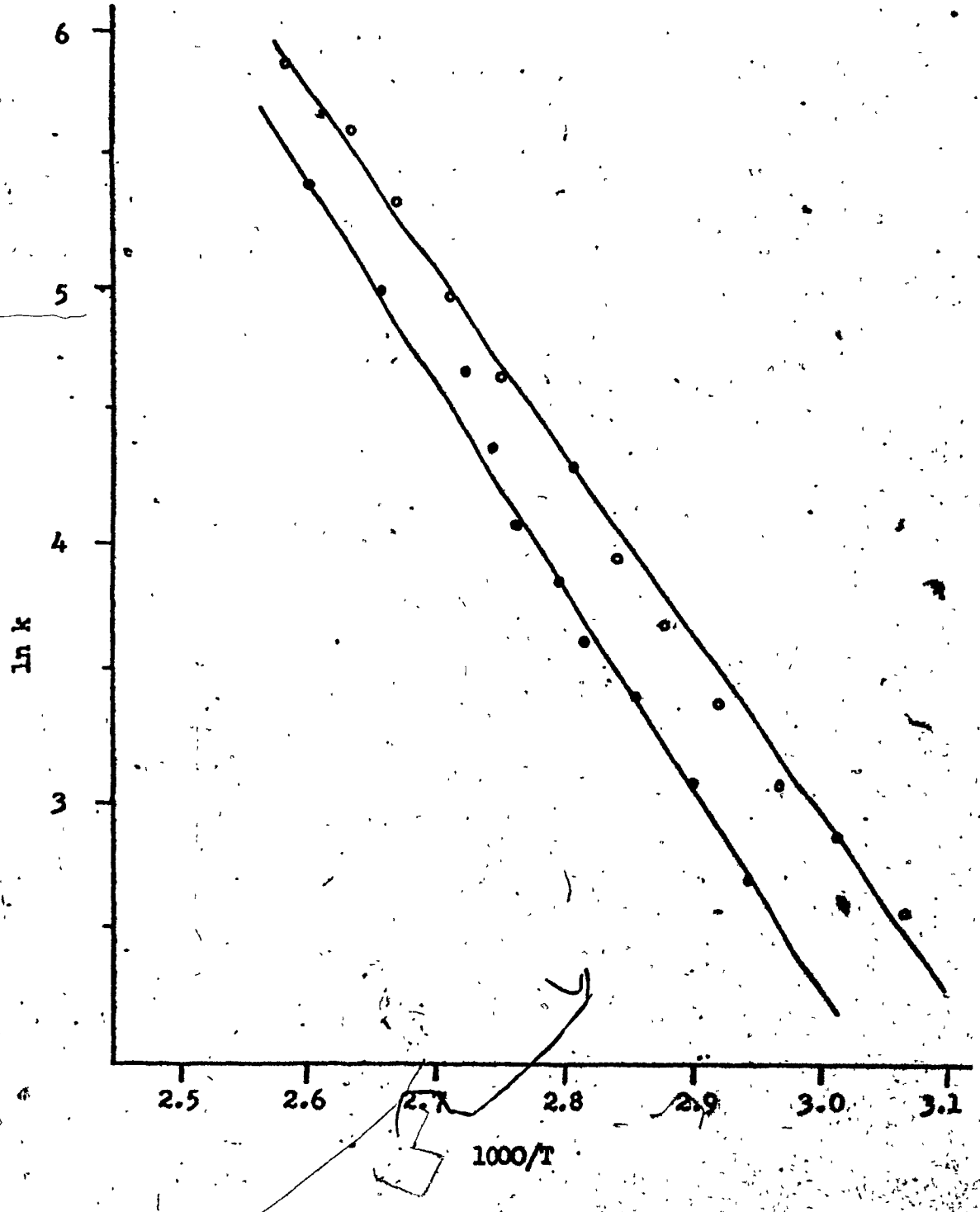

Figure I-18 : Arrhenius Plot for 2-(o-Tolyl)-5,5-dimethyl hydantoin (XIII) in DMSO-d_6 (•) and Pyridine (○) Solutions

Table I-12 : Lifetimes and Rotational Rates for 1-(α-Naphthyl)-5,5-dimethyl hydantoin (XIV) in DMSO-d_6 Solution at Various Temperatures, Calculated at a Line Width of 1.0 Hz and Constant Chemical Shift Difference.

Temperature (°C)	Lifetime (Sec)	Standard Error	Rate Constant (Sec-1)	Chemical Shift Diff. (Hz)
Average of Tau A and Tau B for the Collapse of the C-5 Methyl Signals				
83.0	0.0882	0.0027	11.3	32.8
92.0	0.0480	0.0009	20.8	32.8
105.0	0.0267	0.0004	37.6	32.8
113.0	0.0154	0.0001	64.9	32.8
122.0	0.0090	0.0001	111.1	32.8
130.0	0.0053	0.0001	188.7	32.8
140.0	0.0035	0.0001	285.7	32.8
149.0	0.0023	0.0001	434.8	32.8

Table I-13 : Lifetimes and Rotational Rates for 1-(α-Naphthyl)-5,5-dimethyl hydantoin (XIV) in 2-Chloropyridine Solution at Various Temperatures, Calculated at a Line Width of 1.0 Hz and Constant Chemical Shift Difference.

Temperature (°C)	Lifetime (Sec)	Standard Error	Rate Constant (Sec-1)	Chemical Shift Diff. (Hz)
Average of Tau A and Tau B for the Collapse of the C-5 Methyl signals				
86.0	0.0521	0.0007	19.2	32.2
93.0	0.0378	0.0011	26.5	32.2
97.5	0.0287	0.0006	38.8	32.2
106.2	0.0174	0.0003	57.5	32.2
110.0	0.0140	0.0001	71.4	32.2
113.0	0.0113	0.0001	88.5	32.2
117.5	0.0085	0.0001	117.6	32.2
121.0	0.0065	0.0001	153.8	32.2
127.0	0.0052	0.0001	196.1	32.2

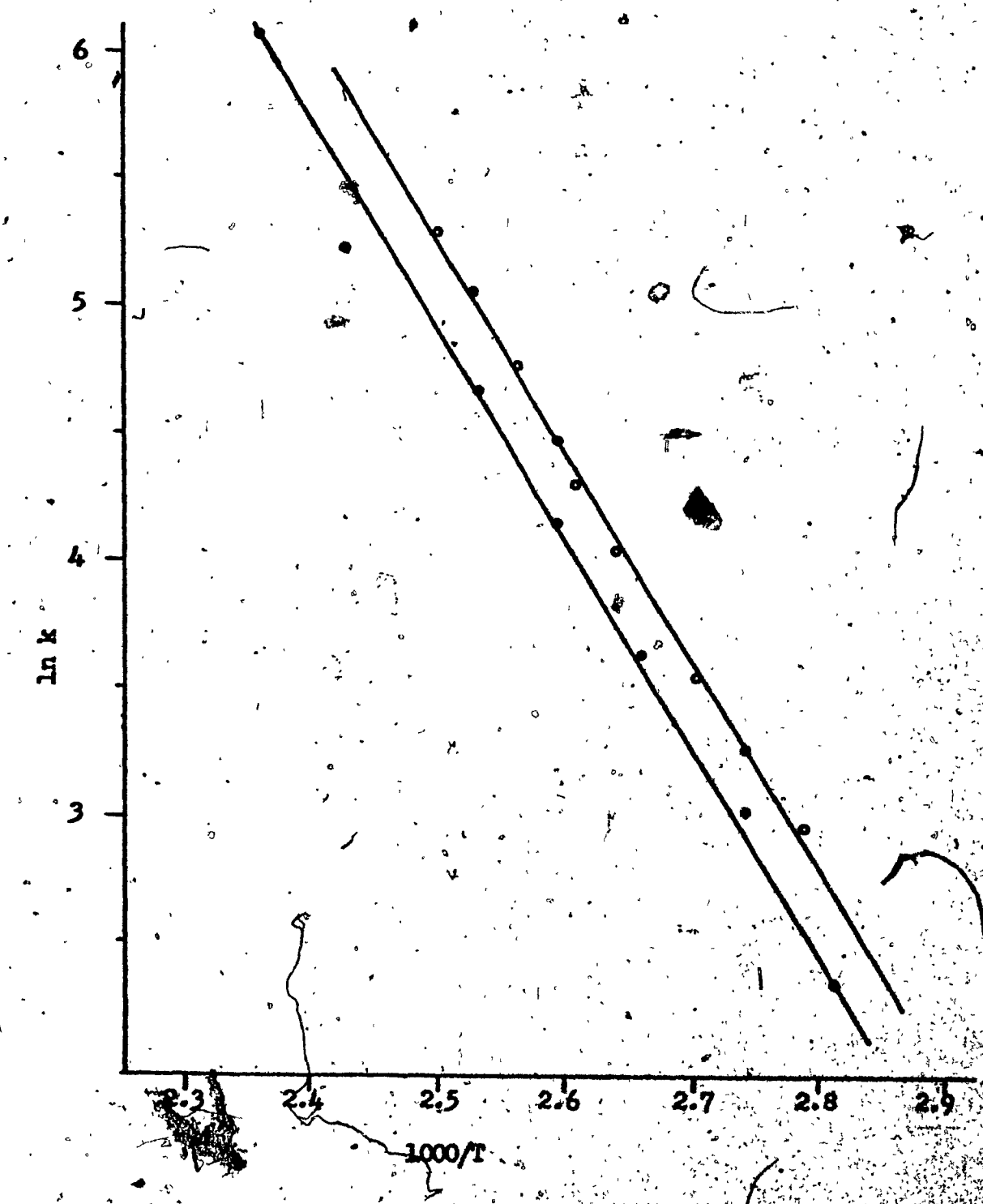

Figure I-19 : Arrhenius Plot for 1-(α-Naphthyl)-5,5-dimethyl hydantoin (XIV) in DMSO-d$_6$ (•) and 2-Chloro-pyridine (o) Solutions.

Table I-14 : Lifetimes and Rotational Rates for 1-(2,3-Dimethylphenyl)- 5,5-dimethyl hydantoin (XVIII) in DMSO-d_6 Solution at Various Temperatures, Calculated at a Line Width of 1.0 Hz and Constant Chemical Shift Difference.

Temperature (Sec)	Lifetime (Sec)	Standard Error	Rate Constant (Sec-1)	Chemical Shift Diff. (Hz)
Average of Tau A and Tau B for the Collapse of the C-5 Methyl Signals				
115.2	0.0635	0.0031	15.7	25.0
121.5	0.0526	0.0017	19.0	25.0
126.5	0.0404	0.0012	24.7	25.0
131.5	0.0283	0.0004	35.3	25.0
136.5	0.0221	0.0002	45.2	25.0
137.8	0.0214	0.0002	46.7	25.0
142.0	0.0173	0.0002	57.8	25.0
147.5	0.0146	0.0001	68.5	25.0
153.0	0.0106	0.0001	97.1	25.0
159.5	0.0078	0.0001	128.2	25.0
165.0	0.0062	0.0001	161.3	25.0

Table I-15 : Lifetimes and Rotational Rates for 1-(2,3-Dimethylphenyl)- 5,5-dimethyl hydantoin (XVIII) in 2-Chloropyridine Solution at Various Temperatures, Calculated at a Line Width of 1.1 Hz and Constant Chemical Shift Difference.

Temperature (°C)	Lifetime (Sec)	Standard Error	Rate Constant (Sec-1)	Chemical Shift Diff. (Hz)
Average of Tau A and Tau B for the Collapse of the C-5 Methyl Signals				
118.0	0.0455	0.0012	21.9	26.0
125.5	0.0319	0.0007	31.3	26.0
133.0	0.0220	0.0007	45.4	26.0
140.5	0.0168	0.0006	59.9	26.0
145.0	0.0132	0.0003	75.8	26.0
147.5	0.0117	0.0001	85.5	26.0
153.5	0.0087	0.0001	114.9	26.0
155.5	0.0080	0.0001	125.0	26.0

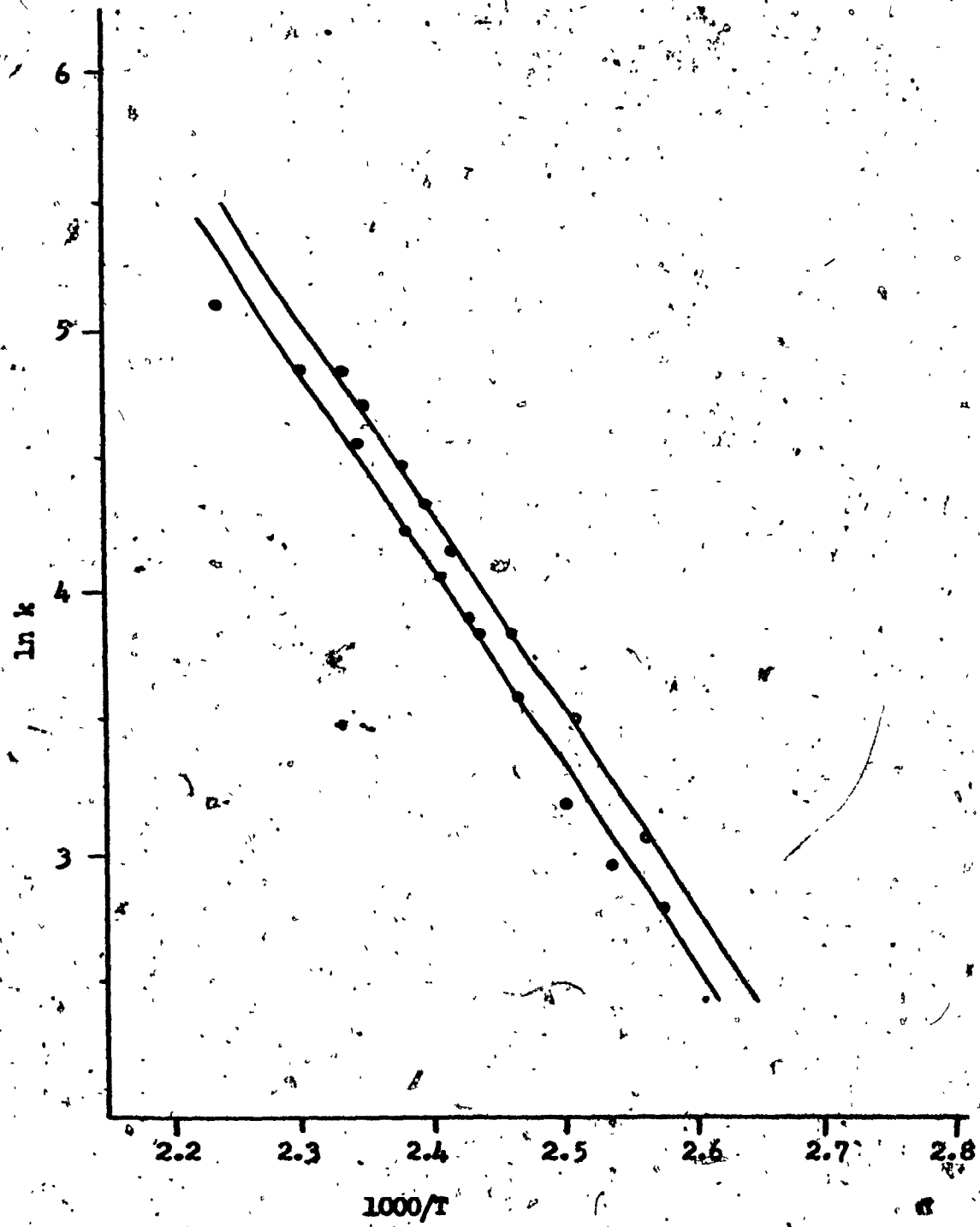

Figure I-20 : Arrhenius Plot for 1-(2,3-Dimethylphenyl)-5,5-dimethyl hydantoin (XVIII) in DMSO-d_6 (•) and 2-Chloro-Pyridine (o) Solutions.

Table I-16: Kinetic Parameters for Rotation in some 1-Aryl-5,5-dimethyl Hydantoins, Calculated at 100°C.[a]

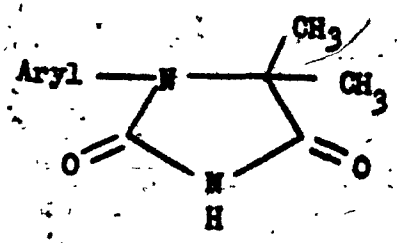

XII Aryl = o-Chlorophenyl

XIII Aryl = o-Tolyl

Compound	Solvent	E_a (kcal/mol)	$\Delta H^{\neq}$ (kcal/mol)	$\Delta S^{\neq}$ (e.u.)	$\Delta G^{\neq}$ (kcal/mol)	τ (sec)
XII	Pyridine	12.9±0.8	12.2±0.8	-14.7±2.3	17.7±0.1	0.0029
	DMSO-d_6	14.4±0.6	13.7±0.6	-11.2±1.7	17.9±0.1	0.0039
XIII	Pyridine	13.8±0.7	13.1±0.7	-13.8±2.0	18.2±0.1	0.0059
	DMSO-d_6	16.0±0.5	15.2±0.5	- 8.6±1.4	18.5±0.1	0.0083

[a]Errors are 90% confidence limits.

Table I-16 : (Cont.)

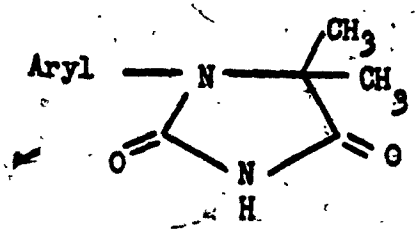

XIV Aryl = α-Naphthyl

XVIII Aryl = 2,3-Dimethylphenyl

Compound	Solvent	E_a (kcal/mol)	$\Delta H^{\neq}$ (kcal/mol)	$\Delta S^{\neq}$ (e.u.)	$\Delta G^{\neq}$ (kcal/mol)	τ (sec)
XIV	o-Chloropyridine	16.6±0.7	15.8±0.7	-9.2±1.9	19.2±0.1	0.024
	DMSO-d_6	16.7±0.7	16.0±0.7	-9.3±1.9	19.4±0.1	0.031
XVIII	o-Chloropyridine	15.4±0.6	14.6±0.6	-15.6±1.4	20.4±0.1	0.121
	DMSO-d_6	16.3±0.7	15.5±0.7	-13.7±1.6	20.7±0.1	0.163

DISCUSSION

The study of hindered rotation about the aryl C-N bond in 1-aryl substituted hydantoins by pmr line shape analysis has yielded stereochemical information which complements that obtained from earlier studies of 3-aryl substituted hydantoins. Differences in the nature of the steric interactions between the heterocyclic moiety and the ortho-substituted aryl group when the latter is in the 1- and the 3-position significantly affect the thermodynamic parameters calculated for the restricted rotational processes. Information obtained from the 1-aryl series has proven useful in clarifying the interpretation of some of the results of the study of the 3-aryl series, such as the question of the relative effective sizes of the ortho chloro and ortho methyl substituents. As a result of this study, new information on steric and electronic influences on conformations and on rotational barriers, on anisotropic shielding, and on solvent effects, has been obtained.

In the 3-aryl hydantoins the bulky ortho substituent on the aryl group must pass the C-2 or the C-4 carbonyl group in the transition state for internal rotation. The steric component of the rotational barrier must arise from interaction between the carbonyl oxygen atoms and the aryl group. In the previous studies of Fehlner,[12] Granata,[15] and Giles,[14] the free energies of activation for internal

rotation were found to be about 20 kcal/mol for 3-aryl hydantoins with bulky ortho substituents. These studies have demonstrated that changes in the bulkiness of the C-5 substituent have little effect on the rotational barriers.

In contrast, barriers to restricted rotation about the C-N bond in 1-aryl hydantoins are significantly affected by the steric requirements of the C-5 substituents. This is expected, since the C-5 substituents in 1-aryl hydantoins are capable of interacting directly with the aryl group. Compounds I, II, III and IV (Table I-I), in which the C-5 positions are unsubstituted, failed to exhibit individual signals from the enantiomeric C-5 protons in their pmr spectra, even at temperatures as low as -75°C. Although it is possible that the failure to observe splitting of the methylene proton signal resulted from accidental chemical shift equivalence, it is considered more probable that rotation about the C-N bond was fast enough on the nmr time scale at this temperature that time averaged spectra were observed. Similar results were found for compounds IX, X, XI in which the C-5 substituent is a phenyl group. No distinguishable spectra of the diastereomeric rotational isomers were observable at low temperatures. It appears that the planar character of the 1-phenyl group enables it to take up such a conformation in the transition state for the rotation of 1-phenyl group, that steric interaction between the 5-phenyl and the

N-1 aryl groups is small. Thus a 5-phenyl substituent does not behave as a bulky group in this series. Although an α-naphthyl group has been shown to exert substantial steric barriers to C-N bond rotation in earlier studies, the two compounds in this series containing 1-(α-naphthyl) groups, IV and XI, failed to show any evidence for restricted rotation at the lowest attainable temperatures.

1-Aryl-5-methyl hydantoins:

In contrast to those compounds unsubstituted, or carrying a phenyl group in the 5-position, the 1-aryl-5-methyl hydantoins, V, VI, VII, and VIII, exhibited restricted internal rotation. In all cases, time averaged spectra were observed at normal probe temperatures. As the temperatures of the samples were lowered, the spectra broadened, passed through a coalescence region, and eventually were resolvable into the superimposed spectra of the two diastereomeric rotational isomers. Temperature dependent spectra arising from the 5-methyl group of VI, VII, and VIII are shown in Figures I-3 to I-6. The kinetic parameters calculated for these compounds are presented in Table I-7. Difficulty in obtaining accurate measurements of chemical shifts, due to overlapping of methyl doublets, caused large errors in the determination of all the activation parameters except the free energies of activation, which are rather insensitive to errors of this origin. In spite of this problem, some

significant correlations were obtained, and are discussed later. The $\Delta G^{\ddagger}$ values calculated at the coalescence points for this group of compounds ranged from 11.1 to 13.3 kcal/mol in the expected order of increasing bulkiness of the aryl substituent, from ortho-chlorophenyl to α-naphthyl.

1-Aryl-5,5-dimethyl hydantoins:

With one exception the C-5 dimethyl compounds exhibited substantially larger barriers to internal rotation than did the monomethyl analogues. Internal rotation was sufficiently slow that doublets were observed for the diastereotopic methyl group signals when the samples were at normal probe temperatures. These doublets collapsed to singlets as time averaging of the environments of the methyl groups became significant at higher probe temperatures. The coalescence temperatures of the compounds XII, XIII, XIV, and XVIII, in which the aryl groups are o-tolyl, o-chlorophenyl, α-naphthyl, and 2,3-dimethylphenyl were found to be 69.0°C, 87.5°C, 114°C, and 138°C respectively, in DMSO-d_6 solutions. The kinetic parameters were calculated for an average temperature of 100°C and are given in Table I-16. These compounds exhibit free energies of activation for restricted rotation of 18-21 kcal/mol. Variations in the values of $\Delta G^{\ddagger}$ within this group are consistent with the expected steric effects of the aryl groups. The relative effective sizes of

chloro and methyl subatituents, which differ from those in 3-aryl series, are discussed later. The steric hindrance to internal rotation produced by the α-naphthyl substituent is found to be higher than that of o-chloro or o-methyl substituents, probably due to an increase on the effective bulkiness of the aryl substituent. However, the 2,3-dimethylphenyl substituent, which exerts a buttressing effect as discussed later, showed higher free energies of activation for restricted rotation.

In general, the barriers to internal rotation in 1-aryl-5,5-dimethyl hydantoins are similar in magnitude to those in 3-aryl hydantoips.

In the case of 1-(o-fluorophenyl)-5,5-dimethyl hydantoin, XVI, the diastereotopic C-5 methyl groups did not exhibit any doubling of signals, even at low temperatures. Fluorine is the smallest ortho substituent other than hydrogen in the series, having a van der Waals radius of 1.35 A°.[27] It appears that steric interaction is too small to cause a sufficiently large barrier to internal rotation about the aryl C-N bond. The ortho fluoro substituent caused higher barriers to hindered rotation in the 3-aryl hydantoins and the 3-aryl 2-thiohydantoins than in 1-aryl hydantoins but the $\Delta G^{\neq}$ value was the lowest calculated in those series[14]. It is probable that electronic repulsive forces between the fluorine and the carbonyl oxygen atoms increases the energy levels of the transition states in

the 3-aryl hydantoins and the 3-aryl 2-thiohydantoins to the extent that rotation becomes slow on the nmr time scale. For this reason, an ortho fluorine atom appears to be larger in the 3-aryl hydantoin and 3-aryl-2-thiohydantoin series than it does in the 1-aryl hydantoin series.

Similar results are seen for 1-(o-methoxyphenyl)-5,5-dimethyl hydantoin, XVII. The methoxy moiety is bulkier than the fluorine atom. Thus one may expect slower rotation around the C-N bond, at least at low temperatures. It may be that the chemical shift difference between enantiomeric methyl protons is too small to be observed. On the other hand, a methyl group bonded to oxygen can bend back in the transition state in order to decrease the steric constraint, and the oxygen atom itself, which has a van der Waals radius of 1.40 Å,[27] exerts a bulk effect similar to fluorine atom. In 3-(o-methoxyphenyl)-5-methyl-2-thiohydantoin, where electronic repulsive forces must again be in effect, rotation about the C-N bond is found to be highly hindered.

Ground State Conformations of Diastereomers:

In the pmr spectra of diastereomeric 1-aryl hydantoins, the C-5 methyl protons of the hetero ring showed a triplet at low temperatures. Coincidence of the chemical shift differences with the coupling constants (J=7 Hz) caused overlapping of the methyl doublets. In the case of compounds,

VI, VII, and VIII, where the bulky ortho substituents are alkyl or aryl, the high field peak of the triplet is more intense than the low field peak. However, in the spectrum of the compound V, in which the ortho substituent is a chlorine atom, the intensities of the high and the low field peaks are more nearly equal. This observation is reflected in the calculated equilibrium constants. The equilibrium constants of compounds VI, VII, and VIII are higher than unity, being 1.25 ± 0.20, 1.26 ± 0.20 and 1.26 ± 0.20 respectively, but that of compound V is closer to unity, being 0.96 ± 0.20 (Table I-7).

It seems that the preference for one of the diastereomers in the ground state conformations is higher when the electronic interactions between the ortho aryl substituent and the heterocyclic moiety are minimal. Such is the case when the ortho substituent is an alkyl or an aryl group, rather than a chlorine atom. Electronic repulsive interaction between the C-2 carbonyl and the ortho chloro substituent may influence the relative stability of the diastereomers. Solvation from strongly polar solvent molecules (acetone-dimethylsulfoxide mixtures) may also affect the ratio of diastereomers.

The existence of chemical shifts between diastereomeric methyl protons, located on the hetero ring, is attributed to the anisotropic shielding of the aryl substituent. In the case of the more stable diastereomer, the peak for the C-5

methyl protons appears at high field, indicating that the shielding from the aryl ring is higher in this conformation than in the ground state conformation of the less stable diastereomer. The shielding of the benzene ring is maximized in the z direction, while the zone of deshielding falls on the ρ axis, as shown in the figure below.[24]

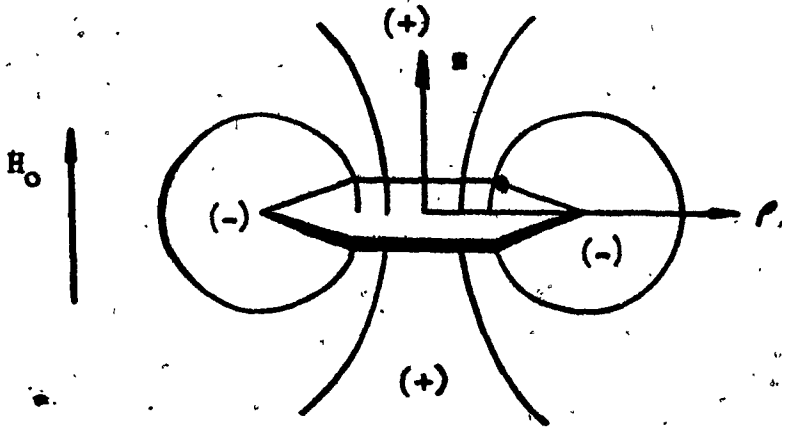

Johnson and Bovey[24], and several other authors [25] have studied the long range shielding of the benzene ring as a function of distance along the z and ρ axes. The diagrams in Figure I-21 represent the shielding zones of the benzene ring as chemical shift lines in ppm. If one can estimate z and ρ distances at various dihedral angles in the diastereomers, some information may be deduced about the ground state conformations, with the assistance of known chemical shift differences. This has been done by using the bond lengths and angles obtained from an x-ray crystallographic study of 3-(o-bromophenyl)-5-methyl-2-thiohydantoin[26]. The bond angles that were not available from this source were

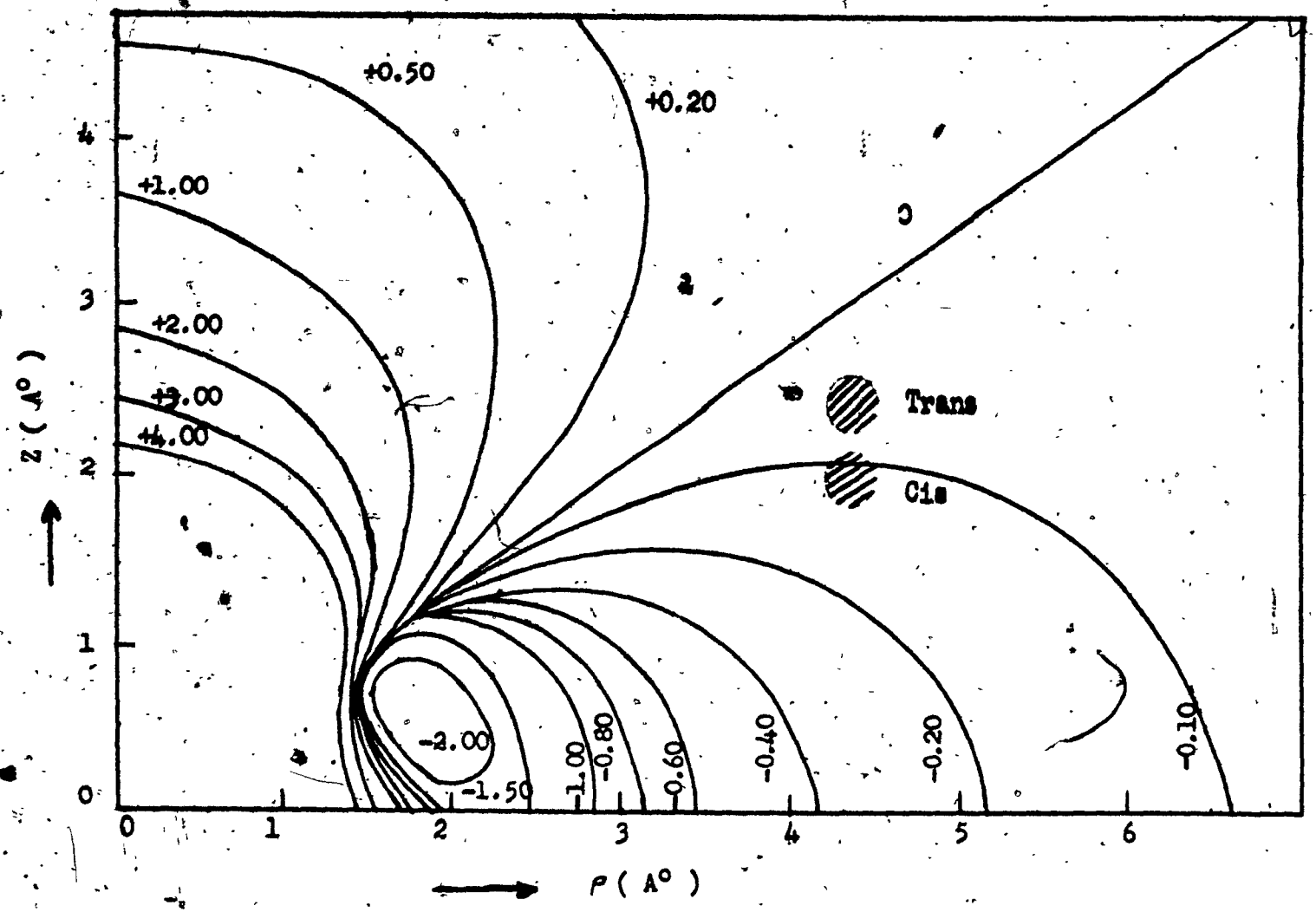

Figure I-21: Shielding Zones of Benzene Ring Relative to the Center of Sixfold Axis.

estimated from molecular models. Table I-17 lists the bond angles and bond lengths which were used in the calculations. From the figure in Table I-17, it can be seen that ρ, which is the distance between the methyl group and the center of the phenyl ring reflected on the plane of the C-N bond and phenyl ring, remains constant during hindered rotation. It is calculated to be 4.3 ± 0.1 A^{o}. The z distance from the methyl group to the plane of the aryl ring varies with the dihedral angle Φ between the aryl and the hetero rings. Values of z at various dihedral angles have been calculated. Figure I-23 shows the sinusoidal curve of Φ versus z. The methyl protons are most deshielded when the dihedral angle is 29^{o}(± 3), that is, when the methyl group is in the plane of the phenyl ring (Table I-18). At a dihedral angle of 119^{o} the distance between the plane of the phenyl ring and the methyl group reaches a maximum value of 2.49 A^{o}, where the methyl protons are least deshielded. Since ρ remains constant, the maximum value of z will coincide with the maximum shfelding zone of the benzene ring (Table I-17) In Table I-18, the chemical shifts corresponding to the dihedral angles or z distances are listed, determined using the Johnson-Bovey diagrams. At all angles of rotation, the methyl groups are found to lie in the deshielding region. This is reflected in the downfield chemical shifts.

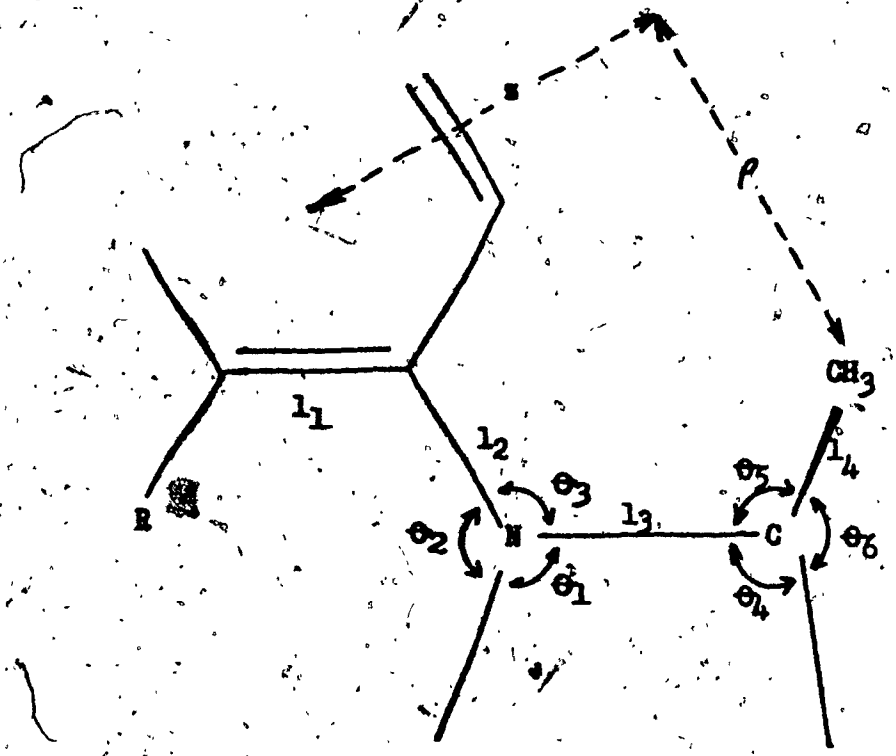

Bond Angle		Bond Length (A°)	
θ_1	114 ± 1	l_1	1.40 ± 0.01
θ_2*	130	l_2	1.46 ± 0.01
θ_3*	116	l_3	1.54 ± 0.01
θ_4	100 ± 1	l_4	1.54 ± 0.01
θ_5	114 ± 1		
θ_6	109 ± 1		

*Estimated

Table I-17 : Various Bond Angles and Bond Lengths for 1-Aryl Hydantoin.

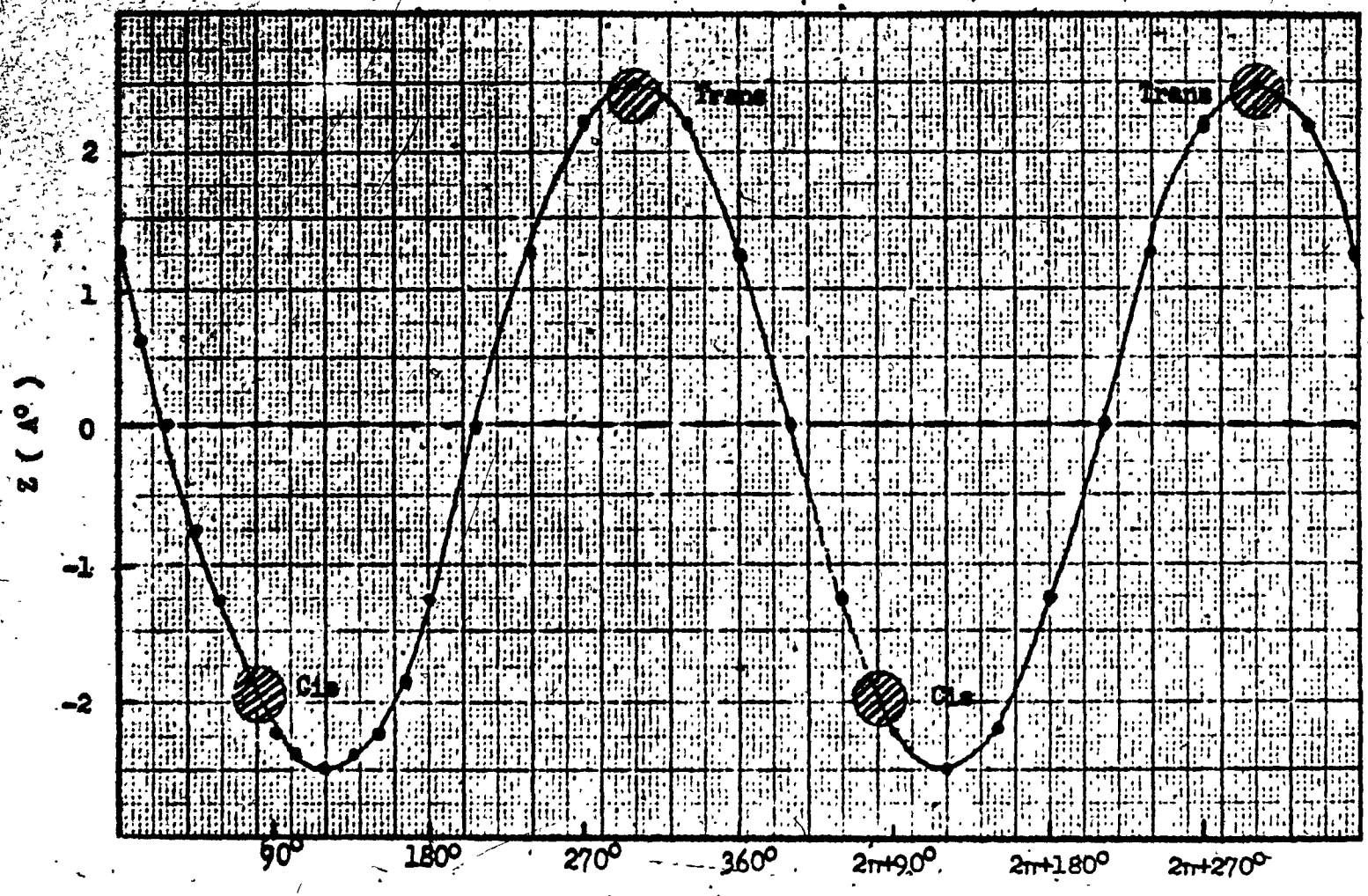

Figure I-22 : Sinusoidal Curve of Hindered Rotation in 1-Aryl Hydantoin Diastereomers as a Function of z Distances and Dihedral Angle, θ.. Trans and Cis Ground State Conformations are shown in Figure.

Table I-18 : Deshielding Chemical Shifts, δ , and z Distances of C-5 Methyl Protons at Various Dihedral Angles, θ , in 1-Aryl Hydantoins

θ	z (A°)	δ (ppm)
0°	1.27	-0.25
15°	0.64	-0.34
29°	0.0	-0.38
45°	-0.76	-0.33
60°	-1.27	-0.25
75°	-1.85	-0.14
90°	-2.20	-0.09
105°	-2.38	-0.07
119°	-2.49	-0.05
135°	-2.38	-0.07
150°	-2.20	-0.09
165°	-1.85	-0.14
180°	-1.27	-0.25

To estimate the dihedral angles in the ground state conformations, one has to consider the steric interactions. Since a carbonyl group appears to be more bulky in these compounds than a methyl group or a proton, the ortho aryl substituent will be pushed away from the C-2 carbonyl towards the C-5 position in the ground state conformations of the diastereomers. When one views the 1-aryl hydantoin molecule in the direction of the C-N bond rotational axis, the cis and the trans ground state conformations would be seen as shown in the figures below.

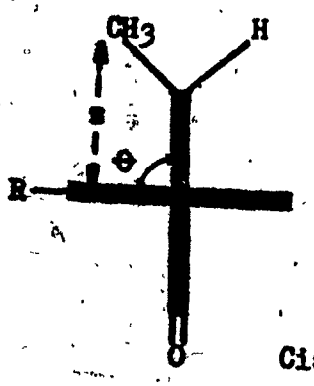

Cis-

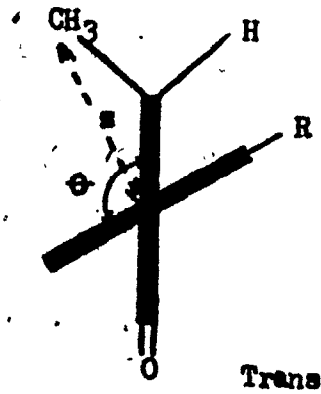

Trans-

The aryl ortho substituent, R, can approach closer to the less bulky proton in the trans isomer, than to the more bulky methyl in the cis isomer. Thus θ will be closer to a right angle in the cis isomer. Also, it is expected that the cis diastereomer will be less stable, due to steric crowding of the carbonyl, methyl, and R groups. Experimental evidence confirms this assumption. In the cis ground state conformation the methyl group is more deshielded, since $z_1 < z_2$. Hence methyl peaks from this conformation will be shifted

downfield. This was observed in the pmr spectra. Thus the trans diastereomer is the more stable isomer in the 1-aryl hydantoins.

By comparison of chemical shifts at various θ, (Table I-18 and Figure I-21), the dihedral angle in the cis conformation may be estimated to be about 80°, corresponding to a deshielding chemical shift of -0.12 ppm. Chemical shift differences between diastereomeric protons are found in the pmr spectra of compounds V, VI, VII and VII to be about 0.06-0.08 ppm. Assuming that the deshielding of the aryl ring is the major factor determining the chemical shift differences, the dihedral angle in the trans diastereomer will be about 120°, which will correspond to a chemical shift of -0.05 ppm. However, since these estimates are not very accurate, the possible ranges of the cis and trans diastereomer parameters are shown as shaded areas in Figures I-21 and I-22.

From the above discussion on the shielding interactions of the aryl and hetero rings and on steric factors, and the observed pmr spectra the trans ground state conformation is clearly defined as the more stable one. This result is in contrast with the x-ray crystallographic study of 3-(p-bromophenyl)-5-methyl-2-thiohydantoin,[26] which showed that the cis diastereomer is the more stable isomer. It should be noticed that the ortho substituent in the 3-aryl 2-thiohydantoin is bromine, a strongly electronegative atom. Another anomaly is

observed in the diastereomeric ratios of 1-(o-chlorophenyl) -5-methyl hydantoin, V , where the ortho substituent is chlorine. In 3-aryl hydantoins the aryl ring is far removed from the C-5 substituents, so that shielding and steric interactions between them are expected to be small during internal rotation. Solvation phenomena and electronic repulsive interactions would be the major factors in determining the ground state conformations. The presence of polar solvent molecules around the carbonyl groups and the ortho bromo substituent may significantly affect the ground state energies. In the ground state conformation of the cis isomer, polar solvent molecules may approach closer to the hydantoin molecule than is possible for the trans isomer, due to reduced steric hindrance, and may effect a greater degree of solvation. The solvation energy, which originates from the exothermic reaction between the solute and solvent molecules, is expected to decrease the ground state energy. Thus, the ground state energy of the cis isomer will be lower than that of the trans isomer in the 3-aryl hydantoins

This hypothesis, which proposes that the cis isomer is the more stable due to its solvation energy, remains to be proven through a study of 3-aryl hydantoins in non-polar solvents. The solubility of hydantoins in non-polar solvents is poor. A proton Fourier transform and pulse nmr technique could be used to study hindered rotation. Because of the rapid scanning ability of the pulsed nmr instrument over short periods

of time, a distinguishable spectrum can be obtained by accumulation when the concentrations of the nmr samples are low.

Solvent Effects on Rotational Enthalpy and Entropy of Activation:

Solvent effects may critically influence the magnitudes of the kinetic parameters obtained from a study of internal rotation. Polar interactions and solvation processes involving solute and solvent molecules, together with steric barriers produced by solvated solvent molecules may make substantial contributions to the rotational enthalpy and entropy of activation. Polar solvent molecules may stabilize polar mesomeric structures of solute molecules. The resulting change in bond lengths could alter the energy levels which determine rotational enthalpies of activation. The formation of solvent shells around polar centers of solute molecules may cause internal rotation to be sterically hindered. Solvation of a solute molecule in a favored solvent is an exothermic reaction. Energy released from this reaction could alter the ground state and transition state energy levels of rotamers. If solvation in the ground and transition states is different due to conformational variations, then the enthalpy and entropy of activation would be affected. A more solvated transition state will correspond to a lower rotational enthalpy of

activation assuming that solvent induced steric effects are absent. On the other hand, a more solvated transition state would be a more ordered one, corresponding to a more negative rotational entropy of activation.

These factors together could modify the rotational enthalpies and entropies of activation due to unsolvated solute molecules in a manner which would depend upon the structural and physical properties of the solute-solvent associated species. Thus one must carefully consider the contribution of each of these factors to the activation parameters, when interpreting measured activation parameters. It is desirable that a study be made using several types of solvents with different polar and structural properties. The contribution of each interaction may then be estimated more accurately.

Some of the solvent effects which are discussed below may be responsible for the unusual values of the activation parameters obtained by line shape and equilibration analysis such as the large negative rotational entropies of activation in 3-aryl hydantoin and quinazolinone diastereomeric rotational isomers.[12,14,15] No studies of the effects of a variety of solvents on the activation parameters for hindered rotation in these heterocyclic compounds were carried out, so no evidence for the contribution of solvent effects to the large negative values of $\Delta S^{\ddagger}$ and to the other activation parameters was available. In order to provide more information

in the present study of 1-aryl hydantoins, the rotational kinetic parameters of the compounds shown below are calculated for two different types of solvents. Tables I-7 and I-16 list the calculated parameters.

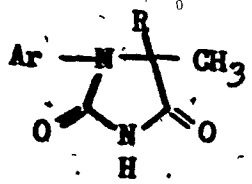

	Ar	R	Solvent I	Solvent II
XIII	o-Tolyl	CH_3	Pyridine	*DMSO-d_6
XII	o-Chlorophenyl	CH_3	Pyridine	DMSO-d_6
XIV	o-Naphthyl	CH_3	2-Chloropyridine	DMSO-d_6
XVIII	2,3-Dimethylphenyl	CH_3	2-Chloropyridine	DMSO-d_6
VIII	2,3-Dimethylphenyl	H	Pyridine	Acetone-d_6/ DMSO-d_6

*DMSO = Dimethylsulfoxide

The choice of solvent is limited because of the poor solubility of hydantoins in non-polar nmr solvents. Despite this restriction, the solvents that have been selected cause substantial variations in the kinetic parameters due to structural and polar differences. The dipole moments of the chosen solvents are listed below are obtained from the handbook of chemistry and physics.

Solvent	Dipole Moment
Pyridine	2.19 D
Acetone	2.88 D
2-Chloropyridine	3.0 D
DMSO	3.96 D

In all of the 1-aryl hydantoins studied, (Tables I-7 and I-16), $\Delta G^{\neq}$ and $\Delta H^{\neq}$ increase, while $\Delta S^{\neq}$ values became more negative, in the order of increasing polarity from pyridine or 2-chloropyridine to DMSO-d_6 or acetone-d_6/DMSO-d_6 mixtures.

Hydantoins are expected to show amide-type resonance. A polar solvent should increase the stability of polar resonance contributors such as B, due to charge stabilization.

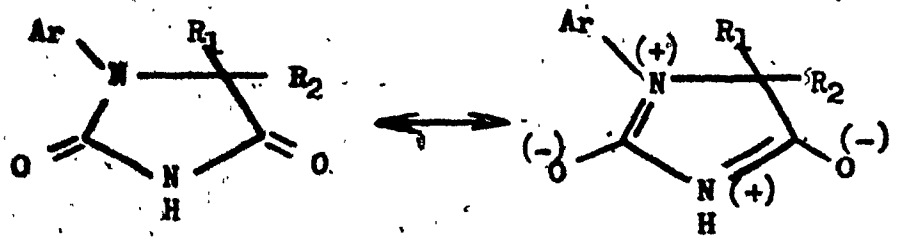

(A) (B)

In the polar contributor, formation of a double bond between the carbon and nitrogen atoms would bring the carbonyl group closer to the aryl moiety. Also, singly bonded oxygen would approach nearer to the ortho aryl substituent. Thus one would expect higher barriers to hindered rotation in the more polar solvent. The enthalpies

of activation will increase with the increasing difference between the ground state and transition state energies. In addition, it is reasonable to assume that the hydantoins will be solvated around the carbonyl groups in polar solvents. The bulky solvent shell around the C-2 carbonyl position could interfere with an ortho aryl substituent in the transition state. This would again cause an increase in the enthalpy value.

Enthalpies of activation were found to increase in all the compounds by about 1-2 kcal/mol in the more polar solvent, except the α-naphthyl substituted hydantoin, XIV, which showed an increase of only 0.2 kcal/mol. There may be large experimental errors in this case, and the polarity difference of the solvents employed, 2-chloropyridine and DMSO-d_6, is rather small. Consistent with this observation, the difference in $\Delta H^{\ddagger}$ values of 1-(o-tolyl)-5,5-dimethyl hydantoin, XIII, in pyridine and in DMSO-d_6 is 2.2 kcal/mol, whereas the difference for 1-(2,3-dimethylphenyl)-5,5-dimethyl hydantoin, XVIII, in 2-chloropyridine and DMSO-d_6 is only about 1 kcal/mol, even though both compounds have similar structures.

A reverse order of solvent effects is observed in the entropy values, compared to the enthalpy values, the values becoming more positive in the more polar solvent DMSO-d_6, relative to those in pyridine. Less negative entropies of activation in DMSO-d_6 solutions cannot be explained by

consideration of polarity and steric interactions. Solvation phenomena and structural differences between pyridine and dimethyl sulfoxide type molecules have to be considered. The solvation of the ground and the transition states may not differ greatly when the relatively small DMSO-d_6 molecules are present, as they can possibly approach the hetero ring to the same extent at all dihedral angles. As experimental evidence, the rotational entropies of activation of hydantoins XII, XIII, XIV and XV are the least negative, between -8 and -13 e.u.. in DMSO-d_6 solutions. In pyridine and 2-chloropyridine solutions, the more negative entropies suggest that the transition states are more ordered. Pyridine is not only a larger molecule than dimethyl sulfoxide and acetone, but it also has a planar shape and contains π electrons. Rather than simply forming bulky solvent shells around the carbonyl group, it will probably also be involved in π-π and charge transfer interactions. Maximum π-π electron cloud interactions between pyridine and 1-aryl hydantoin molecules would occur when the aryl and the hetero rings are co-planar, since under these circumstances delocalization of π-electrons in both rings reaches a maximum and the geometry of the solute molecules is most favorable for close approach of solvent molecules. Since the co-planar conformations correspond to the transition states, solvation energies for transition states should be higher than for the ground states in pyridine solutions. The exothermic

solvation energy would exert an effect opposed to the endothermic rotational enthalpy of activation, so as to cause an effective decrease in the energy of rotation to the transition state. This was observed for pyridine solutions. At the same time, the sandwich type positioning between the solute and the solvent molecules should cause the transition state to become more ordered, so that the entropies of activation for the rotational process would be more negative.

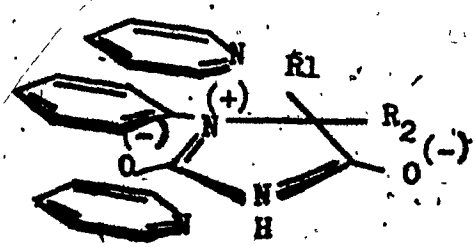

In compound XIV, where the α-naphthyl group is the aryl substituent, the entropy of activation did not vary much for the two solvents. This result may be due to the more effective π – π interactions between pyridine-naphthyl groups, so that in the ground and transition states, delocalisation in the hydantoin ring did not contribute extensively. The solvation energies for the ground and transition states probably did not differ greatly.

A highly negative value of the entropy of activation, -23 e.u. in DMSO-d_6 and -37 e.u. in pyridine, was found for

compound VIII, consistent with the behaviour of the other diastereomeric rotamers listed in Table I-7. Large errors were present in the values of the kinetic parameters estimated for these compounds due to experimental difficulties. However, the change in the enthalpy and entropy of activation from pyridine to acetone-dimethyl sulfoxide mixtures as solvents, is in the expected order. The equilibrium constant, Keq, decreased to 1.15± 0.20 in pyridine from 1.26 ± 0.20 in acetone-DMSO solutions. As this difference is within the range of experimental error, no meaningful interpretation can be made. The thermodynamic parameter calculated most accurately is the free energy of activation, $\Delta G^{\neq}$. The 0.4 kcal/mol increase from 14.1 kcal/mol in pyridine to 14.5 kcal/mol in acetone-d_6/DMSO-d_6 represents the overall variation in the enthalpy and entropy values, since

$$\Delta G^{\neq} = \Delta H^{\neq} - T.\Delta S^{\neq}$$

The change in enthalpy must be the major factor contributing to the overall value of the free energy of activation, as in all the other compounds.

Unusually high negative entropies of activation are also found for 3-aryl hydantoins and quinazolinone diastereomeric rotamers.[12, 14, 15] Solvation differences might be one of the factors to be taken into account, but they could not alone explain the entropy difference of about -15 e.u. between the

monomethyl substituted diastereomeric rotamers and the enantiomeric rotamers. Further study with various types of solvents may resolve this still unanswered question.

Effective Sizes of Methyl and Chlorine Substituents:

In 1-aryl hydantoins the importance of steric interactions on restricted rotational processes is indicated by the reversed order of the effects of methyl and ortho chloro substituents relative to 3-aryl hydantoins.[13] In 3-aryl hydantoins and 3-aryl 2-thio-hydantoins, an ortho chloro substituent is effectively larger than an ortho methyl group in restricting rotation about the aryl C-N bond, whereas in 1-aryl hydantoins the reverse order of sizes is observed.

The methyl group is expected to exert a steric effect greater than that of a chlorine atom, consistent with the relative sizes of these groups as determined by X-ray crystallographic measurements of their van der Waals radii[27]. This order of relative size applies in 1-aryl hydantoins. As shown in Tables I-7 and I-16 the free energies of activation, $\Delta G^{\ddagger}$, are 0.6 - 1.5 kcal/mol higher for the ortho-methyl compounds, VI and XIII, than for the ortho chloro compounds, V and XII. The change in solvent from pyridine to DMSO-d_6 for hydantoins XII and XIII did not effect the relative order of sizes.

In contrast, the free energies of activation of the 3-aryl hydantoins and the 3-aryl 2-thio hydantoins indicate a reversed order of sizes in the relative steric effects of the ortho methyl and ortho chloro substituents. These types

of compounds, which were studied by Fehlner,[12] Giles[14] and Granata[15] are shown in Table I-19 with the calculated free energies of activation. The free energy barriers to rotation about the aryl C-N bonds are 0.9 - 2.1 kcal/mol higher for the ortho chloro compounds than for the corresponding ortho methyl compounds.

Steric, electronic and mesomeric effects can be considered in order to clarify this reversal of order. In the internal rotational ground states, hydantoins are expected to adopt conformations with large dihedral angles between the two cyclic moieties, because of steric interaction between the ortho substituents of the aryl group and the hetero ring. Since the molecule should have sufficient flexibility in the ground state to minimize steric interactions between the two ring systems, it is probable that the most important influence on the values of $\Delta G^{\neq}$ arises from interactions in the transition states. The ground state effects of substituents are most easily recognized when the rotational isomers are diastereomeric Comparison of the equilibrium ratios of rotamers of the methyl and the chloro compounds reveals differences consistent with the reversal of the effective sizes of these groups in the 1-aryl and the 3-aryl series. The equilibrium constants at coalescence temperatures of compounds VI and V are 1.26 ± 0.20 and 0.96 ± 0.20 respectively. This is

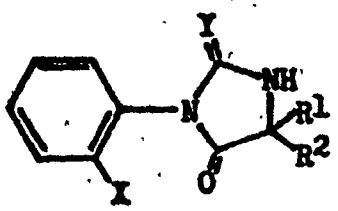

	X	R^1	R^2	Y
3a	CH_3	CH_3	CH_3	O
3b	Cl	CH_3	CH_3	O
3c	CH_3	H	C_6H_5	O
3d	Cl	H	C_6H_5	O
3e	CH_3	H	CH_3	O
3f	Cl	H	CH_3	O
3g	CH_3	H	CH_3	S
3h	Cl	H	CH_3	S

	Solvent	Temperature[a]	$\Delta G^{\ddagger b,c}$	$\Delta G^{\ddagger b,d}$
3a	Pyridine	60	18.3 ± 0.1	
3b	Pyridine	60	19.8 ± 0.2	-1.5
3c	DMSO-d_6	70	18.7 ± 0.2	
3d	DMSO-d_6	70	20.8 ± 0.2	-2.1
3e	DMSO-d_6	70	19.3 ± 0.1	
3f	Pyridine	70	20.0 ± 0.1	-0.7
3g	Pyridine	57.5	24.8 ± 0.1	
3h	Pyridine	58.5	25.7 ± 0.1	-0.9

[a] Degrees C.
[b] Kcal/mol.
[c] 90% confidence limits.
[d] $\Delta G^{\ddagger}_{CH_3} - \Delta G^{\ddagger}_{Cl}$.

Table I-19 : Free Energies of Activation for 3-Aryl Hydantoins and 3-Aryl 2-thiohydantoins.[12, 14, 15]

expected if the methyl group is effectively larger than chlorine in the rotational ground states. In contrast, the equilibrium ratios at ambient temperatures of the 3-aryl 2-thiohydantoins, 3g and 3h, are 1.4 ± 0.1 and 1.7 ± 0.1, respectively, the chloro substituent exerting a greater influence than the methyl group in the ground states.

In the 1-aryl hydantoins there are two possible transition states for rotation, with the ortho aryl substituent passing either the substituents in the 5-position or the C-2 carbonyl group. The significant differences between the rotational barriers of 1-aryl hydantoins (in which the ortho aryl substituent must pass a carbonyl group), the large increase in $\Delta G^{\ddagger}$ with the introduction of a second methyl group in the C-5 position, and the failure to observe restricted rotation at temperatures as low as - 78° C in 1-aryl hydantoins lacking a substituent in the C-5 position, can be taken as evidence that the more bulky ortho substituent must pass the C-5 position in the preferred transition state for rotation in the 1-aryl hydantoin series. This conclusion is supported by a study of Dreiding models. In this series the interaction between the substituents in the C-5 position of the heterocyclic moiety and the ortho chloro or ortho methyl group should be of a normal steric character.

In the 3-aryl hydantoin or 3-aryl 2-thiohydantoin series the ortho chlorb or ortho methyl substituent must pass a carbonyl oxygen atom in the transition state for rotation. The preferred pathway in the 2-thiohydantoins must be the one in which the bulky ortho substituent passes the carbonyl rather than the more bulky thiocarbonyl group. The two possible transition states in the 3-aryl hydantoins are expected to be very similar in energy, the ortho substituent passing either the C-2 or C-4 carbonyl oxygen atom. It is likely that the increase in the effective size of chlorine relative to methyl results from electrostatic repulsion between the electronegative chlorine and oxygen atoms, which increases the energy of the transition states. This influence is lacking in the preferred transition state for rotation in the 1-aryl hydantoins.

In addition to its steric effects and through space electronic effects as an ortho substituent, a chlorine substituent on the aryl group may possibly influence the barriers to rotation through mesomeric effects. These are likely to be significant only in or near the transition state for rotation of the aryl group. In the transition state, the aryl and heterocyclic moieties must be approximately co-planar allowing maximum or near maximum conjugation between the aryl π-electron system and the lone pair of electrons on the heterocyclic nitrogen atom at the point of attachment. Through-bond field effects may operate in both the transition and the

ground states. By influencing the electron distribution in the hetero ring, a chloro substituent might cause sufficient changes in bond lengths and bond angles in the ground and transition states to influence the free energies of activation.

However, no significant changes in the values of $\Delta G^{\neq}$ are observed when the para positions are substituted with chlorine atoms in 3-aryl hydantoins, while the ortho methyl groups remain unchanged.[15] Since the mesomeric influence of an ortho chloro substituent should be similar to that of a para chloro substituent it is concluded that the observed influence of an ortho chloro substituent is primarily a through-space effect.

The discussion above on the effective sizes of a methyl group and a chlorine atom is mainly directed towards the rotational free energies of activation. In 1-aryl hydantoins XII and XIII the enthalpies of activation, which are the true indicators of steric factors, indicate the same trend, with $\Delta H^{\neq}$ being 0.9 - 1.5 kcal/mol higher for the ortho methyl compound than the ortho chloro compound in pyridine and DMSO-d_6 solutions, respectively. The differences in entropies of activation are negligibly small and within the range of experimental error, ±2 e.u.. No attempt has been made to correlate the enthalpy and entropy of activation values in compounds V and VI, which are C-5 mono methyl substituted

1-aryl hydantoins, since large experimental errors are present in the calculation of both parameters due to experimental difficulties.

The complete line shape analysis results for 3-aryl hydantoins with o-chloro and o-methyl substituents,[13] indicated the reversal of the sizes of methyl and chlorine with respect to 1-aryl hydantoins. In the case of compounds 3c and 3d, and 3e and 3f, the enthalpies of activation were found to be 1.2 and 3.1 kcal/mol higher, respectively, for the ortho chloro compounds than the ortho methyl compounds. The entropies of activation were same for 3c and 3d, -22 e.u.. The $\Delta S^{\neq}$ values, calculated for 3e and 3f could not be correlated, because the type of solvent employed was different for both types of compounds. The entropies of activation in rotational studies of this type are strongly solvent dependent and do not relate closely to the internal steric interactions.

Buttressing Effect:

When restricted rotation of an aryl group results from steric interactions of an ortho substituent , the introduction of an adjacent bulky meta substituent may increase the effective size of the ortho group by restricting its ability to bend in the transition state for rotation in order to relieve steric strain. This phenomenon is known as the buttressing effect.

The earliest reports of the buttressing effect originated from studies on biphenyl isomerism. Bell and Kenyon[28] studied the energy barriers to racemization of ortho and meta substituted biphenyls. They concluded that biphenyls with ortho substituents can not readily exist in a planar form as was suggested in the work of Kaufler[29], because of steric interference of the bulky ortho substituents. Furthermore, the energy barriers to racemization are found to vary with the bulkiness of the ortho and meta substituents.

The effects of substituents on the racemization rates have been reported for the biphenyls listed in Table I-20[29]. In compound A the bulk of the ortho substituents, fluorine and methoxy groups, is very small. Racemization occurs so quickly that it is impossible to resolve the two enantiomers. When one pair of small ortho substituents and one pair of medium-sized ortho groups are juxtaposed, as in compounds B and C, resolution becomes possible, although the enantiomers are racemized in 10 and 78 minutes, respectively, by boiling in acetic acid. When large meta substituents are introduced, as in compound D, optically stable enantiomers are obtained. The relative capacities of the ortho substituents to interfere with passage through the planar transition state were found to be in the order $Br>>CH_3>Cl>NO_2>CO_2H>F$, which roughly parallels the size of the groups as determined by x-ray crystallographic measurements of van der Waals radii.[29]

A)

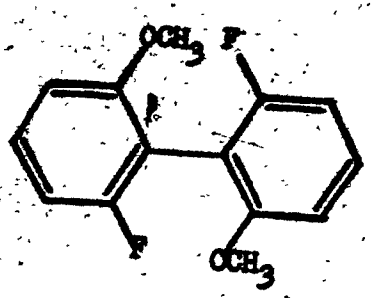

Non-resolvable

B)

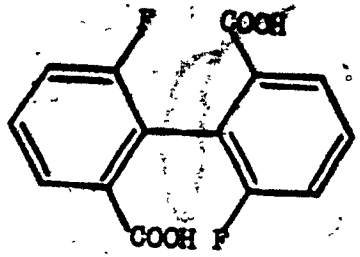

Racemization in 10 minutes

C)

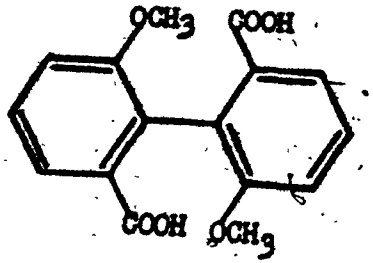

Racemization in 78 minutes

D)

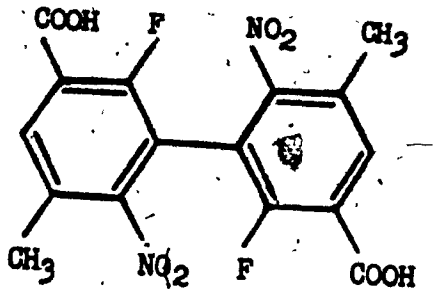

Optically Stable

Table I-20 : Relative Influence of Ortho and Meta Substituents on the Racemization Rates in Biphenyls.

There is no parallel between group interference and polar properties. This order represents a decrease of the barriers to hindered rotation and is in agreement with that observed in the 1-aryl hydantoins, XII, XIII, XVI and XVII, where the ortho substituents are Cl, CH_3, F and OCH_3, respectively. The free energy of activation about the aryl C-N bond for the ortho methyl group is found to be higher than for the ortho chlorine, as discussed previously in the thesis. However the free energy barriers to rotation for the methoxy and fluoro substituted compounds could not be calculated because of fast rotation.

Westheimer and co-workers[30] were able to correctly estimate the enthalpy of activation for racemization in ortho and meta substituted biphenyls from the van der Waals radii and stretching and bending force constants of the appropriate bonds. A buttressing effect clearly became evident as enthalpies of activation for racemization increased 6-7 kcal/mol when the meta positions were filled with bulky groups, while ortho substituents remain unchanged. Relatively minor changes in the activation energy, up to 1.5 kcal/mol, were reported for the substituents in the para position.

Biphenyls with various substituents were also studied by pmr line shape analysis by Bentz.[10] Giles[14] estimated the buttressing effect on 2,2-bis-(bromomethyl)-1,3-dinitrobiphenyl, where the minimum free energy of activation was

calculated from the chemical shift difference to be 23.9 kcal/mol, which is about 2.9 kcal/mol higher than for the non-meta substituted compound. The same author also reported high rotational barriers about C-N bonds in the bulky meta substituted quinazolinone, E, triazine, F, and 3-(β-naphthyl-2-thiohydantoin, $\Delta G^{\neq}$, all of which lack a bulky ortho substituent. This may represent a buttressing effect by the bulky meta groups on the ortho hydrogen of the aryl rings.

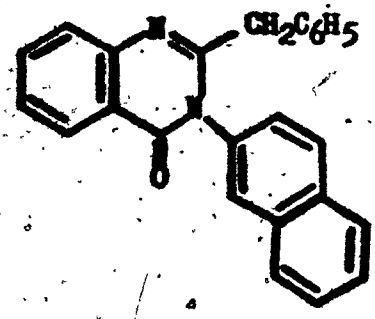

(E)

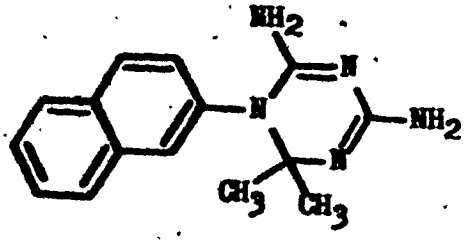

(F)

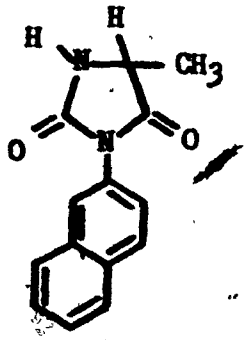

(G)

The 1-(β-naphthyl)-5,5-dimethyl hydantoin, XV, was prepared in the present study in order to detect this type of buttressing effect in 1-aryl hydantoins.

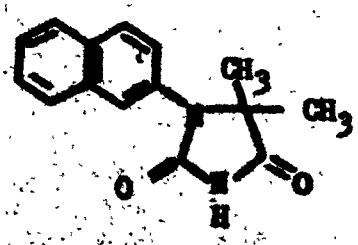

(XV)

Unfortunately, the steric barriers to rotation were not sufficient to obtain slow rotational rates at temperatures as low as -60°C.

In an earlier study, Fehlner[12] observed a buttressing effect in quinazolinones of the type shown below. The free energy of activation and entropy of activation of compounds H and J were calculated through line shape analysis.

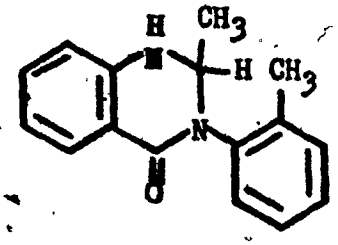

(H)

$\Delta G^{\neq}$ = 16.3 kcal/mol

$\Delta S^{\neq}$ = -31.4 e.u.

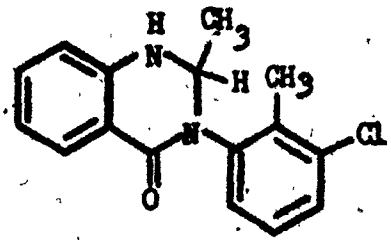

(J)

$\Delta G^{\neq}$ = 18.4 kcal/mol

$\Delta S^{\neq}$ = -21.5 e.u.

The less negative entropy value for compound J was considered by Fehlner to be due to a decrease in the rocking motion of the aryl ring in the ground state, resulting from the effectively larger size of the ortho methyl group.

Buttressing Effect in 1-Aryl hydantoins:

Substantial increases in the free energies of activation and the enthalpies of activation due to buttressing effects were found in 1-aryl hydantoins in the present investigation.

The compounds studied are shown below.

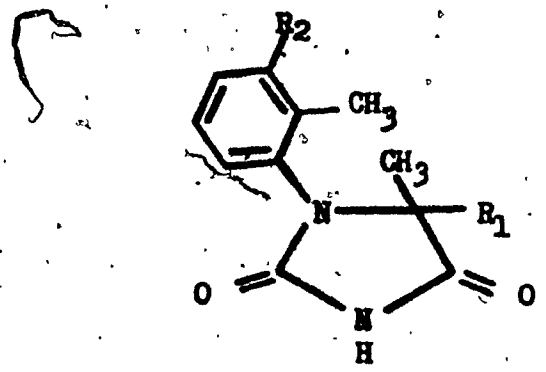

VI $R_1 = R_2 = H$

VIII $R_1 = H$, $R_2 = CH_3$

XIII $R_1 = CH_3$, $R_2 = H$

XVIII $R_1 = R_2 = CH_3$

The free energy of activation of 12.7 kcal/mol for compound VI is increased on the introduction of a methyl group to 13.9 kcal/mol in compound VIII, in acetone-d_6/DMSO-d_6 mixtures. However, between XIII and XVIII the enhancement is from 18.5 kcal/mol to 20.4 kcal/mol in pyridine and 2-chloropyridine solutions, respectively. Thus it seems that the buttressing influence is somewhat less in C-5 monomethyl substituted hydantoins, the difference being 1.2 kcal/mol in C-5 monomethyl hydantoins compared to 1.9 kcal/mol in C-5 dimethyl hydantoins. In the transition state the ortho methyl group of the aryl ring passes a less sterically crowded C-5 position in the hetero ring in compounds VI and VIII, so that in the transition state, the ortho group bends backward to a lesser degree than in the transition states of compounds XIII and XVIII. In consequence, a smaller buttressing effect is observed.

The enthalpies of activation show substantial increases due to the buttressing effect in all of the compounds which

were used to study such steric interactions. However, the variation in the entropies of activation is more difficult to interpret. They all appear to become more negative due to buttressing effects, although the variations are in the range of experimental error. Similar results were obtained by Granata in the study of 3-aryl hydantoins.[15]

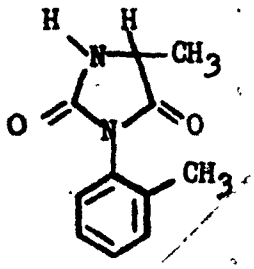

$\Delta G^{\neq}$ = 18.0 kcal/mol

$\Delta S^{\neq}$ = -24 e.u.

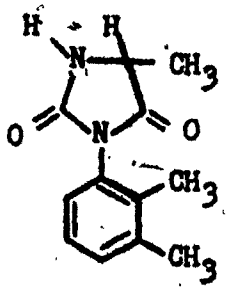

$\Delta G^{\neq}$ = 19.1 kcal/mol

$\Delta S^{\neq}$ = -27 e.u.

It may be assumed that the entropies of both the ground and the transition states are affected to a similar degree by buttressing interactions, since the variations are within the range of experimental error, i.e., ± 2 e.u.. However, the entropies of activation tend to become more negative in both hydantoin series when a buttressing effect is present. The more negative entropy values suggest more ordered transition states, in the aryl substituted hydantoins when the buttressing effect is present.

Due to the absence of sufficient accurate data, the question of the influence of the buttressing effect on the rotational entropies of activation still seems to be open.

SUMMARY

The following results were obtained in the pmr study of restricted rotation about C-N bonds in 1-aryl hydantoins.

a) The barriers to restricted rotation introduced by the ortho substituted aryl groups are consistent with the normally expected order of relative sizes of these groups. In contrast to 3-aryl hydantoins, the rotational barriers are largely determined by the bulk effect of the C-5 substituents.

b) Also in contrast to the previously studied 3-aryl hydantoins, the trans isomer corresponds to the more stable ground state conformation in 1-aryl hydantoin diastereomers.

c) Solvent molecules have critical effects on rotational enthalpies and entropies of activation in 1-aryl hydantoins. The polar solvent DMSO-d_6 increases the $\Delta H^{\neq}$ values of exchanging rotamers 1-2 kcal/mol relative to pyridine, while the $\pi - \pi$ electron cloud interactions cause the observation of more negative $\Delta S^{\neq}$ values in pyridine solutions. Solute-solute interactions may possibly also influence activation parameters.

d) An ortho chloro substituent in 1-aryl hydantoins exerts a lower barrier to internal rotation than an ortho methyl substituent. This is the reverse of the situation in 3-aryl hydantoins. It is caused by the lesser importance of polar repulsive interactions with the carbonyl oxygen atom in

the 1-aryl hydantoin series.

c) Bulky meta substituent or buttressing effects have considerable influences on barriers to internal rotation in 1-aryl hydantoins which increase with an enhancement of steric crowding in the C-5 position.

PART II

CARBON-13 NMR STUDY OF 1-ARYL HYDANTOINS

INTRODUCTION

The application of carbon-13 nmr spectroscopy to chemistry problems has a very recent history. Although the first nmr observations of C-13 nuclei were reported in 1957,[31] extensive and valuable results, particularly in the field of organic chemistry, have begun to appear in the literature only in the last three or four years. The slower rate of development of C-13 nmr spectroscopy relative to that of pmr is due to the experimental difficulties involved in detection of C-13 resonance signals. The isotope 13 of carbon has a nuclear spin of 1/2 (similar to H-1) and a natural abundance of 1.1%. This low natural abundance decreases the sensitivity of carbon resonances considerably. Another factor which further lowers the effective sensitivity of a C-13 nmr experiment is the magnetogyric ratio, γ, which is about 1/4 that of H-1 nuclei. Since the sensitivity of a nucleus in a magnetic resonance experiment is proportional to the cube of γ, a C-13 nucleus gives rise to 1/64 the signal intensity that a proton nucleus would yield on excitation. Thus the overall decrease in sensitivity in a C-13 nmr experiment is by a factor of 6000 relative to a proton experiment. In addition, carbon resonances are found over a chemical shift range of about 600 ppm, compared with about 20 ppm for proton nuclei.[32,33] Although

it is seen in Figure II-1 that most of the carbon-13 shieldings of organic compounds fall over a range of 250 ppm, a wide sweep capability is needed in a C-13 nmr instrument. However, the rapid technological advances of the last decade coupled with the availability of computers for accumulating spectra, have largely overcome these problems. The fast scanning capability of the pulse and Fourier transform C-13 nmr techniquesavailable with the most modern instruments provides the possibility of determining C-13 resonance signals in a routine fashion.[34]

It is expected that in the near future carbon-13 nmr studies will prove to be of far greater importance than pmr studies, as they offer the direct observation of molecular backbones, of carbon reaction sites of interest, and of enhanced effective resolution because of the wide range of carbon chemical shifts.

This carbon-13 nmr study of 1-aryl hydantoins is directed towards obtaining information about the substituent effects on the carbon shieldings through various factors (steric, inductive, conjugation, etc.), the influence of restricted rotation on the observation of nonequivalent carbon nuclei in the ground states of the rotamers, the solvent molecule environment effects on the carbon resonances, and possible conformational analysis by the C-13 nmr technique. The carbon-13 shielding data of 1-aryl hydantoins in a new solvent and reference compound are

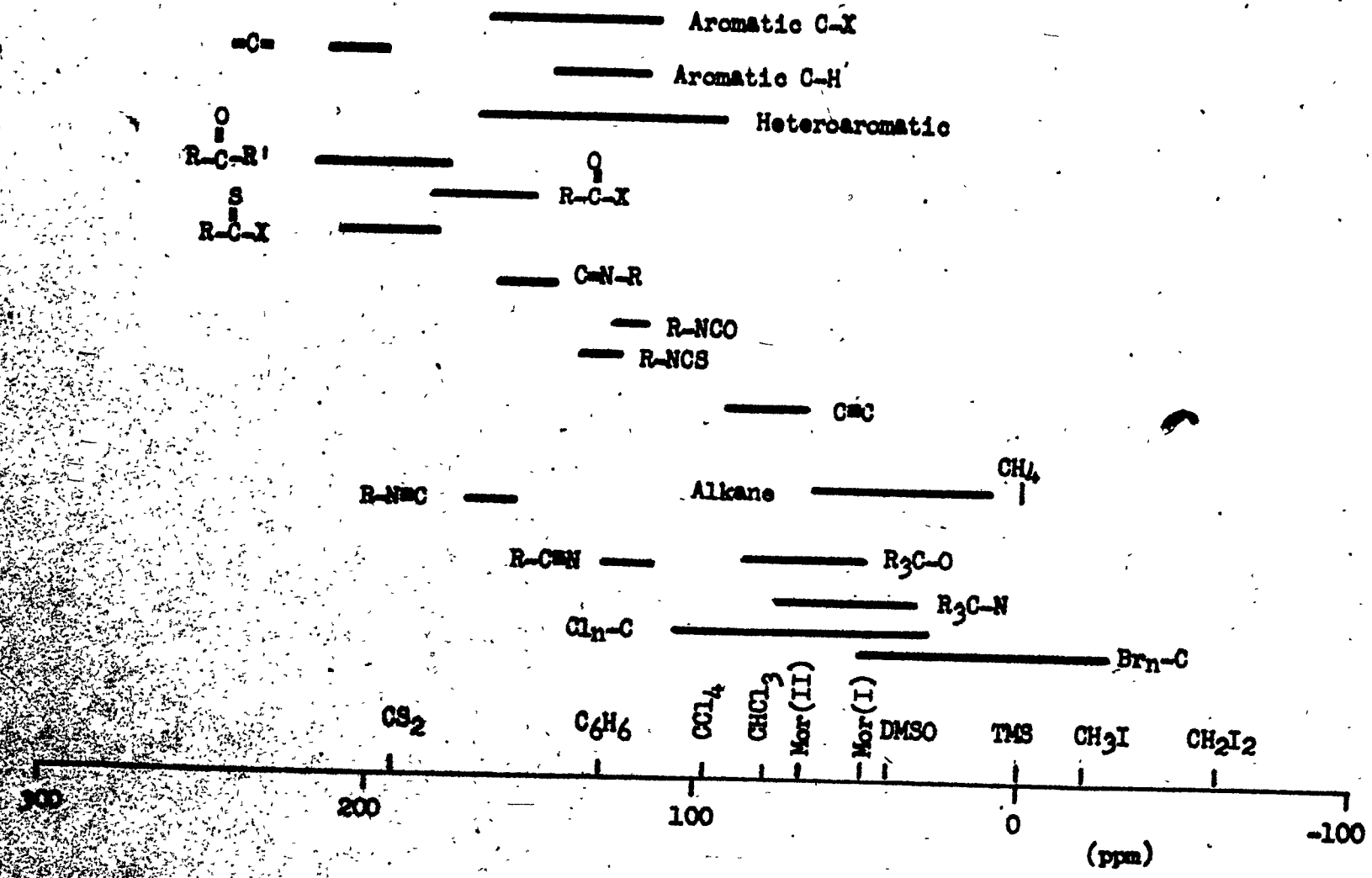

Figure II-1 : Range of Carbon-13 Shieldings in Organic Compounds.

compared with previously studied carbon shielding data of 3-aryl hydantoins[16] and data in the current literature through correlations involving the consideration of concentration and solvent effects. The importance of conformational analysis in the interpretation of activation parameters is discussed for the carbon resonances of aryl-substituted hydantoins. In conclusion, the results of this study introduce valuable and interesting information applicable to future carbon-13 nmr studies on heterocyclic compounds, in relation to the investigation of hindered rotational processes and the probable variations of carbon chemical shifts under the influences of the various factors mentioned above.

THEORY

The carbon-13 magnetic field, H_c, is related to the applied field, H_o, at the irradiating frequency of a carbon nucleus by the expression given below;[32]

$$H_c = H_o(1 - \sigma_c)$$

where σ_c, the screening constant, is a function of the chemical environment of the atom, and thus a direct indication of the carbon-13 shielding or chemical shift.

Saika and Slichter[35] divided the screening expression into three components for theoretical consideration, using molecular orbital calculations:

$$\sigma_c = \sigma_d + \sigma_n + \sigma_p$$

where σ_d, σ_n and σ_p are called the diamagnetic, neighbouring atom, and paramagnetic terms, respectively.

The diamagnetic term, σ_d, which results from the circulation of the local electrons induced by the applied field about the nucleus of interest, represents a small contribution to σ_c. It is a function of the reciprocal of the distances from the nucleus of interest to the overall electrons. Slater atomic orbital calculations have shown that the variation in shielding of the carbon nucleus in question by the influence of σ_d is negligibly small.[35]

The neighbouring-atom term, σ_n, includes the shielding contributions from all the other atoms and electrons in the molecule. Studies on ring currents of π-electrons moving in interatomic currents have proven that the change in carbon-13 chemical shifts produced by this factor does not exceed a few ppm. Although σ_n makes little contribution to the overall σ_c, it is important in stereochemical analysis, since it is dependent on geometry.

LCAO-MO treatment of carbon shieldings in conjugated and aromatic molecules by Karplus and Pople[36] demonstrated that the paramagnetic term, σ_p, is the dominant factor governing C-13 shifts, as was similarly found for F-19 shifts. It is a function of the mean excitation energy, ΔE, the atomic 2p orbital dimensions, $\langle r \rangle_{2p}$, and a term containing the elements of the charge density and bond order matrix, Q_{AB}, in the MO description of the unperturbed molecule. The last term takes into account the p orbitals of the carbon nucleus of interest and of the neighbouring nuclei. Thus bond orders and charge densities of σ as well as π bonds are added to the total paramagnetic term.

Carbon-13 shieldings have been studied in various organic structures by a number of workers. Interesting results were obtained by Grant and Paul[37] on linear alkanes. Replacement of α,β and γ hydrogens with methyl groups caused considerable changes in the carbon shieldings. A γ methyl substituent showed a -2.5 ppm shielding effect, while α and β

methyl substituents both resulted in deshielding effects of about 9 ppm. The types of interactions are quite different in each case. α and β deshielding effects are mainly induced through bonds, while the γ effect must be operative through space. Substitution on more remote regions in alkanes did not result in any considerable contribution to the shielding of carbon.

The quantitative influences on additive α,β and γ-effects of alkanes cannot be generalized to other organic structures, where the additive shift parameters are expected to vary owing to differences in steric effects, the presence of hetero atoms, π-electrons involved in ring currents; etc. . However, the general formulation employed for the additive carbon-13 shielding in alkanes by Paul and Grant may be used in a family of compounds, providing substituent parameters for the series:

$$\sigma'_c = B + \Sigma_j A_j n_{ij}$$

where σ'_c is the shielding of the i^{th} carbon. A_j is the additive shift parameter, n_{ij} is the population factor and B is a constant which corresponds to the shielding of a parent compound. Determination of the substituent parameters for a family of compounds may prove valuable in structural elucidations where information on steric and inductive polarization can be rationalized by stereochemical assignments.

In summary, the shielding effects of the following three factors can be interpreted through stereochemical assignments.

-Steric interaction usually gives rise to an upfield shift, due to the change in the polarization of the carbon atom resulting from through-space repulsive interactions. The electron density on the nuclei which are bonded to carbon, in most cases hydrogens, and which face steric repulsion, decreases due to perturbation of the bond to the carbon atom, while the carbon atom becomes more shielded. This effect is found in cyclohexane derivatives where the protons are deshielded by the increasing repulsive interaction. The γ-effect of alkanes can be given as another example of steric interaction.

- Conjugation effects also cause upfield shifts. Delocalization of π-electrons from aryl rings, olefinic carbons, or hetero atoms may enhance the charge density on neighbouring carbon atoms, thereby causing substantial upfield shifts. A prime example is the shielding increase of methyl and carbonyl carbons from acetone to acetophenone;[39]

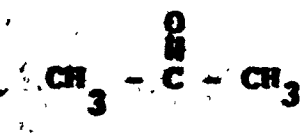

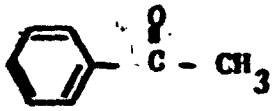

$\delta_c^{CH_3}$ = 28.1 ppm

$\delta_c^{CH_3}$ = 24.9 ppm

$\delta_c^{C=O}$ = 204.1 ppm

$\delta_c^{C=O}$ = 196.9 ppm

-The inductive effect resulting from the substitution of a nucleus other than hydrogen on a carbon atom in most cases causes a decrease in C-13 nuclear shieldings. It is dependent upon the electron releasing or withdrawing ability of the substituent and the polarization of the bond between the carbon nucleus in question and the substituent. Examples are the α and β methyl substituent shifts of polarized C-C bonds in alkanes and the downfield shifts of methoxy and N-methyl carbons due to electronegativity effects.[32,33] Increasing electronegativity of the substituent enhances the deshielding of the carbon nucleus while, conversely, an increase of the electron releasing ability of the substituent shields the carbon nucleus in question, as in the case of the upfield shifts of methyl iodides in Figure II-1.

Carbon shielding is assumed to arise from the bare molecular models in the above descriptions. However, the solvent molecule environment is also expected to contribute to the carbon chemical shifts. Therefore a complete screening constant expression for a carbon nucleus should include a term introducing solvent effects.

Buckingham, Schaefer and Schneider[40] proposed a four term equation to express the contribution to the screening constant of the solvent effects:

$$\sigma_{solvent} = \sigma_b + \sigma_a + \sigma_w + \sigma_E$$

where σ_b is the contribution to screening which is proportional to the bulk magnetic susceptibility of the medium, σ_a is due to anisotropy in the molecular susceptibility of the solvent molecules, σ_w arises from the van der Waals interactions between solute and solvent molecules, and σ_E is the polar effect on the electronic structure of the solute caused by the electric field due to the charge distribution in neighbouring solvent molecules. In agreement with results of Buckingham et al, solvent effect studies by Maciel and Natherstad[41] and other workers [42] have demonstrated that the last two terms, σ_w and σ_E, play the most prominent role in influencing C-13 chemical shifts.

Conformational Analysis by C-13 NMR:

Conformational inversion rates occurring on the nmr time scale and activation parameters of intramolecular rotation processes can be calculated from the carbon-13 spectra.

The kinetic information obtained is potentially more valuable than the pmr results, since the carbon skeleton of the molecular model has been investigated. Dalling, Grant and Johnson[43] have applied the technique to dimethylhexanes and some cis-decalins. The rate constant equations that are used in this study were described by Anet and Bourn[44].

$$k_a = \pi(\nu_{AB})^2/2 \qquad k_b = \pi\delta\nu \qquad k_c = \pi\nu_{AB}/\sqrt{2}$$

where k_a, k_b and k_c are the rate constant expressions for above coalescence, below coalescence and at coalescence temperatures, respectively. ν_{AB} is the chemical shift in Hz between carbons which interchange environments due to conformational inversion, and $\delta\nu$ is the corrected line width at half height (in Hz).

Once the rate constant is calculated for the coalescence temperature, the free energy of activation, $\Delta G^{\neq}$ and other activation parameters can be determined approximately.

$$\Delta G^{\neq} = 2.303\ RT(10.319f + \log T - \log k)$$

$$\Delta G^{\neq} = \Delta H^{\neq} - T\Delta S^{\neq}$$

Overhauser Effect:

The Overhauser effect, or Overhauser enhancement, is a common term used in C-13 studies.[32] In order to identify the origin of this effect, a short description is given.

The intensities of C-13 signals from carbons in the same molecule or from molecular systems in similar concentrations are found to vary doublefold or triplefold in some cases.[45] The enhancement occurs only when the protons of the neighbouring carbons are decoupled, and when the saturation of protons gives rise to a non-equilibrium polarization of the C-13 nuclei, greater than the thermal value. As a result, an increase of the signal strength is observed. This phenomenon

is called a nuclear-nuclear Overhauser effect, since it appears to be very similar in a theoretical sense to the nuclear-electron Overhauser effect which was observed by Overhauser in electron spin resonance (esr) studies.[46]

The nuclear-electron Overhauser effect, not applicable to the C-13 data considered here, causes enhancement of nmr signals several hundredfold under conditions of strong irradiation of esr transitions, when magnetic coupling between nuclei and unpaired electrons is present. Saturation of electron transitions, by the double resonance technique, causes an increase in the Boltzman population in the upper nuclear energy levels, so that a nuclear resonance signal becomes an emission signal and the intensity increases about 400 fold.

The nuclear-nuclear Overhauser effect yields rather moderate results, only a maximum of threefold enhancement being observed for carbon atoms substituted by protons. For the simplest case of a carbon nucleus coupled to a proton, the energy levels and possible transitions among them are shown in the figure below.

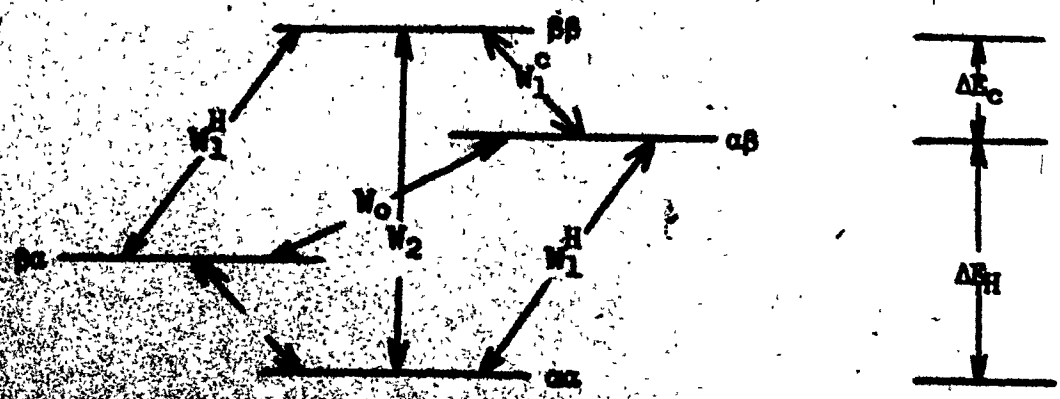

In the dipole-dipole coupling mechanism of a proton and a carbon nucleus, the transitions W_2, W_1^C and W_o have relative probabilities of 1,1/4 and 1/6, respectively, when the W_1^H transition is saturated at the decoupling frequency of proton resonances. These values are substituted in the equation below, which gives the ratio of relative intensities of C-13 signals with and without proton decoupling.

$$\frac{I}{I_o} = 1 + \frac{W_2 - W_o}{2W_1^c + W_2 + W_o}\left(\frac{\gamma_H}{\gamma_c}\right)$$

where $\frac{\gamma_H}{\gamma_c} = 3.976$

A theoretical value of 2.988 for the nuclear Overhauser enhancement has been calculated. This value has been verified by the experimental work of Kuhlman and Grant[45] on systems where the dipole-dipole relaxation mechanism has major importance.

However, this theoretical value of the Overhauser enhancement is not always observed in experimental studies, due to presence of some other competing relaxation mechanisms. Jones et al[47] have derived the equation for the relative intensities of a given carbon atom, taking into

account all the factors.

$$I/I_o = 1 + [\alpha \gamma_H / 2\gamma_C (\alpha + \chi)]$$

$$\alpha = \sum_i (r_i^{CH})^{-6}$$

where r_i^{CH} is the distance between the directly bonded carbon and proton nuclei and % is a relative measurement based on contributions of all the other relaxation mechanisms. It is evident in the equation above that the Overhauser enhancement will depend on C-H separations, when competing relaxation mechanisms are present.

EXPERIMENTAL

Preparation of C-13 NMR Samples:

The choice of solvent in C-13 nmr studies is more critical than in proton nmr studies. Not only is the solubility of the hydantoins a limiting factor, but the availability of a fairly intense carbon lock signal from the solvent also plays an important role. An internal lock on the solvent carbons is preferable in C-13 nmr studies to a co-axial capillary lock.

Dimethyl sulfoxide, DMSO, was used as an internal lock and solvent in the previous C-13 nmr study of 3-aryl hydantoins. However in this C-13 nmr study of 1-aryl hydantoins, morpholine was chosen to be the solvent and the internal reference compound because of the advantages described later in the thesis. The C-13 spectra of one of the 1-aryl hydantoin in DMSO were taken in order to compare the solvent effects of DMSO and morpholine.

Solubility of the hydantoins in morpholine was found to be as high as in DMSO. Table II-3 shows the concentrations of the nmr samples prepared. The highest concentration prepared for a 1-aryl hydantoin in morpholine was 23 mole % at the C-13 probe temperature (55°C). These concentrations provide fairly intense hydantoin carbon peaks for a reasonably small number of scans in the C-13 spectrometer. In order to enhance the signal-to-noise ratio (S/N) due to the low natural abundance of carbon-13 nuclei (1.1%), I am

nmr sample tubes were used instead of the regular 5 mm proton nmr sample tubes.

Solutions were prepared by dissolving 0.4-0.6 g of the hydantoin in 1 g of morpholine. DMSO and morpholine were obtained from Fisher Chemical Co. and were certified ACS reagents. p-Dioxane (Fisher Chem., Cert. ACS) and morpholine were mixed in several ratios (Table II-4) to study the concentration dependence of the morpholine carbon peaks. A Merck, Sharp and Dohme C-13 enriched methyl iodide (85%) capillary was used as an external capillary lock in a concentration dependence study of the morpholine carbons at various hydantoin concentrations.

Instrumentation:

The instrumentation requirements for C-13 nmr spectroscopy are different from those of proton nmr spectroscopy. In addition to the change in the Larmor frequency of the carbon nucleus (25.15 MHz at an external field of 23,490 Gauss), the wide range of carbon chemical shifts and the low natural abundance of carbon-13 necessitate the introduction of additional electronic components.

A V-4335-1 carbon-13 constant temperature probe and a V-4311 transmitter receiver unit operating at 25.15 MHz were employed as accessories of the basic Varian HA-100

continuous wave (C.W.) nmr spectrometer. Wide range sweep capability was provided by the attachment of a V-3530 wide sweep accessory. The addition of this unit is of prime importance, since the proton chemical shifts cover a range of only about 10 ppm whereas most carbon-13 shieldings fall within a range of about 250 ppm (Figure II-1).

Two instrumental techniques are used to overcome the problem of the low detection sensitivity of C-13 relative to protons. One method is the attachment of a Varian C-1024 time averaging computer (CAT), which accumulates the spectra through coherent addition of successive scans, so that for for "n" scans the signal to noise ratio is theoretically increased by "$\sqrt{n}$". The other consists of proton spin-decoupling by means of a V-3512-1 heteronuclear decoupler unit, which enhances the C-13 signal intensity through multiplet collapse and the nuclear Overhauser effect.

The frequency-sweep mode was employed for carbon spectra, rather than the field-sweep operational mode commonly used for protons, in order to simplify decoupling of the proton nuclei. In an operation using the frequency-sweep mode, the transmitted radio frequency (RF) of the spectrometer is fixed and the audio frequency (AF) is swept. The swept AF generates the sidebands used in the detection of the absorption mode signals of an nmr spectrum using the analytical channel phase detector. If the sweep range of the AF frequency is wide, the phase of the signal from the analytical channel phase

detector also changes substantially, causing distortion of the recorded spectrum. In sweep ranges of 10 ppm, the changes in the RF during the sweep are negligible compared to the magnitude of the RF. To overcome the phase problem associated with a wide AF sweep, the RF is swept instead. The lock signal is derived from a swept AF sideband but the position of the lock signal is maintained constant by sweeping the RF the same amount in the opposite direction, both sweeps being driven by a voltage ramp generated in the C-1024. A voltage controlled Hallicrafter oscillator (nominally 25.147 MHz) and a Wavetek model 111 oscillator in the V-3530 wide sweep unit provide the swept RF and AF frequencies, respectively. The analytical channel sideband signal is derived from a fixed frequency Hewlett-Packard 4204A audio oscillator. Since the RF is swept, the analytical channel frequency is effectively swept, and a frequency sweep spectrum is obtained from the analytical channel phase detector.

The C-1024 time averaging computer (CAT) drives the AF and RF sweeps by means of a stepped voltage ramp and at the same time controls the number of scans, the sweep width and the sweep time settings. A sweep interrupt circuit in the C-1024 CAT also monitors the presence of a lock signal and halts the scanning sequence if the lock is lost so that the spectrum accumulated before the lock is lost can be recorded

Figure II-2 represents a schematic drawing of a C-13 nmr spectrometer.

Operational Procedure:

A 60% carbon-13 enriched sample of methyl iodide in a 5 mm nmr tube was used as a reference for homogeneity adjustments and audio frequency settings. The 250 ppm range for carbon-13 chemical shifts corresponds to a 6.5 kHz audio frequency range at a magnetic field of 23.49 kGauss. Thus the AF range covered the range, from 3 to 9.5 kHz. The reference CH_3I peak was set on an AF frequency of 3220 Hz and the audio frequency of other common carbon-13 reference compounds or solvents were calculated with the assistance of C-13 chemical shifts quoted in the recent literature. Table II-1 lists the chemical shifts in ppm from TMS with the corresponding audio frequency settings. The shielding values for morpholine, which is found to be a good C-13 solvent and reference compound, were measured in this laboratory.

In order to obtain the maximum S/N ratio, the RF power attenuator was set at 20 db, and the probe leakage was balanced to a minimum following the tuning of the probe receiver circuit, providing that the sample temperature was in equilibrium with the probe temperature. Higher power levels were found to lead to saturation of the signal.

The magnetic field was adjusted to display the methyl

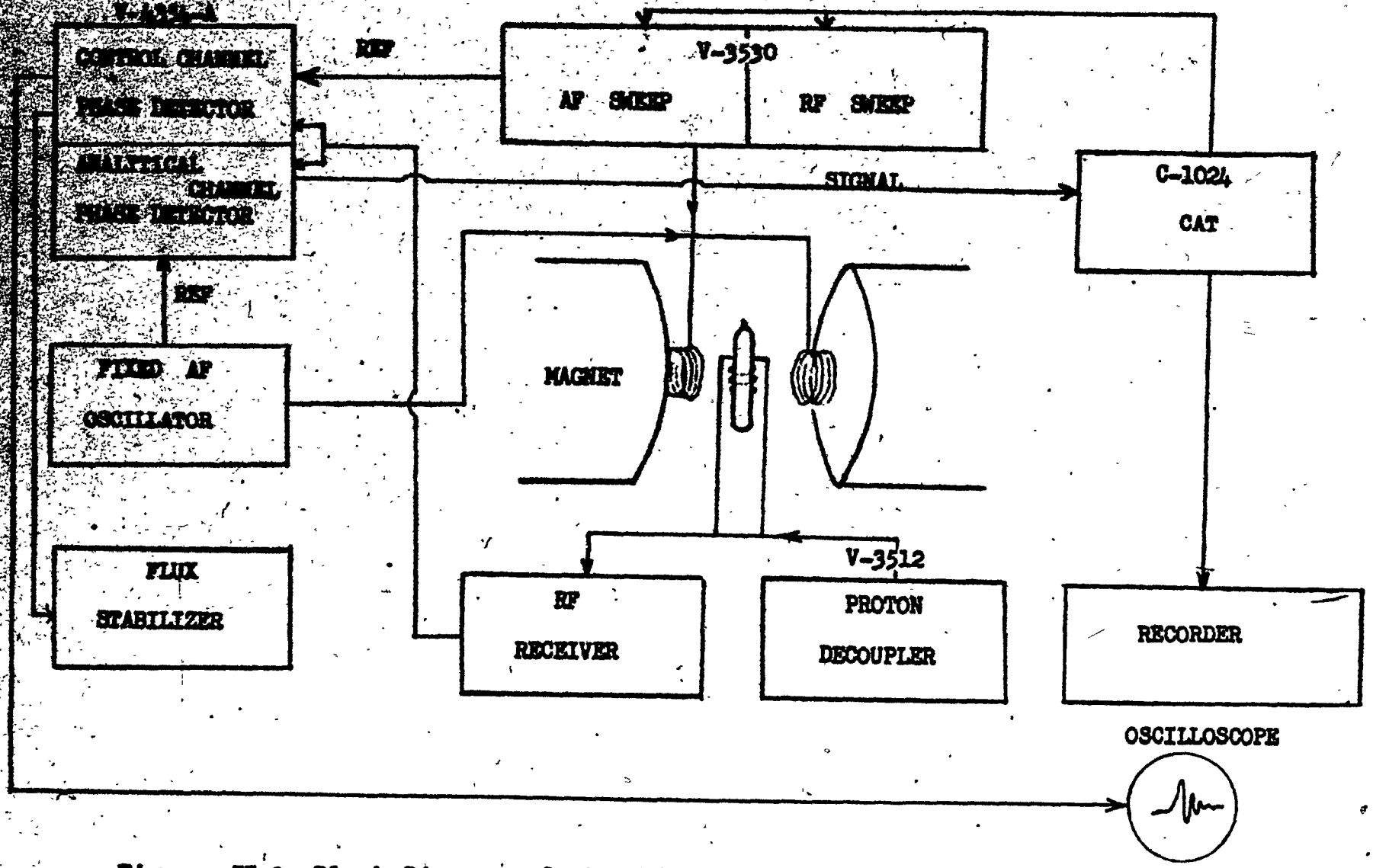

Figure II-2: Block Diagram of the C.W. Carbon-13 NMR Spectrometer.

Table II-1 : C-13 Shieldings and Audio Frequency Settings of Some Common Solvents and Reference Materials

Compound	Chemical Shift (ppm from TMS)	Audio Frequency (Hz)
Carbon disulfide	192.8	8584
Benzene	128.7	6965
Carbon tetrachloride	96.0	6147
Chloroform	77.2	5673
Morpholine (II)	68.3	5452
p-Dioxane	67.4	5427
Morpholine (I)	46.9	4915
Dimethyl sulfoxide	40.5	4754
Cyclohexane	27.7	4430
Methyl iodide	-20.5	3220

iodide quartet on the oscilloscope and the first upper sideband was centered at the AF start frequency of 3220 Hz. The super stabilizer was put on "operate" to prevent fluctuations of the field and frequencies. Magnetic field homogeneity was maximized while observing the ringing from the peaks of the methyl iodide quartet.

In order to achieve a stable lock and accurately measurable spectra, the AF and RF sweeps must be of exactly the same magnitude. This correspondence was achieved by observing a peak of the methyl iodide quartet on the oscilloscope, and then sweeping the AF/RF frequencies using the C-1024 CAT. If the AF/RF sweeps were not of the same number of Hz, then the peak position observed on the oscilloscope moved during the sweep. The sweep width was set at 100 Hz to increase the sensitivity for observing displacement of the signal. The RF sweep width adjusted until a stable signal on the oscilloscope is found.

After these initial adjustments using the reference methyl iodide sample were completed the heteronuclear decoupler unit V-3512 was put on "operate". The high power output of this unit causes the temperature in the carbon-13 probe to increase. To minimize the rise in the temperature, ice cold air was passed into the probe when the heteronuclear decoupler was operating. The change in probe temperature also required renewed balancing of the probe leakage to a minimum at the new equilibrium conditions. The noise band

width was set at 2 kHz while the output on the proton decoupler was set at a maximum of 3.00. The coarse and fine frequency calibrations were adjusted so as to collapse the methyl iodide quartet to a singlet in coherent mode. In order to increase the sensitivity of the adjustment, the sweep width on the scope was reduced with the linear sweep unit so that distortion of the singlet, due to poor frequency calibration of the heteronuclear decoupler could be easily detected.

At this point, the instrument was ready for locking. The RF phase detector was adjusted to obtain the decoupled methyl iodide signal in dispersion mode. Using the slow sweep unit, the field was swept until the lock dc level showed a positive excursion. The lock dc level signal was displayed on the oscilloscope rather than the sine wave lock signal, because the latter could not be observed above the noise. The locking process using the methyl iodide peak was used as a test of the stability of the spectrometer and of the homogeneity adjustments.

If the heteronuclear decoupler were not warmed up, or the probe were not at equilibrium temperature, or the RF power level were too high, intense instability in the lock dc level was observed, implying instability of the lock. The relative voltage height of the lock dc level on the oscilloscope, which is proportional to the intensity of the lock signal, gives visual evidence of the quality of the

homogeneity adjustments and of the frequency calibration of the proton decoupler.

Following satisfactory stability and homogeneity adjustments, the reference methyl iodide sample was replaced with the C-13 sample to be studied, which in most cases was a hydantoin-morpholine solution. Morpholine contains two non-equivalent groups of carbons in its molecular structure. The carbon-13 peak at the lower field, found at an audio frequency of 5452 Hz and a chemical shift from TMS of 68.27 ppm, was chosen as the lock signal. There are two reasons for this choice. First, this signal is very close to the carbon signal of p-dioxane (at AF 5427 Hz). Owing to the twofold enhancement of the relative magnitude of the C-13 signal in p-dioxane because of the presence of four equivalent carbons, it is easily located on the oscilloscope, and consequently may be used to locate the low field morpholine peak when difficulty arises due to saturation or high noise level. Secondly, the majority of the hydantoin carbon peaks fall on downfield ranges. If the lock signal is too far away from the carbons being studied, the RF phase detector requires readjustments in order to obtain absorption mode peaks in the spectra recorded, which would result in distortion of the lock signal phase and reduction in the stability of the lock.

Each change of sample required rebalancing of the probe leakage to a minimum, recalibration of the proton decoupler frequency and a slight homogeneity adjustment on the y-axis,

while the signal was observed on the oscilloscope. The adjustments could be done initially on a pure solvent sample, where the lock signal intensity is higher relative to the solution, so that better sensitivity can be obtained. Minimal changes in frequency calibration and homogeneity adjustment are always desirable on solutions, due to a low S/N ratio and lower sensitivity. Typical instrumental parameters for a stable lock on the morpholine low field peak are given below.

RF attenuation (db)	25
AF start	5452
RF phase detector	25
Spectrum amplitude	6000
Noise bandwidth (kHz)	2
Output	3

The last two parameters pertain to the V-3512 proton decoupler unit which is switched to the incoherent mode after frequency calibration. The fine frequency dial settings of the decoupled protons are not given, as these settings vary under the daily instrumental conditions. It is best to obtain the frequency dial settings for each sample, while observing the signal on the oscilloscope. Thus the calibration chart of Williams[16], in which fine and coarse frequency dial settings are plotted against the chemical shifts of common solvents, was not found to be valid in most cases.

Before proceeding to obtain a C-13 spectrum of the hydantoin carbons, a final check on the homogeneity adjustments was made. The high field carbon signal of morpholine was scanned a few times and the spectrum was recorded. This peak was not locked, so that distortions of the lock signal would not be expected. A narrow and intense peak at a line width of 4 Hz with ringing was taken as evidence of satisfactory homogeneity adjustments. (Figure II-3)

Homogeneity adjustments are very critical in a C.W. carbon-13 nmr study. It is always desirable to obtain a spectrum using the least possible number of scans. Otherwise fluctuations of field and frequency might introduce errors to the measurement of the spectrum and unusually broadened peaks would be observed.

Measurement of Spectra:

The carbon peaks of 1-aryl hydantoins in morpholine were found to be distinguishable after 50-200 scans. The sweep widths of the spectra, when scanned at 10 sec. periods, were chosen to be 100 Hz or 200 Hz. The scanning rate of the spectra at higher sweep width was selected as 25 sec., in order to avoid broadening of the peaks. The minimum line-widths of the carbon peaks were found to be 4 Hz under best resolution conditions.

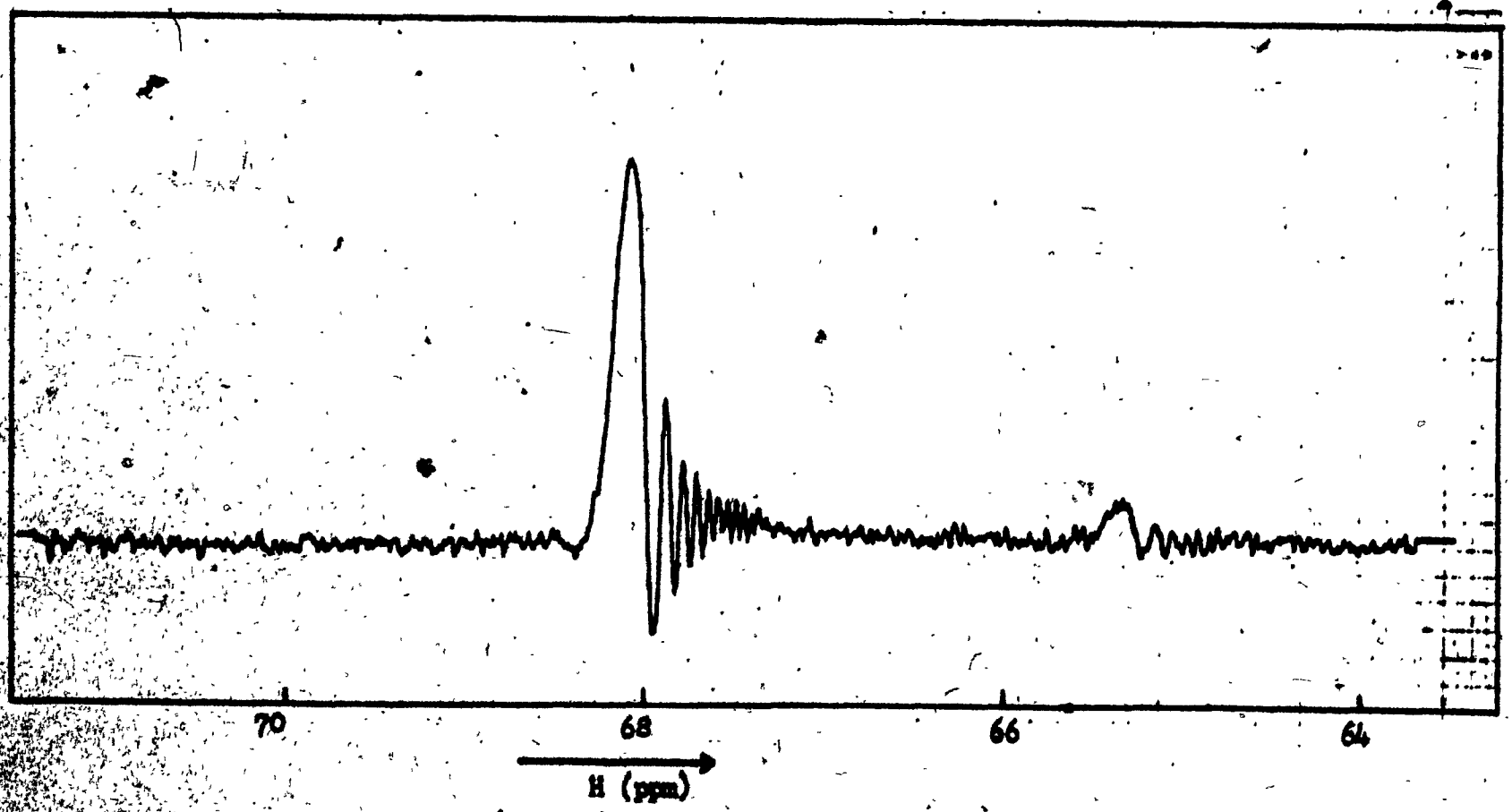

Figure II-3: High Resolution Carbon-13 NMR Spectrum of the Lowfield Morpholine Carbon and the C-5 Carbon of 1-(p-Methoxyphenyl)-5,5-dimethylhydantoin, XVII (50 Scans).

Following the recording of each spectrum, the frequency readings were noted for the sweep start and sweep end during scanning with the C-1024 CAT. The frequency difference that is measured corresponds to the width of the spectrum. These readings were accurate to ± 1 Hz. The AF frequency, which was set by the HP 4204-A oscillator, was recorded to an accuracy of ± 1 Hz or ± 0.04 ppm.

The chemical shifts of the hydantoins are calculated in ppm from TMS. Recent literature data have established the chemical shifts of methyl iodide and p-dioxane as being -20.5 and 67.4 ppm, respectively, where a positive value indicates a downfield shift. Table II-1 shows the audio frequencies of common solvents with the corresponding carbon shielding values. Table II-2 is prepared by selecting an AF of 3220 Hz for methyl iodide. In Figure II-4 a plot of the audio frequencies versus the chemical shifts in ppm from TMS is presented.

Table II-2 : Carbon-13 Chemical Shifts from TMS with the Corresponding Audio Frequency Settings

Chemical Shift (ppm from TMS)	Audio Frequency (Hz)
-30	2980
-20	3232
-10	3483
0	3735
10	3986
20	4238
30	4489
40	4741
50	4992
60	5244
70	5495
80	5747
90	5998
100	6250
110	6501
120	6753
130	7004
140	7256
150	7507
160	7759
170	8010
180	8262
190	8513
200	8765
210	9016
220	9268
230	9519

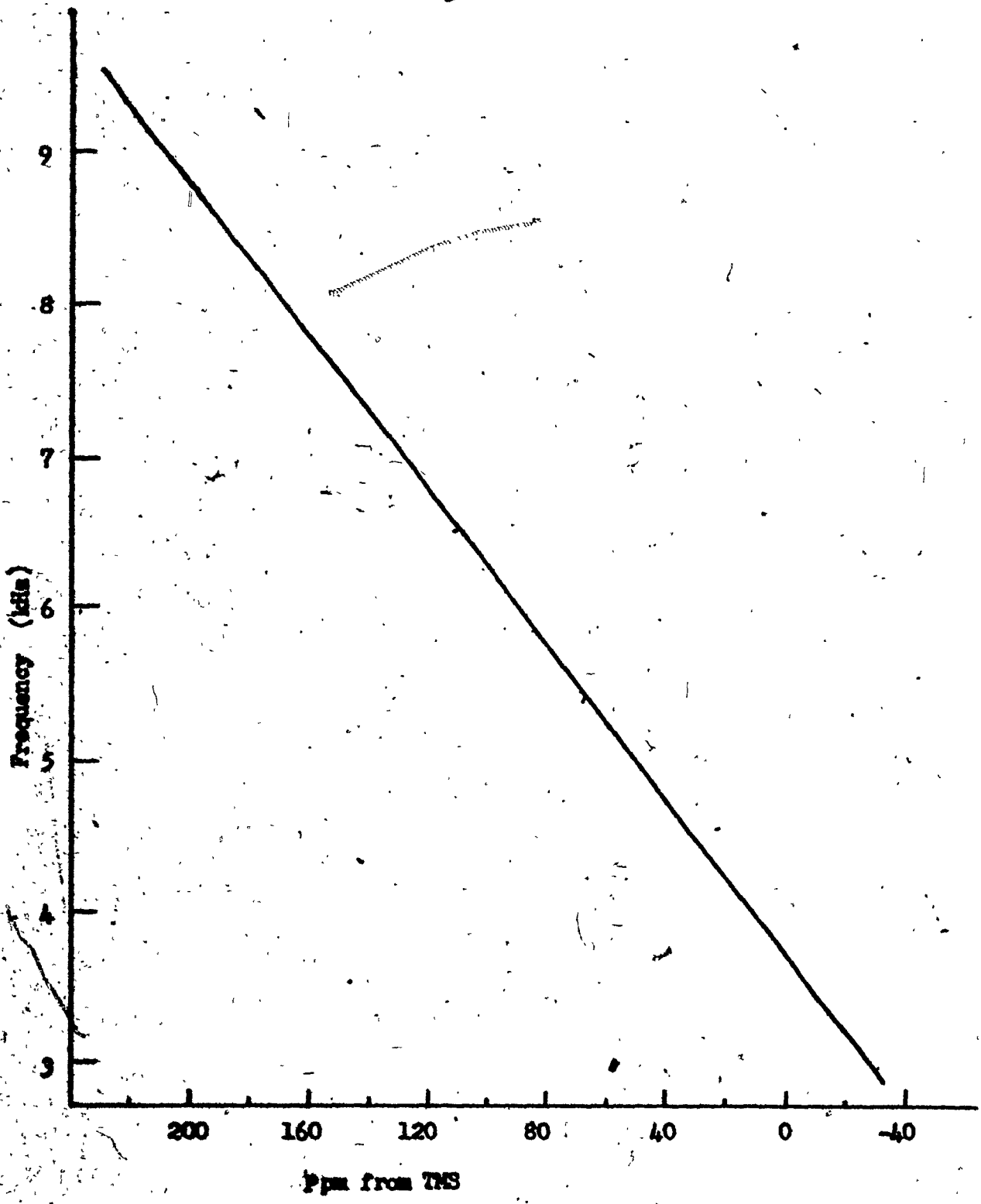

Figure II- 4: A Plot of Frequency versus Ppm from TMS for C-13 NMR.

RESULTS AND DISCUSSION

The 1-aryl hydantoins that were studied by C-13 nmr are listed in Table II-3 with their mole % concentrations in morpholine.

For clarity in the following discussions and tabulations, the C-13 chemical shift data are divided into tables which contain only the chemical shifts of corresponding nuclei. All the C-13 data on hydantoins and any other compounds have been converted to the TMS scale and are reported in parts per million (ppm) with increasing positive values in the direction of decreasing field. This is, in effect, a deshielding scale.

For 1-aryl hydantoin concentrations in the region of 11 to 23 mole % in morpholine, the peaks of the solvent carbons are relatively easily observed in the C-13 nmr spectrometer. Figure II-3 shows the carbon-13 spectrum of the unlocked morpholine peaks and the C-5 carbon peak of 1-(o-methoxyphenyl)-5,5-dimethyl hydantoin, XVII, which was recorded using a 200 Hz sweep width and 50 scans at 10 sec scanning periods. Even though the concentration of XVII, 14.3 mole %, was comparatively low, the C-5 carbon peak is distinguishable without overloading of the solvent peak.

Table II-3 : Some of the 1-Aryl Hydantoins Studied by C-13 NMR, with the Mole % Concentrations in Morpholine

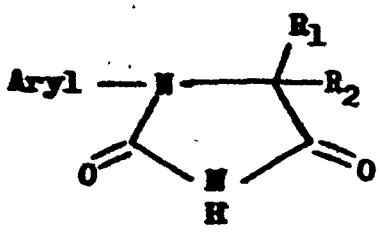

Hydantoin	Aryl	R_1	R_2	Concentrations Mole % in Morpholine
I	Phenyl	H	H	22.9
II	p-Tolyl	H	H	21.5
V	p-Chlorophenyl	CH_3	H	11.2
VI	p-Tolyl	CH_3	CH_3	22.7
VIII	2,3-Dimethylphenyl	CH_3	H	21.4
XII	p-Chlorophenyl	CH_3	CH_3	12.4
XIII	p-Tolyl	CH_3	CH_3	14.7
XIV	α-Naphthyl	CH_3	CH_3	14.9
XV	β-Naphthyl	CH_3	CH_3	15.9
XVI	p-Fluorophenyl	CH_3	CH_3	10.9
XVII	p-Methoxyphenyl	CH_3	CH_3	14.3
XVIII	2,3-Dimethylphenyl	CH_3	CH_3	14.8

A Preferred C-13 Solvent and Reference Compound:

The carbon shieldings of common solvents and reference compounds reported in the literature are shown in Table II-1 (excluding morpholine). Of these, dimethyl sulfoxide (DMSO) was previously chosen for the C-13 nmr study of 3-aryl hydantoins.[16] The main reason for this choice was the high solubility of hydantoins in DMSO. Most other solvents dissolve hydantoins very poorly, and a distinguishable C-13 spectrum on the C.W. spectrometer could not be obtained at these low concentrations. A disadvantage of DMSO is that it provides a poor locking signal, because of the low intensity of the peak due to the equivalent methyl carbons.

An attempt was made to find a more suitable solvent, in order to correlate the solvent dependency of the carbon-13 shifts in hydantoins and to permit better instrumental conditions. The solubility of hydantoins in various solvents containing equivalent carbons was tested. For a number of reasons morpholine was found to be a very favorable solvent and reference compound for the C-13 nmr study of 1-aryl hydantoins:

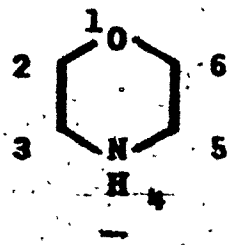

-Morpholine remains a liquid over a wide temperature range, which enables one to do a variable temperature C-13 study if required (m.p.: -5°C; b.p.: 128°C).

-Morpholine has two groups of equivalent carbons. These pairs of carbons, in the 2,6 and 3,5 positions, are found at 68.27 ppm and 46.92 ppm, respectively. In Figure II-5 their C-13 spectrum is shown. The low intensity peak which is visible, is due to the C-5 carbon of the hydantoin which was present in the morpholine solution. The morpholine carbon signals have three advantages relative to that of DMSO:

a- The intensities of the peaks are found to be increased twofold compared to DMSO, even though the same number of carbons are involved in both compounds. A favorable over-hauser enhancement could be responsible for this observation, since in DMSO, competing relaxation mechanisms due to the presence of a sulfoxide group probably decrease the S/N ratio. Thus, the stability of the lock is enhanced in morpholine.

b- The higher intensity of the carbon peaks and the presence of a second solvent peak, which was free from the distortions of the lock signal simplified the homogeneity adjustments (cf. Figures II-3 and II-5). Loss of ringing and broadening of the second morpholine peak indicates to the operator that the homogeneity adjustment is poor, before the scanning on

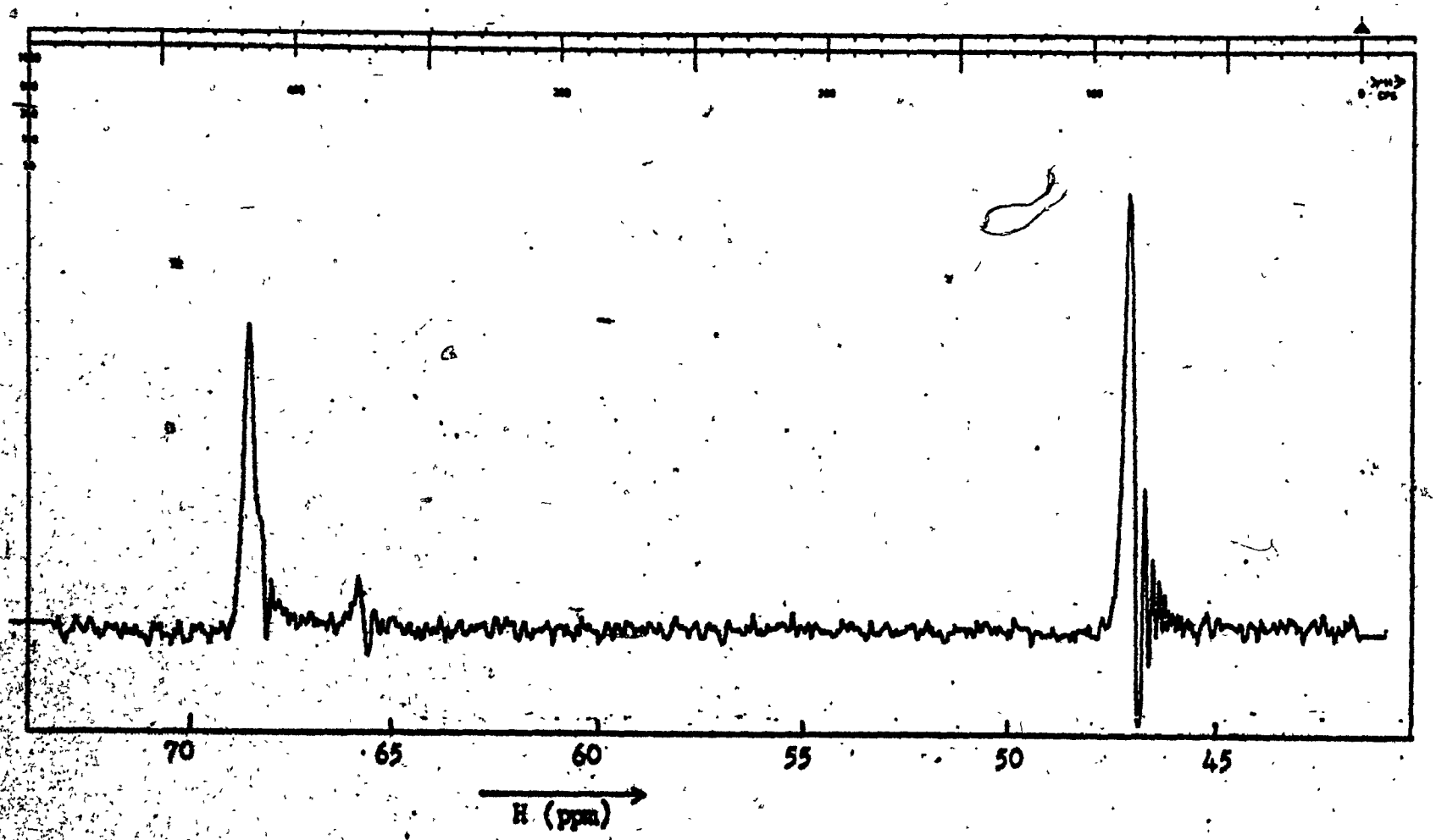

Figure II-5 : Carbon-13 Spectrum of the Morpholine Carbons and the C-5 Carbon of 1-(2,3-Dimethylphenyl) Hydantoin, XVIII (80 Scans).

solute carbons is begun. It is also fairly easy to locate the low field morpholine peak on the C-13 spectrometer if difficulty arises due to high noise. This signal is only 22 Hz away from the p-dioxane (67.4 ppm) carbon peak, whose intensity (four equivalent carbons) is double that of morpholine.

c- It can be seen in Figure II-1 that morpholine shifts occur in the middle of the range of known C-13 shieldings. It is desirable to choose a reference peak close to the signals of carbons to be studied, since scanning of the carbon signals which are distant from the lock signal would require RF phase adjustments, and a major RF phase adjustment would cause a loss of the disperaion mode of the lock signal and result in unstable instrumental conditions. The low field peak of morpholine is found to give the best RF phase adjustments for the hydantoins. It is 27.8 ppm downfield from the DMSO peak, and closer to the aromatic and carbonyl carbons of the hydantoins.

- Tables II-4 and II-5 show the concentration dependence of the morpholine carbon shifts in p-dioxane (internal lock) and in hydantoin II (external lock on enriched methyl iodide in a capillary). The variation of the chemical shifts in p-dioxane is found to be 0.002 ppm per mole % morpholine. Considering the precision of the experiments, the morpholine C-13 shifts can be assumed to be independent of the p-dioxane

Table II-4 : Dependence on Concentration of the Morpholine Carbon Shieldings[a] in p-Dioxane[b]

Reference: $\delta_c^{\text{p-dioxane}}$ = 67.40 ppm (internal lock)

Sample	Concentration Mole % Morpholine	Morpholine-I	Morpholine-II
C-1	20.0	47.04	68.38
C-2	50.1	46.94	68.35
C-3	63.3	46.93	68.32

[a]ppm from TMS

[b]error limits are ± 0.05 ppm

Table II-5 : Dependence on Concentration of the Morpholine Carbon Shieldings[a] in 1-(o-Tolyl) hydantoin(II)

Reference: $\delta_c^{CH_3I}$ = -20.50 ppm (external lock)

Sample	Concentration Mole % Morpholine	Morpholine-I	Morpholine-II
C-1	87.8	46.88	68.25
C-2	84.3	46.86	68.23
C-3	81.5	46.74	68.14

[a]ppm from TMS

[b]error limits are ± 0.05 ppm

concentrations. However, with increasing concentration of the hydantoins, the downfield shifts of the morpholine peak are about 0.015 ppm per mole % morpholine. Even so, the error which could be introduced into the measurements of the C-13 chemical shifts of hydantoins would be sufficiently low, compared to the normal experimental errors on measurements of ± 0.05 ppm, for concentration effects to be considered negligible.

Morpholine is less polar than DMSO. Thus it is expected that the aryl hydantoins would be less perturbed in morpholine, and the observed C-13 chemical shifts would provide better data for the stereochemical assignment of the unsolvated molecule. The following discussion on the concentration dependence of the C-13 shifts of 1-aryl hydantoins supports this hypothesis.

Concentration Dependence of Carbon Shieldings for 1-Aryl Hydantoins in Morpholine:

The concentration effect on the carbon-13 chemical shifts of 1-(o-tolyl) hydantoin, II, was studied at four different concentrations in morpholine. The data from Table II-6 for the methyl, C-5, C-2 and C-4 carbons are plotted in Figure II-6. A small downfield shift with increasing concentration is observed. It is in the same direction as that reported by Williams[16] for 3-aryl hydantoins in DMSO,

Table II-6 : Dependence on Concentration of the Carbon Shieldings[a] of 1-(o-Tolyl) Hydantoin (II) in Morpholine[b]

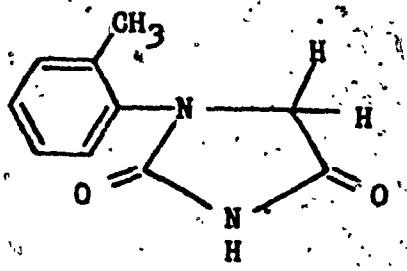

Sample	Concentration Mole % in Morpholine	CH_3	C-5	C-2	C-4
C-1	12.2	17.99	54.30	157.00	172.88
C-2	15.7	18.01	54.43	157.02	172.91
C-3	18.5	18.02	54.42	157.12	172.90
C-4	21.5	18.09	54.47	157.08	172.96

[a] ppm from TMS

[b] errors limits are ± 0.05 ppm

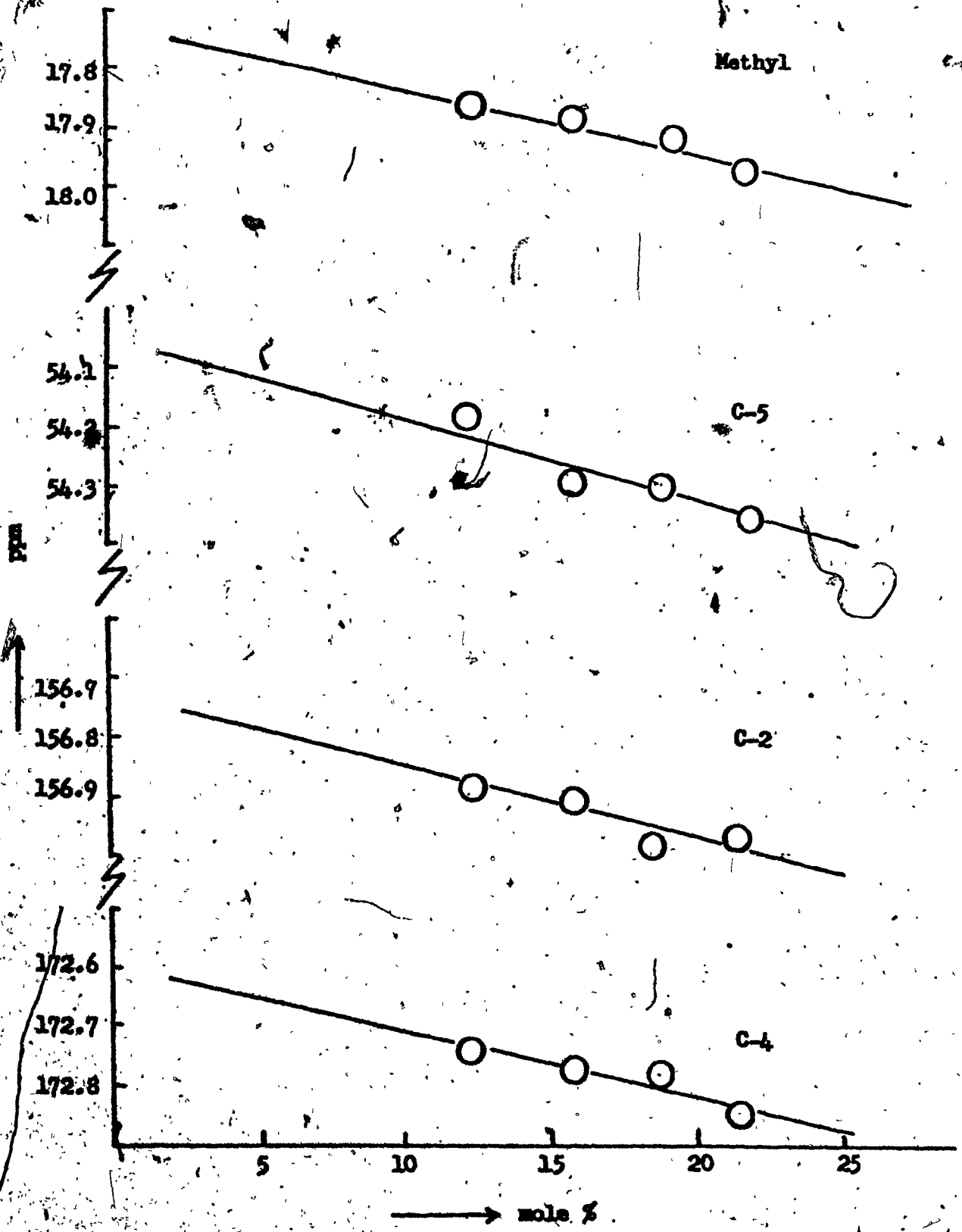

Figure II-6 : Dependence on Concentration of the Carbon Shieldings of 1-(o-Tolyl) Hydantoin (II) in Morpholine.

but the concentration dependence is about three times smaller, being 0.01 ppm per mole % in morpholine, compared to 0.03 ppm per mole % in DMSO. Thus it is evident that morpholine is preferable to DMSO in this respect. Since the magnitude of the concentration effect on each carbon is the same, and the concentration dependence falls within the limits of experimental error, one would expect to correlate the C-13 shifts for 1-aryl hydantoins in morpholine independently of the concentration effects.

Solvent Effects:

In contrast to the extensive investigation of solvent effects on proton chemical shifts, comparatively little attention has been paid to such effects on the chemical shifts of carbon nuclei. A large proportion of C-13 nmr studies in the literature do not include solute-solvent interactions in their data and correlations so that the choice of solvent has generally been dictated by practical rather than theoretical considerations, especially in the area of structural elucidation problems.

In addition to the quantum chemical discussion of solvent effects on carbon shieldings by Buckingham et al[40], other workers[42] have indicated the potential usefulness of carbon

shifts when applied to structural assignments, studies of solute-solvent associations, and other areas. Stothers and Lauterbur[39] and Maciel and Natterstad[4], reported C-13 shifts of the carbonyl carbons in a large number of compounds as a function of solvent. In addition, some earlier C-13 shift studies indicated the uncertainties involved in the interpretation of results without a knowledge of the solvent effects.

Thus the solvent effects in aryl hydantoins will be discussed prior to any further correlation of the C-13 nmr data. The applicability of morpholine as a solvent for the C-13 nmr study of hydantoins has enabled comparison with the carbon shifts in the strongly polar solvent DMSO. Table II-7 lists the C-13 chemical shifts of 1-phenyl hydantoin, I_o, in morpholine and in DMSO. A downfield shift of 3 ppm of the carbonyl carbons, compared to about a 1 ppm downfield shift of the C-5 and aryl carbons, is observed in morpholine. These results reflect the far greater importance of a change in solvent than change in concentration on the carbon-13 shieldings of hydantoins.

The shielding of the carbonyl carbons is most severely affected in changing from morpholine to DMSO, relative to the other parts of the molecule. Carbonyl solvent shifts in aprotic solvents show a general trend towards lower field

Table II-7: Carbon Shieldings[a] of 1-Phenyl Hydantoin (Io) in Dimethylsulfoxide (DMSO) and in Morpholine Solutions

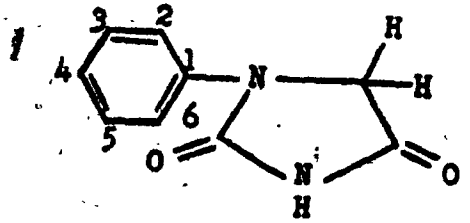

Solvent	C-5	C-2	C-4	1	2	3	4	5	6
Io DMSO	50.8	154.6	169.8	137.9	117.4	128.3	123.3	128.3	117.4
Io Morpholine	52.0	157.6	172.8	139.3	118.8	129.5	123.8	129.5	118.8

[a] ppm from TMS

with increasing solvent polarity, while in protic solvents, the increasing hydrogen bonding deshields the carbonyl carbon. Morpholine is expected to be less polar than DMSO, but it possesses an amine hydrogen. Therefore the low field shifts of the carbonyl carbons in morpholine can be attributed to a hydrogen bonding effect.

An investigation of the contributions to nuclear screening from the molecular interactions of the morpholine and the DMSO solvent molecules could clarify the differences between the carbon-13 shieldings of hydantoins in both solvents. The screening contribution due to the presence of a solvent is expressed with four different terms by Buckingham, Schaeffer and Schneider.[40]

$$\sigma_{solvent} = \sigma_b + \sigma_a + \sigma_W + \sigma_E$$

The bulk magnetic susceptibility effect, σ_b, depends upon the shape of the sample in the external field and is zero for a sphere. Because the same sample shape was used, the change in bulk magnetic susceptibility between DMSO and morpholine will be zero, or $\Delta\sigma_b=0$.

Anisotropy in the susceptibility of the solvent molecules, σ_a, causes high field shifts of solute molecules in solvents when they are disk-shaped molecules with large diamagnetic anisotropies. A reversed effect on the induced magnetic moment in rod-shaped solvent molecules leads to low field

shifts of solute molecules[40]. Morpholine is a disk-shaped molecule but lacks the π electrons necessary to cause substantial diamagnetic anisotropy, such as occurs in the benzene ring. The low field shifts of hydantoins in morpholine shows the unimportance of the anisotropy contribution to the change of the nuclear screening of hydantoin carbons.

Van der Waals interactions between solute and solvent molecules perturb the electronic structure of the solute molecules, and the resulting distortion leads to a solvent-dependent nuclear screening constant, σ_W. It is quite difficult to interpret the relative influence of the van der Waals forces on the carbon chemical shifts in complex molecules, such as aryl-substituted hydantoins. The distortions due to these interactions might be expected to be higher in DMSO, since the relatively small DMSO molecules could closely approach the nuclei of the hydantoin molecule and diminish the diamagnetic screening by electron attraction, thereby causing a deshielding effect on the carbon nuclei. The observed upfield shifts in DMSO might suggest that either a major contribution due to polar effects, σ_E, cancels the σ_W effect, or that competing van der Waals interactions in morpholine outweigh the σ_W effect of DMSO.

The polar effect caused by the charge distribution in the neighbouring solvent molecules leading to an electric field, E, acting on the solute, and thereby perturbing its electronic structure and nuclear screening constant, σ_E, could introduce a shielding or deshielding effect depending on the position of the nucleus relative to the polar groups in the solvent molecule. A reversal of the electric field in changing from DMSO to morpholine may have contributed to the downfield shifts in morpholine. The polarising electric field of the solvent acting along the axis of a H-C bond of the solute tends to draw electrons away from the carbon, thus causing a shift to low field. The opposite sign for E causes high field shifts, as expressed in the equation below.[40]

$$\sigma_E = 2 \times 10^{-12} E_z - 10^{-18} E^2$$

where E_z is the component of the total field E along the H-C bond. Structural differences between morpholine and DMSO might have resulted in reversal of the sign of E_z during solvation, whereby a positive or less negative E_z could have caused the downfield shifts of carbon resonances in morpholine.

The 1 ppm chemical shift differences of the C-5 and aryl carbons in DMSO and morpholine can be attributed largely to

polar solvent effects, since a similar magnitude for the σ_E contribution has been found by Buckingham[40] for cyclohexane compared to nitrobenzene. However, the 3 ppm downfield shifts of the carbonyl carbons cannot be explained by the σ_E term. Hydrogen bonding between the carbonyl oxygen and the amine hydrogen of morpholine must have influenced the carbonyl carbon shifts. Maciel and Natterstad[41] have demonstrated that carbonyl carbon shifts in simple ketones display great sensitivity to the environment if proton donors are present.

$$\text{C} = \text{O} + \text{H} - \text{X} \rightleftharpoons \text{C}^{+} - \text{O} \ldots \text{HX}^{-} \rightleftharpoons \text{C}^{+} - \text{OH} + \text{X}^{-}$$

As shown in the above equilibrium, hydrogen bonding deshields the carbonyl carbon. Lichter and Roberts[42] suggested that the dominant paramagnetic term of C-13 shieldings, σ_p which is proportional to the mean excitation energy, ΔE, and the 2p atomic orbital dimension, $\langle r \rangle_{2p}$, could produce the substantial downfield shifts observed, through a decrease in the average orbital radius r. (See page 114). A similar type of mechanism involving the carbonyl carbons is expected to be valid in the case of morpholine.

In summary, the polarity and proton donor ability of the solvent molecules have pronounced effects on the carbon shieldings of hydantoin molecules. Thus care must be taken when correlations are performed on chemical shift data which have been obtained in various solvents.

Correlations of C-13 Chemical Shifts in Hydantoins

All the groups of corresponding carbons (C-5, C-5 methyl, carbonyl, aromatic, aryl-methyl) in 1-aryl hydantoins are discussed with respect to conjugation, and inductive, steric and polar interactions. The results are compared with the C-13 data in the literature and reported by Williams[16] for the 3-aryl hydantoins, always taking into account the solvent shift effects. Following the discussions on the information obtained an overall summary and conclusion is given.

The C-13 chemical shift data which were measured by Williams[16] for 3-aryl hydantoins in DMSO have been converted to the TMS scale. For comparison, chemical shift differences - from DMSO to morpholine - of 3 ppm for the carbonyl carbons and 1 ppm for the other carbons are introduced into the shielding data of the 3-aryl hydantoins in this thesis. A correction factor of 0.6 ppm has been introduced into the chemical shift values of the 3-aryl hydantoins, for consistency with the literature data on the DMSO shift, which was assigned by Williams as 39.9 ppm from TMS. The more generally accepted value is 40.5 ppm.

C-5 Carbon-13 Chemical Shifts of Hydantoins:

The chemical shift values of the 1-aryl hydantoins and some of the previously studied 3-aryl hydantoins are shown in Tables II-8 and II-9.

Table II-8 : The C-5 Carbon Shieldings[a] of the 1-Aryl Hydantoins in Morpholine

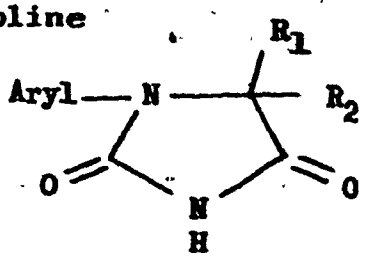

Hydantoin	Aryl	R_1	R_2	C-5
I_o	Phenyl	H	H	52.0
II	o-Tolyl	H	H	54.5
V	o-Chlorophenyl	CH_3	H	59.7
VI	o-Tolyl	CH_3	H	60.1
VIII	2,3-Dimethylphenyl	CH_3	H	60.6
XII	o-Chlorophenyl	CH_3	CH_3	65.9
XIII	o-Tolyl	CH_3	CH_3	65.8
XIV	α-Naphthyl	CH_3	CH_3	66.0
XV	β-Naphthyl	CH_3	CH_3	65.5
XVI	o-Fluorophenyl	CH_3	CH_3	65.4
XVII	o-Methoxyphenyl	CH_3	CH_3	65.4
XVIII	2,3-Dimethylphenyl	CH_3	CH_3	65.1

[a] ppm from TMS

Table II-9 : The C-5 Carbon Shieldings[a] of some 3-Aryl Hydantoins.[16]

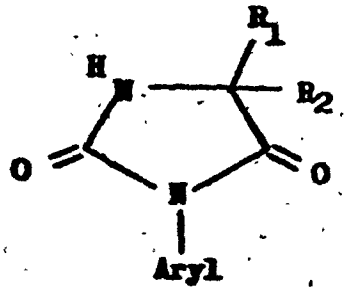

Hydantoin	Aryl	R1	R2	C-5
3-I	o-Chlorophenyl	H	H	47.2
3-II	o-Chlorophenyl	H	CH_3	53.3
3-III	o-Tolyl	H	CH_3	53.6[b]
3-IV	Phenyl	CH_3	CH_3	58.6
3-V	o-Chlorophenyl	CH_3	CH_3	59.2
3-VI	o-Tolyl	CH_3	CH_3	59.0
3-VII	α-Naphthyl	CH_3	CH_3	59.4

[a] ppm from TMS [b] center of doublet, $\Delta\delta$ = 0.1 ppm.

The C-5 carbon signal in 1-aryl hydantoins is shifted about 6.5 ppm to low field, relative to 3-aryl hydantoins This deshielding influence in 1-aryl hydantoins is attributed to the β effect of the aryl carbon.

In both series the C-5 chemical shift values fall mainly into three groups, corresponding to the number of substituents at the C-5 position. However the hydantoin I_o, which lacks a bulky orthosubstituent, may be excluded from the first group. The C-5 carbon signal of this compound is shifted upfield by 2.5 ppm from the shielding value of 1-(o-tolyl) hydantoin, II. The 54.5 ppm shielding of the C-5 carbon in I could not be rationalized in terms of steric interactions. On the other hand, increasing conjugation accompanying a decrease in the dihedral angle between the aryl and hetero rings could result in shielding of the C-5 carbon. However, a better explanation for the downfield shift of the 5-carbon signal might be based on the δ-effect recently proposed by Stothers.[80] The C-5 carbon of 3-phenyl-5,5-dimethyl hydantoin, 3IV, experiences only a 0.4 ppm upfield shift effect from the ortho tolyl substituted hydantoin, 3VI. This is to be expected, since the C-5 carbon is further away from the aryl ring and may well be insensitive to the shielding contribution due to conjugation.

Lauterbur[48] has reported an increasing deshielding effect in N,N-dimethyl anilines as the ortho hydrogen is replaced with a methyl group, which is consistent with the data for 1-aryl hydantoins.

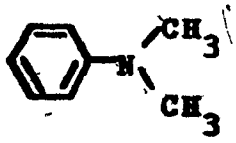

$\delta_c^{CH_3}$ = 41.1 ppm

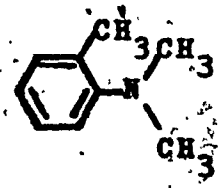

$\delta_c^{CH_3}$ = 45.2 ppm

Stothers[32] rationalized the above observation by assuming that electron release from the ring to the nitrogen nucleus is reduced in the hindered form, thus increasing the polarization of the N-CH_3 bond. The N-methyl carbons of unhindered N,N-dimethyl m-toluidine absorb consistently at 40.9 ppm.

The relative insensitivity of the C-5 carbons to the ortho substituents in 3-aryl hydantoins and the increasing deshielding effect with increasing bulkiness of the ortho substituents in the 1-aryl hydantoins V,VI and VIII, where the C-5 chemical shift values are 59.7, 60.1 and 60.6 ppm, respectively, is consistent with the above hypothesis.

The shielding of the C-5 carbon in XV by 0.5 ppm from the 66.0 ppm shift value of the α-naphthyl substituted hydantoin, XIV could be attributed to δ-effect.

The C-5 carbon chemical shifts of hydantoins XII, XVI, and XVII with the polar ortho chloro, fluoro, and methoxy moieties, respectively, appear insensitive to the steric influence of the aryl substituent. An upfield shift of 0.5 ppm in XVI and XVII relative to XII might indicate the difference in the value of the δ-effect with various polar ortho substituents. It is expected that the polarity of the ortho substituent would contribute to the shielding of the C-5 carbon. The dominance of steric and δ-effects on C-5 carbon shielding and the relatively minor variations introduced by polar ortho aryl substituents creates difficulty in the interpretation of polar effects.

In summary, the variations in the shielding values of the C-5 carbon are dominated largely by the δ-effect. The conjugation shielding contribution could not be correlated with the twist angle, due to complications arising from δ-effects. It is expected to make a negligibly small contribution to the overall changes of the C-5 carbon chemical shifts.

Separate signals from the non-equivalent C-5 carbons of the diastereomeric 3-aryl hydantoins, 3II and 3III were observed at normal probe temperature[16] (~55°C), but the lower barriers to hindered rotation in the corresponding 1-aryl hydantoins, V, VI and VIII, prevented a similar observation. All the C-5 carbon signals were observed as singlets in the 1-aryl hydantoin spectra.

Additive α-Methyl Shift Parameters:

Methyl substituents on the C-5 carbons cause substantial low field shifts of the C-5 signal due to through bond inductive effects. Table II-10 lists the chemical shift differences in 1-aryl and 3-aryl hydantoins caused by methyl substitution. Values of $\Delta\delta$ are calculated for the hydantoins with identical aryl substituents. The α-methyl substituent shifts, for the addition of two successive methyls to the C-5 carbon, do not seem to vary for different ortho aryl substituents. Therefore,

Table II-10: The C-5 Carbon Additive Shift Parameters[a] of some 1-Aryl Hydantoins and 3-Aryl Hydantoins.[16]

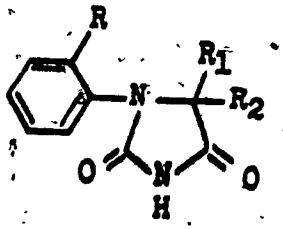

II R=CH_3, R_1=R_2=H

V R=Cl, R=CH_3, R_2=H

VI R=R_1=CH_3, R_2=H

XII R=Cl, R_1=R_2=CH_3

XIII R=R_1=R_2=CH_3

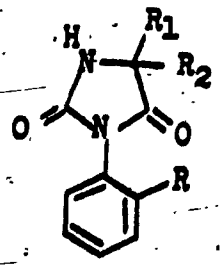

3I R=Cl, R_1=R_2=H

3II R=Cl, R_1=CH_3, R_2=H

3III R=R_1=CH_3, R_2=H

3V R=Cl, R_1=R_2=CH_3

3VI R=R_1=R_2=CH_3

Hydantoin	$\Delta\delta$C-5	Hydantoin	$\Delta\delta$C-5
II - VI	5.6	(3-I) - (3-II)	6.1
VI - XIII	5.6	(3-II) - (3-V)	5.9
V - XII	6.2	(3-III) - (3-VI)	5.4

[a] ppm

an average value of 5.8 ppm can be taken as the additive α-methyl shift parameter on the C-5 carbon of hydantoins.

This parameter is somewhat smaller than the α-methyl substituent shift on a secondary carbon, 9.1 ppm, calculated by Grant and Paul[37]. This difference can be justified in the sense that the C-5 carbon is bonded to an electron attracting nucleus, the N-1 nitrogen, and thus the effect of release of electrons by an α-methyl substituent is reduced. The addition of a second methyl substituent results in a 6.1 ppm shift in linear alkanes[37], which is closer to the value obtained for the hydantoins.

C-5 Methyl Carbon-13 Chemical Shifts of Hydantoins.

Tables II-11 and II-12 show the chemical shift values of the C-5 methyl carbons in the 1-aryl hydantoins and some 3-aryl hydantoins. The first striking feature is that the C-5 methyl carbons from either enantiomeric or diastereomeric rotamers of hydantoins showed distinguishable peaks only when the barriers to hindered rotation were sufficiently high that rates of rotation were slow at the probe temperatures. The 1-aryl hydantoins of Table II-11, XII, XIII, XIV and XVIII, and the 3-aryl hydantoins of Table II-12 with C-5 methyl carbon doublets, were known to have high coalescence temperature, from pmr line shape analysis. The methyl proton peaks from the ground state conformations of the rotational isomers were found to be distinguishable at normal probe temperatures.

Table II-11: The C-5 Methyl Carbon Shieldings of the 1-Aryl Hydantoins in Morpholine

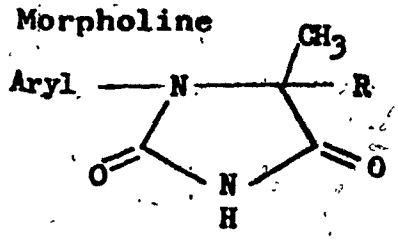

Hydantoin	Aryl	R	C-5 Methyl	
V	o-Chlorophenyl	H	17.9	
VI	o-Tolyl	H	15.7	
VIII	2,3-Dimethylphenyl	H	14.6	
XII	o-Chlorophenyl	CH_3	22.49	24.75
XIII	o-Tolyl	CH_3	22.38	25.05
XIV	α-Naphthyl	CH_3	22.94	24.72
XV	β-Naphthyl	CH_3	24.1	
XVI	o-Fluorophenyl	CH_3	23.4	
XVII	o-Methoxyphenyl	CH_3	23.4	
XVIII	2,3-Dimethylphenyl	CH_3	22.22	25.01

[a] ppm from TMS

Table II-12: The C-5 Methyl Carbon Shieldings[a] of some 3-Aryl Hydantoins[16]

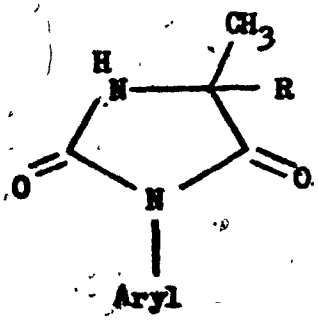

Hydantoin	Aryl	R	C-5	Methyl
3-II	o-Chlorophenyl	H	18.00	18.48
3-III	o-Tolyl	H	18.10	18.61
3-IV	Phenyl	CH_3	25.8	
3-V	o-Chlorophenyl	CH_3	25.13	25.93
3-VI	o-Tolyl	CH_3	25.42	26.12
3-VII	α-Naphthyl	CH_3	25.64	26.27

[a] ppm from TMS

This can be taken as evidence that the double carbon peaks also correspond to the ground state conformations of the rotamers. As further evidence, the C-5 methyl doublet, of 1-(o-chlorophenyl)5,5-dimethyl hydantoin, XII, was found to be broadened, indicating that the probe temperature was close to the coalescence temperature (T_c). The pmr coalescence temperature was found to be 58°C in pyridine. It is expected, as found in earlier studies[44], that the coalescence temperatures for H-1 and C-13 nuclei in these compounds could not differ drastically, (i.e. by not more than 10-20°C) and the coalescence temperature ranges could overlap for both nuclei. A detailed analysis on the non-equivalency of the isomeric carbons is given in the discussion of conformational analysis.

Table II-13 shows the chemical shift differences of the methyl carbons and protons in 1-aryl and 3-aryl hydantoins. Both $\Delta\delta_{C-13}$ and $\Delta\delta_{H}$ are higher in the 1-aryl hydantoins. An increase in the shielding contribution of the aryl ring could explain this result, since in the 3-aryl hydantoins the C-5 methyl groups are further away from the aryl ring so that the magnetic anisotropy difference is reduced.

The slightly lower $\Delta\delta_{C-13}$ of XII, 2.26 ppm, is due to partial collapse of the lines near the coalescence point. The 1 ppm decrease in the chemical shift difference of the α-naphthyl substituted hydantoin, XIV, ($\Delta\delta_{C-13}$ = 1.78 ppm) may be taken as evidence of the effect of anisotropy differences on the

Table II-13: The C-5 Methyl Carbon and Proton Chemical Shift Differences[a] of 1-Aryl Hydantoins and 3-Aryl Hydantoins[16]

1-Aryl Hydantoin	$\Delta\delta_C$	$\Delta\delta_H$	3-Aryl Hydantoin	$\Delta\delta_C$	$\Delta\delta_H$
XII	2.26[b]	0.26[c]	3-II	0.48[e]	0.04[c]
XIII	2.67[b]	0.27[c]	3-III	0.51[e]	0.04[c]
XIV	1.78[b]	0.32[d]	3-V	0.80[e]	0.06[c]
XVIII	2.79[b]	0.26[d]	3-VI	0.70[e]	0.04[c]
			3-VII	0.63[e]	0.08[c]

[a] ppm [b] in morpholine [c] in pyridine [d] in o-chloropyridine [e] in DMSO

Table II-14: The C-5 Methyl Carbon Additive Shift Parameters[a] of 1-Aryl Hydantoins and 3-Aryl Hydantoins[16]

1-Aryl Hydantoins	$\Delta\delta_{CH_3}$	3-Aryl Hydantoins	$\Delta\delta_{CH_3}$
V - XII	5.7	(3-II) - (3-V)	7.4
VI - XIII	8.0	(3-III) - (3-VI)	7.3
VIII - XVIII	9.0		

[a] ppm

non-equivalency of enantiotopic carbon atoms. The shielding difference between the geminal C-5 carbons is smaller when a naphthyl substituent is present. This is probably due to the flatter structure of the naphthyl group relative to the ortho substituted phenyl group, affecting the ground state conformation.

In both series of hydantoins the ratio of the C-13 chemical shift difference to the proton chemical shift difference, $\Delta\delta_{C-13}/\Delta\delta_{H}$ is about 10 (in units of ppm) for phenyl substituents, while in the naphthyl-substituted hydantoins XIV and 3VII, the ratio drops to 6 and 8, respectively. In units of Hz these ratios are divided by a factor of four, due to the change in frequency from proton to carbon nuclei. On the average, a twofold increase of the chemical shift differences (in Hz) of non-equivalent rotamers is evident in the C-13 spectra, suggesting that the coalescence temperatures would be higher for carbon resonances.

Since the C-5 methyl carbons lie out of the plane of hetero ring, shielding changes should be dominated largely by the steric interaction of the ortho aryl substituent and the β-effect of the additional C-5 methyl substituent. Shielding contributions from the hetero ring, such as conjugation, are expected to be much less important than in the case of the C-5 carbon.

It can be seen in Table II-11 that the chemical shift values of the 1-aryl hydantoins appear to be shielded in the order of increasing bulk effect of the ortho substituent, as is evident for the C-5 mono methyl-substituted hydantoins, V, VI and VIII. The methyl carbons absorb at 17.9, 15.7 and 14.6 ppm, respectively. Another example of the steric effect, may be seen with the α- and β-naphthyl-substituted hydantoins XIV and XV. The decreased influence of the bulk effect for the β-naphthyl substituted hydantoin shifts the methyl carbons by 0.7 ppm to low field.

The C-5 methyl carbon shieldings of the 5,5-dimethyl substituted hydantoins, XII, XIII and XVIII, with bulky ortho aryl substituents appear insensitive to the ortho aryl substituent. The average shift values of the methyl doublets are 23.6, 23.7 and 23.6 ppm, respectively. The lack of hydrogen atoms on the C-5 methyl carbon may be responsible for this observation.

The shieldings of the C-5 methyl carbons in the 1-aryl hydantoins with the polar ortho aryl substituents chlorine,

fluorine and methoxy, i.e. XII, XVI and XVII, show a small deviation from those of the non-polar o-tolyl substituted hydantoin XIII. In both hydantoins XVI and XVII, the methyl carbons absorb at 23.4 ppm, while the average value for the chemical shifts of the C-5 methyl doublets in XIII is 23.6 ppm. The average chemical shift value of the C-5 methyl carbons in the non-polar o-tolyl substituted hydantoin XII is 23.7 ppm. About a maximum of 0.3 ppm upfield shift in polar, ortho aryl substituted hydantoins may be explained through polar effects, as with the C-5 carbon shieldings.

The polar groups in intermolecular systems build up electric fields, and the directional orientation of the neighborhood nuclei to these polar electric fields would thus lead to upfield or lowfield shifts. Polar ortho aryl substituents seem to cause slight upfield shifts on the C-5 carbon and C-5 methyl carbons (0.3 ppm).

It is evident from Table II-12 that the C-5 methyl carbon shieldings of 3-aryl hydantoins are not sensitive to the nature of the ortho aryl substituents. With respect to measurement precision, the C-5 methyl carbon shieldings are quite similar and seem not to be affected by polarity or bulk of the ortho aryl substituent. This result can be attributed to the more distant placement of the aryl substituent from the C-5 position of the hetero ring in 3-aryl hydantoins.

Additive β-Shift Parameters of C-5 Methyl Carbons:

In both Tables II-11 and II-12, the C-5 methyl carbon signals are seen to fall into two distinct groups, corresponding to the number of methyls at the C-5 position. The downfield shifts of the methyl carbons in 5,5-dimethyl hydantoins with respect to 5-monomethyl hydantoins, are attributed to dominant through-bond inductive effects or, as they are called by Grant and Paul, β-effects. Table II-14 lists the chemical shift differences of the methyl carbons in 1-aryl and 3-aryl hydantoins with identical aryl substituents.

In contrast to the additive α-shift parameters of the C-5 carbon, the β-shift parameters of the C-5 methyl carbons of the 1-aryl hydantoins differ from those of the 3-aryl hydantoins. This is expected since the C-5 methyl carbons in 1-aryl hydantoins undergo intense steric interaction with the bulky ortho aryl substituent. The steric influence would differ in the C-5 dimethyl and C-5 monomethyl-substituted hydantoins, due to differences in the steric crowding of the methyl groups.

A value of 7.2 ppm was found by Grant and Paul[37] for β-methyl substituent shifts on the addition of a second methyl to a tertiary carbon atom in linear alkanes. This parameter is equal to the shift difference obtained with the 3-aryl hydantoins, where the intermolecular interactions on the

C-5 methyl carbons are minimized.

In the 1-aryl hydantoins a constant parameter could not be obtained, due to steric influences. It can be seen in Table II-14 that the additive shift effect varies between 5.7-9.0 ppm, depending on the ortho aryl substituent.

Carbonyl Carbon Shieldings:

The chemical shifts of the C-2 and C-4 carbonyl carbons of the 1-aryl hydantoins and some previously studied hydantoins are shown in Tables II-15 and II-16.

In both series it is expected that shielding of the C-2 carbonyl would be affected by conjugation, through-space steric interactions, and the polarity contribution of the ortho aryl substituent. Any variations in the C-4 carbonyl carbon shielding would be caused largely by the through-bond inductive effects of the C-5 methyl substituents. In the 3-aryl hydantoins, the inductive effects could be relatively less important due to through-space interactions with the neighbouring aryl moiety.

An unusual feature is that both the C-2 and C-4 carbonyl shieldings remain almost unaffected by the degree of conjugation with the aryl group, especially when the ortho aryl substituents are non-polar. As the ortho hydrogen is replaced by a methyl group in hydantoins I_o and II, the C-2

Table II-15 : Carbonyl Carbon Shieldings[a] of the 1-Aryl Hydantoins in Morpholine Solution.

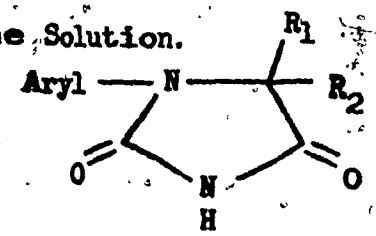

Hydantoin	Aryl	R_1	R_2	C-2	C-4
I.	Phenyl	H	H	157.6	172.8
II	o-Tolyl	H	H	157.1	173.0
V	o-Chlorophenyl	CH_3	H	157.0	176.5
VI	o-Tolyl	CH_3	H	156.2	176.3
VIII	2,3-Dimethylphenyl	CH_3	H	157.0	177.0
XII	o-Chlorophenyl	CH_3	CH_3	156.0	179.4
XIII	o-Tolyl	CH_3	CH_3	155.4	178.9
XIV	α-Naphthyl	CH_3	CH_3	156.7	179.5
XV	β-Naphthyl	CH_3	CH_3	157.0	179.3
XVI	o-Fluorophenyl	CH_3	CH_3	156.5	179.3
XVII	o-Methoxyphenyl	CH_3	CH_3	156.0	179.2
XVIII	2,3-Dimethylphenyl	CH_3	CH_3	155.7	179.0

[a] ppm from TMS

Table II-16: Carbonyl Carbon Shieldings[a] of some 3-Aryl Hydantoins[16]

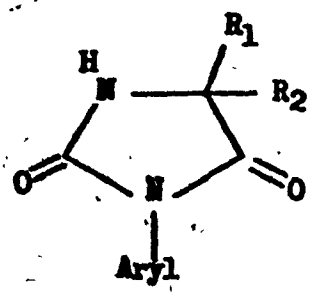

Hydantoin	Aryl	R1	R2	C-2	C-4
3-I	o-Chlorophenyl	H	H	158.5	173.2
3-II	o-Chlorophenyl	H	CH_3	157.4[b]	176.6
3-III	o-Tolyl	H	CH_3	158.2	176.9
3-IV	Phenyl	CH_3	CH_3	157.2	179.3
3-V	o-Chlorophenyl	CH_3	CH_3	156.3	178.6
3-VI	o-Tolyl	CH_3	CH_3	157.1	179.3
3-VII	α-Naphthyl	CH_3	CH_3	157.7	180.2

[a]ppm from TMS [b]center of doublet, $\Delta\delta$ =0.12 ppm

and C-4 carbonyl carbons experience a 0.5 ppm upfield shift and a 0.2 ppm downfield shift, respectively. The increased shielding of the C-2 carbonyl might be attributed to steric perturbation. In the 3-aryl hydantoins (3IV and 3VI), substitution of a similar type does not give rise to any shielding contribution on the C-2 and C-4 carbonyls that is observable within the limits of experimental error. The conjugation effect is negligibly small in the case of hydantoins XIV and XV, with α and β-naphthyl substituents, respectively. The C-4 carbonyl carbon of the β-naphthyl compound is shielded by only 0.2 ppm, while the C-2 carbonyl carbon is deshielded by 0.3 ppm compared to the C-2 and C-4 carbonyl carbon chemical shifts in the α-naphthyl substituted hydantoin XIV, although a substantial decrease in the dihedral angle is expected.

Stothers et al[49] have found that, Table II-17, both non-polar and polar bulky ortho aryl substituents cause pronounced deshielding of the carbonyl carbons of methyl-aryl ketones. Decreasing conjugation associated with an increase in the van der Waals radius of the ortho substituent deshields the carbonyl carbon by up to 4 ppm. However, this relation between the carbonyl shielding and the dihedral angle (i.e. bulk effect) is not applicable to hydantoins. The insensitivity to conjugation may be rationalized by the presence of 8 π-electrons (the lone-pair electrons of N-1 and N-3, and the π-electrons of the carbonyl groups) in the hydantoin ring. Through amide type

Table II-17: Carbonyl Carbon Shieldings[a] in some Ketones [147]

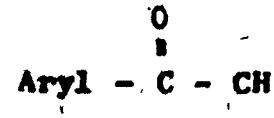

Aryl	$\delta_{C=O}$
Phenyl	196.0
o-Methoxyphenyl	197.8
o-Chlorophenyl	198.7
o-Bromophenyl	199.3
o-Tolyl	199.3
2,3-Dimethylphenyl	200.6
α-Naphthyl	199.5
β-Naphthyl	195.8

[a] ppm from TMS.

resonance, contributions which are stabilized by polar solvent molecules, the carbonyl carbons should have quite a high π-electron density. Therefore the carbonyl carbons would not encourage the release of π-electrons from the aryl ring. The upfield shifts of the hydantoin carbonyl carbons compared to the ketones of Table II-17 indicate that a higher overall charge density occurs primarily in the hetero ring, with respect to that in non-cyclic alkyl-aryl ketones.

The addition of polar ortho aryl substituents in hydantoins produces somewhat different results in the 1-aryl and the 3-aryl series. For hydantoins 3II and 3V, replacement of the ortho methyl group with a chlorine atom shifts the C-2 and C-4 carbonyl carbon signals upfield 0.8 - 0.3 ppm and 0.8 - 0.7 ppm, respectively. Williams[16] suggested that the shielding increase associated with the o-chloro substituent, is due to an increase of the dihedral angle, since a chlorine atom is effectively larger than a methyl moiety in 3-aryl hydantoins. He gives a relative order of bulk effect which is reversed compared to that of the alkyl-aryl ketones.

The carbonyl carbon shieldings of 1-aryl hydantoins with polar ortho substituents are found to differ in an opposite manner. In 1-aryl hydantoins a chlorine atom is found to be effectively smaller than a methyl group and the C-2 carbonyl

carbon is deshielded 0.8 and 0.6 ppm in the o-chloro substituted hydantoins V and XII, from those in o-tolyl substituted hydantoins VI and XIII, respectively. With a less bulky o-fluoro substituent, XVI, deshielding reaches 1.1 ppm. However, in contrast, the o-methoxy substituent, which is effectively less bulky than a chlorine atom causes a shielding effect on the C-2 carbon in XVII which is similar in magnitude to that of XII. In all cases shielding of the C-4 carbon remained unaffected by the polar substituents.

The relatively minor shielding changes on the carbonyl carbons with various polar ortho substituents and differences in the order of bulk effects serve to point out that different types of polarity mechanism are involved, in the 1-aryl and 3-aryl hydantoins, rather than a general bulk effect versus a conjugation-dihedral angle relation.

In order to avoid a through-space repulsive interaction with the carbonyl group, a polar substituent is expected to be closer to the C-5 carbon than to the carbonyl group in the ground state conformations of 1-aryl hydantoins. Thus the most important electronic factor which would influence the C-2 carbonyl carbon shielding is a through-bond inductive effect. It seems that the carbonyl carbon is deshielded in line with the electron withdrawing ability of the ortho aryl substituent.

The δ-effect of the ortho aryl substituent would have been expected to cause an upfield shift of the C-2 carbon signals. The unexpected direction of the shifts indicates the difficulty in interpretation of these values.

Levy and Nelson [33,50] have reported a similar type of polar aryl substituent effect in acetamides, where

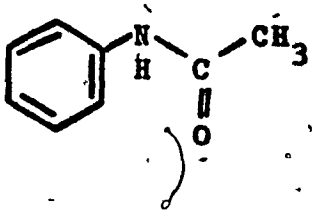

$\delta_{C=O}$ = 168.3 ppm

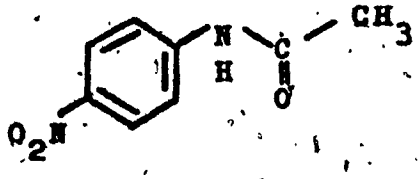

$\delta_{C=O}$ = 169.2 ppm

a 0.9 ppm low field shift also cannot be explained by the electron withdrawing or mesomeric effect of the polar nitro substituent. As with hydantoins, Williams[16] found that the non-polar ortho methyl substituent does not introduce any shielding effect on the carbonyl carbon of N-phenyl ureas.

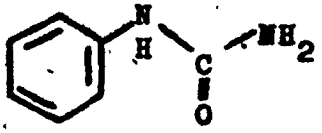

$\delta_{C=O}$ = 156.5 ppm

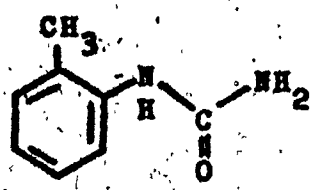

$\delta_{C=O}$ = 156.4 ppm

In 3-aryl hydantoins the ortho aryl substituent is located between two carbonyl oxygens. The carbonyl shielding changes are expected to be influenced by the through-space repulsive interactions of the polar ortho substituents, rather than by through-bond inductive effects. Repulsion of electrons from the carbonyl oxygen in the direction of carbonyl carbons would enhance the shielding on these carbons, as is experimentally observed. Polarization of the C=O bond by the polar substituent would depend on the strength of the electric field build-up by the ortho aryl substituent, and the distance from it to the carbonyl group, but not on the conjugation between the ortho substituent and carbonyl group.

In general, the shielding effects of ortho aryl substituents on carbonyl carbons are complicated by polar factors, through-bond inductive effects, and δ-effects. It seems rather difficult to give any quantitative correlation between the shielding data and the contributing factors, since the changes are rather small and influenced by various factors in an unpredictable manner.

Additive Shift Parameters of Carbonyl Carbons:

The most dominant effects on the shielding of carbonyl carbons are obtained with C-5 substitution. In both hydantoin series the addition of a methyl group to the C-5 carbon deshields

the C-4 carbon by about 3.3 ppm, while a second methyl causes downfield shifts of 2.0 - 2.9 ppm. These chemical shift differences are shown in Table II-18 for both series. The deshielding of the C-4 carbonyl carbon by the C-5 methyl substituent could be termed a β- effect.

The C-2 carbonyl carbons experience a γ-effect due to the C-5 methyls in all cases studied. An average upfield shift of -1 ppm is observed, as shown in Table II-18. In agreement with the results on hydantoins, Stothers[32] has reported a β-effect of 2 ppm and a γ effect of -1 ppm for acyclic ketones. Tarples and Goldstein[51] have reported β - and γ-effects in uracils A and B, although to a lesser degree.

A

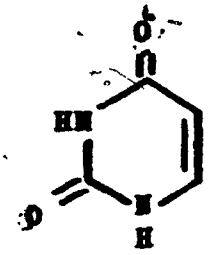

B

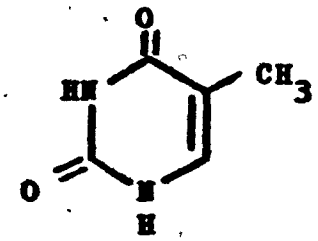

$\delta_{C=O}^{C-2}$ = 152.8 ppm

$\delta_{C=O}^{C-4}$ = 165.3 ppm

$\delta_{C=O}^{C-2}$ = 152.3 ppm

$\delta_{C=O}^{C-4}$ = 165.7 ppm

Table II-18: Carbonyl Carbon Additive Shift Parameters[a] of some 1-Aryl Hydantoins and 3-Aryl Hydantoins[16]

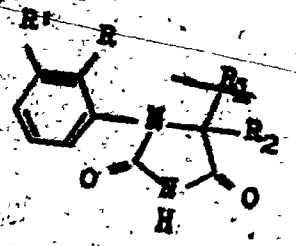

II R=CH_3, R'=R_1=R_2=H

V R=Cl, R_1=CH_3, R=R_2=H

VI R=R_1=CH_3, R'=R_2=H

VIII R=R'=R_1=CH_3, R_2=H

XII R=Cl, R_1=R_2=CH_3, R=H

XIII R=R_1=R_2=CH_3, R'=H

XVIII R=R'=R_1=R_2=CH_3

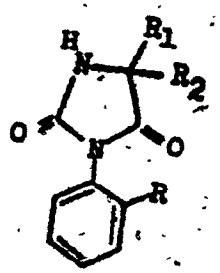

3I R=Cl, R_1=R_2=H

3II R=Cl, R_1=CH_3, R_2=H

3III R=R_1=CH_3, R_2=H

3V R=Cl, R_1=R_2=CH_3

3VI R=R_1=R_2=CH_3

Hydantoin	$\Delta\delta^{C-2}_{C=O}$	$\Delta\delta^{C-4}_{C=O}$
II - VI	-0.9	3.3
V - XII	-1.0	2.9
VI - XIII	-0.8	2.6
VIII - XVIII	-1.3	2.0

Hydantoin	$\Delta\delta^{C-2}_{C=O}$	$\Delta\delta^{C-4}_{C=O}$
(3-I) - (3-II)	-1.1	3.4
(3-II)-(3-V)	-1.1	2.0
(3-III) -(3-VI)	-1.1	2.4

[a] ppm

Aryl Carbon Chemical Shifts :

The carbon-13 chemical shifts of the aryl carbons in 1-aryl hydantoins are given in Table II-19. With two exceptions, all the carbons absorb in the range 110-140 ppm. The signal of the strongly deshielded aromatic carbon bonded to the methoxy oxygen atom in compound XVII is found at 158.1 ppm. In addition, the peak of the aryl carbon bonded to fluorine in XVI is expected to appear at ~164 ppm, as in fluorobenzene. This signal was not recorded.

Useful information about conjugation to the hetero ring or about the dihedral angle and intermolecular steric interactions could not be obtained from the shielding data of the aromatic carbons. Aryl carbon shieldings are most sensitive to perturbations caused by the electronic effects of the substituents. Thus it was not possible to detect the relatively small shielding or deshielding contributions of the heterocyclic ring.

The aryl C-13 chemical shift values of the unsubstituted 1-phenyl hydantoin, I_o were found useful in assigning the chemical shift data to the ring carbons in the other 1-aryl hydantoins. Figure II-7 shows the carbon-13 spectrum of the aryl carbons in I_o. The electron-withdrawing N-1 nitrogen substituent of the hetero-ring reduces the electron density on the C-1 carbon of the phenyl ring, so that it is deshielded to 139.3 ppm. Through-bond mesomeric effects increase the

Table II-19 : Aryl Carbon Shieldings[a] of the 1-Aryl Hydantoins in Morpholine

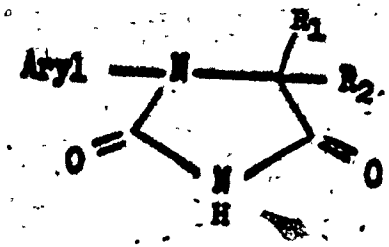

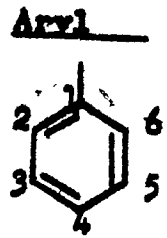

Hydantoin	Aryl	R_1	R_2	1	2	3	4	5	6
Io	Phenyl	H	H	139.3	118.8	129.3	123.8	129.5	118.8
II	o-Tolyl	H	H	136.7	131.4	136.4	127.6	128.1	127.1
V	o-Chlorophenyl	CH_3	H	134.1	130.8	133.6	129.8	133.6	128.3
VI	o-Tolyl	CH_3	H	137.5	131.6	135.3	128.3	138.3	127.2
VIII	2,3-Dimethylphenyl	CH_3	H	138.7	119.9	136.3	128.9	135.2	126.6

[a] ppm from TMS

Table II-19: (Cont.)

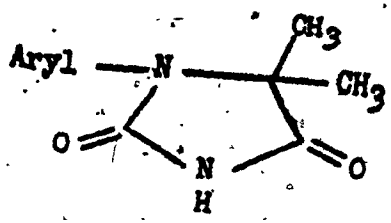

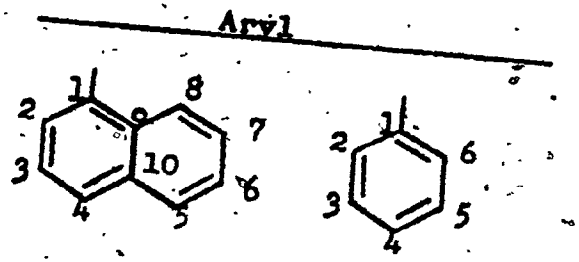

Hydantoin	Aryl	1	2	3	4	5	6	7	8	9	10
XII	o-Chlorophenyl		135.6	131.0	132.9	130.3	132.5	128.0			
XIII	o-Tolyl		138.9	130.3	133.8	128.8	130.3	126.7			
XIV	α-Naphthyl		135.1	124.2	129.6	125.8	128.8	126.7	126.7	127.1	131.9	132.9
XV	β-Naphthyl		128.1	134.1	127.2	132.9	128.4	127.0	127.0	129.3	133.5	134.1
XVI	o-Fluorophenyl	130.8	[b]		122.6	124.8	137.2	124.2			
XVII	o-Methoxyphenyl		131.8	158.1	113.2	130.1	123.9	121.1			
XVIII	2,3-Dimethylphenyl	138.6	130.1	137.4	128.0	133.6	126.0				

[b] not recorded

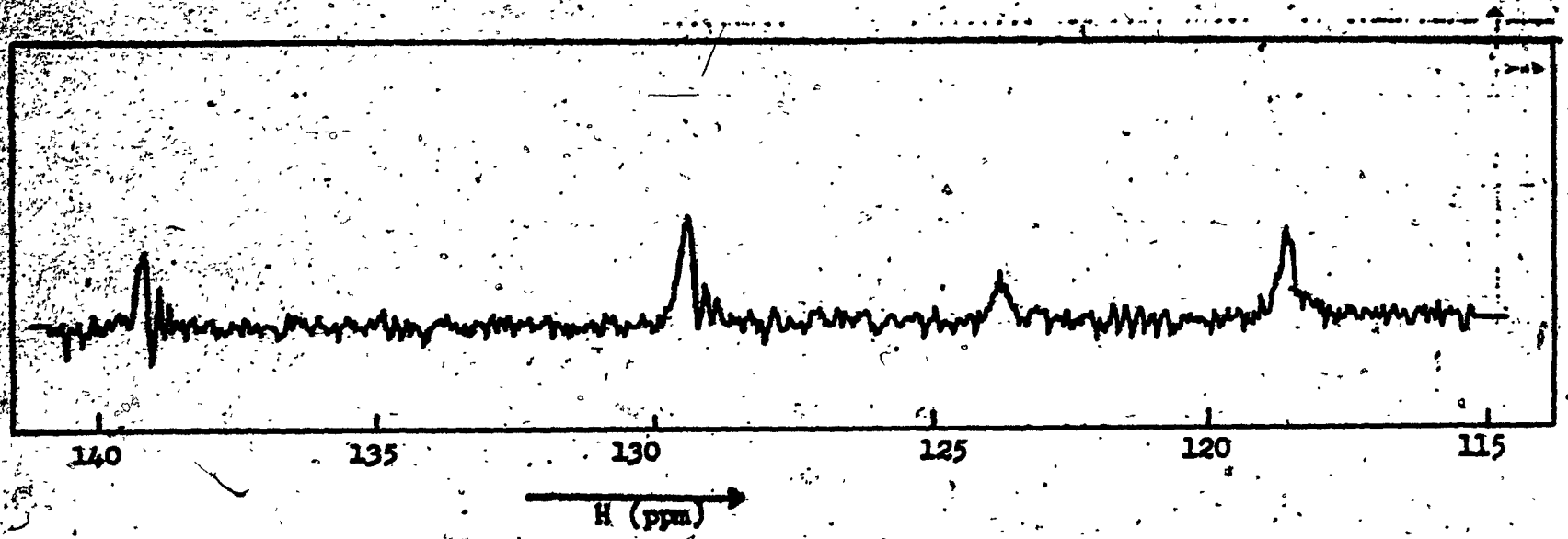

Figure II-7 : The Carbon-13 NMR Spectrum of the Aryl Carbons of 1-Phenyl Hydantoin (I_o) in Morpholine. (104 Scans).

shielding of the ortho and para carbons to 118.8 ppm and 123.8 ppm respectively, while the meta carbons are deshielded to 129.5 ppm, relative to the 128.7 ppm shielding of the benzene carbons.

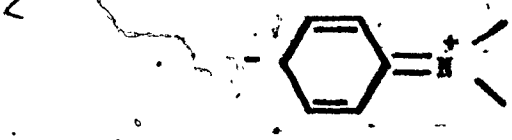

These results are in very good agreement with the carbon shielding data of acetanilide, reported by Maciel and Natterstad.[52]

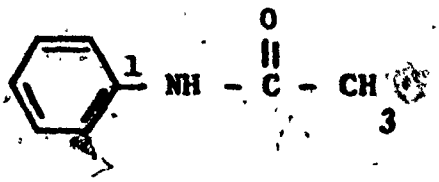

C - 1	Ortho	Meta	Para
139.8	118.8	128.9	123.1

Further ortho or meta substitution on the phenyl ring either shields or deshields the carbons, depending on the electron-withdrawing or electron-releasing ability of the substituent, so that interpretation of the chemical shifts becomes more complicated. Table II-20 lists the literature data[32] for aryl carbon shieldings in benzene with substituents similar to those in 1-aryl hydantoins. From a knowledge of the shielding effects of the ortho substituent and the N-1 nitrogen of the hydantoin, the relative order of the shielding contributions

Table II-20: Aryl Carbon Shieldings[a] in some Substituted Benzenes, $C_6H_{(5-n)}X_n$ [32]

	ppm from TMS				ppm from C_6H_6			
X	C-1	Ortho	Meta	Para	C-1	Ortho	Meta	Para
Hydantoin	139.3	118.8	129.5	123.8	10.6	-9.9	0.8	-4.9
CH_3	137.8	129.3	128.5	125.6	9.1	0.6	-0.2	-3.1
2,3-$(CH_3)_2$	136.4	136.4[b] 129.9[c]	129.9[d] 126.1[e]	126.1	7.7	7.7[b] 1.2[c]	1.2[d] -2.6[e]	-2.6
OCH_3	158.9	113.2	128.7	119.8	30.2	-19.5	0.0	-8.9
Cl	135.1	128.9	129.7	126.7	6.4	0.2	1.0	-2.0
F	163.8	114.6	130.3	124.3	35.1	-14.1	1.6	-4.4

[a] ppm from TMS

[b] ortho carbon 2

[c] ortho carbon 6

[d] meta carbon 3

[e] meta carbon 5

on each carbon in the aryl ring was calculated and the observed chemical shifts were assigned to the ring carbons, as shown in Table II-19.

In the case of naphthyl substituents, assignment of the C-13 carbon shifts became difficult due to lack of sufficient literature data. Carbon shielding data were given by Alger, Grant and Paul[53] for the unsubstituted naphthalene molecule. The α- and β carbons absorb at 128.6 ppm and 126.5 ppm respectively, while the quaternary carbons absorb at 133.9 ppm. For the hydantoins XIV and XV, the lowest field shift value was assigned to the carbon which is bonded to the nitrogen atom. The shieldings of the quaternary carbons (9,10) and the carbons of the unsubstituted ring (5,6,7,8) are expected to be similar to the shielding values of the unsubstituted naphthalene molecule. Chemical shifts, which are in agreement with the data for naphthalene, were assigned to these carbons. The remaining carbon chemical shifts were interpreted through comparison with the shielding data of I_o. The results are shown in Table II-19.

The only meaningful correlation which could be made between the aryl carbon chemical shifts and the hetero ring substitution pattern was a through-bond inductive effect of the C-5 methyls. In the series of ortho tolyl-substituted hydantoins II, VI and XIII, the C-1 aryl carbons are deshielded 0.8 and 1.4 ppm, respectively, by the successive addition of methyl groups to

the C-5 carbon. Similarly, the ortho chloro phenyl hydantoins V and XII show a downfield shift of 1.5 ppm on the addition of a 5-methyl group. When the phenyl ring is ortho-meta dimethyl substituted, the inductive effect is diminished, as in the case of hydantoins VIII and XVIII, where the C-1 aryl carbons absorb at 138.6 and 138.7 ppm, respectively.

Carbon Chemical Shifts of Methyl Groups Substituted on the Aromatic Ring:

Shielding data for methyl carbons on the aromatic ring are shown in Table II-21. The ortho tolyl methyls in hydantoins II, VI and XIII absorb in the range 18.1 - 18.5 ppm. In the 3-aryl hydantoins similar carbons absorb consistently at 17.9 ppm. The methoxy methyl carbon signal of XVII is shifted downfield to 56.1 ppm, due to the withdrawal of electrons by the oxygen atom. It is reported by Dhami and Stothers [54] that the methyl carbon of anisole absorbs at 54.0 ppm. The 2 ppm deshielding of the methyl carbon in XVII indicates that the methoxy moiety experiences electronic effects rather than steric shifts, due to the bending of the methyl group in the methoxy moiety in order to reduce steric hindrance. In confirmation of this, a relatively minor shielding variation is reported for o-methyl anisole[54], for which δ_{CH_3} = 53.7 ppm. Levy and Nelson[33] also report methoxy

Table II-21: Aryl Methyl Carbon Shieldings[a] of 1-Aryl Hydantoins

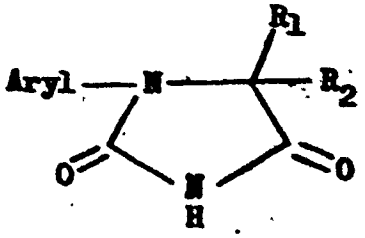

Hydantoin	Aryl	R_1	R_2	Methyl	
II	o-Tolyl	H	H	18.1	
VI	o-Tolyl	H	CH_3	18.1	
VIII	2,3-Dimethylphenyl	H	CH_3	15.7	20.4[b]
XIII	o-Tolyl	CH_3	CH_3	18.5	
XVII	o-Methoxyphenyl	CH_3	CH_3	56.0[c]	
XVIII	2,3-Dimethylphenyl	CH_3	CH_3	15.3	20.3[b]

[a]ppm from TMS [b]meta methyl [c]methoxy methyl

shifts of equal magnitude in ortho and para-dianisyl methanes.

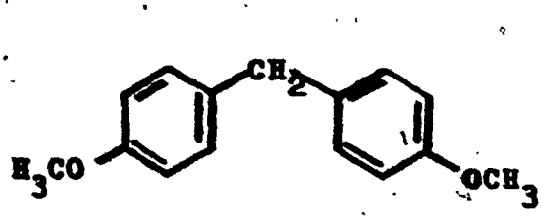

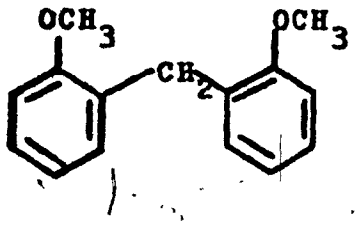

The ortho methyl carbons of the 2,3-dimethylphenyl substituted hydantoins VIII and XVIII are shielded 2.4 ppm and 3.2 ppm, respectively, with respect to the corresponding o-tolyl carbons. The upfield shifts can be attributed to the γ-effect of the meta methyl and steric effect of the C-5 methyl groups. The increased steric crowding of the C-5 position in XVIII caused a larger steric shift, compared to the C-5 position in VIII. A similar trend in upfield shifts was observed in methyl substituted anilines.

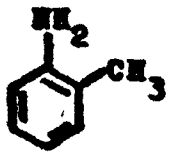

$\delta^{ortho}_{CH_3}$ = 18.2

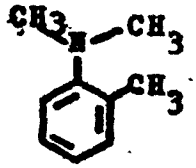

δ^{ortho}_{C} = 19.4 ppm

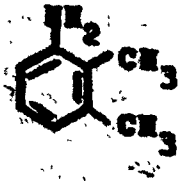

$\delta^{ortho}_{CH_3}$ = 13.6

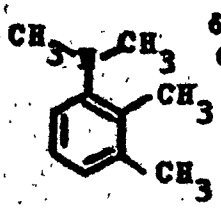

δ^{ortho}_{C} = 15.0 ppm

$\delta^{meta}_{CH_3}$ = 21.5

δ^{meta}_{C} = 21.7 ppm

The insensitivity of the non-polar methyl carbons to the steric, polar and inductive effects of the hetero ring (excluding XVIII) prevents one from forming stereochemical conclusions about the aryl hydantoin molecules based on the methyl chemical shift data. The chemical shifts of these carbons are influenced largely by the additional substituents on the aromatic ring, relatively minor correlations with hetero ring substituents being observable.

Conformational Exchange Analysis of Hydantoins:

Carbon-13 magnetic resonance is an alternative to proton nmr which under favorable circumstances offers one the possibility of calculating conformational inversion rates. The non-availability of a variable temperature C-13 probe precluded a kinetic study of the hydantoins by C-13 nmr. However, the proximity of the probe temperature to the coalescence point in one of the 1-aryl hydantoins (XII) permitted calculation of the rate constant and the free energy of activation from the C-13 data.

The C-5 methyl peaks of 1-(o-chlorophenyl)-5,5-dimethyl hydantoin, XII, are found to be broadened at probe temperature. Employing the rate constant equation, $k_b = \pi\delta$, of Anet and Bourn[44] for temperatures below coalescence, where the pair of lines are broad but not overlapping, a rate constant value

of 53.4 sec-1 was calculated.

The line width, δ , was found to be 17 Hz, following a correction of 5 Hz for the natural broadening due to magnetic field inhomogeneties and sweep rate broadening. The contribution of the transverse relaxation time, T_2, to the broadening was neglected, since it was expected to have a sufficiently large value.

The Eyring equation, $\Delta G^{\neq} = 2.303RT(10.319 + \log T - \log k)$, yielded a value of 16.7 kcal/mol for the rotational free energy of activation using the calculated rate constant and the estimated probe temperatures of 55°C.

This value is lower than the $\Delta G^{\neq}$ value found from the pmr line shape analysis study of XII, which was 17.7 kcal/mol in pyridine. The errors introduced into the calculation of in the C-13 study are higher. The primary source of error arises in the estimation of the temperature of the recorded spectrum. The probe temperature was measured at the maximum output of the heteronuclear decoupler by Williams, and found to be 55°C, but the accuracy is not expected to be better than ± 5°C. The line width measurements and the estimation of correction factors introduce an error limit of ± 5 sec^{-1} into the calculation of the rate constant. Thus the overall error would produce scatter in the value of $\Delta G^{\neq}$ of at least ± 1 kcal/mol. Therefore, within the limits of experimental

error, the free energy of activation from the proton and the carbon-13 study may be said to coincide with each other.

The chemical shift differences of the carbon-13 peaks are larger compared to the proton shifts of the rotamers. This result would be reflected in higher coalescence temperatures of the carbon resonances. The conformational inversion rate at the coalescence temperature is given by:

$$k_c = \pi\nu_{AB}/\sqrt{2}$$

where ν_{AB}, the chemical shift difference of enantiotopic carbon peaks, can be assumed to be equal for o-chlorophenyl and o-tolyl substituted hydantoins, based on the pmr results. Thus, using the chemical shift separation of 65 Hz for XIII, the rate constant equation yields a value of 14.3 sec^{-1}. One can calculate the coalescence temperature of the enantiomeric C-5 methyl carbons of XII in the $\Delta G^{\ddagger}$ equation, assuming that $\Delta G^{\ddagger}$ is 16.7 k cal/mole at the coalescence temperature. The calculation results in a value of 69°C for the coalescence temperature (T_c). The accuracy of the estimation is low, but an increase in the coalescence temperature is evident; from pmr spectra the T_c of XII was found to be 58° in pyridine solution.

The coalescence temperatures of some of the 3-aryl hydantoins were also in the region of the probe temperature, but a similar analysis could not be performed. The carbon chemical shift differences of 3-aryl hydantoins are too low (10-15 Hz), for one to measure reasonably accurate line widths independent of natural broadening, within the precision of the C-13 experiments.

In general, the exchange analysis of hindered rotation processes in hydantoins or similar heterocyclic structures by c.w. C-13 nmr could possess the following advantages and disadvantages.

- Even though the errors in the calculation of the thermodynamic parameters could be reduced by more careful temperature measurements, the overall errors are higher in conformational analysis of carbon resonances. The line width measurements of the carbon peaks are four times more inaccurate than for proton lines, due to the low S/N ratio and the accumulated sweep rate broadening. Considering the approximately two-fold larger chemical shift differences of the carbon peaks, the error limits for the free energies of activation may be estimated to be 0.2 - 0.3 kcal/mol, while pmr analysis gives maximum errors of 0.1 kcal/mol.

- In order to obtain the most accurate results, it is best to select the compound and solvents which will provide the highest shift differences between the non-equivalent isomeric nuclei. Such is the case for the 1-aryl and 3-aryl hydantoins.

-The coalescence temperatures of carbon resonances are higher than those of the corresponding proton resonances. Thus more accessible temperature ranges could be obtained in some cases.

-Undoubtedly the conformational exchange analysis results from carbon resonances may serve as better approaches for stereochemical assignments and correlations in many instances. However comparison of the thermodynamic parameters from both nuclei could prove to be of value.

SUMMARY

The carbon-13 nmr study of 1-aryl hydantoins has led to a number of interesting observations which are listed below:

a) Morpholine is found to be a good solvent and reference compound for the C-13 nmr study of these compounds.

b) The concentration dependence of aryl hydantoin carbon chemical shifts is negligible in morpholine solutions.

c) The solvent molecules have pronounced effects on the carbon shieldings of aryl substituted hydantoins. The shielding differences for the hydantoin carbons in DMSO and morpholine solutions are believed to be the result of the differences in polar effects and in hydrogen bonding of the carbonyl carbons in morpholine solution.

d) The C-5 carbon shieldings of the 1-aryl hydantoins are influenced by the α-effect of the C-5 substituents and the β-effects of the ortho aryl substituents. A mean value of 5.8 ppm is found for the additive α-methyl shift parameter of 1-aryl hydantoins and 3-aryl hydantoins.

e) Variation in the C-5 methyl carbon shieldings is introduced by the steric effect of the ortho aryl substituent and the β-effect of the C-5 substituent. Separate enantiotopic C-5 methyl carbon peaks are found to be observable in 1-aryl hydantoins with restricted rotation

f) The differences between the C-2 carbonyl carbon shieldings of the 1-aryl hydantoins are complicated by the inductive and the δ-effects of the polar ortho aryl substituent and the γ-effect of the C-5 methyl substituent, while variations in the C-4 carbonyl carbon shieldings are brought about by the β-effect of the C-5 substituent. The through-space interaction of polar ortho aryl substituents appears to influence the carbonyl carbon shieldings in 3-aryl hydantoins. A contribution to the shielding values of carbonyl carbons through conjugation was not evident in either series.

g) Conformational exchange analysis for the internal rotational processes about the C-N bond is found to be applicable to the carbon resonances of the 1-aryl hydantoins. Even though the estimated error limits by c.w. carbon-13 nmr methods in the calculation of the thermodynamic parameters are higher, relative to proton resonance calculations, valuable information could be obtained through a kinetic study of hindered rotation, providing a variable temperature carbon-13 nmr instrument was available. Pulse and Fourier transform carbon-13 nmr methods could yield more accurate values.

PART III

AN INVESTIGATION OF NON-EQUIVALENCY OF H-1 AND C-13 NUCLEI OF 1-ARYL HYDANTOINS IN A CHIRAL SOLVENT

INTRODUCTION

It has been recently demonstrated by Pirkle et al[55] that enantiomers, although exhibiting identical properties in achiral media, may be readily distinguished by nuclear magnetic resonance spectroscopy in appropriate optically active solvents. As a result of this observation, optical purities and absolute configurations of a variety of alchohols[56], α-hydroxy acids,[57] amines[58], sulfoxides[59], and α-amino acids [60] have been directly determined from the relative peak areas and senses of non-equivalence of the resonances of enantiotopic nuclei in chiral solvents.

The optically active solvent, phenyltrifluoromethylcarbinol, selected by Pirkle for these studies provides two advantageous features. First, it contains a

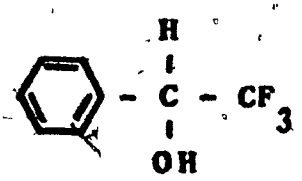

hydroxyl group capable of participating in the formation of strong intermolecular hydrogen bonds. Thus, a close contact between solute and solvent molecules can be provided. Second, the presence of the strongly anisotropic phenyl group enhances the difference in average magnetic environments of nuclei in enantiomers. In all the cases studied, short lived diastereomeric

solvates are formed in which the carbinol-solute hydrogen bonding is the principle mode of interaction. Thus in real terms enantiomeric nuclei of the solute or solvent molecules are diastereomeric and may exhibit distinguishable nmr spectra.

Other workers have also observed the spectral non-equivalence of the protons in enantiomers in an optically active solvent. Dale and Mosher[61] determined the stereochemical purity of diastereomeric esters of α-substituted phenylacetic acids. Mislow[62] has reported the magnetic non-equivalence of all corresponding protons in the enantiomeric isomers resulting from slow pyramidal inversion at nitrogen in 1,2,2-trimethylaziridine in optically active carbinol as solvent. Spectral dissimilarities of enantiomerically pure (-)-cocaine in the two enantiomers of methylphenylcarbinol were found by Jochius, Taigel and Seeliger[63]. Whiteside and Lewis[64] introduced chiral lanthanide shift reagents as probes to determine enantiomeric purity from pmr spectra. Also very recently Fraser, Stothers, and Tan[65] have demonstrated the magnetic non-equivalency of carbons of asymmetric carbinols and amines in chiral lanthanide shift reagents by C-13 nmr spectroscopy.

Hund[11] has made an attempt to apply the technique to the investigation of enantiomeric rotational isomers resulting

from restricted C-N bond rotation processes in the aryl substituted heterocyclic compounds which were studied in these laboratories previously. Resonance doubling for the ortho tolyl methyl protons of 3-(o-tolyl)-5,5-dimethyl hydantoin (3VI) was observed in (-)-phenyltrifluoromethyl-carbinol as solvent.

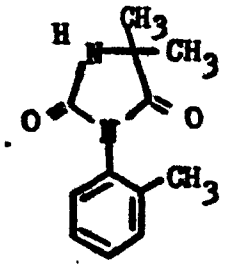

Since Hund observed this effect in only one compound, his data are not sufficient to yield any information on the structure of solute-solvent complex.

Upon observation of a similar result for 1-(o-tolyl) -5,5-dimethyl hydantoin, XVIII, namely, doubling of the tolyl methyl signal, the nmr study was extended to the series of 1-aryl hydantoins shown in Table III-1.

Table III-1: Aryl Hydantoins Studied in an Optically Active Solvent

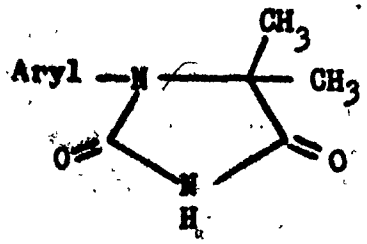

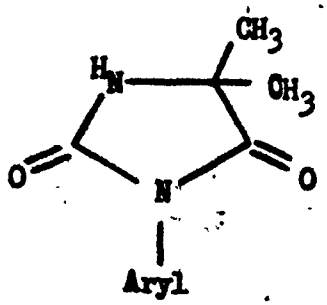

Hydantoin	Aryl
XIII	o-Tolyl
XVIII	2,3-Dimethylphenyl
XIX	2,4-Dimethylphenyl
XX	2,5-Dimethylphenyl
3VI	o-Tolyl

These compounds all have sufficiently high barriers to hindered rotation that diastereomeric interconversion of the solute-solvent complexes is slow on the nmr time scale. In consequence, total splitting of signals is observable. A total line shape analysis of XIII has been carried out in order to obtain the thermodynamic parameters in the chiral solvent (+)-phenyltrifluoromethylcarbinol. Carbon-13 nmr spectra of one of the hydantoins in an optically active solvent were also taken in order to obtain more information on chiral solvent interactions. The absolute configuration of the association complex for 1-aryl hydantoins has been determined from these nmr studies.

THEORY

The shielding contribution of the solvent to a nucleus in a solute molecule is included as one of five separate effects as shown in the equation below:

$$\sigma_{\text{Solvent}} = \sigma_b + \sigma_a + \sigma_w + \sigma_e + \sigma_B$$

The origins of the first four terms are explained in Part II of the thesis. The fifth screening constant expression, σ_B, is designed to include interactions such as charge transfer and hydrogen bonding, which lead to some form of complex in which solute and solvent molecules are specifically oriented with respect to each other. The interactions between solute and solvent which give rise to σ_B are referred to as collision complex formation. These effects are particularly important, because they can cause much larger changes in shieldings than are likely to arise from the other four terms. Shift differences introduced by σ_B could be of the order of 1 ppm for proton nuclei [66]. For carbon atoms the variation could reach higher values, for example 40 ppm chemical shift differences for carbonyl carbons of simple ketones are found in protic solvents. Hydrogen bonding interactions may prove to have useful applications, since they can be used to remove overlap of absorption lines of potentially non-equivalent nuclei in asymmetric molecules

and because they can yield both structural and stereochemical information.

In solute-solvent collision complexes, formed by bonding of a type which is associated with a specific geometry, the various portions of the solute molecules will bear different spatial relationships to the complexed solvent molecules. They will, therefore, experience at least in principle, different magnetic environments associated with any long range effects due to the solvent molecules. However, the solute must contain sites capable of specific bonding with the solvent. The secondary interactions of diamagnetic anisotropy, dipole-dipole, or charge transfer would enhance the long range effects, thus magnifying the chemical shift differences of diastereomeric nuclei in the collision complex.

EXPERIMENTAL

The experimental procedures followed for the line shape analysis and carbon-13 spectra in this study are described in previous chapters of Part I and Part II.

The optically active solvent, (+)-phenyltrifluoromethylcarbinol, was obtained from Burdick and Jackson Inc. A 0.5 g sample of 1-(2,3-dimethylphenyl)-5,5-dimethyl hydantoin was dissolved in 1 g of chiral solvent for C-13 nmr samples. The hydantoin concentrations of proton nmr samples were similar. Racemic dl-α-phenylethylamine (obtained from Matheson Coleman & Bell Inc.) was dissolved in optically pure (+)-phenyltrifluoromethylcarbinol at 39 mole % concentrations for the purpose of the carbon-13 and proton nmr studies.

RESULTS AND DISCUSSION

Non-equivalency of Enantiomeric Protons:

Following the observations of Pirkle[55-60] that enantiomeric protons may give rise to distinguishable signals in the optically active carbinol PTMC, Hund[11] investigated the behaviour of 3-aryl hydantoins in this solvent. He found that the ortho methyl protons of 3-(o-tolyl)-5,5-dimethyl hydantoin (3VI) displayed double multiplicity, while the C-5 methyl protons remained unaffected. The multiplicity of the aryl methyl signals was attributed to the presence of diastereomeric solute-solvent complexes, which enabled a distinction to be made between the rotational isomers of the solute. No splitting of the potentially diastereomeric 5,5-dimethyl signals in the 3-aryl hydantoins of the type investigated by Hund was observable.

It was thought that the 1-aryl hydantoins with enantiomeric rotamers would exhibit similar behaviour in the optically active solvent. This prediction was confirmed by experiment. All of the 1-aryl hydantoins listed in Table III-1, which were studied in the chiral solvent, exhibited non-equivalent ortho and meta methyl groups for the rotational isomers, while the C-5 methyl doublets were somewhat broadened. Distinguishable doubling of the hetero ring methyl signals could not be observed, presumably because the chemical shift differences were too small for resolution to be possible.

Useful data were obtainable from the spectra of the methyl groups substituted on the aromatic ring. The magnitude of the non-equivalence of the aryl methyl groups in the chiral solvent is strongly dependent on the location of the methyl group, i.e. ortho, meta, or para to the hetero substituent. Table III-2 lists the coalescence temperatures and chemical shift differences for the C-5 methyl and the aromatic methyl protons in the optically active carbinol. The chemical shift difference for the meta methyl protons of XVIII, 0.12 ppm, is slightly less than the chemical shift difference for the ortho methyl protons, 0.13 ppm. The coalescence temperatures are the same, within the precision of the measurements. In compound XX, which has a 2,5-dimethyl substitution pattern on the aromatic ring, the chemical shift difference of the meta methyl groups of the two rotamers is decreased to 0.06 ppm. In contrast to the other aryl methyl groups, the para methyl protons of XIX (with a 2,4-dimethyl substitution pattern) showed a single peak at the lowest attainable temperatures ($\sim 0^{\circ}C$). The spectra of the methyl protons of XX in DMSO-d_6 and in (+)-phenyl-trifluoromethylcarbinol (PTMC) solutions are shown in Figure III-1. Doubling of both the ortho and meta methyl signals is clearly evident in the spectra. The site specificity of the degree of non-equivalence of the aromatic ring methyl protons and the broadening of the C-5 methyl signals suggest that secondary anisotropy

Table III-2: Coalescence Temperatures and Chemical Shift Differences of Methyl Doublets for some 1-Aryl Hydantoins in (+)-Phenyltrifluoromethylcarbinol.

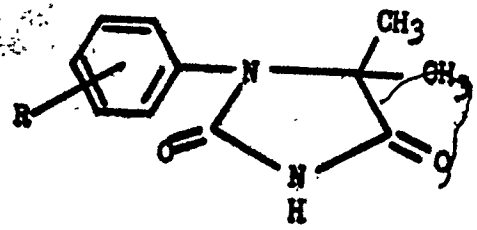

XIII	R=2-Methyl
XVIII	R=2,3-Dimethyl
XIX	R=2,4-Dimethyl
XX	R=2,5-Dimethyl

Hydantoin	Coalescence Temperature (°C)			Chemical Shift Difference (ppm)		
	R Methyl		C-5 Methyl	R Methyl		C-5 Methyl
	Ortho	Meta		Ortho	Meta	
XIII	81.5		105.0	0.12		0.24
XVIII	117.0	117.0	150.0	0.13	0.12	0.24
XIX	81.0		102.0	0.13		0.23
XX	80.5	68.5	101.5	0.13	0.06	0.25

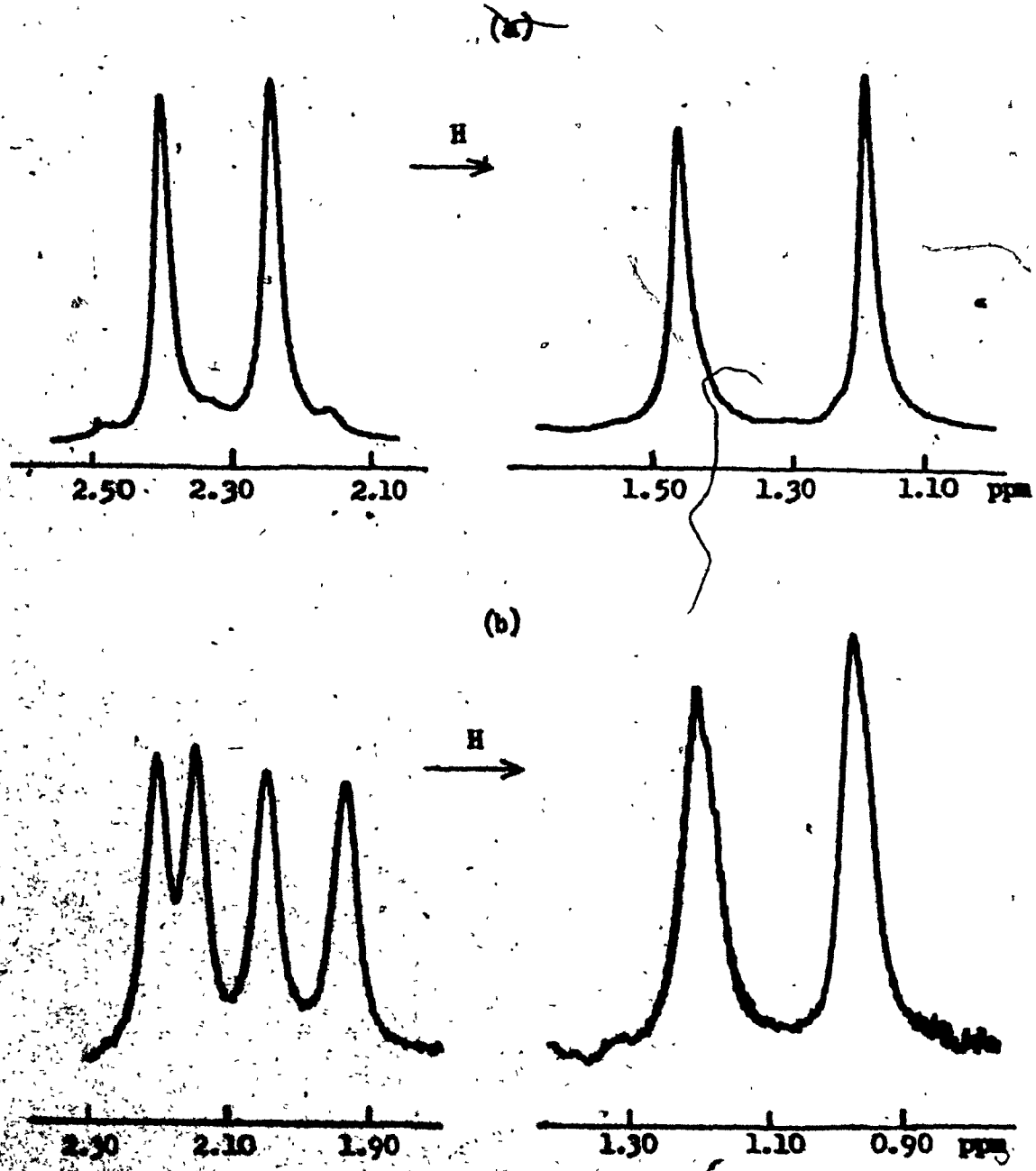

Figure III-1: Proton NMR Spectrum of the Methyl Protons of 1-(2,5-Dimethylphenyl)-5,5-dimethyl hydantoin (XX) in DMSO-d6 (a) and (+)-Phenyltrifluoromethylcarbinol (b).

interactions of solute and solvent molecules are the dominant factors which influence the magnetic non-equivalence of diastereotopic nuclei in diastereomeric hydantoin-carbinol solvates. The aryl moiety of the hydantoin molecule is probably influenced largely by the through space $\pi-\pi$ interactions with the π-electron cloud of the phenyl group of the chiral solvent. Differences in the shielding effects of the solvent phenyl group in the two ground state conformations of the solute molecules are presumably responsible for the non-equivalence of the methyl groups on the aromatic ring. The more remote location of the C-5 methyl protons with respect to the region of $\pi-\pi$ electron interaction, resulting in a smaller influence of the solvent phenyl group, is considered to be responsible for the unresolvable chemical shift difference between the diastereotopic methyl groups.

The chemical shift difference, 0.12 ppm, between the ortho methyl groups of the rotamers of XIII in (+)-PTMC is higher than that (0.05 ppm) of the corresponding protons of the 3-aryl hydantoin 3VI. This observation is consistent with the higher chemical shift differences found for the C-5 methyl protons of the 1-aryl hydantoin enantiomeric rotamers compared to the 3-aryl enantiomeric rotamers in achiral solvents. In the latter case the influence of the aryl group on the C-5 methyl group chemical shifts is less because of the more distant location of these groups.

Coalescence of the aromatic ring methyl doublets (resulting from diastereomeric solute-solvent interactions) occurs at temperatures about 20°C lower than the coalescence temperatures of the C-5 methyl doublets (due to restricted rotation about the aryl C-N bond) (Table III-2). This is an indication that the non-equivalences have different origins in the two cases. The nature of the interactions involved is discussed later.

Either exchange between solute and solvent molecules in the associated complex or internal rotation about the C-N bond in the hydantoin could account for the coalescence of the aryl methyl group signals at elevated temperatures. In all cases coalescence of the aryl methyl doublets is complete before the increased rate of internal rotation as the temperature is raised causes collapse of the 5-methyl doublet, suggesting that it is the solute-solvent exchange process which is primarily responsible for the temperature dependence of the aryl methyl group spectra.

The coalescence temperature of the aryl methyl doublets of 1-(2,3-dimethylphenyl)-5,5-dimethyl hydantoin, XVIII, in the chiral solvent is 117°C, compared to an average of 81°C for the coalescence temperatures of the ortho methyl doublets of XIII, XIX, and XX. Compound XVIII is known to experience an internal buttressing effect which influences the coalescence of the enantiotopic C-5 methyl proton signals. These data suggest that there is a correlation between the coalescence temperatures for collapse of splitting resulting from solute-

Table III-3: Proton Shieldings[a] for Some 1-Aryl hydantoins in Various Solvents (100 MHz)

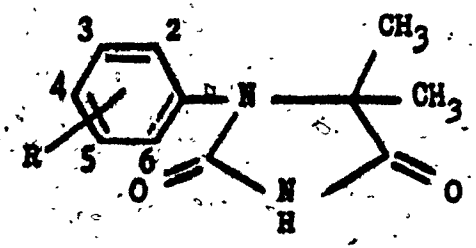

XIII R= 2-Methyl

XVIII R= 2,3-Dimethyl

XIX R= 2,4-Dimethyl

XX R= 2,5-Dimethyl

Hydantoin	C-5 Methyl			Ar	Methyl (R)	
	(+)-PTMC	DMSO-d_6	Pyridine	(+)-PTMC	DMSO-d_6	Pyridine
XIII	0.95 1.19	1.18 1.45	1.23 1.50	1.93 - 2.05[b]	2.18	2.28
XVIII	0.94 1.18	1.17 1.42	1.27 1.52	1.80 - 1.93[b] 2.02 - 2.14[c]	2.05[b] 2.27[c]	2.17[f]
XIX	0.95 1.18	1.16 1.42	1.29 1.54	1.91 - 2.04[b] 2.17[d]	2.13[b] 2.29[d]	2.24[b] 2.28[d]
XX	0.97 1.22	1.18 1.46	1.25 1.52	1.92 - 2.05[b] 2.14 - 2.20[e]	2.14[b] 2.30[e]	2.26[f]

[a] ppm from TMS [b] 2-methyl [c] 3-methyl [d] 4-methyl [e] 5-methyl [f] not resolved

solvent interaction in the chiral solvent and the barrier to internal rotation process. It does not seem possible to evaluate the relative contributions of these two processes to the temperature dependence.

Proton Shieldings:

Comparison of the proton chemical shifts of the 1-aryl hydantoins in achiral and chiral solvents indicates the presence of a strong association complex between the hydantoins and (+)-PTMC (Table III-3). Consistent upfield shifts for both the C-5 and the aromatic ring protons were found in the optically active solvent. The shielding enhancement follows the order: pyridine, DMSO-d_6 and (+)-PTMC. All the methyl proton signals are shifted upfield about 0.05-0.10 ppm in DMSO-d_6 compared to pyridine. This effect may be attributed to an increase in the polarity of the solvent, which results in close contact between the solute and the solvent molecules due to polar interactions in DMSO, thus shielding the methyl group. In the optically active solvent the C-5 methyl protons are relatively more shielded than the aromatic ring methyl protons, upfield shifts of about 0.30 ppm and 0.20 ppm, compared to the chemical shifts in pyridine, being observed. This is an indication that the point of attachment of the association complex is on the hetero ring. The complex probably

involves hydrogen bonding between the hydroxyl proton of the carbinol and a carbonyl oxygen atom of the hydantoin.

Rotational Activation Parameters:

Line shape analyses were carried out for the collapse of the C-5 methyl doublets of the 1-aryl hydantoins in the optically active solvent. The free energies of activation, calculated at the coalescence temperatures in three solvents, are listed in Table III-4, together with the chemical shift differences and the calculated lifetimes. Complete line-shape analysis data, the Arrhenius plot, and kinetic parameters for XIII in (+)-PTMC are presented in Table III-5, Figure III-2, and Table III-6, respectively. These calculations were carried out for the sake of comparison of solvent effects on thermodynamic parameters in achiral and chiral media.

A similar analysis of the collapse of the ortho and meta methyl doublets arising from the chiral solvent-solute interactions was not attempted because of uncertainty concerning the origin of the non-equivalence, and the behaviour of the system with changing temperature. It is expected that the lifetimes of the sites occupied by the non-equivalent nuclei of diastereomeric solvates would be affected by the rate of exchange between associated solute and solvent molecules, as well as by internal C-N bond rotation. The collapse of the enantiotopic C-5 methyl doublets, which should be

Table III-4 Free Energies of Activation and Mean Lifetimes for 1-Aryl Hydantoins in Various Solvents at Coalescence Temperatures, Calculated at Constant Chemical Shift Differences and at a Line Width of 1.1 Hz.

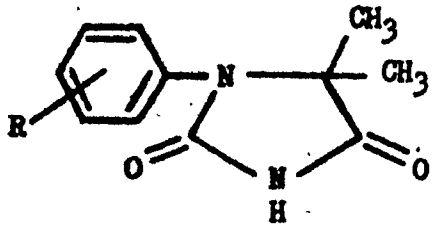

XIII R= 2-Methyl

XVIII R= 2,3-Dimethyl

XIX R= 2,4-Dimethyl

XX R= 2,5-Dimethyl

Hydantoin	Solvent	Temperature (Coal., °C)	Chemical Shift Diff.(Hz)	Lifetime (Sec)	$\neq$ ΔG (Kcal/mol)
	Pyridine	80.5	27.2	0.0203	18.1
XIII	DMSO-d_6	87.5	27.6	0.0195	18.4
	(+)-PTMC[a]	101.0	23.8	0.0217	19.2
	2-Chloropyr.	135.0	26.0	0.0210	21.0
XVIII	DMSO-d6	138.0	25.0	0.0213	21.2
	(+)-PTMC[a]	150.0	22.7	0.0216	21.8
	Pyridine	81.0	25.3	0.0212	18.1
XIX	DMSO-d_6	86.0	26.7	0.0203	18.4
	(+)-PTMC[a]	102.0	22.8	0.0220	19.3
	Pyridine	81.5	26.0	0.0221	18.2
XX	DMSO-d_6	90.5	27.3	0.0195	18.6
	(+)-PTMC[a]	102.0	23.0	0.0226	19.3

[a]Calculated at a Line Width of 2.5 Hz.

Table III-5: Lifetimes and Rotational Rates for 1-(o-Tolyl)-5,5-dimethyl hydantoin (XIII) in (+)-Phenyltrifluoromethylcarbinol Solution at Various Temperatures, Calculated at a Line Width of 2.5 Hz and Constant Chemical Shift Difference.

Temperature (°C)	Lifetime (Sec)	Standard Error	Rate Constant (Sec-1)	Chemical Shift Diff. (Hz)
	Average of Tau A and Tau B for the Collapse of C-5 Methyl Signals			
84.5	0.0561	0.0017	17.8	23.8
89.5	0.0413	0.0006	24.2	23.8
93.0	0.0320	0.0005	31.2	23.8
96.5	0.0262	0.0004	38.2	23.8
97.5	0.0240	0.0003	41.7	23.8
101.0	0.0217	0.0005	46.1	23.8
107.5	0.0151	0.0003	66.2	23.8
110.5	0.0113	0.0003	88.5	23.8

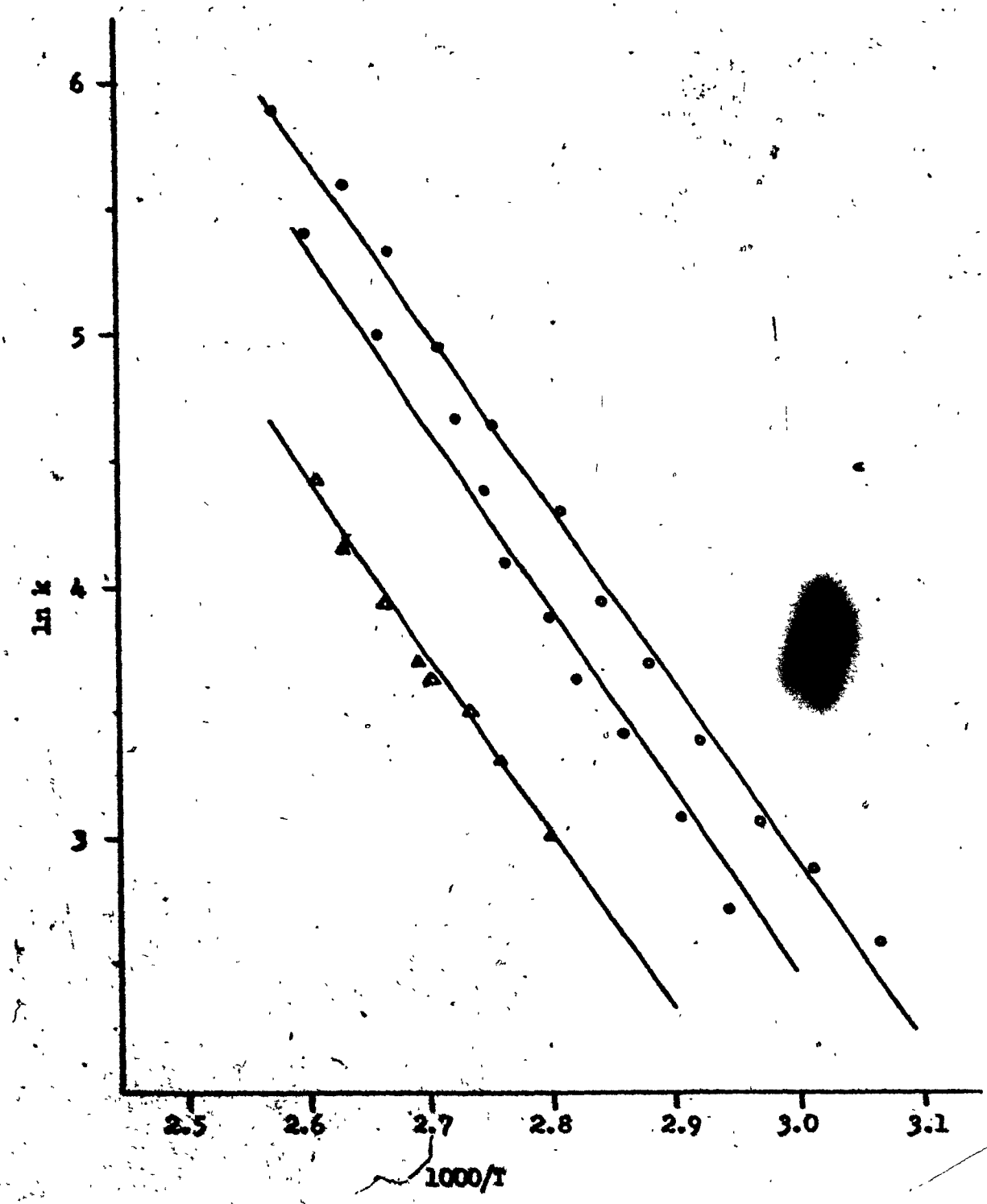

Figure III-2: Arrhenius plot for 1-(o-Tolyl)-5,5-dimethyl hydantoin in DMSO-d_6 (o), Pyridine (o) and (+)-Phenyl-trifluoromethyl-carbinol (o) Solutions.

Table III-6: Kinetic Parameters for Rotation in 1-(o-Tolyl)-5,5-dimethyl Hydantoin, Calculated at 100°C.[a]

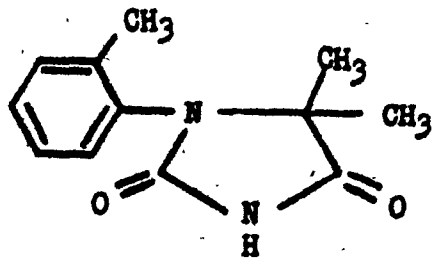

XIII

Solvent	E_a (kcal/mol)	$\Delta H^{\neq}$ (kcal/mol)	$\Delta S^{\neq}$ (e.u.)	$\Delta G^{\neq}$ (kcal/mol)	τ (sec)
Pyridine	13.8±0.7	13.1±0.7	-14±2	18.2±0.1	0.0059
DMSO-d_6	16.0±0.5	15.2±0.5	- 9±2	18.5±0.1	0.0083
(+)-PTMC	16.1±1.1	15.4±1.1	-10±3	19.2±0.1	0.0218

[a]Errors are 90% confidence limits.

independent of the association interaction at the temperatures employed, can be assumed to result only from the hindered ipternal rotation process.

Evidence for the relative importance of these two factors which may influence the lifetimes of diastereotopic methyl groups on the aromatic ring is found in the coalescence temperature ranges. The chemical shift differences between diastereotopic methyl groups began to decrease linearly with increasing temperature about 50°C below the coalescence points. This range is two to three times greater than the coalescence range of the methyl protons, which results only from an increased rate of rotation. The temperature dependence of these chemical shift differences can be attributed to a decrease in hydrogen bonding with an increase in temperature, resulting in an increase in the rate of exchange between optically active solvent molecules and the enantiomeric solute pair.

Higher barriers to hindered rotation in the chiral solvent for all the compounds are evident in Table III-4. Free energies of activation are about 1.1 kcal/mol higher in (+)-PTMC than in pyridine solution. Coalescence temperatures are raised about 20°C, from about 81°C in pyridine to about 101°C in (+)-PTMC. An exception is the internally buttressed hydantoin, XVIII, which exhibits an increase of about 15°C in its coalescence temperature in (+)-PTMC compared to 2-chloropyridine. This difference

may result from use of a more polar achiral reference solvent. The increase in free energy of activation in (+)-PTMC is attributed to an increase in the steric barrier to rotation resulting from close contact between solute and solvent molecules due to association through hydrogen bonding.

Table III-6 shows the rotational activation parameters for XIII calculated for three solvents. The errors involved in the determination of kinetic and thermodynamic parameters are higher in the optically active solvent, due to difficulty in the estimation of the correct natural linewidth. At normal probe temperatures the C-5 methyl peaks are broadened due to solute-solvent interaction. At the higher temperatures required for observation of the collapse of the C-5 methyl doublet resulting from the increased rate of rotation about the C-N bond the line broadening resulting from association is expected to disappear. However, it was not possible to measure or make an accurate estimate of the natural linewidth at the higher temperatures because exchange broadening affected the linewidths as association broadening was removed. An average value of 2.5 Hz was taken as the best estimate for the natural linewidth in the temperature range in which collapse was observed. The rotational enthalpy of activation of XIII in (+)-PTMC was found to be 15.4 kcal/mol, which is 0.2 and 2.3 kcal/mol higher than the enthalpy values in DMSO-d_6 and in pyridine, respectively. The

is expected since steric hindrance to rotation should be enhanced in the chiral solvent due to close contact between solute and solvent molecules. The rotational entropy of activation of XIII in (+)-PTMC is -10.2 e.u., which lies between the $\Delta S^{\neq}$ values of XVIII in pyridine and in DMSO-d_6 as solvents. This result would indicate that the transition states of the rotational isomers are more ordered in the chiral solvent with respect to DMSO-d_6, probably because of favorable π-π interactions between the aryl groups of the solute and the solvent molecules. But the degree of order in the transition state appears to be higher in pyridine, which is a planar molecule with π-electrons.

Carbon-13 Shieldings in the Optically Active Solvent:

It is known that carbon-13 chemical shifts are more sensitive to conformational changes and steric effects than are proton chemical shifts. The relatively large magnitudes of the resulting chemical shift effects, such as were found in the hydantoins (Part II), suggested that studies of the magnetic non-equivalence of the carbon atoms, associated with molecular dissymmetry in optically active solvents, might yield useful information. An example of molecular asymmetry effects on carbon-13 shieldings in freely rotating systems has been provided by Kroschwitz et. al.[67] from their results for compounds of the following type:

$(CH_3)_2CH(CH_2)_nCH(OH)R$

R = alkyl

The isopropyl methyl carbons exhibited non-equivalent peaks, similar to the C-5 methyl carbons in the aryl substituted hydantoins, the degree of non-equivalence being increased with the increasing bulk effect of the R' alkyl substituent. The magnetic non-equivalence of the isopropyl methyl carbons has been attributed to steric effects in the asymmetric molecule. Solvent effects on the magnetic non-equivalence of the carbon resonances were neglected in the study of Kroschwitz et. al.. However, doubling of the resonances of the enantiomeric carbons in racemic mixtures of phenylethylamines and phenylethylcarbinols has recently been reported by Fraser, Stothers and Tan[65] in chiral lanthanide complexes. Unfortunately, an adequate explanation of the origin of the non-equivalence of nuclei in diastereomeric solute-solvent complexes was not given. Even so, this study has proven that potentially non-equivalent carbon nuclei, resulting from chiral solvent interactions, may give rise to observable carbon-13 chemical shift differences.

It was thought, therefore, that the methyl carbons of the aryl substituted hydantoins might show double multiplicity, as was found in the pmr spectra. However the experimental results showed no such doubling of signals. It can be seen

in Figure III-3 that the aromatic ring methyl carbons (at 17.9 and 20.5 ppm) and the C-5 methyl carbons (at 21.8 and 24.3 ppm) of 1-(2,5-dimethylphenyl)-5,5-dimethyl hydantoin, XX, exhibited the normal multiplicity in the chiral solvent (+)-PTMC. The higher intensities observable in Figure III-3 for the aryl methyl carbons relative to the C-5 methyl carbons may be due to a more favorable Overhauser enhancement or to differences in relaxation times. The same phenomenon was observed in achiral solvents such as morpholine.

The carbon-13 chemical shift data for the 1-aryl hydantoins in morpholine and (+)-PTMC solutions for the methyl carbons and the hetero ring carbons are given in Table III-7. The chemical shift differences between the aryl methyl carbon peaks and the C-5 methyl carbon peaks are not affected by the change in solvents. The slight shift in the chemical shifts in (+)-PTMC could be attributed to the use of an external lock in the latter case. The carbonyl carbon shieldings are similar in morpholine and the chiral solvent, which is evidence that similar types of solvation processes are involved in both cases, i.e. a hydrogen bonding interaction. In agreement with this interpretation, the carbonyl carbon signals of 3-(o-tolyl)-5,5-dimethyl-hydantoin, XVI, in (+)-PTMC are shifted down field about 2 ppm with respect to the chemical shifts in DMSO (Table III-8). The ortho methyl and the C-5 methyl carbon shieldings of XVI in (+)-PTMC exhibit chemical shifts

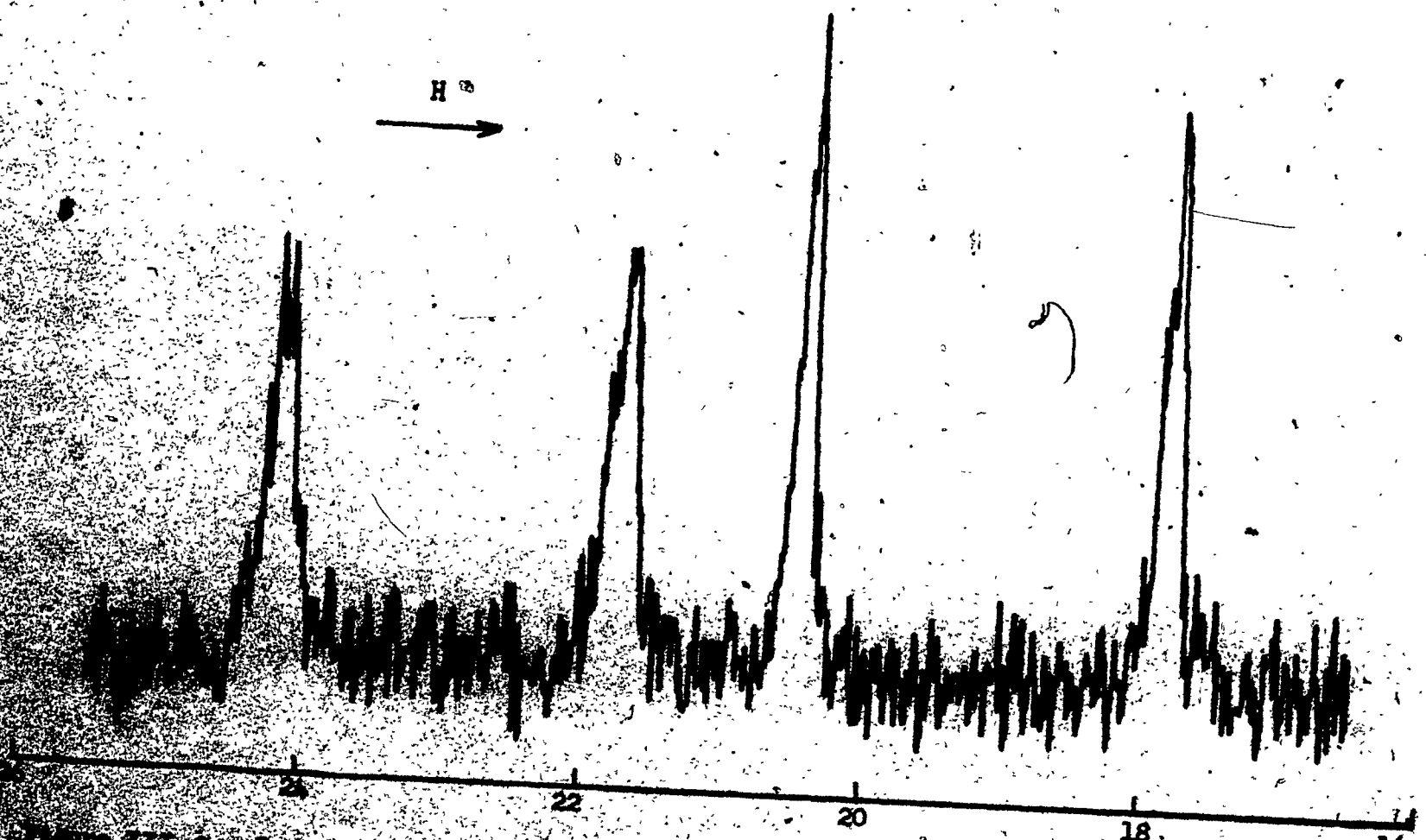

Figure III-3: Carbon-13 NMR Spectrum of the Methyl Carbons of 1-(2,5-Dimethylphenyl)-5,5-dimethyl [illegible] (II) in (+)-Phenyltrifluoromethylcarbinol (PTMC)(110 Scans).

Table III-7: Carbon-13 Shieldings[a] of the 1-Aryl Hydantoins in Morpholine and (+)-Phenyltrifluoromethylcarbinol (PTMC) Solutions.

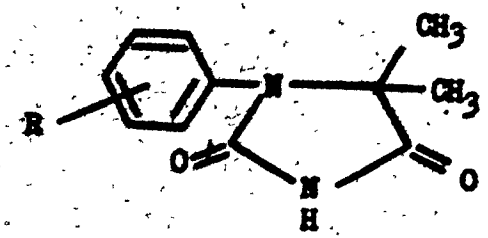

XII	R=2-Methyl
XVIII	R=2,3-Dimethyl
XIX	R=2,4-Dimethyl
XX	R=2,5-Dimethyl

Hydantoin	Solvent	R Methyl	C-5 Methyl	C-5	C-2	C-4
XIII	Morpholine	18.5[b]	22.4 - 25.1	65.8	155.4	178.9
XVIII	Morpholine	15.3[b] - 20.3	22.2 - 25.0	65.1	155.7	179.0
XIX	Morpholine	18.5[b] - 20.7	22.3 - 25.0	65.5	155.4	178.9
XX	Morpholine	18.1[b] - 20.6	22.3 - 25.1	65.7	155.6	179.1
XX	(+)-PTMC	17.9[b] - 20.5	21.8 - 24.3	66.7	155.4	179.0

[a]ppm from TMS. [b]ortho methyl.

Table III-8: Carbon-13 Shieldings[a] of 3-(o-Tolyl)-5,5-dimethyl Hydantoin in DMSO and (+)-Phenyltrifluoromethylcarbinol (PTMC)

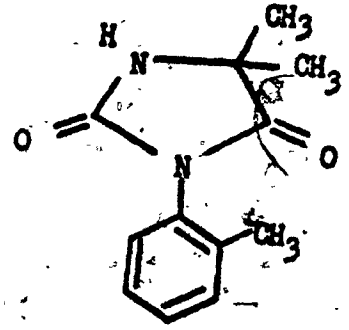

3VI

Hydantoin	Solvent	Aryl Methyl	C-5 Methyl	C-5	C-2	C-4
3VI	DMSO	16.9	24.4-25.1	58.0	154.1	176.3
3VI	(+)-PTMC	17.2	24.1-24.8	59.6	156.3	178.1

[a] ppm from TMS

similar to those found for the 1-aryl hydantoin, XX. The C-5 carbon signal of the hetero ring is deshielded 1.0 ppm and 1.6 ppm for XX and 3VI, respectively, in the chiral solvent compared to DMSO. This downfield shift probably results from the presence of the hydrogen bonded association complex of the solute and solvent molecules. However, it is difficult to interpret the origin of the deshielding effect on the C-5 carbon.

The solvent carbon signals of (+)-PTMC were also recorded in the hope of obtaining some information. The trifluoromethyl carbon exhibited a quartet at 72.9 ppm (J = 33 Hz) due to coupling with the fluorine atoms, while the carbinol signal was observed at 88.9 ppm as a single peak. No additional multiplicity for any of the solvent carbon signals was observable.

The aryl carbon chemical shifts of the aryl substituted hydantoins in morpholine and in (+)-PTMC solutions are listed in Table III-9. Since the range of aryl carbon peaks of XX and 3VI overlapped the range of aryl carbon signals of the chiral solvent, an assignment of the chemical shifts of the aryl carbons could not be made. The aryl carbon peaks of hydantoins XIX and XX in morpholine, which are not reported earlier in the thesis, were assigned by the method described in Part II. Aryl carbon chemical shifts of the reference compounds m-xylene and p-xylene were obtained from the literature[68]. In general, the aryl carbon chemical shifts did not provide any useful information on chiral solvent

Table III-9. : Aryl Carbon Shieldings[a] of some Hydantoins in Achiral and Chiral Solvents.

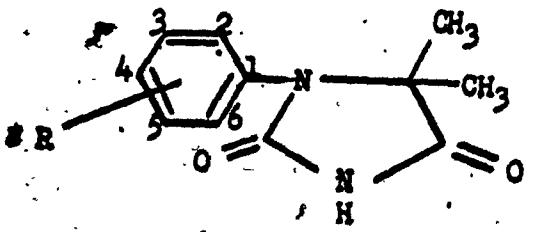

XIX R=2,4-Dimethyl

XX R=2,5-Dimethyl

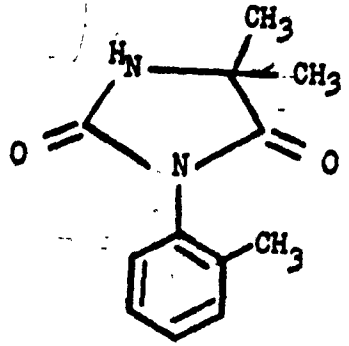

3VI

Hydantoin	Solvent	1	2	3	4	5	6		
XIX	Morpholine[c]	138.5	131.2	132.2	134.7	130.0	127.4		
XX	Morpholine	136.4	131.3	133.6	130.8	135.6	129.5		
XX	(+)-PTMC[B]	128.1	128.9	129.6	130.7	132.0	135.4	137.2	
3VI	(+)-PTMC[b]	127.4	127.9	128.7	129.5	130.6	131.6	135.2	136.9

[a] ppm from TMS. [b] aryl carbons are not assigned.

interactions.

In conclusion, failure to observe doubling of the carbon-13 signals of hydantoins could be attributed to relative insensitivity of the carbon resonances for the distinguishability of the anisotropic shielding effects in these systems. In compounds previously studied by Pirkle et al.[55-60], and in aryl substituted hydantoins the secondary anisotropic effects between solute and solvent molecules in the associated complexes have been considered responsible for the non-equivalence of diastereotopic protons or fluorine nuclei. One may expect that the non-equivalence of diastereotopic nuclei arising from anisotropy interactions would be similar in ppm for both proton and carbon resonances, in contrast to the general trend of higher chemical shift differences in carbon resonances for diastereotopic nuclei subject to steric influences. The chemical shift difference of aromatic methyl proton doublets are 0.13 ppm in (+)-PTMC (Table III-2), measured at proton probe temperatures (~30°C). At the carbon probe temperatures (~55°C), the $\Delta\delta$ is estimated to decrease to about 0.08 ppm, based on pmr data, while the accuracy of measurements in the C-13 spectra is ± 0.05 ppm. Thus it would be expected that the carbon resonances would be insensitive to these small chemical shift differences.

In order to test the validity of this assumption the carbon-13 spectrum of dl-α-phenylethylamine in (+)-PTMC

was taken.

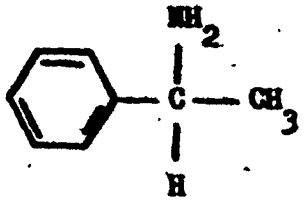

Pirkle et al.[55] previously made a study of this compound in the optically active carbinol and observed doubling of the proton and fluorine resonances in both solute and solvent molecules. At the concentration of the C-13 nmr sample (38.9 % in (+)-PTMC) the methine proton of dl-α-phenylethylamine showed two sets of quartets with a chemical shift difference of 0.04 ppm. However, any double multiplicity in the C-13 nmr spectrum was not observable. The carbinyl and methyl carbon signals of the racemic amine were found as singlets at 51.0 and 24.5 ppm, respectively. The solvent also did not show any evidence of doubling of signals, the carbinol and trifluoromethyl signals being observed at 94.9 ppm and 72.2 ppm (J=33 Hz), respectively.

It has been shown by Pirkle et al.[55], that secondary anisotropy interactions cause the non-equivalency of diastereotopic protons in amine-carbinol association complexes. This is also believed to be the case for hydantoin-carbinol pairs. Failure to observe the non-equivalency of the carbon resonances in amine-carbinol mixtures, with a $\Delta\delta$ of only 0.04 ppm for diastereotopic proton nuclei, is consistent

with the explanation given above for the hydantoin-carbinol interactions.

Configuration of Association Complex:

The configuration of the diastereomeric solvates between the 1-aryl hydantoin and (+)-PTMC molecules could be determined from the available proton and C-13 nmr data. The proton shielding data and the carbonyl carbon shielding data of the 1-aryl hydantoins clearly indicate the presence of a hydrogen bonding interaction through the carbonyl oxygens of the hydantoin molecule, and the hydroxyl hydrogen atoms of the carbinol molecules. In order to maximize the π-π interactions between the solute and solvent pairs, the phenyl rings of the hydantoin and carbinol molecules would tend to stay parallel to each other in the ground state conformations of the diastereomeric solvates. Dreiding models, studied with the aid of this evidence, have suggested the possible orientations of the chiral solvent molecule relative to the two ground state conformations of the 1-aryl hydantoin. For the first case, the bulky CF_3 group of the (+)-PTMC is placed between the aryl rings of the solute and the solvent, and for the second case it is placed further away from the aryl rings. Due to the effects of steric hindrance, the latter case would be expected to be the preferred configuration. Using these arguments, the structures of the diastereomeric solvates

involving (+)-PTMC for the ground state conformations of the two rotational isomers are shown in the figures below:

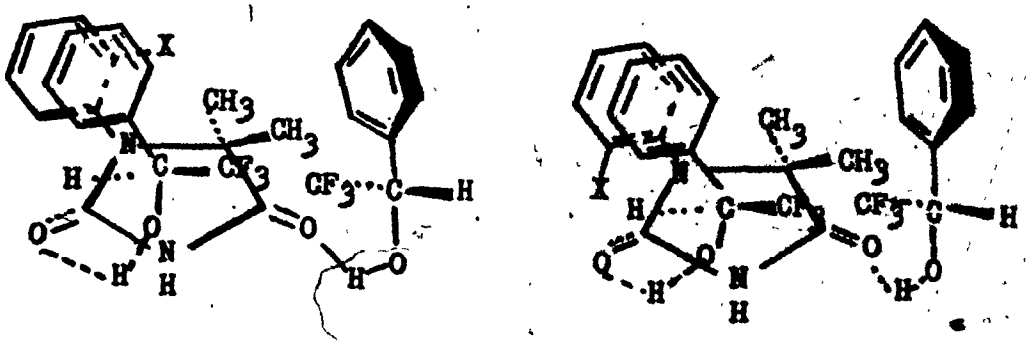

D_I D_{II}

In both configurations the phenyl rings of the solute and the solvent are slightly shifted relative to each other, resulting in unequal shielding of the aryl substituents of the hydantoin molecule. In consequence, the Dreiding models clarify the unequal degree of non-equivalency observed for the ortho, meta and para methyl protons. The ortho methyl protons exhibited the highest chemical shift difference because the phenyl ring of the chiral solvent is placed near to the hetero ring and exerts the maximum anisotropy shielding on the ortho methyl moiety as is seen in the figure showing the D_I configuration whereas in the D_{II} configuration the ortho methyl group is nearer to the deshielding zone of the phenyl ring. The meta methyl protons are placed further away from the phenyl ring, and they experience a lower degree

of shielding interaction. The para methyl substituent is symmetrically positioned in both the D_I and D_{II} configurations and it is expected to be shielded to an equal degree by the chiral solvent phenyl group. Hence no resonance doubling could be observed. The ortho and meta methyl proton peaks arising from the D_I configuration would be found shifted upfield while the proton peak corresponding to D_{II} configuration would be deshielded. These peaks are observed with equal intensities in the nmr spectra, due to the presence of approximately equally populated diastereomeric solvates.

SUMMARY

The following conclusions are drawn in the study of aryl substituted hydantoins in an optically active solvent.

a) The presence of an asymmetric center in the solvent molecules causes the formation of distinguishable diastereomeric solute-solvent pairs in the pmr spectra of aryl substituted hydantoins.

b) The magnetic non-equivalency of enantiotopic protons of aryl substituted hydantoins is observable only for the methyl protons of the aromatic ring. It is suggested that this is due to the presence of favorable anisotropic interactions with the chiral solvent.

c) The proton and the C-13 nmr data indicate that the association of the solute and solvent complexes involves hydrogen bonding between the carbonyl and hydroxyl groups of the hydantoin and the carbinol molecules.

d) Strong solute-solvent interactions in the chiral solvent increase the barriers to hindered rotation about the C-N bond in 1-aryl hydantoins, thus resulting in larger values of rotational free energies of activation and enthalpies of activation.

e) Doubling of signals from the enantiotopic carbon nuclei of aryl substituted hydantoins is not evident in the optically active solvent, probably due to insufficient magnetic non-equivalency of diastereomeric solvates.

f) The configuration of the hydantoin-carbinol

association complex can be deduced from the proton and carbon-13 nmr data, and the degree of non-equivalency of methyl protons on ortho, meta and para positions of the aromatic ring.

SYNTHETIC EXPERIMENTAL

Hydantoins containing a bulky ortho aryl substituent were prepared by mainly two methods. Methods of synthesis and reaction conditions differ from those of previously prepared 3-aryl substituted hydantoins. In this section the preparative description of each method, and the analytical and spectroscopic data of the synthesized compounds are given.

METHOD A

The method of synthesis which was undertaken and applied successfully for the preparation of some of the 1-aryl hydantoins is shown in the scheme below:[69,70]

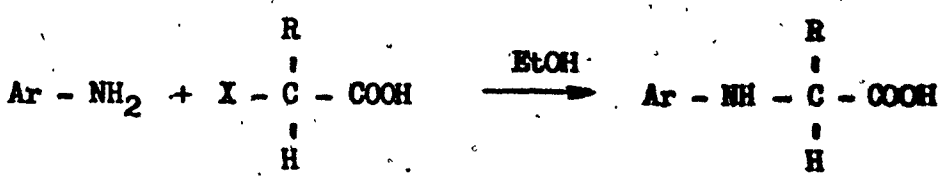

X = Cl, Br

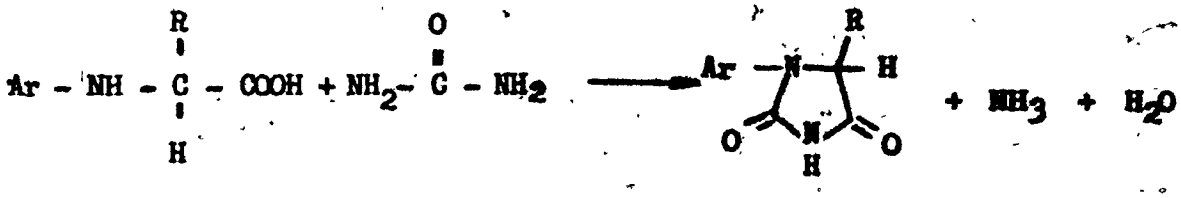

Primary aromatic amines were refluxed in aqueous ethanol (70-80 %) with α-halo carboxylic acids to form N-aryl amino acids. Refluxing periods were varied between

2 and 6 hours, according to the steric hindrance to reaction shown by the R group of the carboxylic acid and the ortho substituent of the anilines. In some cases the ethyl ester of the carboxylic acid was used and the resulting amino acid ester was converted to the free acid by sodium hydroxide hydrolysis. Amino acids were purified by crystallization from aqueous and absolute ethanol and identified by their nmr spectra and physical properties, given in the literature.

Hydantoins were formed by the reaction of N-aryl amino acids with urea in the absence of solvent. Reactants were heated in a 100 ml three neck flask fitted with a thermometer and an air condenser. It was found that the temperature range and the heating period critically affected the yields. Best results were obtained when the reaction phase stayed as a homogeneous liquid, for at least an hour of prolonged heating between temperatures of 140 and 170°C. The hydantoins were extracted from the reaction mixture with warm 10% sodium hydroxide solution. Neutralization of the alkaline solution yielded the crude product. The hydantoins were purified through recrystallization from ethanol and were identified by elemental analysis, nmr , and ir spectra.

N- (o-tolyl) glycine:

10.0 g (0.101 mole) of monochloroacetic acid was dissolved in 30 ml of aqueous ethanol (80%) and 10.0 g (0.093 mole) of o-toluidine was added to the solution. The reaction mixture was refluxed for two hours. The amino acid precipitated upon cooling. Crystallization of the crude product from absolute ethanol yielded 3.4 g (22 % N-(o-tolyl) glycine, m.p.: 148°C (Lit.[73] 149-50°C).

NMR data:

Methyl protons (on aromatic ring): 2.17 ppm, singlet

Methylene protons: 3.38 ppm, singlet

Aromatic protons: 6.40-7.25 ppm, multiplet

Hydroxyl protons: 8.63 ppm, broad singlet

1-(o-tolyl) hydantoin:

2.0 g (0.012 mole) of N-(o-tolyl) glycine was mixed with 1.5 g (0.025 mole) of urea in a 100 ml three neck flask fitted with a thermometer and an air condenser. The reaction mixture was heated for an hour at temperatures in the range 140 to 160°C. Under these conditions the reaction mixture remained a homogeneous liquid. The reaction flask was then cooled to room temperature and 50 ml of warm 10 % sodium hydroxide solution was added. Following vigorous mixing, the suspension was filtered under vacuum. Neutralisation of the filtrate with conc. HCl yielded the crude hydantoin,

The residue was filtered and recrystallized several times from absolute ethanol.

Yield: 1.53 g, 67 % m.p.: 177-8°C

Elemental analysis:

Calculated: % C 63.16, % H 5.26, % N 14.74

Found: % C 63.31, % H 5.55, % N 14.91

NMR data: (in DMSO-d_6)

Methyl protons (on aromatic ring): 2.24 ppm, singlet

Methylene protons: 4.33 ppm, singlet

Aromatic protons: 7.24-7.36 ppm, multiplet

The procedures were the same for the preparation of the following amino acids and hydantoins.

The origin and quality of the chemicals used for the synthesis of the aminoacids and hydantoins, are listed below.

Canlab/J.T. Baker:

Monochloroacetic acid, "Baker Analysed Reagent"

Urea, "Baker A.R."

o-Toluidine, "Baker"

o-Chloroaniline, "Baker"

1-Naphthylamine, "Baker"

Ethyl-2-bromopropionate, "Practical"

Aldrich :

Bromophenylacetic acid, "99.5 %"

o-Toluidine was distilled prior to use.

N-(o-chlorophenyl) glycine:

Starting Materials : 13.0 g (0.102 mole) o-chloroaniline, 10.0 g (0.101 mole) monochloroacetic acid.

Yield : 3.15 g , 17% , m.p.: 169°C (Lit.[74] 171-3°C)

NMR data: (in DMSO-d_6)

Methylene protons : 3.45 ppm, singlet

Aromatic protons : 6.35-7.35 ppm, multiplet

Hydroxyl proton : 8.87 ppm, broad singlet

N-(1-naphthyl) glycine :

Starting Materials : 14.0 g (0.098 mole) 1-naphthylamine, 10.0 g (0.101 mole) monochloroacetic acid.

Yield : 2.32 g , 11% , m.p.: 193-4°C (Lit.[75] 190-1°C)

NMR data : (in DMSO-d_6)

Methylene protons : 3.92 ppm, singlet

Naphthyl protons: 6.20-8.15 ppm, multiplet

Hydroxyl proton : overlapped with naphthyl protons

N-(o-tolyl)-2-phenyl glycine :

Starting Materials : 10.0 g (0.093 mole) o-toluidine, 20.0 g (0.094 mole) α-bromo phenylacetic acid.

Yield : 3.86 g , 16% m.p.: 147°C

NMR data : (in DMSO-d_6)

Methyl protons (on aromatic ring) : 2.20 ppm, singlet

Methine proton : 5.48 ppm, singlet

Aromatic protons : 7.15-7.47 ppm, multiplet

Hydroxyl proton : 9.89 ppm, broad singlet

N-(o-chlorophenyl)-2-phenyl glycine :

Starting Materials : 13.0 g (0.102 mole) o-chloroaniline ,
20.0 g (0.094 mole) α -bromo phenylacetic acid.

Yield : 2.88 g , 11% m.p.: 163°C (Lit.[76] 160°C)

NMR data : (in DMSO-d_6)

Methine proton : 5.16 ppm, singlet

Aromatic protons : 6.55-7.53 ppm, multiplet

Hydroxyl proton : 9.04 ppm, broad singlet

α -N-(o-tolyl) alanine :

Starting Materials : 10.0 g (0.093 mole) o-toluidine ,
17.0 g (0.099 mole) ethyl-2-bromopropionate

Yield : 7.33 g , 14% m.p.: 163°C

NMR data : (in DMSO-d_6)

Methyl protons : 1.51-1.63 ppm, doublet, J=12 Hz.

Methyl protons (on aromatic ring) : 2.20 ppm, singlet

Methine proton : 4.02-4.38 ppm, quartet, J=12 Hz.

Aromatic proton : 6.54-7.28 ppm, multiplet

Hydroxyl proton: 10.01 ppm, broad singlet

α-N-(o-chlorophenyl) alanine:

Starting Materials: 13.0 g (0.102 mole) o-chloroaniline ,
17.0 g (0.099 mole) ethyl-2-bromopropionate

Yield : 1.96 g , 10% m.p.: 149°C (Lit.[74] 148-50°C)

NMR data : (in DMSO-d_6)

Methyl protons : 1.51-1.63 ppm, doublet, J=12 Hz.

Methine protons : 4.01-4.37 ppm, quartet, J=12 Hz.

Aromatic protons : 7.17-7.33 ppm, multiplet

Hydroxyl protons : 10.27 ppm, broad singlet

α -N-(α-naphthyl) alanine :

Starting Materials : 14.0 g (0.098 mole) 1-naphthylamine, 17.0 g (0.099 mole) ethyl-2-bromopropionate.

Yield : 1.57 g , 7.5% m.p.: 163 (Lit.[77] 161°C)

NMR data : (in DMSO-d_6)

Methyl protons : 1.53-1.66 ppm, J=12 Hz., doublet

Methine protons : 4.04-4.40 ppm, J=12 Hz., quartet

Aromatic protons : 6.27-8.16 ppm, multiplet

Hydroxyl proton : 9.46 ppm, broad singlet

1-phenylhydantoin :

Starting Materials : 5.0 g (0.033 mole) N-phenylglycine , 4.0 g (0.067 mole) urea.

Yield : 4.41 g , 76% m.p.: 195.0°C (Lit.[78] 191-4°C)

NMR data : (in DMSO-d_6)

Methylene protons : 4.21 ppm, singlet

Aromatic protons : 7.02-7.33 ppm, multiplet

1-(o-chlorophenyl) hydantoin :

Starting Materials : 2.0 g (0.011 mole) N-(o-chlorophenyl)-glycine, 1.5 g (0.025 mole) urea.

Yield : 1.2 g , 53% m.p. : 188°C

Elemental analysis:

Calculated : C% 51.43 , H% 3.33 , N% 13.33

Found : C% 51.40 , H% 3.34 , N% 13.19

NMR data : (in DMSO-d_6)

Methylene protons : 4.38 ppm, singlet

Aromatic protons : 7.31-7.68 ppm, multiplet

1- (o-trifluoromethylphenyl) hydantoin:

This compound has been prepared by J. R. Fehlner.[12]

M.p. :189-90°C

Elemental analysis:

Calculated : C% 49.18 , H% 2.87

Found : C% 49.08 , H% 2.71

NMR data : (in DMSO-d_6)

Methylene protons : 4.39 ppm, singlet

Aromatic protons : 7.28-7.41 ppm, multiplet

1-(α-naphthyl) hydantoin:

Starting Materials : 2.0 g (0.010 mole) N-(1-naphthyl) glycine, 1.5 g. (0.025 mole) urea.

Yield : 0.95 g., 42% m.p.: 229°C

Elemental analysis:

Calculated : C% 69.03 , H% 4.42 , N% 12.39

Found : C% 69.00 , H% 4.45 , N% 12.29

NMR data : (in DMSO-d_6)

Methylene protons : 4.48 ppm, singlet

Aromatic protons : 7.47-8.06 ppm, multiplet

1-(o-tolyl)-5-phenyl hydantoin :

Starting Materials : 3.0 g (0.012 mole) N-(o-tolyl)-2-phenyl glycine, 2.0 g (0.033 mole) urea.

Yield : 1.46 g., 46% m.p.: 199°C

Elemental analysis:

Calculated : C% 72.18 , H% 5.26 , N% 10.53

Found : C% 72.31 , H% 5.12 , N% 10.53

NMR data : (in DMSO-d_6)

Methyl protons (on aromatic ring) : 2.20 ppm, singlet

Methine proton : 5.64 ppm, singlet

Aromatic protons : 6.92-7.19 ppm, multiplet

1-(o-chlorophenyl) - 5-phenyl hydantoin :

Starting Materials : 2.5 g (0.0096 mole) N-(o-chloro phenyl)-2-phenyl glycine, 2.0 g (0.033 mole) urea.

Yield : 1.21 g , 44% m.p.: 180°C

Elemental analysis:

Calculated : C% 62.83 , H% 3.84 , N% 9.77

Found : C% 62.64 , H% 3.84 , N% 9.98

NMR data : (in DMSO-d_6)

Methine proton : 5.54 ppm, singlet

Aromatic protons : 6.85-7.22 ppm, multiplet

1-(o-tolyl)-5-methyl hydantoin :

Starting Materials : 2.0 g (0.011 mole) α-N-(o-tolyl) alanine, 1.5 g (0.025 mole) urea.

Yield : 1.31 g , 58% m.p.: 168°C

Elemental analysis:

Calculated : C% 64.71 , H% 5.88 , N% 13.72

Found : C% 64.09 , H% 5.99 , N% 14.02

NMR data : (in DMSO-d_6)

Methyl protons : 1.15-1.22 ppm, doublet, J=7 Hz.

Methyl protons (on aromatic ring) : 2.21 ppm, singlet

Methine proton : 4.50-4.71 ppm, quartet, J=7 Hz.

Aromatic protons : 7.24-7.31 ppm, multiplet

1-(o-chlorophenyl)-5-methyl hydantoin :

Starting Materials : 1.6 g (0.008 mole) α -N-(o-chloro-phenyl) alanine, 1.2 g (0.020) mole urea.

Yield : 0.88 g , 49% m.p.: 202°C

Elemental analysis:

Calculated : C% 53.45 , H% 4.01

Found : C% 52.99 , H% 3.94

NMR data : (in DMSO-d_6)

Methyl protons : 1.21-1.28 ppm, doublet, J=7 Hz.

Methine proton : 4.50-4.71 ppm, quartet, J=7 Hz.

Aromatic protons : 7.38-7.62 ppm, multiplet

1-(α-naphthyl)-5-methyl hydantoin :

Starting Materials : 1.3 g (0.006 mole) α-N-(α-naphthyl) alanine, 1.0 g (0.017 mole) urea.

Yield : 0.59 g , 41% m.p.: 224°C

Elemental analysis:

Calculated: : C% 69.99 , H% 5.03

Found : C% 69.83 , H% 5.24

NMR data : (in DMSO-d_6)

Methyl protons : 1.21-1.28 ppm, doublet, J=7 Hz.

Methine proton : 4.50-4.71 ppm, quartet, J=7 Hz.

Aromatic protons : 7.38-7.62 ppm, multiplet

METHOD B

α-Amino acids could not be obtained by the reaction of anilines with α-halo isobutyric acids due to the steric effect of methyl groups. Refluxing in ethanol for 10 days, as suggested in one of the references[70] did not yield any product.

Mazover's method of synthesis[71,72] originally employed for the preparation of 1-(p-sulfamoylphenyl) hydantoin, has been improved and successfully applied to the synthesis of 1-aryl hydantoins with dimethyl groups in the 5-position, and with a bulky ortho substituent on the aryl moiety. Better overall yields were also obtained compared to method A. The scheme below shows the reaction steps for this method:

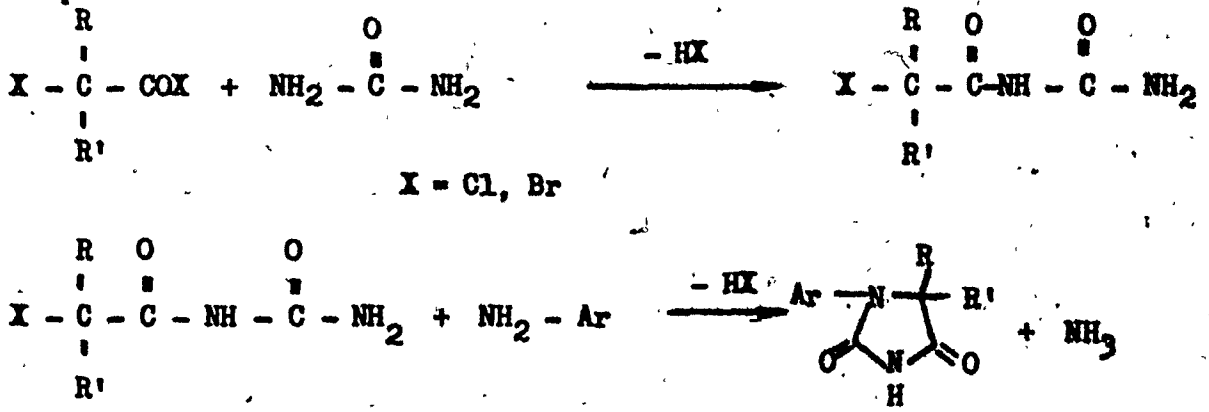

The α-halo acyl halides were reacted with urea on a steam bath, the reaction mixture being heated 0.5 to 1 hour. The mixture first melted and then solidified, forming the urea of the α-halo carboxylic acid. One has to avoid contact between water vapor and acyl halide, otherwise poorer yields were obtained. The reaction was carried out

in a 250 ml. boiling flask fitted with a condenser and a drying tube. The carboxylic acid ureas were crystallized from hot water and ethanol, and dried under vacuum.

The aniline derivatives were heated with the α-halo carboxylic acid ureas in the absence of solvent, as in method A. Due to decomposition of the acyl ureas at high temperatures the yields of the hydantoins were found to be more sensitive and critical to the heating ranges and temperatures. Best results were obtained at temperature ranges of 130-150° C, with reaction times of 1-2 hours in the presence of small quantities of sodium bicarbonate. Slow heating rates (0.5-1 hour) and homogeneous mixing, were necessary, otherwise a sudden solidification occurred and hydantoins could not be isolated. The 1-aryl hydantoins were extracted from the reaction mixtures with warm 10% sodium hydroxide solution. Neutralization of the alkaline solution with conc. HCl yielded the crude product. The hydantoins were purified by crystallization from benzene and ethanol, and were identified by elemental analysis, nmr, and ir spectra.

N-(α-bromopropionyl) urea:

20.0 g (0.09 mole) of α-bromopropionylbromide was added cautiously to 15.0 g (0.25 mole) urea in a 250 ml boiling flask fitted with an air condenser and drying tube. The reaction mixture was heated on a steam bath with vigorous stirring. Following the solidification of the melted mixture (0.5 hr), the oily product was dissolved in 150 ml hot water. Upon cooling, N-(α-bromopropionyl) urea precipitated and was recrystallized from absolute ethanol. The purified product was dried under vacuum.

Yield: 11.6 g, 64% m.p.: 164-5°C

NMR data: (in DMSO d_6)

Methyl protons: 1.61-1.72 ppm, doublet, J=11 Hz

Methine proton: 4.34-4.67 ppm, quartet, J=11 Hz

Amine protons: 7.11-7.37 ppm, broad doublet, 10.32 ppm, singlet

1-(2,3-dimethyl phenyl)-5-methyl hydantoin

2.0 g (0.016 mole) of 2,3-dimethyl aniline was added to 3.0 g (0.015 mole) N-(α-bromopropionyl) urea in a 100 ml three neck flask fitted with a thermometer and an air condenser. The reaction mixture was heated for one hour between 130 and 150°C, following the addition of 0.5 g sodium bicarbonate. The hydantoin was dissolved in 50 ml of warm 10% sodium hydroxide solution. Neutralization of the alkaline solution with conc. HCl yielded the crude product which was filtered and purified by crystallization from benzene and absolute ethanol.

Yield: 1.79 g , 55% m.p.: 176°C

Elemental analysis:

Calculated: % C 66.05, % H 6.42, % N 13.84

Found: % C 66.17, % H 6.09, % N 13.89

NMR data: (in DMSO-d_6)

Methyl protons: 1.13-1.20 ppm, doublet, J=7 Hz

Methyl protons (on aromatic ring): 2.09 and 2.25 ppm, singlets

Methine proton: 4.42-4.63 ppm, quartet, J=7 Hz

Aromatic protons: 7.24 ppm, multiplet

The procedures were the same for the preparation of the following ureas and hydantoins.

The origin and the quality of the chemicals used for the synthesis of the urea derivatives and hydantoins, are listed below.

Camlab/J.T. Baker:

2,3-Dimethylaniline, "Baker"

2,4-Dimethylaniline, "Baker"

2,5-Dimethylaniline, "Baker"

p-Anisidine, "Baker"

α-Bromopropionylbromide, "Baker"

2-Bromo-2-methylpropionylbromide, "Baker"

Benzene, "B. A. R."

Fisher:

o-Fluoroaniline, "highest purity"

Aldrich:

α-Chlorophenylacetylchloride, "97 %"

[illegible], "95 %"

N-(α -chlorophenylacetyl) urea:

Starting Materials : 20.0 g (0.106 mole) α -chlorophenyl acetyl chloride, 15.0 g (0.25 mole) urea.

Yield : 12.8 g , 57% m.p.: 197-9°C (Lit.[79] 200°C)

NMR data : (in DMSO-d_6)

Methine proton : 5.14 ppm, singlet,

Aromatic protons : 7.12 ppm, singlet

Amine protons : 10.25 ppm, singlet, (NH_2 protons overlapped with aromatic ring protons)

N- (2-bromo-2-methylpropionyl) urea:

Starting Materials: 50.0 g (0.217 mole) 2-bromo-2-methyl propionyl bromide, 30.0 g (0.5 mole) urea.

Yield : 16.8 g , 37% m.p.: 138-9°C (Lit.[72] 138-9°C)

NMR data : (in DMSO-d_6)

Methyl protons : 1.92 ppm, singlet

Amine protons : 7.18-7.50 ppm, broad doublet, 9.93 ppm, singlet

1-(α-naphthyl)-5-phenyl hydantoin:

Starting Materials : 2.0 g (0.014 mole) α -napthylamine , 3.0 g (0.014 mole) N-(α -chlorophenylacetyl) urea.

Yield : 1.46 g , 36% m.p.: 225°C

NMR data : (in DMSO-d_6)

Methine proton : 5.51 ppm, singlet

Aromatic protons : 6.97-7.82 ppm, multiplet

Elemental analysis:

Calculated : %C 75.50 , %H 4.64 , %N 9.28

Found : %C 75.87 , %H 4.53 , %N 9.04

1-(o-tolyl)-5,5-dimethyl hydantoin:

Starting Materials : 1.5 g (0.014 mole) o-toluidine, 2.0 g (0.0096 mole) N-(2-bromo-2-methylpropionyl) urea.

Yield : 0.92 g., 44% m.p.: 197-8°C

Elemental analysis:

Calculated : %C 66.06 , %H 6.42 , %N 12.84

Found : %C 66.26 , %H 6.57 , %N 12.87

NMR data : (in DMSO-d_6)

Methyl protons : 1.07-1.33 ppm, doublet,

Methyl protons (on aromatic ring) : 2.11 ppm, singlet

Aromatic protons : 7.13-7.29 ppm, multiplet

1-(o-chlorophenyl)-5,5-dimethyl hydantoin:

Starting Materials : 1.5 g (0.012 mole) o-chloro aniline, 2.0 g (0.0096 mole) N-(2-bromo-2-methyl propionyl) urea.

Yield : 0.66 g., 29% m.p.: 233°C

Elemental analysis:

Calculated : %C 55.35 , %H 4.61 , %N 11.74

Found : %C 55.08 , %H 4.80 , %N 11.70

NMR data : (in DMSO-d_6)

Methyl protons : 1.16-1.28 ppm, doublet,

Aromatic protons : 7.34-7.50 ppm, multiplet

1-(o-Methoxyphenyl)-5,5-dimethyl hydantoin:

Starting Materials : 1.5 g (0.012 mole) o-anisidine, 2.0 g 0.0096 mole) N-(2-bromo-2-methylpropionyl) urea.

Yield : 1.32 g , 59% m.p.: 206°C

Elemental analysis:

Calculated: : %C 61.54 , %H 5.98 , %N 11.96

Found : %C 61.18 , %H 6.31 , %N 11.86

NMR data : (in DMSO-d_6)

Methyl protons : 1.17 ppm, singlet

Methoxy protons : 3.62 ppm, singlet

Aromatic protons : 6.91-7.33 ppm, multiplet

1-(o-Fluorophenyl)-5,5-dimethyl hydantoin:

Starting Materials : 1.5 g . (0.014 mole) o-fluoro aniline, 2.0 g (0.0096 mole) N-(2-bromo-2-methylpropionyl) urea.

Yield : 0.55 g , 26% m.p.:234°C

Elemental analysis:

Calculated : %C 59.46 , %H 4.95 , %N 12.61

Found : %C 59.71 , %H 4.96 , %N 12.84

NMR data : (in DMSO-d_6)

Methyl protons : 1.19 ppm, singlet

Aromatic protons : 7.16-7.38 ppm, multiplet

1-(2,3-dimethylphenyl) -5,5-dimethyl hydantoin:

Starting Materials : g (0.012 mole) 2,3-dimethyl aniline, 2.0 g (0.0096 mole) N-(2-bromo-2-methylpropionyl urea.

Yield : 0.80 g , 36% m.p.: 244-5°C

Elemental analysis :

Calculated : %C 67.24 , %H 6.90 , %N 12.07

Found : %C 67.31 , %H 7.13 , %N 12.11

NMR data : (in DMSO-d_6)

Methyl protons : 1.18-1.43 ppm, doublet

Methyl protons (on aromatic ring) : 2.08 and 2.28 ppm, singlets

Aromatic protons : 7.07-7.30 ppm, multiplets

1-(2,4-dimethylphenyl) -5,5-dimethyl hydantoin:

Starting Materials : 1.5 g (0.012 mole) 2,4-dimethyl aniline, 2.0 g (0.0096 mole) N-(2-bromo-2-methyl propionyl) urea.

Yield : 0.86 g , 39% m.p.: 211-12°C

Elemental analysis:

Calculated : %C 67.24 , %H 6.90 , %N 12.07

Found : %C 67.22 , %H 7.11 , %N 12.05

NMR data : (in DMSO-d_6)

Methyl protons : 1.13-1.38 ppm, doublet

Methyl protons (on aromatic ring) : 2.12 and 2.28 ppm, singlets

Aromatic protons : 7.09-7.28 ppm, multiplet

1-(2,5-dimethylphenyl)- 5,5-dimethyl hydantoin:

Starting Materials : 1.5 g (0.012 mole) 2,5-dimethyl aniline, 2.0 g (0.0096 mole) N-(2-bromo-2-methylpropionyl) urea.

Yield: 0.71 g , 31% m.p.: 198-200°C

Elemental analysis:

Calculated : %C 67.24 , %H 6.90 , %N 12.07

Found : %C 67.16 , %H 7.05 , %N 12.08

NMR data : (in DMSO-d_6)

Methyl protons : 1.21-1.47 ppm, doublet

Methyl protons (on aromatic ring) : 2.18 and 2.33 ppm, singlets

Aromatic protons : 7.05-7.26 ppm, multiplet.

<u>1-(α-naphthyl)-5,5-dimethyl hydantoin:</u>

Starting materials : 1.5 g (0.010 mole) α-naphthylamine, 2.0 g (0.0096 mole) N-(2-bromo-2-methylpropionyl) urea.

Yield : 0.48 g , 20% m.p.: 233°C

Elemental analysis:

Calculated : %C 70.85 , %H 5.55 , %N 11.02

Found : %C 70.41 , %H 5.91 , %N 10.70

NMR data (in DMSO-d_6)

Methyl protons : 1.20-1.53 ppm, doublet

Aromatic protons : 7.51-8.13 ppm, multiplet

<u>1-(β-naphthyl)-5,5-dimethyl hydantoin:</u>

Starting materials : 2.5 g (0.017 mole) β-naphthyl amine, 3.0 g (0.0143 mole) N-(2-bromo-2-methylpropionyl) urea

Yield : 0.50 g , 14% m.p.: 223-5°C

Elemental analysis:

Calculated : %C 70.85 , %H 5.55 , %N 11.02

Found : %C 70.69 , %H 5.40 , %N 11.02

NMR data (in DMSO-d_6) :

Methyl protons : 1.23 ppm, singlet

Aromatic protons : 7.21-7.88 ppm, multiplet

NMR and IR Spectra:

Nmr Spectra of the synthesized compounds were taken on Varian HA-100 100 MHz and A-60A 60 MHz spectrometers. The field sweep mode of operation has been employed for 100 MHz spectra. Two examples of hydantoin nmr spectra are shown in Figure S-1 and Figure S-3 . Methyl protons in the C-5 position of hydantoins absorb between 1.05-1.55 ppm, whereas methyl groups on the aromatic rings are shifted to low field, 2.05-2.35 ppm, due to the deshielding effect of the π-electron system. Hence both types of methyl groups were easily distinguishable. A similar effect was observed on the C-5 methine proton of hydantoins. If the substituent in the C-5 position was a methyl group, the methine proton absorbed between 4.40-4.70 ppm, whereas in 5-phenyl substituted hydantoins it was found between 5.50-5.70 ppm. The NH proton of the hydantoins was broadened by quadrupole relaxation of the nitrogen atom and shifted over a wide range.

Ir spectra of 1-aryl hydantoins were taken through

potassium bromide disks on a Perkin-Elmer 457 Infrared spectrophotometer. Two characteristic modes of vibration are easily recognized in the ir spectra. The first is the NH stretch, which absorbs between 3020-3180 cm-1. The second, the carbonyl stretching mode, gives rise to two bands. One is a moderate intensity absorption between 1760-1780 cm-1 and the other is a strong, broad band between 1690 and 1720 cm-1. Two examples of ir spectra of 1-aryl hydantoins are shown in Figure S-2 and Figure S-4.

All the nmr and ir spectral data of 1-aryl hydantoins were very well in agreement with those of previously studied hydantoins.

Figure 8-I : 100 MHz NMR spectrum of 1-(o-Tolyl) hydantoin (II) in DMSO-d_6 Solution (1000 Hz Scan)

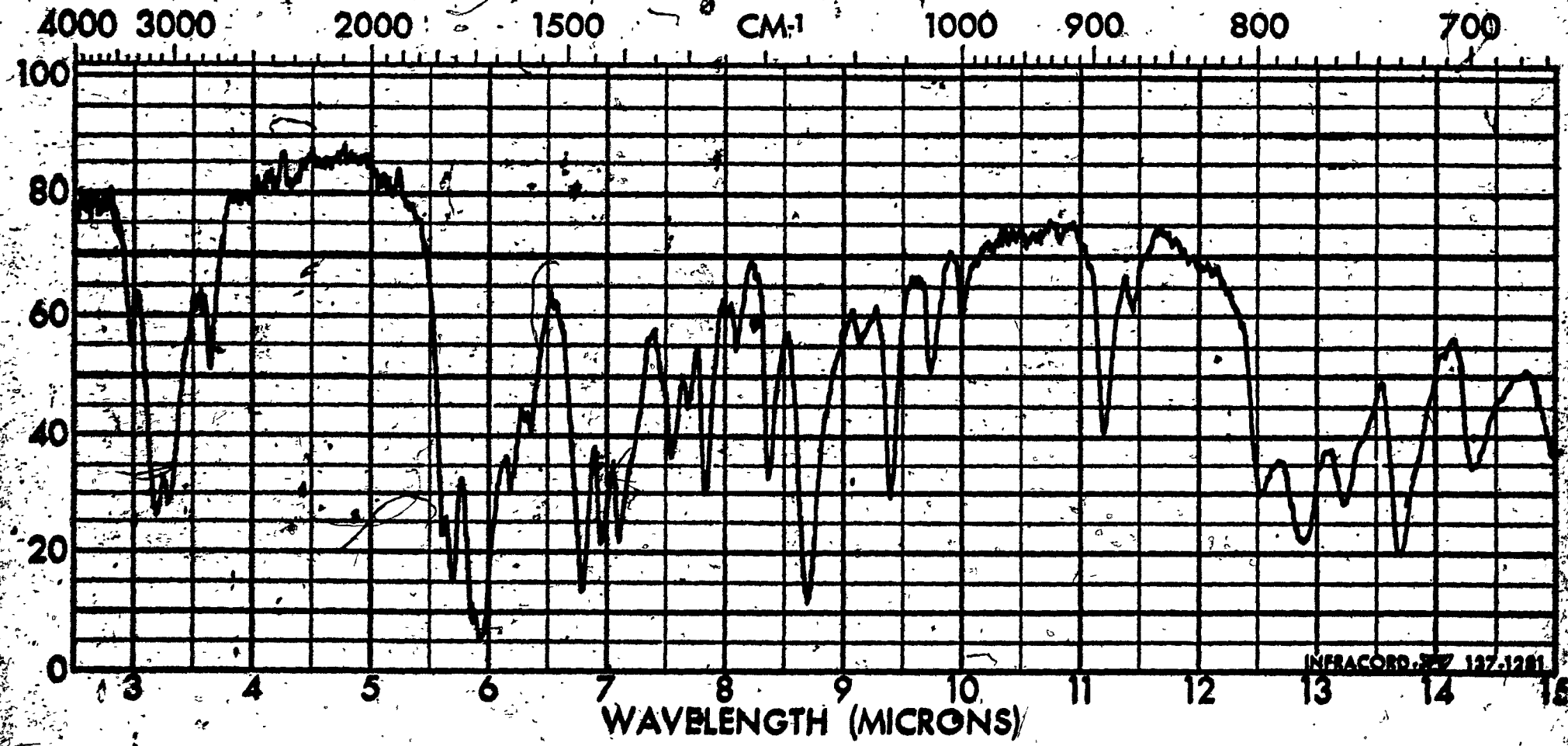

Figure 8-2 : Infrared Spectrum of 1-(o-Chlorophenyl) hydantoin, I.

Figure 8-3 : 100 MHz NMR Spectrum of 1-(2,3-Dimethyl phenyl)-5,5-dimethyl hydantoin (XVIII) in DMSO-d_6 Solution (1000 Hz scan)

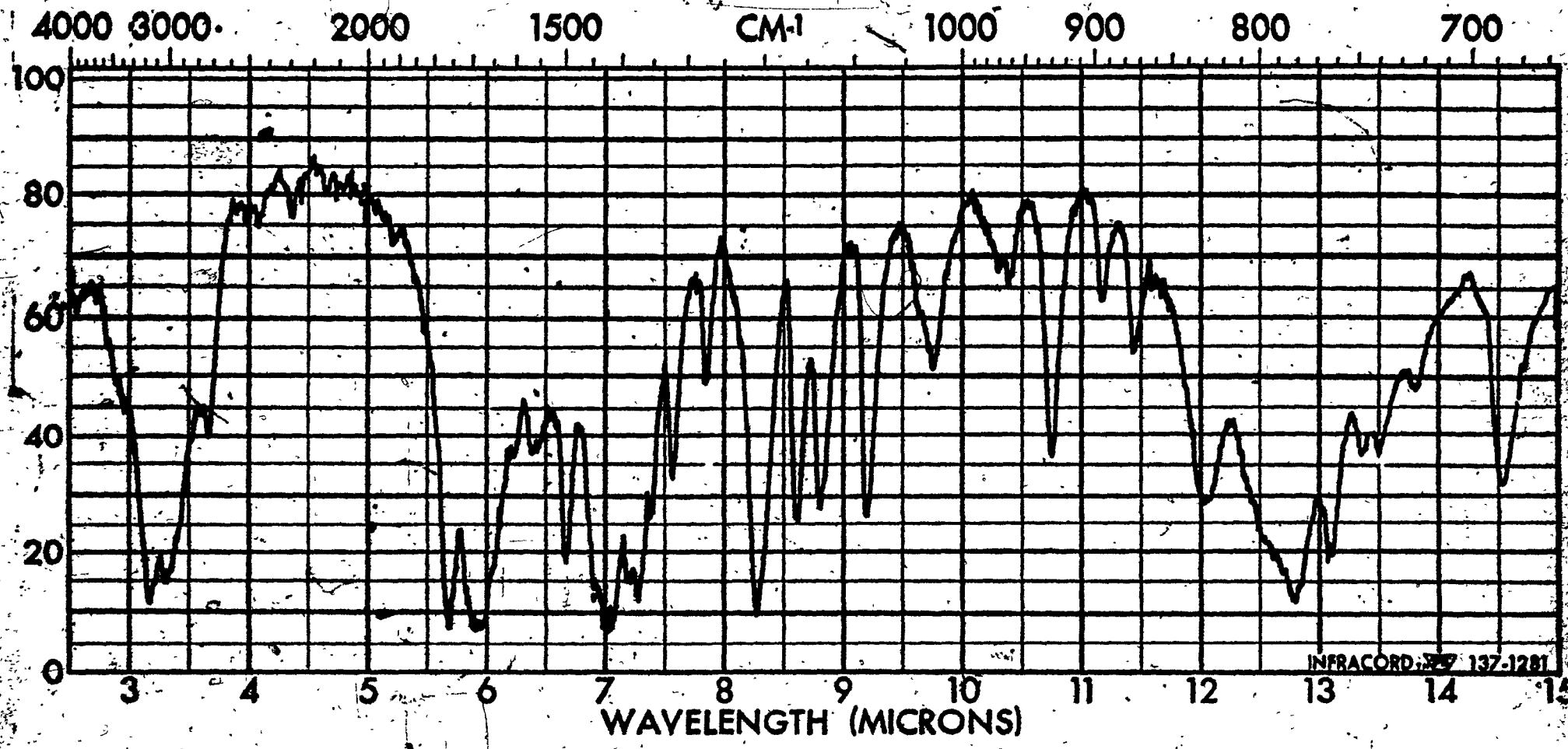

Figure S-4 : Infrared Spectrum of 1-(2,3-Dimethylphenyl)-5,5-dimethyl hydantoin (XVIII)

REFERENCES

1 - D. J. Millen, in "Progress in Stereochemistry", Vol. 3, P.B.D. de la Mare and W. Klyne, Eds., Butterworths, London, 1962, p. 138.

2 - G. Binsch, in "Topics in Stereochemistry", Vol. 3, E. L. Eliel and N. L. Allinger, Eds., Interscience Publishers, New York, 1968, p. 97.

3 - J. A. Pople, W. G. Schneider, H. J. Bernstein, "High Resolution Nuclear Magnetic Resonance", McGraw Hill Pub. Co., N.Y., 1959, p. 365.

4 - W. D. Phillips, J. Chem. Phys., 23, 1363 (1955).

5 - H. S. Gutowsky, C. H. Holm, J. Chem. Phys., 25, 1228 (1956).

6 - J. A. Hirsch, in "Topics in Stereochemistry", Vol. 1, N. L. Allinger, E. L. Eliel, Eds., Interscience, New York, 1967, p. 199.

7 - a) M. Witanowki, J. D. Roberts, J. Am. Chem. Soc., 87, 4878 (1965);
b) G. Fraenkel, D. T. Dix, J. Am. Chem. Soc., 88, 979 (1966).

8 - Y. Shvo, E. C. Taylor, K. Mislow, M. Raban, J. Am. Chem. Soc., 89, 4910 (1967).

9 - L. D. Colebrook, J. A. Jahnke, J. Am. Chem. Soc., 90, 4687 (1968).

10 - a) W. E. Bentz, Ph.D. Thesis, University of Rochester, Rochester, N.Y., 1971;
b) W. E. Bentz, L.D. Colebrook, Can. J. Chem., 47, 2473 (1969).

11 - F. Hund, Ph.D. Thesis, University of Rochester, Rochester, N.Y. 1971.

12 - a) J. R. Fehlner, Ph.D. Thesis, University of Rochester, Rochester, N.Y., 1970;
b) W. E. Bentz, L.D. Colebrook, J. R. Fehlner, Chem. Commun. 974 (1970).

13 - L. D. Colebrook, H. G. Giles, A. Granata, S. Iqli, J. R. Fehlner, Can. J. Chem., 51, 3635 (1973).

14 - a) H. G. Giles, Ph.D. Thesis, Sir George Williams University, Montreal, 1973;
b) L. D. Colebrook, H. G. Giles, A. Rosowsky, Tetra. Lett., 5239 (1972).

15 - A. Granata, M.Sc. Thesis, Sir George Williams University, Montreal, 1972.

16 - D. F. Williams, M.Sc. Thesis, Sir George Williams University, Montreal, 1972.

17 - a) S. Alexander, J. Chem. Phys., 37, 967 (1962);
b) S. Alexander, ibid., 38, 1787 (1963).

18 - a) J. I. Kaplan, J. Chem. Phys., 28, 278 (1958);
J. I. Kaplan ibid., 29, 462 (1958).

19 - A. H. Turner, Ph.D. Thesis, University of Rochester, Rochester, N.Y., 1967.

20 - F. Bloch, Phys. Rev., 70, 460 (1946).

21 - D. W. Marquardt, J. Soc. Ind. App. Math., 11, 431 (1963).

22 - L. D. Colebrook, Personal Communication, Department of Chemistry, Sir George Williams University, Montreal, 1972.

23 - C. E. Johnson, F. A. Bovey, J. Chem. Phys., 29, 1012 (1958).

24 - L. M. Jackman, S. Sternhell, in "Applications of Nuclear Magnetic Resonance Spectroscopy in Organic Chemistry", Pergamon Press, 2nd Ed., London, 1969, p. 94.

25 - J. S. Waugh, R. W. Fessenden, J. Am. Chem. Soc., 79, 846 (1957).

26 - L. D. Colebrook, H. G. Giles, P. H. Bird, A. R. Fraser, Chem. Comm., In Press.

27 - L. Pauling, "The Nature of the Chemical Bond", 3rd Ed., Cornell Univ. Press, Ithaca, N.Y., p. 260.

28 - P. Bell, J. Kenyon, Chem. and Ind., (London), 45, 864 (1926).

29 - E. L. Eliel, "Stereochemistry of Carbon Compounds", McGraw Hill Inc., New York, 1962, p. 156.

30 - a) F. H. Westheimer, J. E. Mayer, J. Chem. Phys., 14, 733 (1946);
b) F. H. Westheimer, in "Steric Effects in Organic Chemistry", M. S. Newman, John Wiley & Sons Inc., New York, 1956, Chap. 12.

31 - a) P. C. Lauterbur, J. Chem. Phys., 26, 217 (1957);
b) C. H. Holm, ibid., 26, 707 (1957).

32 - J. B. Stothers, "Carbon-13 NMR Spectroscopy", Academic Press, New York, 1972.

33 - G. C. Levy, G. L. Nelson, "Carbon-13 Nuclear Magnetic Resonance for Organic Chemists", John Wiley & Sons Inc., New York, 1972.

34 - T. C. Farrar, E. D. Becker, "Pulse and Fourier Transform NMR", Academic Press, New York, 1971.

35 - A. Saika, C. P. Slichter, J. Chem. Phys., 22, 26 (1954).

36 - M. Karplus, J. A. Pople, J. Chem. Phys., 38, 2803 (1963).

37 - D. M. Grant, E. G. Paul, J. Am. Chem. Soc., 86, 2984 (1964).

38 - A. S. Perlin, H. J. Koch, Can. J. Chem., 48, 2639 (1970).

39 - a) J. B. Stothers, P.C. Lauterbur, Can. J. Chem., 42, 1563 (1964);
b) K. S. Dhami, J. B. Stothers, ibid., 43, 498 (1965).

40 - a) A. D. Buckingham, Can. J. Chem., 38, 300 (1960);
b) A. D. Buckingham, T. Schaeffer, W. G. Schneider, J. Chem. Phys., 32, 1227 (1960).

41 - G. E. Maciel, J. J. Natterstad, J. Chem. Phys., 42, 2752 (1965).

42 - R. L. Lichter, J. D. Roberts, J. Phys. Chem., 74, 912 (1970).

43 - D. K. Dalling, D. M. Grant, L. F. Johnson, J. Am. Chem. Soc., 93, 3678 (1971).

44 - F. A. L. Anet, A. J. R. Bourn, J. Am. Chem. Soc., 89, 760 (1967).

45 - K. F. Kuhlmann, D. M. Grant, J. Am. Chem. Soc., 90, 7355 (1968).

46 - A. W. Overhauser, Phys. Rev., 92, 411 (1953).

47 - A. J. Jones, D. M. Grant, K. F. Kuhlmann, J. Am. Chem. Soc., 91, 5103 (1969).

48 - P. C. Lauterbur, J. Chem. Phys., 38, 1415 (1963).

49 - K. S. Dhami, J. B. Stothers, Can. J. Chem., 43, 479 (1965).

50 - G. C. Levy, G. L. Nelson, J. Am. Chem. Soc., 94, 4897 (1972).

51 - A. R. Tarplus, J. H. Goldstein, J. Am. Chem. Soc., 93, 3573 (1971).

52 - G. E. Maciel, J. J. Natterstad, J. Chem. Phys., 42, 2427 (1965).

53 - T. D. Alger, D. M. Grant, E. G. Payl, J. Am. Chem. Soc., 88, 5397 (1966).

54 - K. S. Dhami, J. B. Stothers, Can. J. Chem., 44, 2855 (1966).

55 - a) W. H. Pirkle, J. Am. Chem. Soc., 88, 1837 (1966); b) W. H. Pirkle, T. G. Burlingame, ibid., 4294 (1966).

56 - W. H. Pirkle, T. G. Burlingame, Tetra. Lett., 41, 4039 (1967).

57 - W. H. Pirkle, R. L. Muntz, J. C. Paul, J. Am. Chem. Soc., 93, 2817 (1971).

58 - W. H. Pirkle, T. G. Burlingame, S. D. Beare, Tetra. Lett., 56, 5849 (1968).

59 - a) W. H. Pirkle, S. D. Beare, R. L. Muntz, J. Am. Chem. Soc., 91, 5150 (1969);
b) W. H. Pirkle, S. D. Beare, ibid., 90, 6250 (1968).

60 - W. H. Pirkle, S. D. Beare, J. Am. Chem. Soc., 91, 5150 (1969).

61 - a) J. A. Dale, H. S. Mosher, J. Am. Chem. Soc., 90, 3732 (1968);
b) J. A. Dale, D. L. Dull, H. S. Mosher, J. Org. Chem. 34, 2543 (1969).

62 - J. Andose, B. Egan, K. Mislow, Personal Communication.

63 - J. C. Jochims, G. Taigel, A. Seeliger, Tetra. Lett., 1901 (1967).

64 - a) G. M. Whitesides, D. W. Lewis, J. Am. Chem. Soc., 92, 6979 (1970);
b) G. M. Whitesides, D. W. Lewis, ibid., 93, 5914 (1971).

65 - R. R. Fraser, J. B. Stothers, C. T. Tan, J. Magn., Res., 10, 95 (1973).

66 - L. M. Jackman, S. Sternhell, "Applications of NMR Spectroscopy in Organic Chemistry", Pergamon Press, 2nd Ed., London, 1969, p. 109.

67 - J. I. Kroschwitz, M. Winokur, H. J. Reich, J. D. Roberts, J. Am. Chem. Soc., 91, 5927 (1969).

68 - W. R. Woolfenden, D. M. Grant, J. Am. Chem. Soc., 88, 1496 (1966).

69 - M. Wada, Chem. Ber., 260, 47 (1933).

70 - M. Julia, G. Tchernoff, Bull. Soc. Chim. France, 661 (1958).

71 - Y. G. Mazover, J. Gen. Chem. USSR, 22, 1700 (1952).

72 - S. R. Sadir, H. Dalatian, W. Fanshawe, K. Cyr., R. Lopresti, R. P. Williams, S. D. Upham, L. Goldman, S. Kushner, J. Am. Chem. Soc., 77, 4840 (1955).

73 - D. Vorlander, R. Von Schilling, Chem. Ber., 34, 1646 (1901).

74 - R. E. Miller, D.B. Sharp, J. Org. Chem., 26, 386 (1961).

75 - N. Wada, S. Shimada, S. Nakagawa, A. Inami, Osaka Puritsu Kogyo-Shoreikan Hokoku, 26, 53 (1961).

76 - C. M. Cutter, F.B. Dains, J. Am. Chem. Soc., 50, 2733(1928).

77 - C. A. Bischoff, A. Hausdorfer, Chem. Ber., 25, 2309 (1892).

78 - P. Schwebel, Chem. Ber., 10, 2049 (1877).

79 - Donau-Pharmazie, G.m.b.H. Austrian, 186, 643, Aug. 25, 1956.

80 - S.H. Grover, J.P. Gutherie, J.B. Stothers, J. Mag. Res., 10, 227, (1973).

APPENDIX I

LISTINGS AND DIRECTIONS FOR USE OF THE COMPUTER PROGRAMS USED FOR DATA REDUCTION AND FOR CALCULATION OF KINETIC PARAMETERS

PROGRAM FOR DIGITIZATION OF NMR SPECTRA

The program LINDI is used for the digitization of nmr spectra. A listing of the program is presented in the M.Sc. thesis of Granata.[16] The directions for the use of LINDI are given in the Experimental section-Part I of this thesis. LINDI is written in Fortran and Assembler for the Hewlett-Packard 2114A computer.

PROGRAMS FOR TRANSFER OF DATA

The programs TAPGH, TPDDJ and CHKTP are used for the transfer of digital information from paper tape to magnetic tape. A listing of TAPGH is given in the M.Sc. thesis of Granata.[16] The listings for TPDDJ and CHKTP are presented in the following pages (see also Experimental section-Part I). These programs are written in Fortran for the Hewlett-Packard 2114A computer.

```
FTN,B
      PROGRAM TPDDJ
      COMMON IB(9),B(9),IDEN(35),X(256),KY(256),KKY(4),X
     1X(4)
      K0=0
      K1=1
      K9=9
      FK0=0.0
      WRITE(2,100)
  100 FORMAT(/"PREPARE INPUT TAPE FOR NLINDD"//"USE
     1FREE FIELD FORMAT FOR INPUT"/"NOTE: YES = 1,
     2NO = 0"/"TO ABORT: SET SWITCH 15"/)
      WRITE(2,101)
  101 FORMAT("CAUTION"/"CAUTION"//DO NOT PROCEED UNTIL
     1DATA TAPE IS MOUNTED"/)
      PAUSE
      WRITE(2,102)
  102 FORMAT("PARAMETER IDENTIFICATION:"/"B(1) = TAU(A)
     1"/" B(2) = TAU(B)"/" B(3) = SHIFT(A)"/" B(4) = S
     2HIFT(B)"/" B(5) = COUPLING CONSTANT(A)"/" B(6) =
     3 LINEWIDTH"/" B(7) = SCALING FACTOR"/" B(8) = R
     4ELATIONSHIP FACTOR"/" B(9) = COUPLING CONSTANT
     5(B)"/)
    2 WRITE(2,103)
  103 FORMAT("ENTER SPECT NO")
      CALL RESET
      READ(1,*)NRUN
      WRITE(2,104)
  104 FORMAT("ENT NO OF FIX PRMTS")
      READ(1,*)KP
      IF (KP) 5,3,5
    5 WRITE(2,105)
  105 FORMAT("ENT SUBSC OF FIX PRMTS")
      DO 6 I=1,KP
      READ(1,*)IB(I)
    6 CONTINUE
    3 WRITE(2,106)
  106 FORMAT("ENTER TAU(A)")
      READ(1,*)B(1)
      WRITE(2,107)
  107 FORMAT("ENTER TAU(B)")
      READ(1,*)B(2)
      WRITE(2,108)
  108 FORMAT("ENTER SHIFT(A)")
      READ(1,*)B(3)
      WRITE(2,109)
  109 FORMAT("ENTER SHIFT(B)")
      READ(1,*)B(4)
      WRITE(2,110)
  110 FORMAT("ENTER COUPLING CONSTANT(A)")
      READ(1,*)B(5)
      WRITE(2,114)
  114 FORMAT("ENTER COUPLING CONSTANT(B)")
      READ(1,*)B(9)
```

```
      WRITE(2,111)
  111 FORMAT("ENTER LINE WIDTH")
      READ(1,*)B(6)
      WRITE(2,112)
  112 FORMAT("ENTER SCALING FACTOR")
      READ(1,*)B(7)
      WRITE(2,113)
  113 FORMAT("ENTER RELATIONSHIP FACTOR")
      READ(1,*)B(8)
      IF (ISSW(15))2,7
    7 READ(5,120)IDEN
  120 FORMAT(35A2)
      READ(5,122)NPT
  122 FORMAT(33X,I3,4/)
      N=1
      NC=NPT
      NN=4
    8 READ(5,121)(KKY(I),XX(I),I=1,NN)
  121 FORMAT(3(I5,F8.2,4X)(I5,F8.2))
      DO 9 I=1,NN
      KY(N)=KKY(I)
      X(N)=XX(I)
      N=N+1
    9 CONTINUE
      NC=NC-NN
      IF (NC-4)11,10,10
   10 NN=4
      GO TO 12
   11 NN=NC
   12 CONTINUE
      IF (NPT-N)13,8,8
   13 WRITE(2,133)IDEN
  133 FORMAT("IDENTIFICATION:"//35A2/)
      WRITE(2,135)
  135 FORMAT("TRANSFER TO MAGNETIC TAPE ?")
      READ(1,*)IT
      IF (IT)26,29,26
   26 MAX=KY(1)
      DO 45 I=2,NPT
      IF (MAX-KY(I)) 40,45
   40 MAX=KY(I)
   45 CONTINUE
      SPRD=MAX
      SPRD=0.011*SPRD
      WRITE(7,140)NPT,K9,KP,K1,K1,KO
  140 FORMAT(1213)
      WRITE(7,140)KO,K1,K1,KO,KO,KO
      WRITE(7,145)FKO,SPRD
      IF (KP)30,31,30
   30 WRITE(7,140)(IB(I),I=1,KP),KO,KO,KO,KO,KO
```

```
   31 WRITE(7,142)(FK0,I=1,8)
  142 FORMAT(8F10.0)
      WRITE(7,143)(B(I),I=1,7)
      WRITE(7,143)B(8),B(9),FK0,FK0,FK0,FK0,FK0
  143 FORMAT(7F10.4)
      DO 27 I=1,NPT
      Y=FLOAT(KY(I))/100.0
      WRITE(7,145)Y,X(I)
  145 FORMAT(2F10.3)
   27 CONTINUE
      WRITE(7,146)NRUN,IDEN
  146 FORMAT(I3,35A2)
      WRITE(2,150)
  150 FORMAT("IS ANOTHER DATA SET TO FOLLOW ?")
      READ (1,*)IS
      IF (IS)29,28,29
   28 WRITE(7,146)(K0,I=1,6)
      END FILE 7
      REWIND 7
      WRITE(2,151)
  151 FORMAT("TAPE PREPARATION COMPLETE")
   29 WRITE(2,152)
  152 FORMAT(/"NEXT CASE"/)
      PAUSE
      GO TO 2
      END
      ENDS
```

```
FTN,B
      PROGRAM CHKTP
      DIMENSION B(10),IDEN(36),IB(10),Y(200),X(200)
    1 READ(7,900)N,K,IP,M,IFP,NCONS
      WRITE(2,900)N,K,IP,M,IFP,NCONS
  900 FORMAT(25I3)
      READ(7,900)ISW1,ISW2,ISW3,ISW4,ISW5,ISW6
      WRITE(2,900)ISW1,ISW2,ISW3,ISW4,ISW5,ISW6
      READ(7,930)YMN,SPRD
      WRITE(2,930)YMN,SPRD
  930 FORMAT(7F10.3)
      IF (IP)2,3,2
    2 READ(7,900)(IB(I),I=1,IP)
      WRITE(2,900)(IB(I),I=1,IP)
    3 READ(5,931)FF,T,E,TAU,XL,GA,DEL,ZETA
      WRITE(2,931)FF,T,E,TAU,XL,GA,DEL,ZETA
  931 FORMAT(8F10.3)
      READ(7,930)(B(I),I=1,K)
      WRITE(2,930)(B(I),I=1,K)
      DO 10 I=1,N
      READ(7,100)Y(I),X(I)
      WRITE(2,100)Y(I),X(I)
  100 FORMAT(2F10.3)
   10 CONTINUE
      READ(7,101)NRUN,IDEN
      WRITE(2,101)NRUN,IDEN
  101 FORMAT(I3,36A2)
      GO TO 1
      PAUSE
      END
      ENDS
```

PROGRAMS FOR FITTING OF SPECTRA

The programs NLINDD2, NLINGH, and DD are used to fit the calculated spectra to digitized experimental spectra (see Experimental section-Part I). A listing of NLINGH is presented in the M.Sc. thesis of Granata[16] and in the Ph.D. thesis of Fehlner.[12] The listings of NLINDD2 and DD are given in the following pages. NLINDD2 and NLINGH are written in Fortran for the CDC-6400 computer. Program DD is written in Fortran for the Hewlett-Packard 2114A computer.

```
      PROGRAM NLIN(INPUT,OUTPUT,TAPE3,TAPE5,TAPE6=OUTPUT)
C     CDC 6400 VERSION.  OCTOBER 1971
C     TAPE5 IS USED FOR DATA INPUT
C
C     MODIFIED VERSION.   APRIL 1971
C     PREPARED FOR MAGNETIC TAPE INPUT.
C     RESTRICTED TO TWO DATA VALUES, IN (2F10.0) FORMAT.
C     CERO INPUT MAY BE USED, BUT FORMAT CARD (ITEM 7) MUST BE OMITTED.
C     TO RE-CONVERT TO ORIGINAL VERSION OF NLIN, INSERT AFTER CARD 1250
C     READ(5,902)(FMT(I),I=1,12)
C     REPLACE CARD 1280 WITH
C  56 READ(5,FMT)Y(I),(X(I,L),L=1,M)
C     REMOVE CARD 1281.
C
C     NONLINEAR LEAST SQUARES                                          281
C     BY     D. W. MARQUARDT
C     PROGRAMMED BY       I. BAUMEISTER III,
C                         J. ANN SHELDON AND RUBY M. STANLEY
C                   IBKT=1 MEANS USE UPPER A MATRIX
C                   IBKT=2 MEANS USE TAPE 3
C
      DIMENSION FMT(18),PRNT(5),SPRNT(5)
      DIMENSION BS(50),DB(50),BA(50),G(50),W(51),IB(49),SA(50),P(50),A(5
     10,51),B(50)
      DIMENSION X(500,1),Y(500)
      DIMENSION CONS(25)
      DATA IBCH/1H /,IOCH/1HO/,IPCH/1HP/,IXCH/1HX/,IYCH/1HY/
C
C     ------------------------------------------------------------------
C     MAX NO OF PARAMETERS IS K=50
C     MAX NO OF IND VARS IS M=10
C     MAX NO OF OBSERVATIONS IS N=500
C                   IWHER =-1 MEANS DO ANY SPECIAL INITIALIZING FOR CASE
```

```
C                    IWHER = 0 MEANS START NEW CASE OR END RUN
C                    IWHER = 1 MEANS GET P S AND F
C                    IWHER GREATER THAN 1 MEANS GET F ONLY
C     ------------------------------------------------------------------
C     SET ITERATION LIMIT
      ITLIM=50
C     ------------------------------------------------------------------
      NPRNT=0
  650 IWHER = 0
  652 GO TO 4
  653 IWHER = IWHER
      IF (IWHER.GT.0)GO TO 654
      IF (IWHER.EQ.0)GO TO 660
  651 CONTINUE
C                    CODING FOR CASE INITIALIZING GOES HERE
C     ..................................................................
      CALL SUBZ(Y,X,B,PRNT,NPRNT,N)
C     ..................................................................
      IF (IAOUT.EQ.0) GO TO 652
      GO TO 650
  654 CONTINUE
C                    CODING TO MAKE F GOES HERE
C                    F IS Y HAT (I)
C                    NPRNT IS THE NO OF OTHER WORDS TO BE PRINTED
C                    THE WORDS TO BE PRINTED ARE IN PRNT(1)...PRNT(5)
C     ..................................................................
      CALL      FCODE(Y,X,B,PRNT,F,I,RES)
C     ..................................................................
      IF (IWHER.NE.1)GO TO 652
  656 IF (IFSS2.NE.0) GO TO 652
  658 CONTINUE
C                    CODING TO MAKE DF/DB GOES HERE
C                    MAKE K OF THEM. CALL THEM P(J)
```

```
C                    THEY ARE MADE FROM X(I,L) AND B(J)
C     ..................................................................
      CALL PCODE(P,X,B,PRNT,F,I)
C     ..................................................................
      GO TO 652
  660 STOP 111
C                    THIS IS THE END OF THE MAIN ROUTINE
C     ------------------------------------------------------------------
    4 IWHER = IWHER
C               - 0 +
      IF (IWHER.LT.0)GO TO 59
      IF (IWHER.EQ.0)GO TO 10
C             1  2  3  4
    8 GO TO (75,304,606,620), IWHER
C                    READ FIRST CARD OF NEXT CASE
   10 ITCT=0
      IROUT=0
      K1 = 1
      K2 = 1
      IISS = 0
      READ (5,900) N,K,IP,M,IFP,NCONS
      NTILDA=N+NCONS
      XNT=NTILDA
      IF (N.LE.0)GO TO 20
      READ (5,900) IWS1,IWS2,IWS3,IWS4,IWS5,IWS6
      IFS31=2
      IF (IWS5.EQ.0)GO TO 210
      PAUSE 5
  210 CONTINUE
      WRITE (6,932)
   21 GO TO 21
C                    END OF LAST PROBLEM
   20 GO TO ( 19,  17),IBKT
```

```
   17 REWIND 3
   19 INNER=0
      GO TO 553
   21 IF (IFF.LE.0)GO TO 22
   23 CONTINUE
      READ (5,930)YMN,SPRD
   22 IF(IP.LE.0) GOTO 30
   24 READ(5,900)(IH(I), I = 1,IP)
      DO 26 I=1,IP
      IF (IA(I).GT.0)GO TO 26
   25 WRITE (6,926)
  212 CONTINUE
      IBOUT=I
   26 CONTINUE
   30 READ (5,931) FF,T,E,TAU,XL,GAMCR,DEL,ZETA
C                    DUB IN INPUT CONSTANTS IF NOT SUPPLIED
C                    ( XL IS CHECKED IN FIRST ITERATION )
      IF(FF.GT.0.) GOTO 34
   32 FF=4.
   34 IF(E.GT.0.) GOTO 37
   36 E=.00005
   37 IF(TAU.GT.0.) GOTO 39
   38 TAU=.001
   39 IF(T.GT.0.) GOTO 42
   40 T=2.
   42 IF (K .GT.25)GO TO 46
   44 IAKT=1
      GO TO 50
   46 IAKT=2
      REWIND 3
   50 IF(GAMCR.GT. 0.) GOTO 52
   51 GAMCR = 45.
   52 IF (DEL.GT. 0.) GO TO 55
```

```
      DEL=.00001
   55 IF (ZETA.GT. 0.) GO TO 53
      ZETA=.1E-30
   53 XKDA =-1.
   54 CONTINUE
C                    READ IN INITIAL B GUESSES 7 TO THE CARD
C     READ (5,901)(B(I),I=1,K)
      DO 56 I=1,N
   56 READ(5,950)Y(I),(X(I,L),L=1,M)
  950 FORMAT(2F10.0)
      IWHER=-1
      GO TO 653
   59 IRKA=1
C
C     ..................................................................
C                    START THE CALCULATION OF THE PTP MATRIX
   58 WRITE (6,907)N,K,IP,M,IFP,GAMMA,DEL,FF,T,E,TAU,XL,ZETA
  213 GO TO 61
   60 CONTINUE
      IF (IWS3.NE.0) GO TO 61
      IWS3=IWS3-1
      IWS3=MAX0(IWS3,0)
   61 DO 62 I=1,K
      B(I)=0.
      DO 62 J=1,K
   62 A(I,J)=0.
      GO TO (63,69,69),IRKA
   63 IF (IWS).EQ.0)GO TO 630
  630 IFSS3=IWS3
      IFSS2=IWS2
      GO TO 70
   65 IRKA=2
      GO TO (70,65),IFSS2
```

```
      IFSS=0
      GO TO 70
   68 CONTINUE
      WRITE (6,908) ITCT,(B(J),J=1,K)
  908 CONTINUE
      IF (IFSS3.EQ.0)GO TO 73
      IF (IFP.LE.0)GO TO 68
   67 WS = YMN*SPRD
      WRITE( 6,906)YMN,WS
  906 CONTINUE
      GO TO 73
   68 WRITE( 6,910)
  910 CONTINUE
   73 I=1
      PHI=0.
      PHIN=0.
      ICONS=1
      IF (IFSS2.EQ.0) GO TO 57
      GO TO 600
   72 IF (IFSS2.EQ.1)GO TO 602
C                    THIS IS THE ANALYTICAL P S ROUTINE
C    57 IWHER=1      GET P S AND F
      GO TO 653
   75 IF (IP.LE.0)GO TO 80
   76 DO 77 I=1,IP
      IWSAIA(I)
   77 P(IWS)=0.
      GO TO 80
C     .....
C                    THIS IS THE ESTIMATED P S ROUTINE
  600 CONTINUE
  602 IWHER=3
```

```
      GO TO 653
  606 RWS=RES
      FSAVE=F
      DO 607 II=1,NPRNT
  607 SPRNT(II)=PRNT(II)
      J=1
  608 IF (IP.LE.0)GO TO 618
  610 DO 612 II=1,IP
      IF ((J-IB(II)).EQ.0)GO TO 621
  612 CONTINUE
  618 DBW=B(J)*DEL
      TWS=B(J)
      B(J)=R(J)+DBW
      IWHER=4
      GO TO 653
  620 B(J)=TWS
      P(J)=-(RES-RWS)/DBW
      GO TO 622
  621 P(J)=0.
  622 J=J+1
      IF ((J-K).LE.0)GO TO 608
  624 RES=RWS
      F=FSAVE
      DO 625 II=1,NPRNT
  625 PRNT(II)=SPRNT(II)
C                 END OF ESTIMATED P S ROUTINE
C     ..........................................................
C                 NOW, USE THE P S TO MAKE PARTIALS MATRIX
      DO 80 JJ=1,K
      A(JJ)=A(JJ)+RES*P(JJ)
      DO 80 II=JJ,K
      A(II,JJ)=A(II,JJ)+P(II)*P(JJ)
   80 A(JJ,II)=A(II,JJ)
```

```
      IF (IPP.LE.0)GO TO 318
  800 IF (IFSS3.EQ.0.OR.I.GT.N) GO TO 314
C                   PLOTTING Y(I),F
  802 IO = (Y(I)-YMN)*100./SPRD
      IPP = (F-YMN)*100./SPRD
      IF (IO.EQ.IPP)GO TO 808
      IF (IO.GT. IPP)GO TO 812
C                   Y(I) OUT FIRST
  804 IP1=IOCH
      IP2=IPCH
      I1=IO
      I2=IPP
      GO TO 816
C                   ONLY ONE CHARACTER
  808 IP1=IYCH
      IP2=IBCH
      I1=IO
      I2=IPP
      GO TO 816
C                   F OUT FIRST
  812 IP1=IPCH
      IP2=IOCH
      I1=IPP
      I2=IO
C                   ZERO PLOTS IN THE LEFT HAND COLUMN. SO I1 IS ITS
C                   OWN BLANK COUNTER
C                   OVERFLOWS PLOT X IN COLUMN 102
C                   UNDERFLOWS ALSO PLOT X IN COLUMN ZERO
  816 IF (I2.LE.101)GO TO 819
  817 I2=101
      IP2=IXCH
      IF (I1.LT.101)GO TO 819
  818 I1=101
```

```
      IP1=IXCH
      IP2=IBCH
      GO TO 825
  819 IF (I1.GE.0)GO TO 825
  822 I1=0
      IP1=IXCH
      IF (I2.GT.0)GO TO 825
  823 I2=1
      IP2=IBCH
  825 I1M1=I1
      I1M2=I2-I1-1
      IF (I1M1.GT.0)GO TO 832
  820 IF (I1M2.GT.0)GO TO 828
  824 WRITE (6,928)IP1,IP2
  215 CONTINUE
      GO TO 844
  828 WRITE (6,928)IP1,(IBCH,II=1,I1M2),IP2
  216 CONTINUE
      GO TO 844
  832 IF (I1M2.GT.0)GO TO 840
  836 WRITE (6,928)(IBCH,II=1,I1M1),IP1,IP2
  217 CONTINUE
      GO TO 844
  840 WRITE (6,928)(IBCH,II=1,I1M1),IP1,(IBCH,II=1,I1M2),IP2
  218 CONTINUE
  844 GO TO 314
  310 WS=BES
      IF (IFSS3.EQ.0.OR.1.GT.N) GO TO 314
  309 IF (NPRNT.GT.0)GO TO 312
  311 WRITE (6,925)Y(I),F,WS
  313 CONTINUE
      GO TO 314
  312 WRITE (6,925)Y(I),F,WS,(PRNT(JJ),JJ=1,NPRNT)
```

```
  220 CONTINUE
  314 WS=RES
      PHI=PHI+WS*WS
      IF (I.GT.N) GO TO 313
      PHIN=PHIN+WS*WS
      GO TO 315
  313 CONS(ICONS)=RES
      ICONS=ICONS+1
  315 I=I+1
      IF (I.LE.NTILDA) GO TO 72
   84 IF (IP.LE.0)GO TO 88
   85 DO 87 JJ=1,IP
      IWS=IB(JJ)
      DO 86 II=1,K
      A(IWS,II)=0.
   86 A(II,IWS)=0.
   87 A(IWS,IWS)=1.
   88 GO TO (90,704,703),IBKA
C                    SAVE SQUARE ROOTS OF DIAGONAL ELEMENTS
   90 DO 92 I=1,K
   92 SA(I)=SQRT (A(I,I))
      DO 106 I=1,K
      DO 100 J=I,K
      WS = SA(I)*SA(J)
      IF(WS.GT.0.) GOTO 98
   96 A(I,J) =0.
      GO TO 100
   98 A(I,J)=A(I,J)/WS
  100 CONTINUE
      IF(SA(I).GT.0.) GOTO 104
  102 G(I)=0.
      GO TO 106
  104 G(I)=G(I)/SA(I)
```

```
106 CONTINUE
    DO 110 I=1,K
110 A(I,I)=1.
120 PHIZ=PHI
C                    WE NOW HAVE PHI ZERO
    GO TO (1132,1130),IBKT
1130 WRITE (3)A
    REWIND 3
    GO TO 1134
1132 DO 1133 II=1,K
    II=II+25
    DO 1133 JJ=1,K
1133 A(II,JJ)=A(II,JJ)
C 1134 CONTINUE
    IF (IFCT.NE.0) GO TO 163
C                    FIRST ITERATION
150 IF(XL.GT.0.) GOTO 154
152 XL=0.01
154 DO 161 J=1,K
161 BS(J)=B(J)
C 163 IDIF=1
    ASSN=0.0
    IFCT=IFCT+1
    IF (IFCT.GT.1) GO TO 1800
    IF (IFCT.GT.0)GO TO 165
    IF (XL.GE.0.) GO TO 168
    WRITE (6,1)PHIZ,SE,XLL,GAMMA,XL
    GO TO 170
    WRITE (6,12)PHIZ,SE,XLL,GAMMA,XL
```

```
  222  CONTINUE
       GO TO 169
  165  IF (NCONS.EQ.0) GO TO 166
       WRITE (6,938) (JJ,CONS(JJ),JJ=1,NCONS)
  166  WRITE (6,939)
  111  DO 114 I=1,K
       WRITE (6,937) I, (A(I,J),J=1,K)
  114  CONTINUE
       IF (IFSS2.EQ.0) GO TO 1661
       WRITE (6,903) PHIZ,SE,XL
  223  CONTINUE
       GO TO 169
 1661  WRITE (6,909)PHIZ,SE,XL
  224  CONTINUE
  169  GO TO 200
  164  PHIL=PHI
C                    WE NOW HAVE PHI LAMBDA
       DO 170 J=1,K
       IF (ABS(DB(J)/(ABS(B(J)) + TAU)).GE.E) GOTO 172
  170  CONTINUE
       WRITE (6,923)
  225  CONTINUE
       GO TO 700
  172  IF (IWS5.EQ.0)GO TO 1720
 1720  IF (IWS4.EQ.0)GO TO 173
       IF (IWS4.EQ.1)GO TO 171
       IWS4=IWS4-1
       GO TO 173
  171  WRITE (6,924)
  226  CONTINUE
       GO TO 700
  173  XKDB = 1.
       IF (PHIL.GT.PHIZ)GO TO 190
```

```
  174 XLS=XL
      DO 176 J=1,K
      BA(J)=B(J)
  176 B(J)=BS(J)
      IF (XL.GT..00000001)GO TO 175
 1175 DO 1176 J=1,K
#     B(J)=BA(J)
 1176 BS(J)=B(J)
      GO TO 60
  175 XL=XL/10.
      IRK1=2
      GO TO 200
  177 PHL4=PHI
C                    WE NOW HAVE PHI(LAMBDA/10)
      IF(PHL4.GT.PHIZ) GOTO 184
  182 DO 183 J=1,K
  183 BS(J)=B(J)
      GO TO 60
  184 XL=XLS
      DO 186 J=1,K
      B(J)=BA(J)
  186 BS(J)=BA(J)
      GO TO 60
  190 IRK1=4
      XLS=XL
      XL=XL/10.
      DO 185 J=1,K
  185 B(J)=BS(J)
      GO TO 200
  192 IF (PHI.LE.PHIZ)GO TO 196
  191 XL=XLS
      IRK1=3
  193 XL=XL*10.
```

```
  195 DO 193 J=1,K
  193 B(J)=AS(J)
      GO TO 200
  194 PHIT4=PHI
C                        WE NOW HAVE PHI(10*LAMBDA)
  180  IF (PHIT4.GT.PHIZ)GO TO 198
 #196 DO 197 J=1,K
  197 BS(J)=B(J)
      GO TO 50
  198  IF (GAMMA.GE.GAMCR)GO TO 192
   199 XKDB = XKDB/2.
       DO 1199 J=1,K
       IF (ABS(DB(J)/(ABS(B(J))+TAU)).GE.E)GO TO 195
 1199 CONTINUE
       DO 1200 J=1,K
 1200 B(J)=AS(J)
       WRITE (6,934)
  227  CONTINUE
       GO TO 700
C
C     ..................................................................
C                      SET UP FOR MATRIX INVERSION
   200 GO TO (1102,1100),IBKT
  1100 READ (3)A
       REWIND 3
       GO TO 1104
  1102 DO 1103 II=1,K
       III=II+25
       DO 1103 JJ=1,K
  1103 A(II,JJ)=A(III,JJ)
  1104 DO 202 I=1,K
   202 A(I,I)=A(I,I)+XL
C                    GET INVERSE OF A AND SOLVE FOR DB (J)S
```

```
      IBKM=1
C     ..................................................................
C                    THIS IS THE MATRIX INVERSION ROUTINE
C                    K IS THE SIZE OF THE MATRIX
  404 CALL GJR(A,K,ZETA,MSING)
      GO TO (415,650), MSING
  415 GO TO (416,710), IBKM
C                    END OF MATRIX INVERSION, SOLVE FOR DB(J)
  416 DO 420 I=1,K
      DB(I)=0.
      DO 421 J=1,K
  421 DB(I)=A(I,J)*G(J)+DB(I)
  420 DB(I)=XKDB*DB(I)
      XLL=0.
      DTG = 0.
      GTG = 0.
      DO 250 J=1,K
      XLL=XLL+DB(J)*DB(J)
      DTG = DTG + DB(J)*G(J)
      GTG = GTG + G(J)**2
      DB(J)=DB(J)/SA(J)
  250 B(J)=B(J)+DB(J)
      KIP=K-IP
      IF (KIP.EQ.1) GO TO 1257
      CGAM=DTG/SQRT(XLL*GTG)
      JGAM = 1
      IF(CGAM.GT..0) GOTO 253
  252 CGAM = ABS(CGAM)
      JGAM = 2
  253 GAMMA = 57.2957795*(1.5707288*CGAM*(-0.2121144+CGAM*(0.074261
     1-CGAM*.0187293)))*SQRT(1.-CGAM)
      GO TO (257,255), JGAM
  255 GAMMA = 180.-GAMMA
```

```
      IF (XL.LT.1.0)GO TO 257
1256  WRITE(6,922)XL,GAMMA
      CONTINUE
      GO TO 700
1257  GAMMA=0.
257   XLL=SQRT(XLL)
      IBK2=1
      GO TO 300
252   IF (IFSS3.EQ.0)GO TO 256
254   WRITE (6,904) (DB(J),J=I,K)
229   CONTINUE
      WRITE (6,905)PHI,XL,GAMMA,XLL
230   CONTINUE
250   GO TO (164,177,194,187),IBK1
C
C     ..................................................................
C                    CALCULATE PHI
300   I=1
      PHI=0.
      PHIN=0.
      IWHER=2
      IF (IWSS.EQ.0) GO TO 653
302   GO TO 653
304   PHI=PHI+(RES**2)
      IF (I.GT.N) GO TO 305
      PHIN=PHIN+RES*RES
305   I=I+1
      IF (I.LE.NTILDA) GO TO 302
316   IISS = 1
      K1 = K2
      GO TO 999
C
C
```

962

```
C     ..................................................................
C                    THIS IS THE CONFIDENCE LIMIT CALCULATION
  700 DO 702 J=1,K
  702 B(J)=BS(J)
      WRITE (6,933)N,K,IP,M,FF,T,E,TAU
  23  CONTINUE
      IBKA=2
      NTILDA=N
C                    THIS WILL PRINT THE Y,YHAT,DELTA Y
      ITCT=ITCT-1
      IPSS3=I
      GO TO 61
  704 IF (IFP.LE.0) GO TO 703
  705 IBKA=1
      IFP=0
      GO TO 61
  703 IF (NCONS.EQ.0) GO TO 706
      WRITE (6,938) (JJ,CONS(JJ),JJ=1,NCONS)
  706 WRITE(IP
      WRITE(IP)(PHIZ(MS)
      PHIZ=PHI
      IF (IFPSZ.EQ.0)GO TO 709
      WRITE (6,903)PHIZ,SE,XL
      CONTINUE
      GO TO 710
      WRITE(6,903) PHIZ,SE,XL
      CONTINUE
                    NOW WE HAVE MATRIX A
      GO TO (1)(2,1120),IBKT
      WRITE (IP)A
      GO TO 1124
      DO 1123 I=1,K
```

```
      II1=II+25
      DO 1123 JJ=1,K
 1123 A(II1,JJ)=A(II,JJ)
 1124 IRKM=2
      GO TO 404
C
C                    NOW WE HAVE C = A INVERSE
  710 DO 711 J=1,K
      IF(A(J,J).LT.0.) GO TO 713
  711 SA(J)=SQRT(A(J,J))
      GO TO 715
  713 IROUT=1
  715 KST=-4
      WRITE (6,916)
  234 KST=KST+5
      KEND=KST+4
      IF (KEND.LT.K) GO TO 719
      KEND=K
  719 DO 712 I=1,K
  712 WRITE (6,918)I,(A(I,J),J=KST,KEND)
      IF (KEND.LT.K) GO TO 234
      IF (IROUT.EQ.0) GO TO 717
      WRITE (6,936)
      GO TO 650
  717 DO 718 I=1,K
      DO 718 J=1,K
      WS=SA(I)*SA(J)
      IF(WS.GT. 0.) GOTO 716
  714 A(I,J)=0.
      GO TO 718
  716 A(I,J)=A(I,J)/WS
  718 CONTINUE
      DO 720 J=1,K
```

```
      720 A(J,J)=1.
          WRITE (6,917)
      236 CONTINUE
          KST=0
      721 KST=KST+10
          KEND=KST+9
          IF (KEND.LT.K) GO TO 722
          KEND=K
      722 DO 724 I=1,K
      724 WRITE (6,935) I,(A(I,J),J=KST,KEND)
          IF (KEND.LT.K) GO TO 721
C                         GET T*SE*SQRT(C(I,I))
          DO 726 J=1,K
      726 A(J)=.SE*SA(J)
          GO TO (1112,1110),IBKT
     1110 READ (3)A
          REWIND 3
          GO TO 1114
     1112 DO 1113 II=1,K
          JJ=II+25
          DO 1113 JJ=1,K
     1113 A(II,JJ)=A(II,JJ)
     1114 CONTINUE
      747 WRITE (6,919)
      238 CONTINUE
          IP=K-1
          DO 744 J=1,K
          IF (IP.LE.0)GO TO 743
          DO 742 I=1,IP
          IF (I.EQ.J)GO TO 746
      742 CONTINUE
      743 A(I,J)=SQRT(A(I,I)*A(J,J))*SA(J)
      744 SA(J)=SA(J)
```

```
      OPL=BS(J)-SA(J)*T
      OPU=BS(J)+SA(J)*T
      SPL=BS(J)-HJTD
      WRITE (6,927) J,STE,OPL,OPU,SPL,SPU
      SPU=BS(J)+HJTD
  238 CONTINUE
      GO TO 750
  744 WRITE (6,913)J
  240 CONTINUE
  750 CONTINUE
C                        NONLINEAR CONFIDENCE LIMIT
      IF (IWS6.EQ.1) GO TO 650
      WS=K-IP
      WSI=N-K+IP
      PKN=WS/WSI
      PC=PHIZ*(1.+FF*PKN)
      WRITE (6,920)PC
  241 CONTINUE
      WRITE (6,921)
  242 CONTINUE
      IFSS3=1
      K1 = 1
  999 DO 790 J = K1,K
      K2 = J
      IF(IISS.NE.1) GO TO 998
      IISS = 0
      GO TO (252,780,704,762,766,772),IBK2
  998 IAKP=1
      DO 752 JJ=1,K
  752 B(JJ)=BS(JJ)
      IF (IP.LE.0)GO TO 758
  754 DO 756 JJ=1,IP
      IF (J.EQ.IB(JJ))GO TO 787
```

```
  756 CONTINUE
  758 DD=-1.
      IBKN=1
  760 D=DD
      B(J)=BS(J)+D*SA(J)
      IBK2=4
C     GO TO 300
  762 PHI1=PHI
      IF (PHI1.GE.PC)GO TO 770
  764 D=D+DD
      IF (D/DD.GE.5.)GO TO 788
  765 B(J)=BS(J)+D*SA(J)
      IBK2=5
      GO TO 300
  766 PHID=PHI
      IF (PHID.LT.PC)GO TO 764
      IF (PHID.GE.PC) GO TO 778
  770 D=D/2.
      IF (D/DD.LE..001)GO TO 788
  771 B(J)=BS(J)+D*SA(J)
      IBK2=6
      GO TO 300
  772 PHID=PHI
      IF (PHID.GT.PC)GO TO 770
  778 XK1=PHI2/D+PHI1/(1.-D)*PHID/(D*(D-1.))
      XK2=-(PHI2*(1.+D)/D+D/(1.-D)*PHI1+PHID/(D*(D-1.)))
      XK3=PHI2-PC
      BC = (SQRT(XK2*XK2-4.*XK1*XK3)-XK2)/(2.*XK1)
      GO TO (779,784),IBKN
  779 B(J)=BS(J)-SA(J)*BC
      GO TO 781
  784 B(J)=BS(J)+SA(J)*BC
  781 IBK2=2
```

```
      GO TO 300
  780 GO TO (782,786),IBKN
  782 IBKN=2
      DD=1.
      BL=B(J)
      PL=PHI
C     GO TO 760
  786 BU=B(J)
      PU=PHI
      GO TO (783,795,785,789),IBKP
  783 WRITE (6,918) J, BL, PL, BU, PU
  243 CONTINUE
      GO TO 790
  795 WRITE (6,915) J, BU, PU
  244 CONTINUE
      GO TO 790
  785 WRITE (6,918)J,BL, PL
  245 CONTINUE
      GO TO 790
  787 WRITE (6,913)J
  246 CONTINUE
      GO TO 790
  789 WRITE (6,914)J
  247 CONTINUE
      GO TO 790
  788 GO TO (791,792),IBKN
C                    DELETE LOWER PRINT
  791 IBKP=2
      GO TO 780
  792 GO TO (793,794),IBKP
C                    DELETE UPPER PRINT
  793 IBKP=3
      GO TO 780
```

```
C                    LOWER IS ALREADY DELETED, SO DELETE BOTH
  794 IBKP=4
      GO TO 780
  790 CONTINUE
      GO TO 10
 1800 WRITE(6,1850)
      GO TO 10
C     ..................................................................
  900 FORMAT (2513)
  901 FORMAT (7F10.0)
  902 FORMAT(18A4 )
  903 FORMAT (/13X,4H PHI 14X,4H S E                  9X,7H LAMBDA   6X,
     1 25H ESTIMATED PARTIALS USED  / 5X,2E18.8,  E13.3 )
  904 FORMAT(/12H INCREMENTS 5E18.8/(12X,5E18.8) )
  905 FORMAT (13X,4H PHI 10X,7H LAMBDA 6X,7H GAMMA  6X, 7H LENGTH  /
     1 5X, E18.8, 3E13.3)
  906 FORMAT(1X,1E9.2,86X,1E9.2 /1X,1H+ 99X,1H+ )
  907 FORMAT( 5H1N = I3,5X,5H K = I3,5X,5H P = I3,5X,5H M = I3,5X,
     1 7H IFP = I3,5X,13HGAMMA CRIT = E10.3,5X,6HDEL = E10.3/6H FF =
     2E10.3,5X,5H T = E10.3,5X,5H E = E10.3,5X,7H TAU = E10.3,5X,6H XL =
     3  E10.3 , 4X, 7HZETA = E10.3 /)
  908 FORMAT (/2H (I3,13H) PARAMETERS 5E18.8/(18X,5E18.8))
  909 FORMAT (/13X,4H PHI 14X,4H S E                  9X,7H LAMBDA 6X,
     1 25H ANALYTIC PARTIALS USED   /5X, 2E18.8,  E13.3)
  910 FORMAT(1H /5X,9X,4H OBS 13X,5H PRED 13X,5H DIFF  )
  911 FORMAT (/13X,4H PHI 14X,4H S E 11X,7H LENGTH 6X, 7H GAMMA 6X,
     2 7H LAMBDA 6X, 25HESTIMATED PARTIALS USED  /5X, 2E18.8, 3E13.3)
  912 FORMAT (/13X,4H PHI 14X,4H S E 11X,7H LENGTH 6X, 7H GAMMA 6X,
     1 7H LAMBDA 6X, 24HANALYTIC PARTIALS USED  /5X, 2E18.8, 3E13.3)
  913 FORMAT(12X,I3,20H PARAMETER NOT USED  )
  914 FORMAT(2X,I3,12H NONE FOUND  )
  915 FORMAT(2X,I3,36X,2E18.8  )
  916 FORMAT(1H /13H PTP INVERSE )
```

```
  917 FORMAT(1H /30H PARAMETER CORRELATION MATRIX  )
  918 FORMAT( 2X,I3,5E18.8)
  919 FORMAT( 1H /1H / 13X,4H STD 17X, 16H ONE - PARAMETER 21X,
     1 14H SUPPORT PLANE / 3X, 2H B 7X,6H ERROR 12X, 6H LOWER 12X,
     2 6H UPPER 12X, 6H LOWER 12X, 6H UPPER   )
  920 FORMAT( 1H /1H /30H  NONLINEAR CONFIDENCE LIMITS - / /
     $ 1 16H PHI CRITICAL = E15.8    )
  921 FORMAT(1H / 6H  PARA 6X,8H LOWER B 8X,10H LOWER PHI 10X,8H UPPER B
     1 8X,10H UPPER PHI  )
  922 FORMAT (1H1,60X,17HGAMMA LAMBDA TEST 6X,2E13.3)
  923 FORMAT (1H1,90X,12HEPSILON TEST )
  924 FORMAT (1H1,90X,10HFORCE OFF  )
  925 FORMAT (5X,6E18.8/59X,2E18.8)
  926 FORMAT ( 40H BAD DATA, SUBSCRIPTS FOR UNUSED BS = 0   / / / )
  927 FORMAT(2X,I3,5E18.8 )
  928 FORMAT(1H , 110A1  )
  929 FORMAT(10A1)
  930 FORMAT (7F10.0)
  931 FORMAT (8F10.0)
  932 FORMAT(1H1)
  933 FORMAT(5HON = ,I3,5X,5H K = ,I3,5X,5H P = ,I3,5X,5H M = ,I3,5X,
     1/6H FF = ,E10.3,5X,5H T = ,E10.3,
     25X,5H E = ,E10.3,5X,7H TAU = ,E10.3/)
  934 FORMAT (1H1,80X,18HGAMMA EPSILON TEST )
  935 FORMAT (3X,I5,2X,10F10.4)
  936 FORMAT (27H0 NEGATIVE DIAGONAL ELEMENT   )
  937 FORMAT (3X,I5,2X,10F10.4/(10X,10F10.4))
  938 FORMAT (1H /25H CONSTRAINT RESIDUALS .../(3X,I5,33X,E18.8))
  939 FORMAT (1H /23H PTP CORRELATION MATRIX )
 1450 FORMAT(///41H ITERATION LIMIT EXCEEDED, RUN TERMINATED)
      END
      SUBROUTINE GJR(A,N,EPS,MSING)
C     GAUSS-JORDAN-RUTISHAUSER MATRIX INVERSION WITH DOUBLE PIVOTING.
```

```
      DIMENSION A(50,50),B(50),C(50),P(50),Q(50)
      INTEGER P,Q
      MSING=1
      DO 10 K=1,N
C     DETERMINATION OF THE PIVOT ELEMENT
      PIVOT=0.
      DO 20 I=K,N
      DO 20 J=K,N
      IF(ABS(A(I,J))-ABS(PIVOT))20,20,30
   30 PIVOT=A(I,J)
      P(K)=I
      Q(K)=J
   20 CONTINUE
      IF(ABS(PIVOT)-EPS)40,40,50
C     EXCHANGE OF THE PIVOTAL ROW WITH THE KTH ROW
   50 IF(P(K)-K)60,80,60
   60 DO 70 J=1,N
      L=P(K)
      Z=A(L,J)
      A(L,J)=A(K,J)
   70 A(K,J)=Z
C     EXCHANGE OF THE PIVOTAL COLUMN WITH THE KTH COLUMN
   80 IF(Q(K)-K)85,90,85
   85 DO 100 I=1,N
      L=Q(K)
      Z=A(I,L)
      A(I,L)=A(I,K)
  100 A(I,K)=Z
   90 CONTINUE
C     JORDAN STEP
      DO 110 J=1,N
      IF(J-K)130,120,130
  120 A(I,J)=1./PIVOT
```

```
      C(J)=0.
      GO TO 140
  130 B(J)=-A(K,J)/PIVOT
      C(J)=A(J,K)
  140 A(K,J)=0.
  110 A(J,K)=0.
      DO 10 I=1,N
      DO 10 J=1,N
   10 A(I,J)=A(I,J)+C(I)*B(J)
C     REORDERING THE MATRIX
      DO 155 M=1,N
      K=N-M+1
      IF(P(K)-K)160,170,160
  160 DO 180 I=1,N
      L=P(K)
      Z=A(I,L)
      A(I,L)=A(I,K)
  180 A(I,K)=Z
  170 IF(Q(K)-K)190,155,190
  190 DO 150 J=1,N
      L=Q(K)
      Z=A(L,J)
      A(L,J)=A(K,J)
  150 A(K,J)=Z
  155 CONTINUE
  151 RETURN
   40 PRINT 45,P(K),Q(K),PIVOT
   45 FORMAT(16HOSINGULAR MATRIX3H I=I3,3H J=I3,7H PIVOT=E16.8/)
      MSING=2
      GO TO 151
      END
      SUBROUTINE SUBZ(Y,X,B,PRNT,NPRNT,N)
      DIMENSION Y(500),X(500,1),B(50),PRNT(5),IDEN(7)
```

```
      READ(5,800) NRUN,IDEN
      WRITE(6,801) NRUN,IDEN
      WRITE (6,802)
      NPRNT=1
  800 FORMAT(I3,7A10)
  801 FORMAT(1HH NLIN DDJJ///14H RUN NUMBER = ,I3,5X,7A10///)
  802 FORMAT (25H PARAMETER IDENTIFICATION//5X,12H B(1) = TAUA/5X,12H B(
     12) = TAUR/5X,11H B(3) = AMU/5X,11H B(4) = BNU/5X,10H B(5) = JA/5X,
     29H B(6) = W/5X,22H B(7) = SCALING FACTOR/5X,27H B(8) = RELATIONSHI
     3P FACTOR/5X,10H B(9) = JB)
      RETURN
      END
      SUBROUTINE FCODE(Y,X,B,PRNT,F,I,RES)
      DIMENSION Y(500),X(500,1),B(50),PRNT(5)
      PI=3.1415927
      TPI=6.2831853
      RIT=PI*B(6)
      TOR=(B(1)*B(2))/(B(1)+B(2))
      DELP=(B(1)-B(2))/(B(1)+B(2))
      SNU=(B(3)+B(4))/2.0
      DNU=(B(3)-B(4))/2.0
      SNO=(B(3)+B(5)+B(4)+B(9))/2.0
      DNO=(B(3)+B(5)-B(4)-B(9))/2.0
      DLGNU=SNU-X(I,1)
      DLGNO=SNO-X(I,1)
      PU=TOR*(RIT*RIT-TPI*TPI*(DLGNU*DLGNU-DNU*DNU))+RIT
      PO=TOR*(RIT*RIT-TPI*TPI*(DLGNO*DLGNO-DNO*DNO))+RIT
      QU=TOR*TPI*(DLGNU-DELP*DNU)
      QO=TOR*TPI*(DLGNO-DELP*DNO)
      RU=TPI*(DLGNU*(1.0+2.0*TOR*RIT)+DELP*DNU)
      RO=TPI*(DLGNO*(1.0+2.0*TOR*RIT)+DELP*DNO)
      F1=B(7)*(PU*(1.0+TOR*RIT)+QU*RU)/(PU*PU+RU*RU)
      F0=B(8)*B(7)*(PO*(1.0+TOR*RIT)+QO*RU)/(PO*PO+RO*RO)
```

```
      F=FU+F0
      RES=Y(I)-F
      PRNT(1)=X(I,1)
      RETURN
      END
      SUBROUTINE PCODE(P,X,B,PRNT,F,I)
      DIMENSION P(50),X(500,1),B(50),PRNT(5)
      RETURN
      END
```

```
FTN,B,L
      PROGRAM DD
      COMMON Y(256)
      WRITE(2,10)
   10 FORMAT("NMR LI
    1 WRITE(2,11)
   11 FORMAT("LIFETIME ON SITE A (SEC) =")
      READ(1,*)TAUA
      WRITE(2,12)
   12 FORMAT("LIFETIME ON SITE B (SEC) =")
      WRITE(2,20)
   20 FORMAT("NOTE:Y
      READ(1,*)TAUB
      WRITE(2,13)
   13 FORMAT("CHEMICAL SHIFT A (HZ) =")
      READ(1,*)ANU
      WRITE(2,14)
   14 FORMAT("CHEMICAL SHIFT B (HZ) =")
      READ(1,*)BNU
      WRITE(2,15)
   15 FORMAT("COUPLING CONSTANT (HZ) =")
      READ(1,*)CUP
      WRITE(2,16)
   16 FORMAT("LINE WIDTH (HZ) =")
      READ(1,*)WIDTH
      WRITE(2,17)
   17 FORMAT("RELATIONSHIP FACTOR =")
      READ(1,*)FAC
      WRITE(2,18)
   18 FORMAT("FREQUENCY LOWER LIMIT =")
      READ(1,*)FREQL
      WRITE(2,19)
   19 FORMAT("FREQUENCY UPPER LIMIT =")
      READ(1,*)FREQH
    5 FORMAT(F10.0)
      WRITE(2,40)
   40 FORMAT(//"PARAMETERS:"/)
      WRITE(2,41)TAUA,TAUB
   41 FORMAT(13H    TAU(A) =
      WRITE(2,42)ANU,BNU
   42 FORMAT(13H  SHIFT(A)
      WRITE(2,43)CUP,WIDTH,FAC
   43 FORMAT("COUPLING CONSTANT
      WRITE(2,44)FREQL,FREQH
   44 FORMAT("FREQUENCY RANGE= "F6.2" TO "F6.2)
      WRITE(2,45)
   45 FORMAT("IS A RE-START REQUIRED?")
      READ(1,*)IR
      IF (IR)60,46,60
   46 CONTINUE
```

```
      PI=3.1415927
      TPI=6.2831853
      RIT=PI*WIDTH
      TOR=(TAUA*TAUB)/(TAUA+TAUB)
      DELP=(TAUA-TAUB)/(TAUA+TAUB)
      SNU=0.5*(ANU+BNU)
      DNU=0.5*(ANU-BNU)
      SNO=0.5*(ANU+BNU+2.0*CUP)
      FREQI=(FREQH-FREQL)/255.0
      FREQ=FREQL
      DO 111 N=1,256'
      DLGNU=SNU-FREQ
      DLGNO=SNO-FREQ
      PU=TOR*(RIT*RIT-
      PO=TOR*(RIT*RIT-
      QU=TOR*TPI*(DLGNU-DELP*DNU)
      QO=TOR*TPI*(DLGNO-DELP*DNU)
      RU=TPI*(DLGNU*(1.0+2.0*TOR*RIT)+DELP*DNU)
      RO=TPI*(DLGNO*(1.0+2.0*TOR*RIT)+DELP*DNU)
      FU=(PU*(1.0+TOR*RIT)+QU*RU)/(PU*PU+RU*RU)
      FO=FAC*(PO*(1.0+TOR*RIT)+QO*RO)/(PO*PO+RO*RO)
      Y(N)=FU+FO
      FREQ=FREQ+FREQI
  111 CONTINUE
      YHI=Y(1)
      DO 115 N=1,256
      IF(YHI-Y(N))114,115,115
  114 YHO=Y(N)
      YHI=YHO
  115 CONTINUE
      WRITE(2,50)
   50 FORMAT("IS PLOT SIZE ADJUSTMENT REQUIRED?")
      READ(1,*)IP
      IF(IP)116,38,116
  116 WRITE(2,30)
   30 FORMAT("RAISE PEN")
      WRITE(2,31)
   31 FORMAT("SET SIZE OF PLOT")
      WRITE(2,32)
   32 FORMAT("ON PAUSE, ADJUST X AND Y ZERO")
      CALL PLOT(0.0)
      PAUSE
      WRITE(2,33)
   33 FORMAT("ON PAUSE, ADJUST X AXIS")
      CALL PLOT(255,0)
      PAUSE
      WRITE(2,34)
   34 FORMAT("ON PAUSE, ADJUST Y AXIS")
      CALL PLOT(255,255)
      PAUSE
```

```
      CALL PLOT(0,0)
      WRITE(2,35)
   35 FORMAT("LOWER PEN")
   38 PAUSE
      DO 121 J=1,256
      Z=Y(J)/YHI
      IY=Z*255.0+0.5
      IX=J-1
      CALL PLOT(IX,IY)
  121 CONTINUE
      CALL PLOT(IX,0)
      CALL PLOT(0,0)
      WRITE(2,36)
   36 FORMAT("PLOT COMPLETED"//)
      WRITE(2,70)
   70 FORMAT("IS A RE-PLOT REQUIRED?")
      READ(1,*)JP
      IF(JP)115,71,115
   71 PAUSE
   60 WRITE(2,61)
   61 FORMAT("RE-STA
      GO TO 1
      END
      ENDS
```

PROGRAMS FOR CALCULATION OF ARRHENIUS AND EYRING ACTIVATION PARAMETERS

Program ACTPAR is used for the calculation of Arrhenius and Eyring activation parameters. A listing and directions for the use of ACTPAR is given in the M.Sc. thesis of Granata.[16]

PROGRAMS FOR PLOTTING OF FITTED SPECTRA IN THE THESIS

The programs PUNNLIN, STACKGH and STACKDD are used for the plotting of fitted digitized and calculated spectra in the thesis. PUNNLIN uses the output of TAPGH and TPDDJ as input to punch the cards which are used later as input for STACKGH and STACKDD. The listings and directions for the use of PUNNLIN and STACKGH are given in the M.Sc. thesis of Granata.[16]

STACKDD stacks outputs from NLINDD. Plots of the digitized spectra are superimposed on the theoretical spectra (smooth curves) calculated from the "best fit" values of the line shape parameters. The sets of spectra are separated vertically on the plot. The heights and

vertical placing of the spectra are calculated automatically.

The original sets of data cards containing the digitized experimental spectra are used.

Input cards are prepared as follows:

Item 1. NSETS, IDEN Format (I3, 18A4)

NSETS = number of sets of spectra to be stacked on each plot. A zero value for NSETS will terminate the run.

IDEN = alphanumeric identification. This is printed on the plot output.

Item 2. FR1, FR2, SCALE Format(3F10.0)

FR1 = low frequency limit of plot

FR2 = high frequency limit of plot

SCALE = plotting scale in mm/Hz

Item 3. NDATA, TEMP Format(I3,7X,F10.0)

NDATA = number of data pairs of the digitized spectrum

TEMP = temperature of measurement. This is printed on the plot

Item 4. B(1), B(2), B(3), B(4), B(5), B(6), B(7), B(8) Format (8F10.0)

B(1) = mean lifetime on site A (sec)

B(2) = mean lifetime on site B (sec)

B(3) = chemical shift on site A (Hz)

B(4) = chemical shift on site B (Hz)

B(5) = coupling constant (Hz)*

B(6) = natural line width (Hz)

B(7) = scaling factor

B(8) = relationship factor

* An average of the two coupling constants in NLINDD2 is used.

Item 5. SPECY(I), SPECX(I) Format(2F10.0)

Number of cards in Item 5 = NDATA

SPECY(I) = Y co-ordinate of point in experimental spectrum.

SPECX(I) = X co-ordinate of point in experimental spectrum.

Any number of runs may be stacked one after another. Each run produces a separate plot. The job is terminated by a blank card following the last data set. Items 3,4,&5 are repeated for each set spectra, i.e. the total number of sets of spectra comprising 3,4&5 = NSETS for each run.

```
      PROGRAM STACKDD(INPUT,OUTPUT,TAPE3,TAPE60=INPUT,TAPE61=OUTPUT)
C     CDC 6400 FORTRAN,   JULY  1973
C     THIS PROGRAM STACKS OUTPUTS FROM NLINDD
C     A PLOT OF THE DIGITIZED SPECTRUM IS SUPERIMPOSED ON THE SPECTRUM
C     CALCULATED FROM THE BEST FIT PARAMETERS
C     NOTE-FOR THIS PROGRAM CHEMICAL SHIFTS ARE DEFINED  AS THE POSITION
C     OF THE LOW FREQUENCY LINES OF THE DOUBLETS
C     IT IS ASSUMED THAT THE SPECTRUM IS VERY CLOSE TO FIRST ORDER
C
C     B(1) = MEAN LIFETIME IN SECONDS ON SITE A
C     B(2) = MEAN LIFETIME IN SECONDS ON SITE B
C     B(3) = CHEMICAL SHIFT IN HZ ON SITE A
C     B(4) = CHEMICAL SHIFT IN HZ ON SITE B
C     B(5) = COUPLING CONSTANT IN HZ
C     B(6) = LINE WIDTH IN HZ
C     B(7) = SCALING FACTOR
C     B(8) = RELATIONSHIP FACTOR
C
      DIMENSION IDEN(18),Y(3000),B(8),KRAY(14),SPECX(200),SPECY(200)
      WRITE(61,200)
  200 FORMAT(1H1,'PROGRAM STACKDD'//)
      READ(60,201)NSETS,IDEN
  201 FORMAT(I3,18A4)
      IF (NSETS.EQ.0) GO TO 50
      DO 1 I = 1,
      DELTAT=200.0/SETS
      NTEMP=(600/25)+4
      CALL PLYSE
      READ(60,202)FR1,FR2,SCALE
  202 FORMAT(3F10.0)
      WRITE(61,204)IDEN
  204 FORMAT(10X,18A4///)
```

```
      WRITE (6,200)FR1,FR2,SCALE,HEIGHT
  200 FORMAT(20H PLOTTING PARAMETERS//5X,18HFREQUENCY RANGE = ,F8.2,4H T
     1O ,F8.2,3H HZ/5X,9H SCALE = ,F6.2,6H MM/HZ,5X,10H HEIGHT = ,F6.2,3
     2H MM)
      DENS=100.0
      XMAX=SCALE*(FR2-FR1)/25.4
      NPOINT=DENS*XMAX+0.5
      IF (NPOINT.GT.3000) NPOINT=3000
      STEP=(FR2-FR1)/NPOINT
C
C     DRAW AXES AND TICK MARKS
      LY=XMAX+6.0
      YL=(FR2-FR1)*FLOAT(LY)/XMAX
      YLOW=FR1-DENS*STEP*1.5
      CALL SAXES(3,10,LY,1.0,10.0,YL,0.0,YLOW,0.0,YLOW)
      YT=FR1
      CALL PLOTXY(9.90,YT,0,0)
      CALL PLOTXY(10.0,YT,1,0)
   30 YT=YT+5.0
      YLIM=YLOW+YL
      IF (YT.GT.FR2) GO TO 35
      CALL PLOTXY(10.0,YT,1,0)
      CALL PLOTXY(9.95,YT,1,0)
      CALL PLOTXY(10.0,YT,1,0)
      YT=YT+5.0
      IF (YT.GT.FR2) GO TO 35
      CALL PLOTXY(10.0,YT,1,0)
      CALL PLOTXY(9.90,YT,1,0)
      CALL PLOTXY(10.0,YT,1,0)
      GO TO 30
   35 CONTINUE
C
C     PROCESS SETS OF SPECTRA
```

```
      DO 45 II=1,NSETS
      NPLOT=NPLOT +1
      BASE=BASE+RISE
      READ(60,210)NDATA,TEMP
  210 FORMAT(I3,7X,F10.0)
      WRITE(61,211)NPLOT,TEMP
  211 FORMAT(//13H PLOT NUMBER ,I3,10X,14HTEMPERATURE = ,F8.1//)
      READ(60,202)R(1),R(2),R(3),R(4),R(5),R(6),R(7),R(8)
  202 FORMAT(8F10.0)
      WRITE(61,205) R(1),R(2),R(3),R(4),R(5),R(6),R(7),R(8)
  205 FORMAT(23H CALCULATION PARAMETERS//5X,32HMEAN LIFETIME ON SITE A (
     1SEC) = ,F8.4,5X,32HMEAN LIFETIME ON SITE B (SEC) = ,F8.4,/5X,32HCH
     2EMICAL SHIFT ON SITE A (HZ) = ,F8.2,5X,32HCHEMICAL SHIFT ON SITE B
     3 (HZ) = ,F8.2,/12X,25HCOUPLING CONSTANT (HZ) = ,F8.2,20X,17HLINEWI
     4DTH (HZ) = ,F8.2,/20X,17HSCALING FACTOR = ,F8.2,15X,22HRELATIONSHI
     5P FACTOR = ,F8.2//)
      DO 10 I=1,NDATA
   10 READ(60,207)SPECY(I),SPECX(I)
  207 FORMAT(2F10.0)
      WRITE(61,208)
  208 FORMAT(19H DIGITIZED SPECTRUM//5X,9HINTENSITY,5X,9HFREQUENCY/)
      DO 15 I=1,NDATA
   15 WRITE(61,209)SPECY(I),SPECX(I)
  209 FORMAT(3X,F10.3,4X,F10.3)
C
C     CALCULATE THEORETICAL SPECTRUM
      PI=3.141592
      TPI=6.283853
      RII=PI*R(8)
      TOP=R(1)*R(2)*(R(1)+R(2))
      DELP=(R(1)-R(2))/(R(1)+R(2))
      SNUM=.5*(R(3)+R(4))
      ENUM=.5*(R(3)-R(4))
```

```
      SNO=SNU+B(5)
      FREQ=FR1-STEP
      DO 20 I=1,NPOINT
      FREQ=FREQ+STEP
      DLGNU=SNU-FREQ
      DLGNO=SNO-FREQ
      PU=TOR*(RIT*RIT-TPI*TPI*(DLGNU*DLGNU-DNU*DNU))+RIT
      PO=TOR*(RIT*RIT-TPI*TPI*(DLGNO*DLGNO-DNU*DNU))+RIT
      QU=TOR*TPI*(DLGNU-DELP*DNU)
      QO=TOR*TPI*(DLGNO-DELP*DNU)
      RU=TPI*(DLGNU*(1.0+2.0*TOR*RIT)+DELP*DNU)
      RO=TPI*(DLGNO*(1.0+2.0*TOR*RIT)+DELP*DNU)
      FU=(PU*(1.0+TOR*RIT)+QU*RU)/(PU*PU+RU*RU)
      FO=B(6)*(PO*(1.0+TOR*RIT)+QO*RO)/(PO*PO+RO*RO)
   20 Y(I)=(FU+FO)*B(7)
C
C     SCALE BOTH SPECTRA TO CALCULATED HEIGHT
      YMAX=Y(1)
      DO 21 I=2,NPOINT
      IF (YMAX.GT.Y(I)) GO TO 21
      YMAX=Y(I)
   21 CONTINUE
      FACTOR=HEIGHT/(25.4*YMAX)
      DO 28 I=1,NPOINT
   28 Y(I)=Y(I)*FACTOR
      DO 29 I=1,NDATA
   29 SPECY(I)=SPECY(I)*FACTOR
C
C     PLOT THE SPECTRA
      ENCODE(60,110,KRAY(1))TEMP,B(1),B(2)
  110 FORMAT(F6.1,6H DEG.,8X,F6.4,6H SEC.,8X,F6.4,6H SEC.,8X)
      XP1=8.95-BASE
      XP2=9.30-BASE
```

```
      XP3=9.60-BASE
      X=FR1
      YYY=9.85-Y(NPOINT)-BASE
      CALL PLOTXY(YYY,X,0,0)
      DO 24 I=2,NPOINT
      J=NPOINT-I+1
      X=X+STEP
      YYY=9.85-Y(J)-BASE
   24 CALL PLOTXY(YYY,X,1,0)
      CALL PLOTXY(XP1,FR2,0,0)
      CALL LABEL(11,1,3,KRAY(1))
      CALL PLOTXY(XP2,FR2,0,0)
      CALL LABEL(11,1,3,KRAY(3))
      CALL PLOTXY(XP3,FR2,0,0)
      CALL LABEL(11,1,3,KRAY(5))
      IFR1=FR1
      IFR2=FR2
      IRF=0
      ILF=0
      ENCODE(4,111,ILF)IFR1
      ENCODE(4,111,IRF)IFR2
  111 FORMAT(I4)
      Y2=YLOW+YL*(FLOAT(LY)-0.6)/FLOAT(LY)
      Y3=YLOW+0.1*YL/FLOAT(LY)
      XSUM=FR1+FR2
      DO 40 I=1,NDATA
      XX=XSUM-SPECX(I)
      YSPEC=9.85-SPECY(I)-BASE
   40 CALL PLOTXY(YSPEC,XX,0,9)
C
C     PROCESS NEXT PAIR OF SPECTRA
   45 CONTINUE
      CALL PLOTXY(0.0,YLOW,0,0)
```

```
      WRITE(61,100)
  100 FORMAT(///29H SUMMARY OF PLOT CALCULATIONS//)
      WRITE(61,102)NPOINT
  102 FORMAT(9X,28H NUMBER OF POINTS PLOTTED = ,I4)
      WRITE(61,105)LY
  105 FORMAT(37H LENGTH OF FREQUENCY AXIS (INCHES) = ,I3)
C     WRITE(61,106)YL
  106 FORMAT(3X,34H LENGTH OF FREQUENCY AXIS IN HZ = ,F7.2)
      WRITE(61,107)FR1,X
  107 FORMAT(10X,27H FREQUENCY RANGE PLOTTED = ,F7.2,4H TO ,F7.2,3H HZ//
     1//)
      END FILE 3
C
C     START NEXT CASE
      GO TO 1
   50 CONTINUE
      END FILE 3
      REWIND 3
      STOP 1
      END
```

APPENDIX II

AN APPLICATION OF CARBON-13 NMR SPECTROSCOPY TO STRUCTURAL ANALYSIS

In a study by mass spectroscopy of the fragmentation processes of 2-cyclohexene-1-ol following electron impact, the mechanisms of water and methyl radical loss have been investigated by Rye at al.[1] In the course of the project, 2-cyclohexenone was deuterated under the conditions of reaction shown in the scheme below.

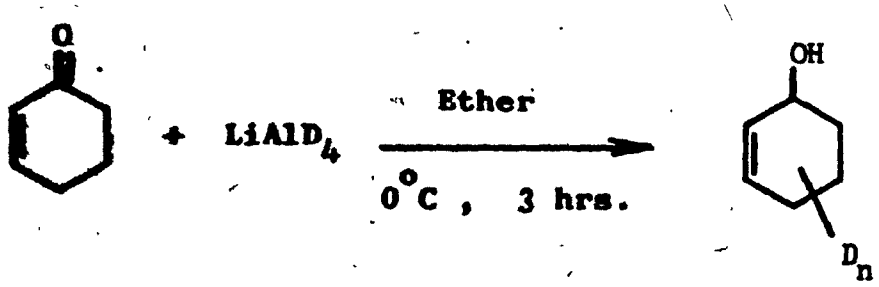

There are two sites of attack for the allylic substitution of deuterium in this compound, leading to the formation of the possible products A and B.

A B

It was necessary to identify the deuterated product before it would be used in the mass spectrometer study. Evidence available from nmr spectra was not adequate for an unambiguous structural assignment, due to overlapping

of the signals from coupled methylene and methine protons. The carbon-13 nmr spectra of undeuterated and deuterated 2-cyclohexene-1-ol were taken in order to identify the deuterated carbon atom. Since the deuterium carbon spin coupling is not affected by the proton-carbon decoupling employed when the spectra are taken, signals from carbon atoms carrying deuterium are easily recognized in the C-13 spectra. Further, the number of deuterium atoms substituted on a carbon atom may be readily deduced from the multiplicity of the signal.

Samples of 2-cyclohexene-1-ol and the deuterated product were prepared for carbon-13 measurements in p-dioxane at 64 mole % and 58 mole % concentrations, respectively. The carbon chemical shifts were measured from the internal reference carbon peak of the solvent, and were converted to the TMS scale in ppm.

Carbon atom chemical shifts for 2-cyclohexene-1-ol are readily assigned since all the carbons are non-equivalent and have appreciable chemical shift differences. The assignments are consistent with data previously reported for cyclohexanes,[2] cyclohexanols,[3] and cyclohexenones.[4]

Table: Carbon-13 Chemical Shifts (ppm from TMS)

	C-1	C-2	C-3	C-4	C-5	C-6
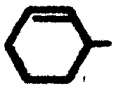	65.5	32.3	19.4	25.2	128.9	131.5
	64.90 (1:1:1 triplet) J=22 Hz	32.4	19.7	25.4	129.1	131.6

It can immediately be seen that the product is B. The signal arising from C-1 of 2-cyclohexene-1-ol-1-d is split into three signals of equal intensity due to coupling with one deuterium atom (Figure a,b). The C-1 carbon signal of 2-cyclohexene-1-ol is observed as a single peak since the proton on this carbon is decoupled under the conditions of measurement. If the deuterated product had been A, the signal from the C-4 carbon would have been split into five peaks due to coupling with two deuterium atoms. Thus the structure of the deuterated product may be assigned without ambiguity.

An upfield shift of 0.6 ppm for the C-1 carbon in B is consistent with the isotopic upfield shifts obtained in benzene (0.53 ppm) and cyclohexane (1.33 ppm) by Gold et al.[5] Other data in the literature also confirm the deuterium shielding effects.[6,7] The C^{13}-D coupling constant is also consistent with C^{13}-D coupling constants in benzene

and cyclohexane: $J_{C-D}^{C-1} = 22$ Hz,

benzene $J_{C-D} = 19$ Hz, cyclohexane $J_{C-D} = 24$ Hz

The isotope effect of deuterium is seen on the α - carbon signal only, since the changes in shielding values of the other carbons are not significant when considered in relation to the precision of the experiments.

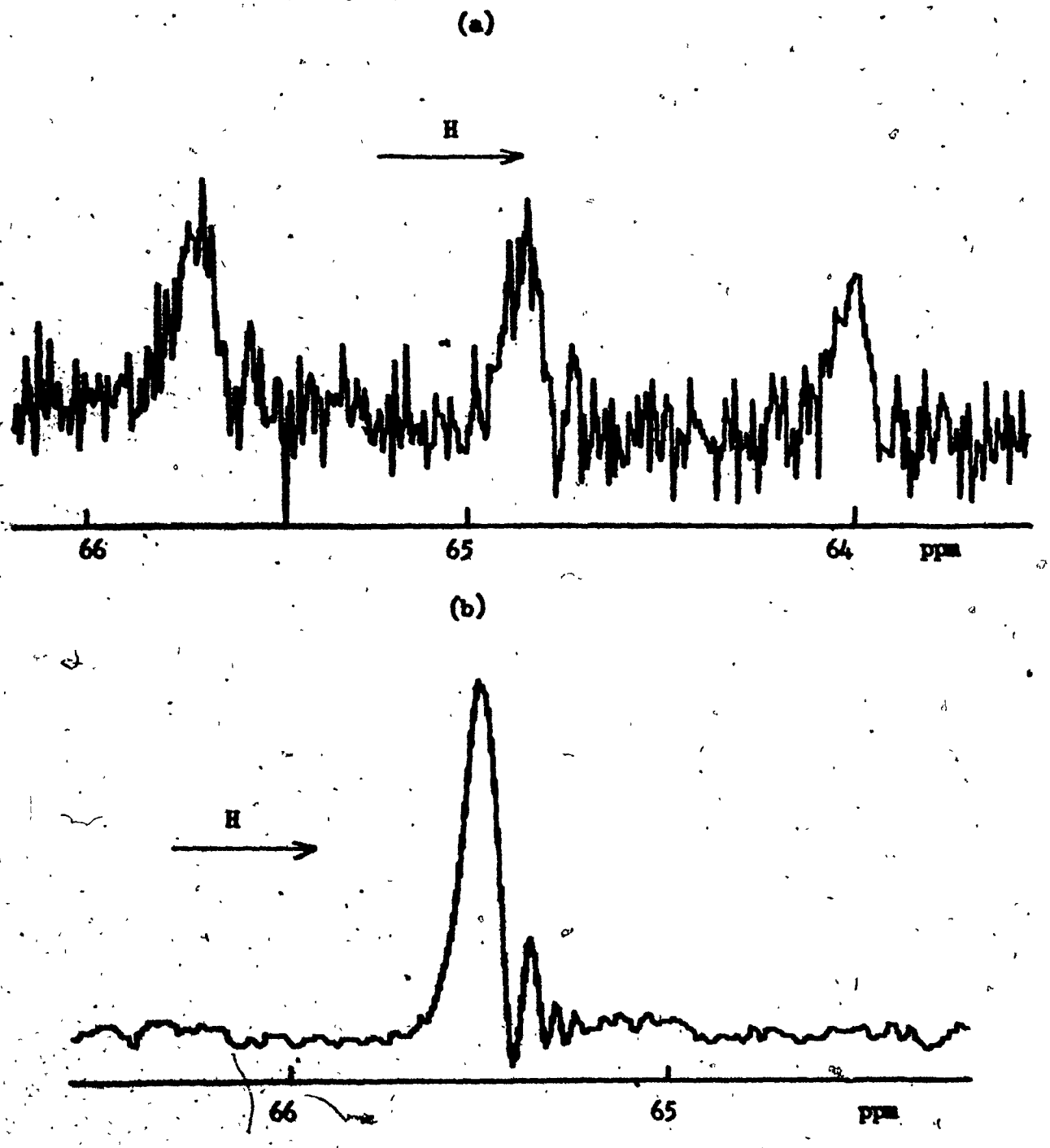

Figure: Carbon-13 NMR Spectra of C-1 Carbon
a) in 2-Cyclohexene-1-ol-1-d, and
b) in 2-Cyclohexene-1-ol

REFERENCES FOR APPENDIX II

1 - R.T.B. Rye, Q.T. Trung, Private Communication, Department of Chemistry, Sir George Williams University, Montreal, 1973.

2 - P. C. Lauterbur, J. Am. Chem. Soc., 83, 1838, 1846 (1961).

3 - J.D. Roberts, F.J. Weigert, J.I. Kroschwitz, H.J. Reich, J. Am. Chem. Soc., 92, 1338 (1970).

4 - D.H. Marr, J.B. Stothers, Can. J. Chem., 43, 596 (1965).

5 - H.N. Colli, V. Gold, J.E. Pearson, Chem. Comm. (J. Chem. Soc.) 12, 408 (1973).

6 - H. Batiz-Hernandez, R.A. Bernheim, Progr. NMR Spectr., 1, 63 (1970).

7 - a) Yu. K. Grishin, N.M. Sergeyev, Yu. A. Ustynyuk, Mol. Phys. 22, 711, (1971);

b) D. Laver, E. L. Motell, D.D. Traficate, G.E. Maciel J. Am. Chem. Soc., 94, 5335 (1972).